Synthesis and pharmacological characterization of dibenzodiazepinone-type heterodimeric and fluorescently labeled muscarinic receptor ligands

Dissertation

zur Erlangung des Doktorgrades der Naturwissenschaften (Dr. rer. nat.)

an der Fakultät für Chemie und Pharmazie

der Universität Regensburg

vorgelegt von

Xueke She

aus

Chengdu (China)

2017

The experimental part of this work was carried out between April 2013 and October 2016 under the supervision of Prof. Dr. Armin Buschauer and Dr. Max Keller at the Institute of Pharmacy, Faculty of Natural Sciences IV - Chemistry and Pharmacy, University of Regensburg.

The thesis was submitted on: 13nd, March, 2017

Date of the colloquium: 3nd, April, 2017

Board of examiners: Prof. Dr. Alkwin Slenczka (Chairman)

Prof. Dr. Armin Buschauer (1st Referee)

Prof. Dr. Günther Bernhardt (2nd Referee)

Prof. Dr. Sigurd Elz (Examiner)

Acknowledgements

Here I would like to express my sincere gratitude
to my supervisors Prof. Dr. Armin Buschauer and Dr. Max Keller, I am grateful to Prof. Dr. Armin Buschauer gave me the chance to work in his research group and gave me such an interesting project to explore, and the admission of Research Training Group GRK1910; I am grateful to Dr. Max Keller for scientific advices and valuable discussions on my projects, patient explanations for my questions and helping me to solve problems at experiments,

to Prof. Dr. Günther Bernhardt for improving of this thesis and for his scientific discussions,

to Prof. Dr. Nicholas D Holliday (School of Life Sciences, University of Nottingham, UK) and his group members in Nottingham for the excellent cooperation and assistance at high content imaging- based binding studies,

to Prof. Dr. Peter Gmeiner and Dr. Harald Hübner (Department of Chemistry and Pharmacy, Friedrich-Alexander-Universität Erlangen Nürnberg (FAU)) for helping to perform IP1 accumulation assay in Chapter 3,

to Brigitte Wenzl, Maria Beer-Krön, Susanne Bollwein, Elvira Schreiber, Dita Fritsch for excellent technical assistance, patient explanations of assays and Peter Richthammer for helping to solve technical problems, Karin Reindl for helping to solve organizational matters,

to all members of the Buschauer- and Elz- group for their help, ideas and support, especially my lab mates Dr. Carolin Meyer, Kilian Kuhn, Mengya Chen, Jonas Buschmann, Theresa Seiler and Christoph Müller for providing amusing atmosphere in the lab, Dr. Nicole Plank for preparing cell homogenates for me and Andrea Pegoli for exploring our projects together,

to Sabrina Biselli for exciting time of Yoga after work, and Dr. Carolin Meyer for teaching me how to make cakes,

to all my friends especially Dr. Paul Baumeister, Dr. Daniel Bücherl, Marina Hi, Christina Bücherl, Shiwen Xue, Mengya Chen, Shaoyang Qiu and Yanyan Zhang for making my stay in Regensburg wonderful,

to Jianfei for his encouragement and help for solving problems in experiments, and my parents for their supports and concerns,

to China Scholarship Council and project „International Quality Network-Medicinal Chemistry“ for providing financial support to me, and Research Training Group GRK1910 of the Deutsche Forschungsgemein-schaft for financial support and scientific promotion.

Publications (published results prior to the submission of this thesis):

(1) Andrea Pegoli, Xueke She, David Wifling, Harald Hübner, Günther Bernhardt, Peter Gmeiner, and Max Keller. Radiolabeled dibenzodiazepinone-type muscarinic receptor ligands enable unveiling of dualsteric binding at the M_2R. *J. Med. Chem.* **2016**, submitted.

(2) Max Keller, Christian Tränkle, Xueke She, Andrea Pegoli, Günther Bernhardt, Armin Buschauer, Roger W. Read. M_2 Subtype preferring dibenzodiazepinone-type muscarinic receptor ligands: Effect of chemical homo-dimerization on orthosteric (and allosteric?) binding. *Bioorg. Med. Chem.* **2015**, 23, 3970-3990.

Poster Presentations:

(1) Xueke She, Andrea Pegoli, Günther Bernhardt, Armin Buschauer, Max Keller. Synthesis and Pharmacological Characterization of Homo- and Heterodimeric Muscarinic Receptor Ligands. Emil Fischer School Research Day, Erlangen, Germany, 06/2014

(2) Xueke She, Andrea Pegoli, Günther Bernhardt, Armin Buschauer, Roger W. Read, Max Keller. Dibenzodiazepinone Derivatives: Synthesis and Pharmacological Characterization of Homo- and Heterodimeric Muscarinic Receptor Ligands. EFMC-ISMC 2014 XXIII International Symposium on Medicinal Chemistry, Lisbon, Portugal, 09/2014

(3) Xueke She, Andrea Pegoli, Günther Bernhardt, Armin Buschauer, Roger W. Read, Max Keller. Dibenzodiazepinone Derivatives: Synthesis and Pharmacological Characterization of Homo- and Heterodimeric Muscarinic Receptor Ligands. The 7th Summer School in Medicinal Chemistry, Regensburg, Germany, 09/2014

(4) Xueke She, Andrea Pegoli, Jianfei Wan, Sabrina Biselli, Günther Bernhardt, Armin Buschauer, Max Keller. Synthesis and Characterization of Radiolabeled and Fluorescent Pharmacological Tools for Muscarinic Receptors. GLISTEN Meeting, Erlangen, Germany, 04/2016

(5) Xueke She, Andrea Pegoli, Nicholas D Holliday, Günther Bernhardt, Armin Buschauer, Max Keller. Fluorescently Labelled Dibenzodiazepinone-type Muscarinic Receptor Ligands: Characterization of Bitopic (?) Molecular Tools. The 8th Summer School in Medicinal Chemistry, Regensburg, Germany, 09/2016.

Professional Training:

02/2014	Radioanalytical working methods for pharmacists. Regensburg, Germany.
12/2013-03/2017	Associated member of the Research Training Group (Graduiertenkolleg 1910) “Medicinal Chemistry of Selective GPCR Ligands” of the German Research Foundation. Regensburg, Germany.
06/2014-04/2017	Member of the Emil Fischer Graduate School of Pharmaceutical Sciences and Molecular Medicine. Regensburg, Erlangen, Germany.

Contents

Chapter 1

General Introduction

1. General Introduction

1.1. G-protein coupled receptors

1.1.1. GPCRs as drug targets and their classification

The superfamily of G-protein coupled receptors (GPCRs) is one of the largest and most studied families of proteins, over 800 GPCRs are encoded in the human genome[1-2]. A major characteristic of GPCR proteins is that they have seven α-helical transmembrane domains, an extracellular N-terminus and an intracellular C-terminus connected by three intracellular and extracellular loop domains (*cf*. Figure 1). Diverse kinds of endogenous ligands bind to GPCRs, such as biogenic amines, peptides, amino acids, glycoproteins, prostanoids, phospholipids, fatty acids, nucleosides, nucleotides and Ca^{2+} ions, as well as pheromones, fragrances or flavors are recognized by sensory 7TM receptors[3]. Moreover, the endogenous ligands of around 140 GPCRs are not identified, these GPCRs are the so-called orphan GPCRs[4], this field is relatively wide open for new discoveries. GPCR agonist and antagonist drugs have therapeutic benefit across a broad spectrum of human diseases[5], like peptic ulcers, pain, asthma, schizophrenia, depression and hypertension. According to sequence homology and functional roles, the mammalian members of this superfamily can be classified into three major families: A, B and C. Family A, also referred as the rhodopsin-like family, represents the largest and best studied subgroup of 7TM receptors. It includes aminergic and some peptidergic GPCRs as well as receptors addressed by nucleotides, lipids and other small molecules[6]. The other two main subfamilies are the family B (secretin receptor family) and metabotropic glutamate receptors, γ-aminobutyric acid receptors and the Ca^{2+} sensing receptor for family C[7]. The receptor topology varies between the families, e.g. with respect to the location of the orthosteric binding domain (OBD). For family A, the OBD is located within the 7TM domains, for family B in the large extracellular loop regions, and for family C the OBD is existent at the extracellular Venus-flytrap-like domain[8].

The crystal structure of bovine rhodopsin gave the first insight into the three-dimensional architecture of GPCRs[9]. Further structures were solved, e. g. those of the human β_2-adrenoceptor[10-11], the turkey β_1-adrenergic receptor[12], the human adenosine 2A receptor[13], the dopamine D_3 receptor[14], opsin[15-16] and the chemokine CXCR4 receptor[17]. The crystal structures of GPCRs provided insights into the molecular mechanisms of GPCR activation and constitutive activity and served as template for GPCR homology models to study GPCR conformations and ligand receptor interactions. So far, the structures of more than 30 different GPCRs have been solved.

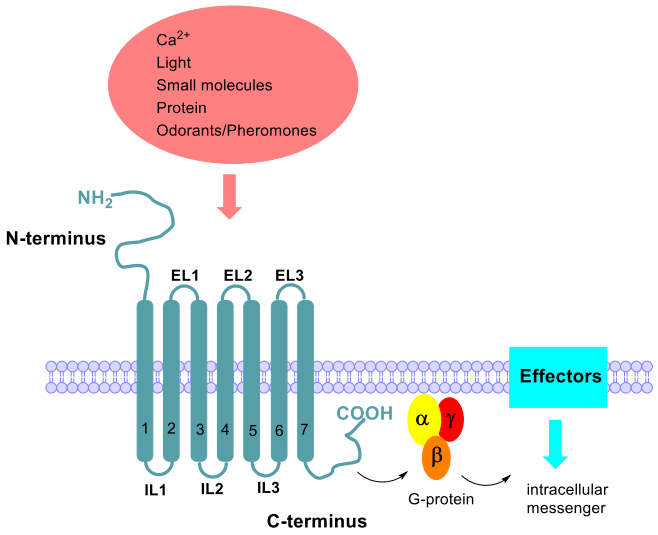

Figure 1. Schematic structure of a generic GPCR. GPCRs all contain a common core composed of seven transmembrane helices (7TM) with an extracellular N-terminal domain and an intracellular C-terminal domain. The TMs are connected by three extracellular loops (EL1-EL3) and three intracellular loops (IL1-IL3). (modified from the literature[8])

1.1.2. GPCR signaling pathways

To explain the interaction between a GPCR (R), its ligand (A) and the respective G-protein (G), several models have been proposed. The ternary complex model was firstly described by DeLean and colleagues[18]. In this model, the binding of the activated receptor to membrane proteins such as G-proteins was taken into account, the process is[19]:

$$A + R \rightleftharpoons AR + G \rightleftharpoons ARG$$

However, the ternary complex model was not able to explain the phenomena such as constitutive activity or inverse agonism. Refinement of the ternary complex model resulted the extended ternary complex model, which additionally implies the equilibrium between the inactive R_i and the active R_a receptor states[19-20]. The active state receptor can form a complex with G-protein (G) to R_aG, or agonist activation can induce a ternary complex AR_aG. The term α refers to the multiple differences in affinity of the ligand for R_a over R_i, and γ refers to the multiple difference in affinity of the receptor for G-protein, when the ligand is bound to the receptor (*cf*. Figure 2A). Moreover, further refinements were made with the cubic ternary complex (CTC) model. The concept of the CTC is shown in Figure 2B. Accordingly, receptors are assumed to exist in inactive (R_i) and active (R_a) conformations, which may or may not be coupled to G-protein. At equilibrium, four receptor species namely R_i, R_a, R_iG, and R_aG make up the native ensemble. K_G, K_{act}, and β are defined as the interconversions between these four species (R_i, R_a, R_iG, and R_aG). Each of the four receptor species in the native ensemble can bind to ligand (refers to A). The equilibrium dissociation constants for the binding of ligand to the members of the native ensemble are K_A, αK_A, γK_A, and $\delta\alpha\gamma K_A$, respectively[21-23].

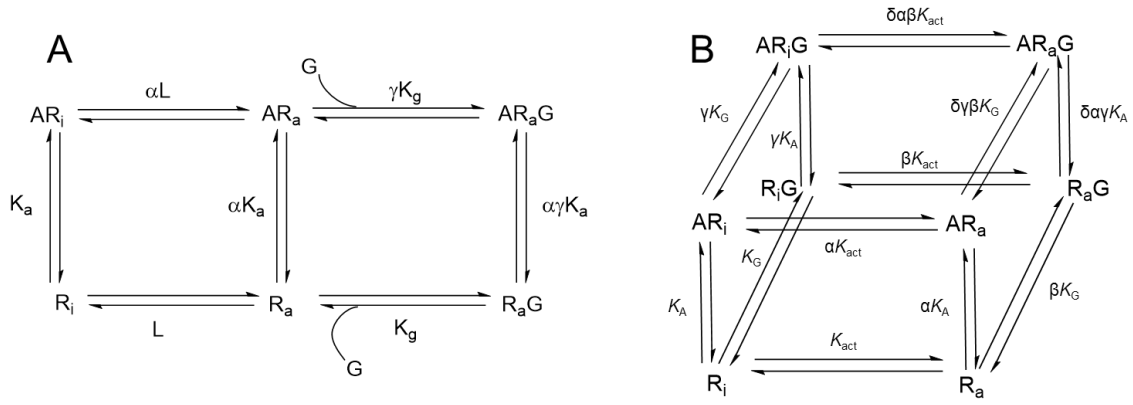

Figure 2. (A) Illustration of the extended ternary complex model[19]: discrimination between R_i and R_a. (B) Scheme of the cubic ternary complex model of GPCR ligand-receptor interactions. The cubic ternary complex model comprises eight distinct types of receptor species: R_i, R_a, AR_i, AR_a, R_aG, R_iG, AR_iG, and AR_aG (R_i = inactive receptor, R_a = activated receptor, A = ligand, G = G-protein). (modified from literature[21-23])

Upon activation (agonist-dependent or independent), GPCRs can transduce signals into cells through G-Protein coupling. There are two main classes of G-proteins, small cytoplasmic G-proteins and heterotrimeric G-proteins[24-26]. In the latter case, α, β and γ subunits constitute a heterotrimeric G-protein. Agonist binding to extracellular or transmembrane domains of a GPCR leads to the stabilization of a certain receptor conformation resulting in binding of the intracellular receptor domains to a heterotrimeric G protein. This agonist-receptor-G-protein complex, is termed ternary complex. Upon receptor activation, the GDP-bound G-protein interacts with the intracellular face and C-terminus of the receptor, inducing GDP to GTP exchange on the Gα subunit and concurrent dissociation of the activated α subunit ($G\alpha^*$) from the βγ-dimer[8]. Both G-protein subunits regulate the activity of enzymatic effectors, such as adenylate cyclases, phospholipase C isoforms, and ion channels, to regulate the production and release of small molecule 'second messengers'. The receptor returns to the inactive state by intrinsic GTPase activity of the Gα subunit: cleavage of the terminal γ-phosphate of GTP, resulting in GDP, gives the inactive GDP-bound Gα and the subunits re-associate allowing a new cycle[24, 27-28]. A scheme of the G-protein cycle is depicted in Figure 3.

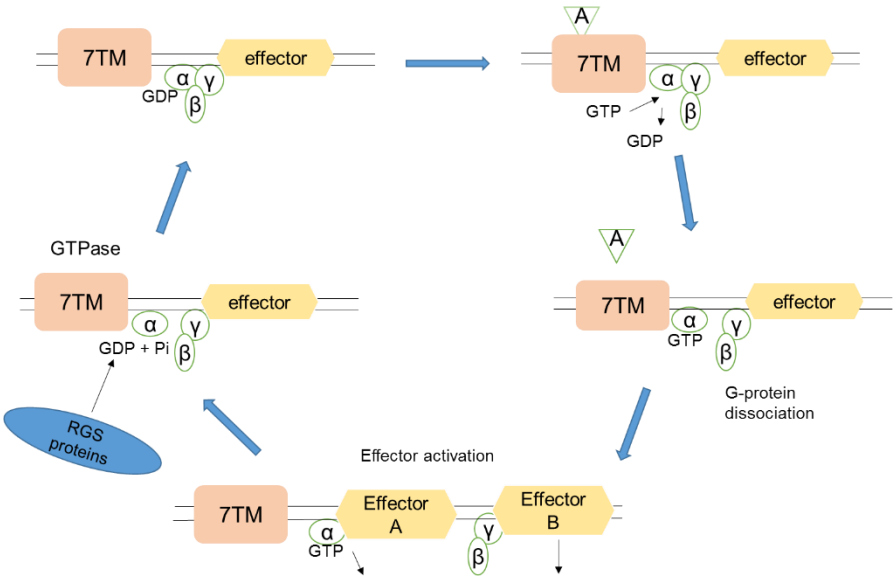

Figure 3. The G-protein cycle. RGS, regulator of G-protein signaling. (adopted and modified from the literature[29])

More than twenty G-protein α-subunits have been described for mammalian systems. Based on the degree of primary sequence similarities and different regulation of effectors[30], G-protein α-subunits can be divided into 4 families, termed as $G_{\alpha s}$, $G_{\alpha i/o}$, $G_{\alpha q}$ and $G_{\alpha 12/13}$[3, 24, 29]. Stimulation of the $G_{\alpha s}$ subfamily activates AC1-9, leading to an increase in intracellular cAMP (3'-5'-cyclic adenosine monophosphate) levels, and consequently, to an activation of proteinkinase A (PKA) or the mitogen-activated protein kinase (MAPK) pathway, which results in a modulation of gene transcription[31]. Activation of the $G_{\alpha i}$ family results in an inhibition of AC5 and AC6, and thus in decreased intracellular cAMP formation. Proteins of the $G_{\alpha q}$ family active phospholipases Cβ1-3 (PLCβ), leading to the hydrolysis of phosphatidylinositol 4,5-bisphosphate (PIP_2) into 1,2-diacylglycerol (DAG) and inositol-1,4,5-trisphosphate (IP_3). IP_3 mediates the release of Ca^{2+} from intracellular compartments in particular from the endoplasmic reticulum. DAG activates protein kinase C (PKC) which phosphorylates of various proteins[32]. It has been difficult to selectively study the cellular processes mediated by G_{12} and G_{13}, for G_{12}/G_{13} as the respective receptors are often simultaneously stimulated by activating members of the G_q-family. It was reported that G_{12}/G_{13} stimulates a Na^+/H^+ exchange and alters a variety of downstream effectors including phospholipase A_2 (PLA_2)[33-34]. Like the GTP-bound α-subunits, the β- and γ-subunits, forming a tightly associated βγ-complex, are also able to interact with effector proteins such as PLCβ and ion channels[24] and regulate their functions. Besides the modulation of GPCR signaling by ligand (agonist) binding, the signaling is also substantially influenced by receptor expression, desensitization, and internalization in response to binding of different ligands[35]. The desensitization of GPCRs occurs through molecular mechanisms, involving phosphorylation of activated receptors by G protein-coupled

receptor kinases (GRKs). The phosphorylation leads to binding of β-arrestin preventing receptor-G-protein interactions while allowing activation of arrestin-dependent signaling pathways[36-37]. β-Arrestin can also induce receptor internalization, this regulates the level of cell surface receptors, thus effecting signaling to downstream effector pathways[38].

1.1.3. Allosteric modulation of GPCRs

The word *allosteric* comes from the Greek *allos*, and the arrangement of atoms in space refers *steric*[19]. The term 'orthosteric ligand' describes a receptor ligand, which binds to the binding site of the endogenous ligand, activating the receptor as agonist/partial agonist, blocking the actions of the endogenous agonist as an antagonist, or suppressing the receptor´s basal activity as an inverse agonist. Most GPCR drug discovery efforts to date have focused on targeting such sites. But as the orthosteric site is often highly conserved across subtypes of a given GPCR subfamily, this approach cannot always lead to highly subtype selective ligands. For example, the development of orthosteric selective ligands for one of the five subtypes of muscarinic acetylcholine receptors (M_1-M_5) is highly challenging. A number of MR agonists such as xanomeline, milameline, sabcomeline, cevimeline and talsaclidine were developed for the treatment of Alzheimer's disease. However, due to their poor subtype selectivity and associated side effects, their use in clinical trials was limited[39]. Meanwhile, in addition to orthosteric sites, potentially all GPCRs possess additional binding sites, which are designated allosteric sites. Ligands, which bind to an allosteric site of a GPCR, can potentially modulate the binding and/or signaling properties of the orthosteric ligand[40-42]. Because they do not face the same evolutionary pressure as orthosteric sites, allosteric sites are less conserved than orthosteric sites, presenting novel avenues for achieving selectivity in drug action[42-44]. Furthermore, allosteric modulators with limited positive or negative cooperativity will have a ceiling level to their effect, it means they might be potentially safer than orthosteric ligands if administered in high doses[44-45]. Finally, given that allosteric modulators can promote a conformational change of the receptor, their ability to effect orthosteric ligand efficacy is not surprising[8]. Some synthetic small molecules acting in such a pathway-selective allosteric modulation are actually reported[46-48].

Modulators binding to an allosteric site to stabilize a certain receptor conformation lead to an increase or decrease of the affinity and/or efficacy of an orthosteric agonist[8]. Such kind of allosteric ligands are termed as positive allosteric modulators (PAMs) and negative allosteric modulators (NAMs), respectively. Besides PAMs and NAMs, some allosteric ligands can be neutral (or silent), showing no cooperativity with the orthosteric ligand despite binding to an allosteric site of the receptor[8]. With the discovery of allosteric modulators and the intricate

mechanisms underlying their pharmacological properties, classical receptor models need to be revised or expanded. The allosteric ternary complex model (ATCM), which also forms the basis for many quantitative studies of GPCR allosterism, is considered as the simplest model to describe allosteric interactions[41] (*cf*. Figure 4A). This model, describing the interactions between an orthosteric agonist, an allosteric modulator and a receptor, was derived from the original TCM, which describes ligand, receptor, and G-protein interactions. A prerequisite for an application of the ATCM is a simultaneous binding of the orthosteric ligand (A) and the allosteric ligand (B) to distinct, i.e. non-overlapping sites of the receptor. The ATCM provides estimates of the respective equilibrium dissociation constants, K_A and K_B, as well as the "cooperativity factor" (α), which is a measure of the mutual effect of the two ligands on each other's affinity to the receptor[49-50]. Values of α > 1 indicate positive cooperativity. In this case an allosteric ligand promotes the binding of the orthosteric ligand. Values of α < 1 refers to negative cooperativity, *i.e.* the allosteric modulator inhibits the binding of the orthosteric ligand, whereas α = 1 means that binding of the allosteric ligand to the receptor does not alter the affinity of the orthosteric ligand. Provided that the two sites are conformationally linked, the orthosteric ligand will modulate the binding of the allosteric ligand in the same way[41-42]. Figure 4C and 4D illustrate another important aspect of such allosteric interactions, namely the fact that these effects are limited, in other words, they are saturable. The extent of the effect is defined by the numerical value of α (the lower the deviation of α from unity, the less pronounced is the modulatory effect of B)[42].

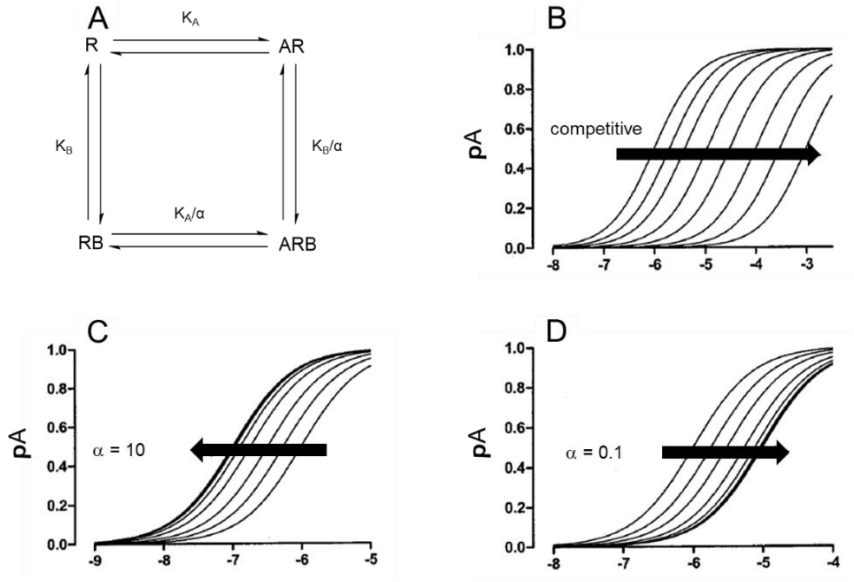

Figure 4. (A) The allosteric ternary complex model (ATCM), which describes the interaction of two ligands (e.g., an orthosteric agonist and an allosteric modulator) on a receptor in terms of their equilibrium dissociation constants (K_A, K_B) and the cooperativity (α) between the ligands. (B) Effect of a competitive antagonist on orthosteric ligand receptor occupancy (**p**A), simple competitive interactions are characterized by mutually exclusive binding of the two ligands for the same site and, thus, allow for a theoretically limitless dextral shift of orthosteric ligand occupancy. (C) An allosteric enhancer (α = 10) or (D) allosteric inhibitor (α = 0.1) on orthosteric ligand receptor occupancy (**p**A) based on the simple

ternary complex model for allosteric interactions. In these examples, ligand affinity is either maximally diminished or enhanced by a factor of 10. (adopted and modified from the literature[41-42])

1.2. Muscarinic acetylcholine receptors

1.2.1. Muscarinic receptors subtypes and signaling pathways

Muscarinic acetylcholine receptors (mAChRs or MRs) belong to class A (rhodopsin-like) GPCRs. In humans, the family of mAChRs comprises five subtypes (M_1-M_5). The M_1, M_3 and M_5 subtypes couple to the $G_{q/11}$ family of G proteins, resulting in phospholipase C activation, hydrolysis of PIP_2 and an increase in intracellular Ca^{2+} (*cf*. Figure 5A). The M_2 and M_4 subtypes couple to the $G_{i/o}$ family, resulting in the inhibition of adenylyl cyclase with a decrease in cAMP formation[45, 51] (*cf*. Figure 5B).

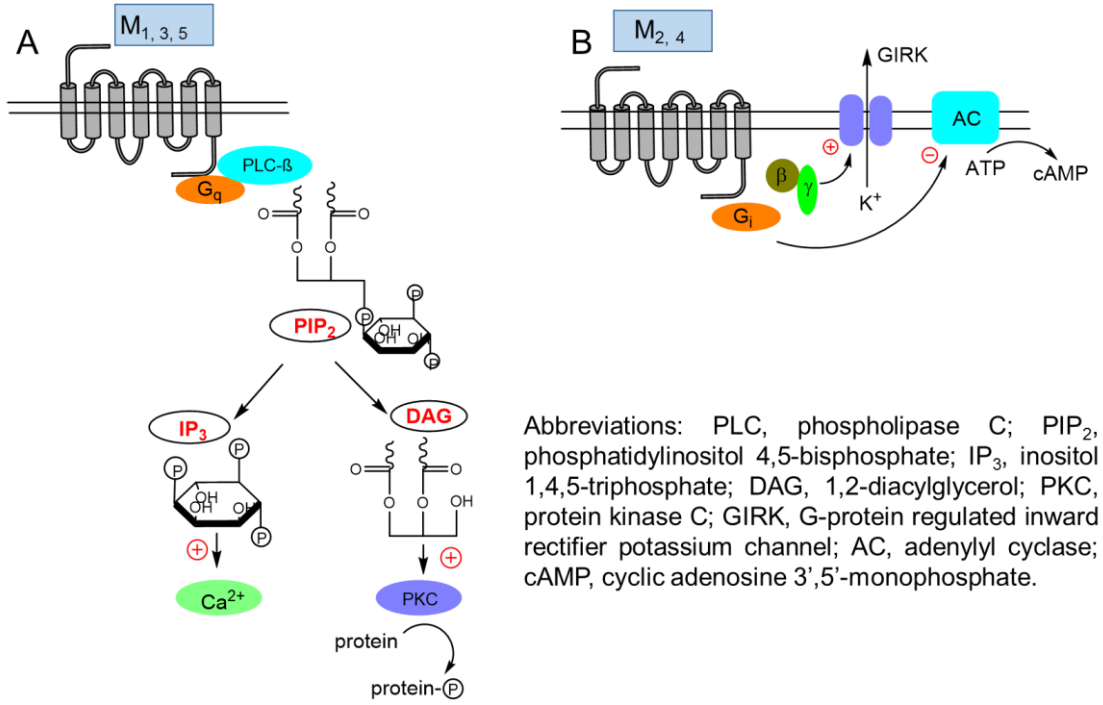

Figure 5. Schematic illustration of the signaling pathway of muscarinic receptors. (adopted and modified from the literature[29])

MRs are widely distributed in the periphery and the central nervous system (CNS), and play important roles in many functions of the CNS. The M_1 subtype is widely expressed in forebrain regions, including the cerebral cortex, hippocampus and striatum[52-55]. It was reported that reduced M_1R signaling in the CNS is associated with cognitive deficits such as Alzheimer's disease[56-57]. Selective agonists of the M_1 mAChR have been pursued as a potential avenue for the treatment of dementia-related disorders[58]. The M_2 mAChRs is located, e.g. in the brainstem, hypothalamus/thalamus, hippocampus, striatum, cortex[52-53] and in the heart[51]. It is suggested that elevated acetylcholine levels through antagonism of presynaptic M_2 muscarinic

autoreceptors may be beneficial in the treatment of psychosis and Alzheimer's disease[59-62]. In this respect, M_1/M_2 selectivity is crucial as antagonism at post-synaptic M_1 receptors is counterproductive, as confirmed by studies with the non-selective antagonists such as scopolamine, which lead to cognitive deficits[63]. In the heart, M_2 receptors may be directly linked through G proteins to ion channels devoid of a second messenger[64-66]. M_3 mAChRs are expressed at low levels in the cortex, the striatum, the hippocampus and the hypothalamus/thalamus[53, 67-68]. M_3 receptors are involved in regulating longitudinal growth by promoting the proliferation of pituitary somatotrophic cells, suggesting the M_3R as a target to treat growth disorders[69]. Furthermore, M_3 receptors participate in the regulation of smooth muscle motility. The M_3 receptor antagonist solifenacin could be bladder-selective to provide new approaches to the pharmacotherapy of an overactive bladder[70]. M_4 mAChRs are found in hippocampus, cortex, hypothalamus/thalamus and striatum[65]. Selective M_4 antagonists could be used as a medication for parkinsonism by controlling the tremor associated with Parkinson's disease[71]. The M_5 mAChR, which is expressed at consistently low levels in the brain, is the least studied subtype among the five muscarinic receptors[72]. The M_5 and the D_2 receptor were found to be co-localized within the pars compacta of the substantia nigra[73], and activation of the M_5R was reported to facilitate the release of dopamine.

Physiologically, each muscarinic subtype is activated by the endogenous ligand acetylcholine (*cf*. Figure 6). Several naturally occurring ligands binding to muscarinic acetylcholine receptors were described, e.g. the agonist muscarine (where the receptors name comes from), and the antagonist atropine (*cf*. Figure 6).

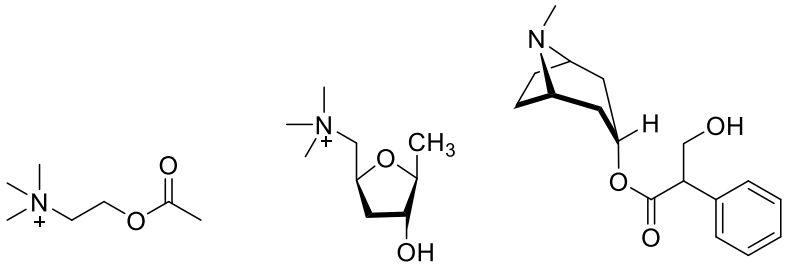

acetylcholine muscarine atropine

Figure 6. Structures of acetylcholine (endogenous MR agonist) and the naturally occurring ligands muscarine (MR agonist from the mushroom *Amanita muscaria* L.) and atropine (MR antagonist from *Atropa belladonna* L.).

For many years, pharmaceutical chemists aimed to find ligands, which bind selectively to one subtype of the MR family. As the five subtypes exhibit a high conservation of the orthosteric binding site, there are only very few subtype selective orthosteric agonists and antagonists. Many ligands exhibit merely a (weak) preference for one subtype. For example, the antagonist pirenzepine[74] shows a preference for the M_1R, the antagonists methoctramine, AF DX 384, tripitramine and himbacine show preference for the M_2R[75-77], the antagonist darifenacin prefers

the M_3R[78], and the antagonist PD102807 prefers the M_4R[79]. These ligands are used as pharmacological tools rather than for therapeutic purposes (*cf*. Figure 7).

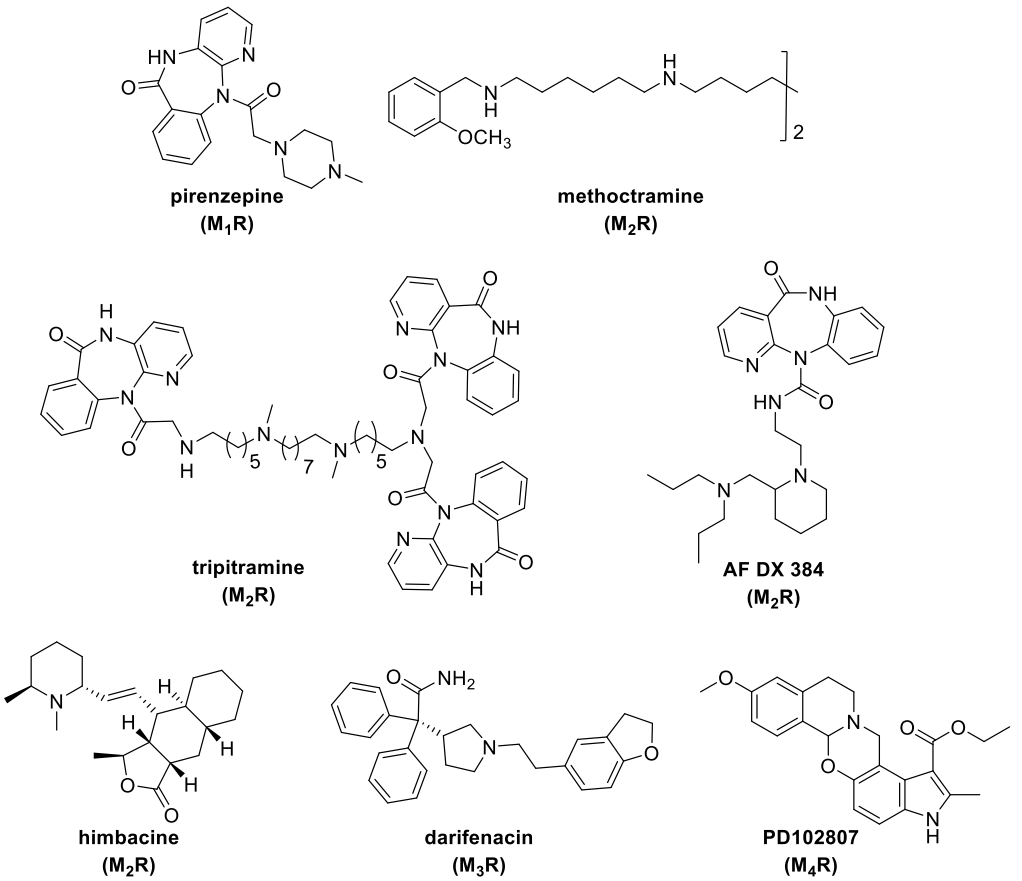

Figure 7. Chemical structures of muscarinic receptor ligands reported to exhibit preference for one muscarinic receptor subtype.

1.2.2. Muscarinic receptor agonists

According to a general trend, MR agonists are small molecules, whereas antagonists are large molecules, often containing an aromatic moiety[51]. Arecoline (*cf*. Figure 8), which is a naturally-occurring MR agonist shows no subtype selectivity. Due to the ester group, being prone to hydrolysis, its clinical application was limited. To improve the pharmacological properties, for example, the ester group was replaced with more stable five-membered heterocyclic rings such as oxadiazole, thiadiazole or tetrazole. The 1,2,5-thiadiazole derivative xanomeline (*cf*. Figure 8), which was reported as a cognition enhancer, potentially useful for the treatment of schizophrenia, has higher potency and efficacy for M_1 and M_4 than for M_2, M_3 and M_5 receptor subtypes[80]. Although xanomeline prefers M_1R with positive effects on verbal learning and short-term memory function[81], it causes side effects including nausea salivation and diaphoresis, presumably due to the activation of other mAChR subtypes[82]. Moreover, it was reported that xanomeline showed a unique mode of mAChR activation, being different from

that of conventional agonists such as carbachol[83], and it was reported to bind to the M_1R in a wash-resistant manner, which may be attributed not only to hydrophobic interactions between xanomeline's O-hexyl chain and the receptor, but also to the binding to a secondary binding site of the receptor[84-85]. Replacement of the side-chain and the azacyclic ring of xanomeline led to the discovery of potent MR agonists. The phenylpropargylthio-1azabicyclo[3.2.1] octane endo analogue (*cf*. Figure 8) is the most selective M_1/M_2 compound in this series, which was suggested to be a drug candidate for AD[86]. Many MR ligands, such as tritiated 3-quinuclidinyl benzilate ([^{3}H]QNB), a non-selective MR antagonist, which is routinely used for receptor binding studies, contain a quinuclidine ring. The same holds for some moderately potent MR agonists, for example, talsaclidine is a quinuclidinyl-propargyl ether (*cf*. Figure 8), which is a selective M_1R agonist[87] and has been reported for therapy of Alzheimer's disease[88]. Another "quinuclidine-related" M_1R agonist is SB202026[89], which contains a cyanooximether group in the structure (*cf*. Figure 8). As a functionally selective M_1R partial agonist, SB202026 was used in the investigation of the cholinergic hypothesis of senile dementia of the Alzheimer type (SDAT). To increase receptor subtype selectivity, several pharmacophores with increased rigidity were developed, for example, the conformationally restricted spiro compound RS-86 (*cf*. Figure 8), which was a M_2R preferable agonist, and some attempts also have been made to change the profile towards M_1R selectivity based on this structure[90]. Oxotremorine (*cf*. Figure 8) has long been known as a partial M_1R agonist[91]. By means of classical isosteric replacement of a methylene group with oxygen and exchange the pyrrolidine moiety of oxotremorine by a trimethylammonium group yielded a trimethylammonium salt related to oxotremorine (*cf*. Figure 8), which displayed binding affinity comparable to that of oxotremorine, but showed a pronounced selectivity for M_2R versus M_1R[92].

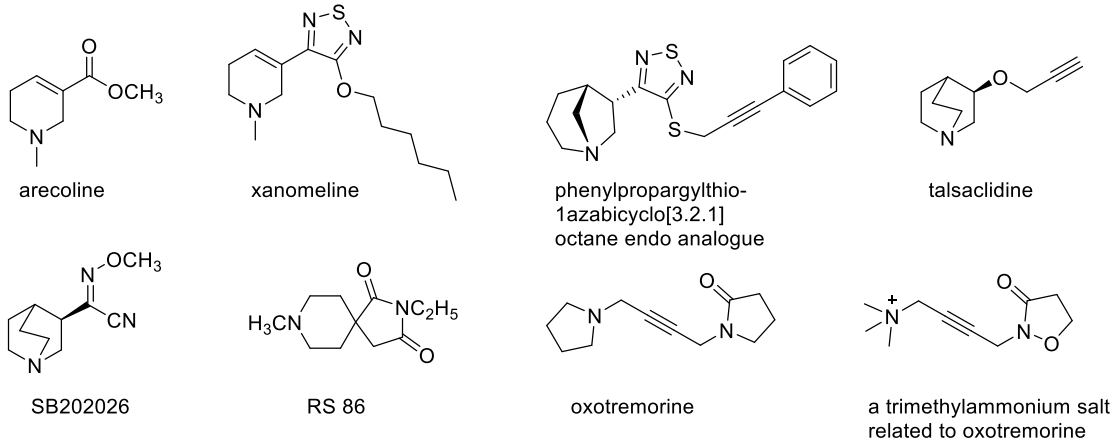

Figure 8. Chemical structures of selected muscarinic receptor agonists.

1.2.3. Allosteric modulation of muscarinic receptors

The lack of highly selective mAChR orthosteric ligands demands alternative approaches to develop subtype selective MR ligands. All five muscarinic receptor subtypes possess at least one extracellular allosteric binding sites for small molecules[93-94]. The M_2 subtype was the first GPCR found to be sensitive to allosteric modulation[95-96], so that the M_2R is one of the most extensively characterized allosteric model systems[45]. The best studied allosteric modulators of the mAChRs are represented by neuromuscular-blocking agents, for example, gallamine, alcuronium, W84 and its heptamethylene congener C7/3-phth, and most of these prototypical common-site modulators have higher affinity to the M_2R than to the other subtypes (*cf*. Figure 10). The allosteric behavior of gallamine can be demonstrated by equilibrium binding assays: Figure 9A and 9B show the effect of the modulator gallamine on the saturation binding of [^{3}H]NMS at the M_2R expressed by CHO cells. Although gallamine is able to shift [^{3}H]NMS binding curves to the right, the allosteric nature of the interaction is revealed as progressively higher concentrations of gallamine fail to cause significant dextral displacements of the [^{3}H]NMS saturation curves, becoming obvious from curvilinear Schild regressions[41]. Also the inhibitory effect of gallamine on equilibrium binding of [^{3}H]NMS could unmask the limited ability of this negative allosteric modulator to inhibit specific [^{3}H]NMS binding. From Figure 9C, it can be seen that when a low concentration of [^{3}H]NMS (0.1 nM) was applied, the increasing concentrations of gallamine resulted in an apparently complete inhibition of specific [^{3}H]NMS binding. However, applying a higher concentration of [^{3}H]NMS (2.0 nM), caused an incomplete [^{3}H]NMS binding by gallamine[41]. Alcuronium was found allosterically increases [^{3}H]NMS binding at M_2 and M_4 subtypes; in contrast, it inhibits [^{3}H]NMS binding at M_1, M_3 and M_5 subtypes[97]. The alkaloid structure of alcuronium lead to the identification of related compounds such as strychnine, vincamine, eburnamonine, and brucine and its analogs as allosteric mAChR modulators[98-99].

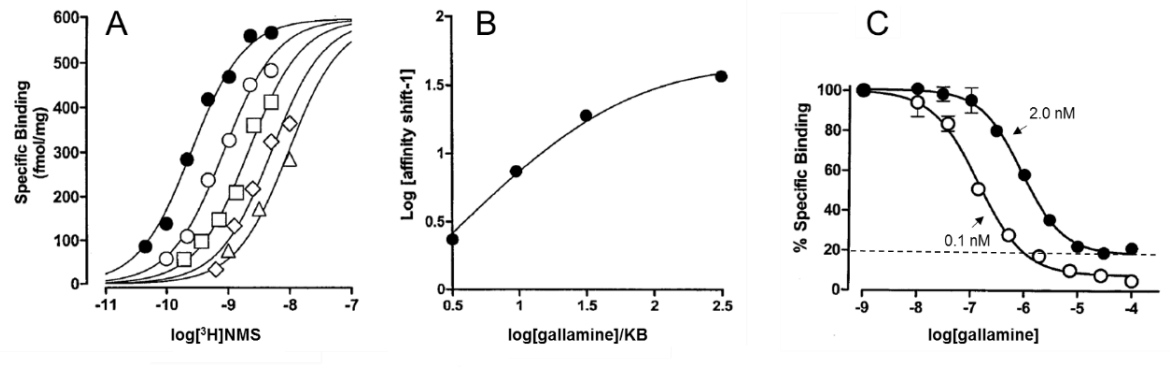

Figure 9. (A) [^{3}H]NMS saturation binding curves obtained in the presence of the following concentrations of gallamine: 0 (●), 1 μM (○), 3 μM (□), 10 μM (◇) and 100 μM (△). (B) Effect of gallamine on the ratio of [^{3}H]NMS K_d values ("affinity-shift") determined in the presence or absence of the modulator. (C) Inhibition of [^{3}H]NMS binding 0.1 nM (○) and 2.0 nM (●) by increasing concentrations of gallamine. Data were taken from the literature[41].

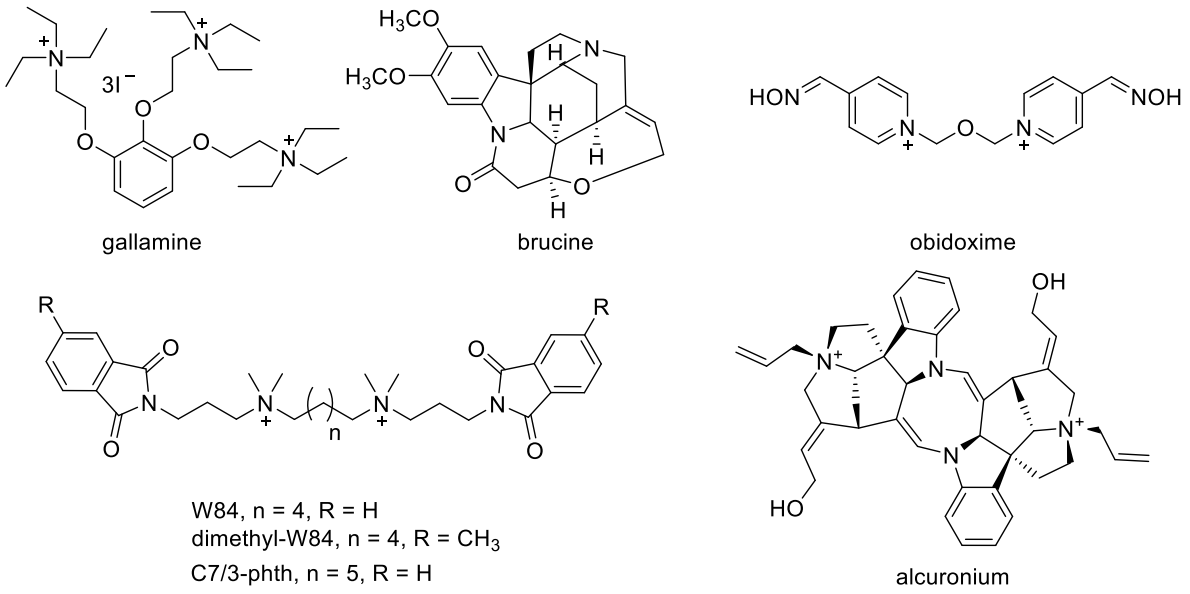

Figure 10. Structures of prototypical “common allosteric” site mAChR modulators.

In addition to the well-studied common mAChR allosteric site, Lazareno, Birdsall and colleagues defined a second allosteric site[94, 100]. For example, depending on the mAChR subtype, several indolocarbazole derivatives of staurosporine (*cf.* Figure 11) were found to show positive, negative and neutral cooperativity with Ach, but did not appear to interact with the prototypical modulators gallamine and brucine[94]. Similarly, WIN 51,708 (*cf.* Figure 11) interacts with staurosporine in a competitive manner, whilst interacting with gallamine and strychnine in a noncompetitive way[100].

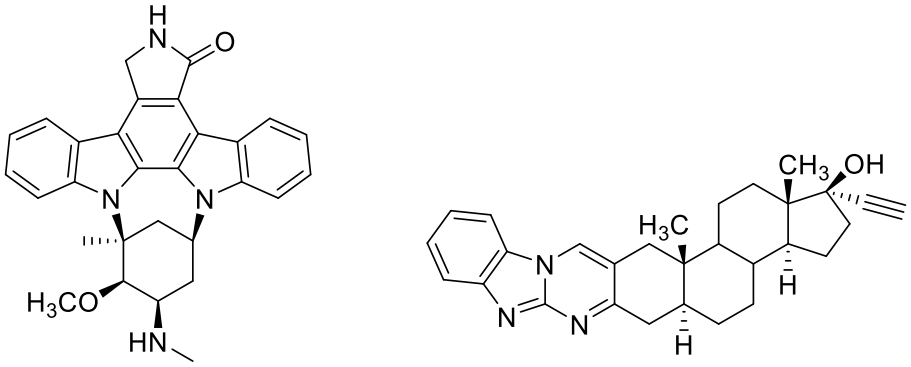

Figure 11. Examples of “second-site” mAChR modulators.

Given that allosteric modulators can induces a unique conformational change of the receptor, it is not surprising that they have the ability to affect orthosteric ligand efficacy. McN-A-343 (*cf.* Figure 12) was the mAChR agonist known to display functional selectivity[101], it was actually found to interact allosterically with [^{3}H]NMS on M_2 mAChRs[102]. Other agents were recently identified as potential mAChR allosteric agonists, such as AC-42 and its close structural

analog 77-LH-28-1. Both AC-42 and 77-LH-28-1 (*cf.* Figure 12) display high selectivity to activate the M_1 mAChR over other mAChR subtypes[103]. TBPB (*cf.* Figure 12) was reported as a novel highly selective agonist for the M_1 receptor with no agonist activity at any other mAChR subtypes, mutagenesis and molecular pharmacology studies revealed that TBPB activates M_1R through an allosteric site rather than the orthosteric ACh binding site[104]. A highly selective and efficacious allosteric potentiator for M_1R is BQCA (benzyl quinolone carboxylic acid) (*cf.* Figure 12)[105]. N-desmethylclozapine (*cf.* Figure 12), the major metabolite of the antipsychotic clozapine, which is a functionally-selective M_1 mAChR agonist that has been suggested to act allosterically[106].

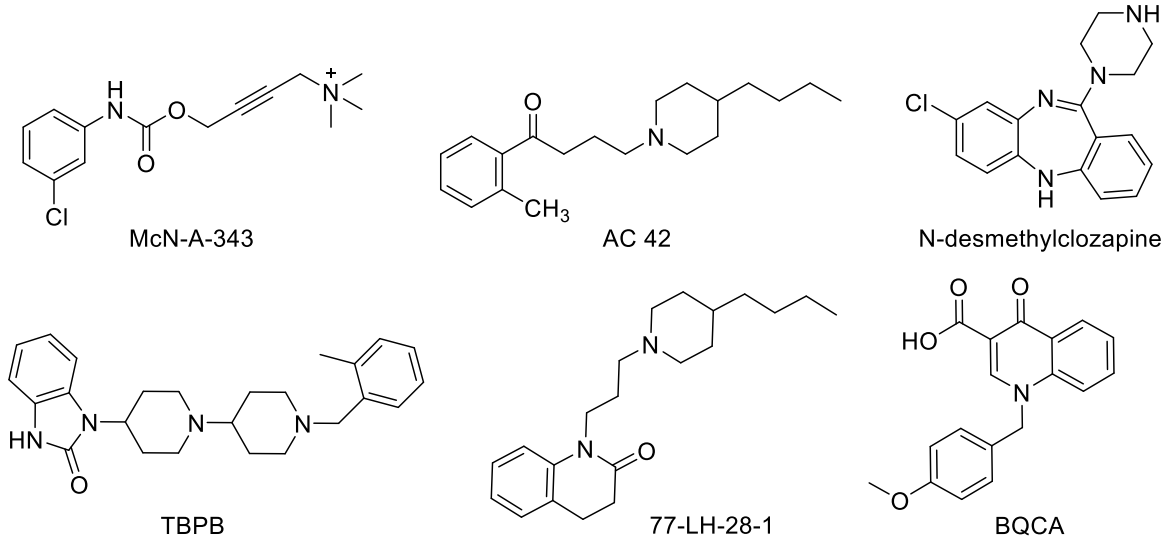

Figure 12. Examples of allosteric mAChR agonists (McN-A-343, AC 42, N-desmethylclozapine, TBPB and 77-LH-28-1) and allosteric potentiators (BQCA).

1.2.4. Crystal structures of muscarinic receptors

Kobilka *et. al* reported the crystal structures of the M_2R (with bound antagonist QNB) and M_3R (with bound inverse agonist tiotropium) in 2012[107-108]. The overall structure of the M_3R is similar to that of the M_2R, structural conservation includes intracellular loops (ICLs) 1 and 2, and extracellular loops (ECLs) 1-3, which share highly similar despite low sequence conservation. The binding poses of QNB (M_2R) and tiotropium (M_3R) were very similar, suggesting this pose to be a conserved binding mode: the ligands are deeply buried within the TM receptor core and covered by a 'lid' consisting of three conserved tyrosines, which separate the orthosteric site from the extracellular vestibule[107-108]. The structures of the inactive M_2 and M_3 receptor suggested that these receptors possess a large extracellular vestibule, which was shown to be addressed by allosteric modulators. In this region of the receptor, the structural diversity is much higher than in the region of the orthosteric binding site. When an allosteric ligand binds to this site, an influence on the association and disassociation rates of orthosteric ligands are

expected. Recently, the M_1 and the M_4 receptor were crystallized in the inactive state bound with the inverse agonist tiotropium bound. The structures of the M_1 and M_4 receptors are similar to the previously solved inactive states of M_2 and M_3 receptors, with similar positioning of the seven-transmembrane (TM1-7) bundle and root mean squared deviations of 0.6-0.9 Å[107-108]. By comparing structures of the M_1 and the M_4 receptor, subtle differences between the receptors are observed on the extracellular and intracellular sides corresponding to regions that are least conserved across the MR subtypes[109]. Further comparison of the orthosteric sites of M_1R and M_4R revealed the M_4R is closer related to the M_1 than to the M_2 subtype. Another breakthrough was the solution of the active-state structure of the M_2R in the presence of the high affinity agonist iperoxo and the positive allosteric modulator LY2119620[110]. This structure revealed that LY2119620 binds to the vestibule just above the orthosteric agonist iperoxo. Moreover, it suggested that the allosteric modulator induces structural changes such as the inward motion of TM6, which directly contacts the allosteric modulator, the orthosteric agonist, and probably, the G protein as well[110]. The MR crystal structures offer important insights into the activation mechanism and allosteric modulation of MRs, and are supposed to contribute to the development of highly selective MR ligands.

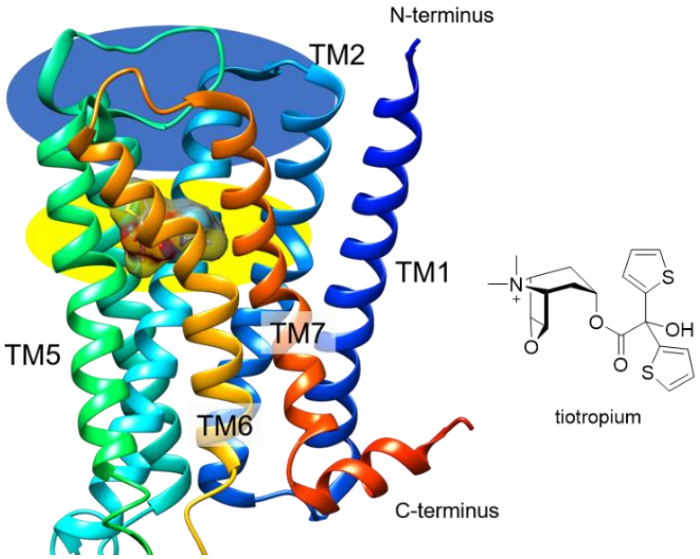

Figure 13. Muscarinic M_3 receptor (PDB code 4U14[108]) bound with tiotropium at the orthosteric pocket. The orthosteric and allosteric sites are indicated in yellow and blue elliptical shaded areas, respectively. Image was generated by UCSF Chimera[111]. (adopted and modified from the literature[108])

1.3. Bivalent ligands

Much of the pioneering work describing bivalent ligands for GPCRs was led by the group of Portoghese[112-115], targeting opioid receptor subtypes. Bivalent ligands are defined as compounds containing two pharmacophores, which are covalently tethered by a linker. Bivalent ligands are divided into two general classes: homobivalent ligands, containing two

identical pharmacophores, and heterobivalent ligands, wherein the two pharmacophores are different[113, 116-117]. A number of homo- and heterobivalent GPCR ligands have been developed in recent years, such as histamine receptor[118-119], dopamine receptor[120-123], muscarinic receptor[124-125], adenosine receptor[126-127] and serotonin receptor[128-129] ligands. There are several hypotheses to explain the enhanced activity and selectivity observed for some bivalent GPCR ligands. The first possibility is through a univalently bound state, the unbound recognition unit being in the locus of neighboring binding sites, in another word, the bivalent ligand increased local concentration of free pharmacophore, which increases the probability of a productive binding event (*cf*. Figure 14A). Secondly, the bivalent ligand interacts simultaneously with two orthosteric binding sites of a dimeric or oligomeric complex of GPCRs, leading to increased affinity and selectivity (*cf*. Figure 14B), and thirdly, the bivalent ligand occupies the orthosteric binding site and a second (low affinity) allosteric binding site at one and the same receptor protomer (*cf*. Figure 14C).

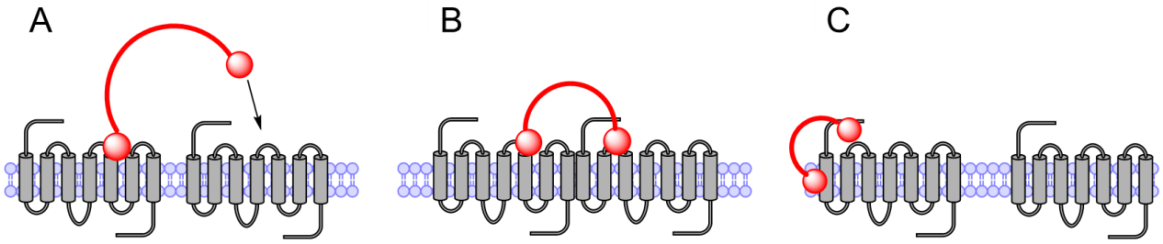

Figure 14. Possible binding modes of bivalent ligands. (A) Increased local concentration of free pharmacophore. (B) Induction of GPCR dimerization. (C) Simultaneous binding to an orthosteric and allosteric binding site of the same receptor molecule (bitopic or dualsteric binding mode). (adopted and modified from the literature[130])

A new concept in drug design derived from bivalent ligand was focusing on bitopic or dualsteric ligands, these ligands can address both the orthosteric and the allosteric site of a receptor protein[131-132]. The reasons to pursue a bitopic ligand approach are various. The most important reason is that a bitopic ligand can theoretically achieve improvements in affinity and selectivity. Another advantage is that the use of pure allosteric modulators relies on the presence of endogenous agonist tone to mediate their effects, whereas the use of a bitopic ligands would engage the orthosteric site irrespective of the presence or absence of endogenous tone[133]. Examples of rationally designed bitopic MR ligands are oxotremorine-related hybrid molecules[134]. These hybrid ligands target the mAChRs, constructed with the agonist oxotremorine (an orthosteric pharmacophore) and hexamethonium derived allosteric modulators (the structure of one of these hybrid ligands will be shown in Chapter 3). Though these hybrid ligands didn't show improved affinity, they gained subtype selectivity as compared with the parent orthosteric agonist (oxoremorine). Mohr and colleagues linked a non-selective, orthosteric agonist iperoxo, with a M_2-selective bis(ammonio)alkane-type allosteric fragment to form hybrid **2** (*cf*. Figure 15). This approach engendered receptor subtype selective

activation compared with the parent agonist[135]. A bitopic ligand was developed for the adenosine A_1 receptor (A_1R) by linking a positive allosteric modulator and an orthosteric pharmacophore through a spacer of 9 carbon atoms. The resulting bivalent ligand LUF6258 (*cf*. Figure 15) did not show significant changes in affinity or potency in the presence of an allosteric enhancer (PD81,723), taken a hint that the bivalent ligand bridges both sites on the receptor[136]. Recently, Christopoulos and colleagues linked the endogenous orthosteric agonist adenosine with a PAM of the A_1 adenosine receptor VCP171, leaded the rational design of a bitopic A_1 adenosine receptor ligand VCP746[137], which displays biased agonism relative to prototypical A_1AR ligands (*cf*. Figure 15). More examples of bitopic ligands such as THRX-160209 will be shown in Chapter 3.

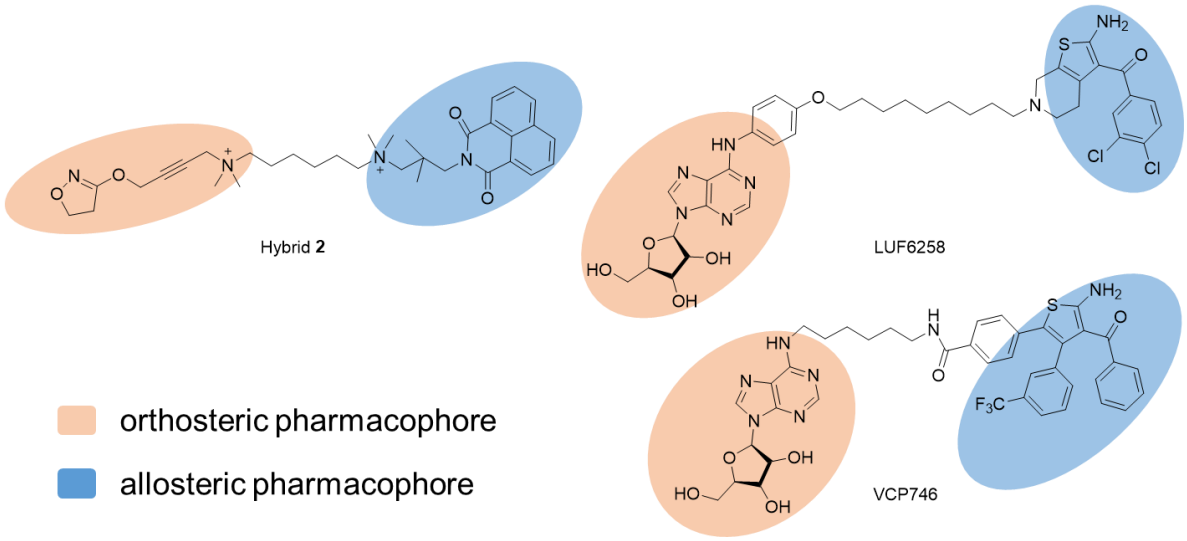

Figure 15. Examples of bitopic GPCR ligands. The non-selective, orthosteric, agonist iperoxo and a M_2 selective bis(ammonio)alkane-type allosteric fragment were linked to form hybrid **2**; Bitopic ligands LUF6258 and VCP746 target the adenosine A_1 receptor.

1.4. Radioligands for muscarinic receptor

Several radioligands were developed as pharmacological tools for studying the receptor binding of MR ligands. For instance, the orthosteric antagonists [^{3}H]QNB[138], [^{3}H]N-methyl scopolamine[91, 139], [^{3}H]pirenzepine[140] and [^{3}H]tiotropium[141], the orthosteric agonists [^{3}H]acetylcholine[142] and [^{3}H]oxotremorine-M[143] have been used as radioligands. Moreover, [^{3}H]NMS has been frequently used to identify allosteric interactions of agents[144-145], and to check the common allosteric site hypothesis for the allosteric modulators alcuronium, W84, and gallamine[146]. One important approach was the development of [^{3}H]dimethyl-W84, the first radiolabeled allosteric modulator of the M_2 mAChR[147]. Table 1 shows the pK_d values of the muscarinic receptor radioligands mentioned above.

Table 1. Reported pK_d values of radioligands binding to muscarinic mAChRs.

Radioligands	pK_d M_1R	pK_d M_2R	pK_d M_3R	pK_d M_4R	pK_d M_5R
[^{3}H]QNB[a]	10.6 - 10.8	10.1 - 10.6	10.4	9.7 - 10.5	10.2 - 10.7
[^{3}H]NMS[a]	9.4 - 10.3	9.3 - 9.9	9.7 - 10.2	9.9 - 10.2	9.3 - 9.7
[^{3}H]pirenzepine[a]	7.9	-	-	-	-
[^{3}H]tiotropium[a]	-	10.3	10.7	-	-
[^{3}H]oxotremorine-M[a]	-	8.7	-	-	-
[^{3}H]acetylcholine[a]	-	8.8	-	8.2	-
[^{3}H]dimethyl-W84[a]		8.5			

[a]pK_d values reported in the literature (data taken from the IUPHAR/BPS database (guidetopharmacology.org) in Nov. 2016).

1.5. Fluorescently labeled GPCR ligands

The major disadvantages of radiolabeled ligands are that they are potentially hazardous to human health, high costs of production and waste disposal and the requirement of special laboratory conditions. Besides label-free ligand binding assays such as affinity selection mass spectrometry (AS-MS)[148] and nuclear magnetic resonance spectroscopy (NMR)-based binding assays[149], fluorescent ligand-based receptor binding assays were developed for several peptide and non-peptide GPCRs as an alternative to radioligand binding assays.

Like radioligands, fluorescent ligands can be used to determine the affinity of unlabeled receptor ligands[150]. Moreover, fluorescent ligands have been used for the screening of small molecules (fragments) in terms of GPCR binding. For instance, one fluorescent ligand was used in a fluorescence resonance energy transfer (FRET)-based assay to identify the first small molecule agonist for the apelin receptor, which may lead to new molecules being developed for the treatment of heart failure[151]. New non-peptide small molecule ligands for the formylpeptide receptor were identified from a library of 880 compounds by using a fluorescein labelled formylmethionine-leucine-phenylalanine-lysine based on high-throughput flow cytometry (HTFC)[152]. In addition, fluorescent ligands can be used to study receptor expression patterns, GPCR localization and internalization as demonstrated for the μ and δ opioid receptor[153] and AT_1 angiotensin receptor[154], as well as ligand-receptor binding kinetics in living cells as demonstrated for the adenosine-A_1 and -A_3 receptor[155-156]. Fluorescent ligands can also be used to investigate the dynamics of GPCR oligomerization in living cells[157-158].

Several fluorescent ligands were also developed as useful pharmacological tools for studying muscarinic receptors. For example, Cu(I)-catalyzed 1,3-dipolar cycloaddition, referred to as

"click" chemistry, was used to incorporate of a fluorophore (Lissamine Rhodamine B) into a MR antagonist scaffold derived from pirenzepine[159]. The high affinity and very slow off-rates of the telenzepine analogs Cy3B-telenzepine (K_d = 35 pM, M_1R) and Alexa488-telenz (K_d = 0.5 nM, M_1R) were applied to investigate the dynamics of M_1 receptor dimerization in living cells[158]. BODIPY-pirenzepine was used to study pirenzepine-induced formation of muscarinic M_1R dimers[160]. A fluorescent tolterodine-BODIPY (boron dipyrromethene) conjugate was described to exhibit affinity for M_1, M_2 and M_4 receptors in the nanomolar range, harboring the potential to be used for high throughput screening. However, a slow degradation of this compound was observed even when stored in the dark ($t_{1/2}$ = 10 weeks)[161]. Ilien and co-workers prepared pirenzepine derivatives linked to the boron-dipyrromethene [Bodipy (558/568)] fluorophore via spacers of varying lengths[162-163] and coupled the lissamine rhodamine B fluorophore (in para position) to AC42 to study bitopic fluorescent ligands[164].

1.6. References

1. Fredriksson, R.; Schiöth, H. B., The repertoire of G-protein-coupled receptors in fully sequenced genomes. *Mol. Pharmacol.* **2005,** *67* (5), 1414-1425.
2. Hanlon, C. D.; Andrew, D. J., Outside-in signaling-a brief review of GPCR signaling with a focus on the Drosophila GPCR family. *J. Cell Sci.* **2015,** *128* (19), 3533-3542.
3. Kristiansen, K., Molecular mechanisms of ligand binding, signaling, and regulation within the superfamily of G-protein-coupled receptors: molecular modeling and mutagenesis approaches to receptor structure and function. *Pharmacol. Ther.* **2004,** *103* (1), 21-80.
4. Tang, X.-l.; Wang, Y.; Li, D.-l.; Luo, J.; Liu, M.-y., Orphan G protein-coupled receptors (GPCRs): biological functions and potential drug targets. *Acta Pharmacol. Sin.* **2012,** *33* (3), 363-371.
5. Wise, A.; Gearing, K.; Rees, S., Target validation of G-protein coupled receptors. *Drug Discovery Today* **2002,** *7* (4), 235-246.
6. Heilker, R.; Wolff, M.; Tautermann, C. S.; Bieler, M., G-protein-coupled receptor-focused drug discovery using a target class platform approach. *Drug Discovery Today* **2009,** *14* (5), 231-240.
7. Jacoby, E.; Bouhelal, R.; Gerspacher, M.; Seuwen, K., The 7 TM G-protein-coupled receptor target family. *ChemMedChem* **2006,** *1* (8), 760-782.
8. Bridges, T. M.; Lindsley, C. W., G-protein-coupled receptors: from classical modes of modulation to allosteric mechanisms. *ACS Chem. Biol.* **2008,** *3* (9), 530-541.
9. Palczewski, K.; Kumasaka, T.; Hori, T.; Behnke, C. A.; Motoshima, H.; Fox, B. A.; Le Trong, I.; Teller, D. C.; Okada, T.; Stenkamp, R. E., Crystal structure of rhodopsin: AG protein-coupled receptor. *Science* **2000,** *289* (5480), 739-745.
10. Rasmussen, S. G.; Choi, H.-J.; Rosenbaum, D. M.; Kobilka, T. S.; Thian, F. S.; Edwards, P. C.; Burghammer, M.; Ratnala, V. R.; Sanishvili, R.; Fischetti, R. F., Crystal structure of the human &bgr; 2 adrenergic G-protein-coupled receptor. *Nature* **2007,** *450* (7168), 383-387.
11. Cherezov, V.; Rosenbaum, D. M.; Hanson, M. A.; Rasmussen, S. G.; Thian, F. S.; Kobilka, T. S.; Choi, H.-J.; Kuhn, P.; Weis, W. I.; Kobilka, B. K., High-resolution crystal structure of an engineered human β_2-adrenergic G protein-coupled receptor. *Science* **2007,** *318* (5854), 1258-1265.

12. Warne, T.; Serrano-Vega, M. J.; Baker, J. G.; Moukhametzianov, R.; Edwards, P. C.; Henderson, R.; Leslie, A. G.; Tate, C. G.; Schertler, G. F., Structure of a &bgr; 1-adrenergic G-protein-coupled receptor. *Nature* **2008,** *454* (7203), 486-491.
13. Jaakola, V.-P.; Griffith, M. T.; Hanson, M. A.; Cherezov, V.; Chien, E. Y.; Lane, J. R.; Ijzerman, A. P.; Stevens, R. C., The 2.6 angstrom crystal structure of a human A_2A adenosine receptor bound to an antagonist. *Science* **2008,** *322* (5905), 1211-1217.
14. Chien, E. Y.; Liu, W.; Zhao, Q.; Katritch, V.; Han, G. W.; Hanson, M. A.; Shi, L.; Newman, A. H.; Javitch, J. A.; Cherezov, V., Structure of the human dopamine D_3 receptor in complex with a D_2/D_3 selective antagonist. *Science* **2010,** *330* (6007), 1091-1095.
15. Scheerer, P.; Park, J. H.; Hildebrand, P. W.; Kim, Y. J.; Krauß, N.; Choe, H.-W.; Hofmann, K. P.; Ernst, O. P., Crystal structure of opsin in its G-protein-interacting conformation. *Nature* **2008,** *455* (7212), 497-502.
16. Park, J. H.; Scheerer, P.; Hofmann, K. P.; Choe, H.-W.; Ernst, O. P., Crystal structure of the ligand-free G-protein-coupled receptor opsin. *Nature* **2008,** *454* (7201), 183-187.
17. Wu, B.; Chien, E. Y.; Mol, C. D.; Fenalti, G.; Liu, W.; Katritch, V.; Abagyan, R.; Brooun, A.; Wells, P.; Bi, F. C., Structures of the CXCR4 chemokine GPCR with small-molecule and cyclic peptide antagonists. *Science* **2010,** *330* (6007), 1066-1071.
18. De Lean, A.; Stadel, J.; Lefkowitz, R., A ternary complex model explains the agonist-specific binding properties of the adenylate cyclase-coupled beta-adrenergic receptor. *J. Biol. Chem.* **1980,** *255* (15), 7108-7117.
19. Kenakin, T. P., A pharmacology primer. Academic Press: 2014.
20. Samama, P.; Cotecchia, S.; Costa, T.; Lefkowitz, R., A mutation-induced activated state of the beta 2-adrenergic receptor. Extending the ternary complex model. *J. Biol. Chem.* **1993,** *268* (7), 4625-4636.
21. Weiss, J. M.; Morgan, P. H.; Lutz, M. W.; Kenakin, T. P., The Cubic Ternary Complex Receptor-Occupancy Model I. Model Description. *J. Theor. Biol.* **1996,** *178* (2), 151-167.
22. Weiss, J. M.; Morgan, P. H.; Lutz, M. W.; Kenakin, T. P., The cubic ternary complex receptor-occupancy model II. Understanding apparent affinity. *J. Theor. Biol.* **1996,** *178* (2), 169-182.
23. Weiss, J. M.; Morgan, P. H.; Lutz, M. W.; Kenakin, T. P., The cubic ternary complex receptor-occupancy model III. Resurrecting efficacy. *J. Theor. Biol.* **1996,** *181* (4), 381-397.
24. Cabrera-Vera, T. M.; Vanhauwe, J.; Thomas, T. O.; Medkova, M.; Preininger, A.; Mazzoni, M. R.; Hamm, H. E., Insights into G protein structure, function, and regulation. *Endocr. Rev.* **2003,** *24* (6), 765-781.
25. Pierce, K. L.; Premont, R. T.; Lefkowitz, R. J., Seven-transmembrane receptors. *Nat. Rev. Mol. Cell Biol.* **2002,** *3* (9), 639-650.
26. Wong, S.-F., G protein selectivity is regulated by multiple intracellular regions of GPCRs. *Neurosignals* **2003,** *12* (1), 1-12.
27. Luttrell, L. M., Reviews in molecular biology and biotechnology: transmembrane signaling by G protein-coupled receptors. *Mol. Biotechnol.* **2008,** *39* (3), 239-264.
28. Johnston, C. A.; Siderovski, D. P., Receptor-mediated activation of heterotrimeric G-proteins: current structural insights. *Mol. Pharmacol.* **2007,** *72* (2), 219-230.
29. Offermanns, S., G-proteins as transducers in transmembrane signalling. *Prog. Biophys. Mol. Biol.* **2003,** *83* (2), 101-130.
30. Simon, M. I.; Strathmann, M. P.; Gautam, N., Diversity of G proteins in signal transduction. *Science* **1991,** *252* (5007), 802-808.
31. Marinissen, M. J.; Gutkind, J. S., G-protein-coupled receptors and signaling networks: emerging paradigms. *Trends Pharmacol. Sci.* **2001,** *22* (7), 368-376.
32. Mikoshiba, K., IP_3 receptor/Ca^{2+} channel: from discovery to new signaling concepts. *J. Neurochem.* **2007,** *102* (5), 1426-1446.
33. Hooley, R.; Yu, C.-Y.; Symons, M.; Barber, D. L., G_{13} stimulates Na-H exchange through distinct Cdc42-dependent and RhoA-dependent pathways. *J. Biol. Chem.* **1996,** *271* (11), 6152-6158.

34. Dhanasekaran, N.; Dermott, J. M., Signaling by the G_{12} class of G proteins. *Cell. Signalling* **1996,** *8* (4), 235-245.
35. Gainetdinov, R. R.; Premont, R. T.; Bohn, L. M.; Lefkowitz, R. J.; Caron, M. G., Desensitization of G protein-coupled receptors and neuronal functions. *Annu. Rev. Neurosci.* **2004,** *27*, 107-144.
36. Premont, R. T.; Gainetdinov, R. R., Physiological roles of G protein-coupled receptor kinases and arrestins. *Annu. Rev. Physiol.* **2007,** *69*, 511-534.
37. Violin, J. D.; DiPilato, L. M.; Yildirim, N.; Elston, T. C.; Zhang, J.; Lefkowitz, R. J., β_2-adrenergic receptor signaling and desensitization elucidated by quantitative modeling of real time cAMP dynamics. *J. Biol. Chem.* **2008,** *283* (5), 2949-2961.
38. Moore, C. A.; Milano, S. K.; Benovic, J. L., Regulation of receptor trafficking by GRKs and arrestins. *Annu. Rev. Physiol.* **2007,** *69*, 451-482.
39. Greenlee, W.; Clader, J.; Asberom, T.; McCombie, S.; Ford, J.; Guzik, H.; Kozlowski, J.; Li, S.; Liu, C.; Lowe, D., Muscarinic agonists and antagonists in the treatment of Alzheimer's disease. *Il Farmaco* **2001,** *56* (4), 247-250.
40. Christopoulos, A., Allosteric binding sites on cell-surface receptors: novel targets for drug discovery. *Nat. Rev. Drug Discovery* **2002,** *1* (3), 198-210.
41. Christopoulos, A.; Kenakin, T., G protein-coupled receptor allosterism and complexing. *Pharmacol. Rev.* **2002,** *54* (2), 323-374.
42. May, L. T.; Leach, K.; Sexton, P. M.; Christopoulos, A., Allosteric modulation of G protein-coupled receptors. *Annu. Rev. Pharmacol. Toxicol.* **2007,** *47*, 1-51.
43. Holzgrabe, U.; Mohr, K., Allosteric modulators of ligand binding to muscarinic acetylcholine receptors. *Drug Discovery Today* **1998,** *3* (5), 214-222.
44. Valant, C.; Robert Lane, J.; Sexton, P. M.; Christopoulos, A., The best of both worlds? Bitopic orthosteric/allosteric ligands of g protein-coupled receptors. *Annu. Rev. Pharmacol. Toxicol.* **2012,** *52*, 153-178.
45. Gregory, K. J.; Sexton, P. M.; Christopoulos, A., Allosteric modulation of muscarinic acetylcholine receptors. *Curr. Neuropharmacol.* **2007,** *5* (3), 157-167.
46. Leach, K.; Loiacono, R. E.; Felder, C. C.; McKinzie, D. L.; Mogg, A.; Shaw, D. B.; Sexton, P. M.; Christopoulos, A., Molecular mechanisms of action and in vivo validation of an M_4 muscarinic acetylcholine receptor allosteric modulator with potential antipsychotic properties. *Neuropsychopharmacology* **2010,** *35* (4), 855-869.
47. Mathiesen, J. M.; Ulven, T.; Martini, L.; Gerlach, L. O.; Heinemann, A.; Kostenis, E., Identification of indole derivatives exclusively interfering with a G protein-independent signaling pathway of the prostaglandin D_2 receptor CRTH2. *Mol. Pharmacol.* **2005,** *68* (2), 393-402.
48. Stewart, G. D.; Sexton, P. M.; Christopoulos, A., Prediction of functionally selective allosteric interactions at an M_3 muscarinic acetylcholine receptor mutant using Saccharomyces cerevisiae. *Mol. Pharmacol.* **2010,** *78* (2), 205-214.
49. Ehlert, F., Estimation of the affinities of allosteric ligands using radioligand binding and pharmacological null methods. *Mol. Pharmacol.* **1988,** *33* (2), 187-194.
50. Stockton, J.; Birdsall, N.; Burgen, A.; Hulme, E., Modification of the binding properties of muscarinic receptors by gallamine. *Mol. Pharmacol.* **1983,** *23* (3), 551-557.
51. Broadley, K. J.; Kelly, D. R., Muscarinic receptor agonists and antagonists. *Molecules* **2001,** *6* (3), 142-193.
52. Levey, A.; Edmunds, S.; Koliatsos, V.; Wiley, R.; Heilman, C., Expression of M_1-M_4 muscarinic acetylcholine receptor proteins in rat hippocampus and regulation by cholinergic innervation. *The Journal of neuroscience* **1995,** *15* (5), 4077-4092.
53. Levey, A.; Kitt, C.; Simonds, W.; Price, D.; Brann, M., Identification and localization of muscarinic acetylcholine receptor proteins in brain with subtype-specific antibodies. *The Journal of Neuroscience* **1991,** *11* (10), 3218-3226.
54. Miyakawa, T.; Yamada, M.; Duttaroy, A.; Wess, J., Hyperactivity and intact hippocampus-dependent learning in mice lacking the M_1 muscarinic acetylcholine receptor. *The Journal of Neuroscience* **2001,** *21* (14), 5239-5250.
55. Oki, T.; Takagi, Y.; Inagaki, S.; Taketo, M. M.; Manabe, T.; Matsui, M.; Yamada, S.,

Quantitative analysis of binding parameters of [^{3}H] N-methylscopolamine in central nervous system of muscarinic acetylcholine receptor knockout mice. *Mol. Brain Res.* **2005,** *133* (1), 6-11.

56. Iversen, S. D., Behavioural evaluation of cholinergic drugs. *Life Sci.* **1997,** *60* (13), 1145-1152.
57. Fisher, A.; Heldman, E.; Gurwitz, D.; Haring, R.; Karton, Y.; Meshulam, H.; Pittel, Z.; Marciano, D.; Brandeis, R.; Sadot, E., M_1 Agonists for the Treatment of Alzheimer's Disease. *Ann. N.Y. Acad. Sci.* **1996,** *777* (1), 189-196.
58. Flynn, D.; Mash, D. C., Multiple in vitro interactions with and differential in vivo regulation of muscarinic receptor subtypes by tetrahydroaminoacridine. *J. Pharmacol. Exp. Ther.* **1989,** *250* (2), 573-581.
59. Cummings, J. L., Cholinesterase inhibitors: a new class of psychotropic compounds. *Am. J. Psychiatry.* **2000**.
60. Wang, Y.; Chackalamannil, S.; Hu, Z.; Greenlee, W. J.; Clader, J.; Boyle, C. D.; Kaminski, J. J.; Billard, W.; Binch III, H.; Crosby, G., Improving the oral efficacy of CNS drug candidates: discovery of highly orally efficacious piperidinyl piperidine M_2 muscarinic receptor antagonists. *J. Med. Chem.* **2002,** *45* (25), 5415-5418.
61. Kozlowski, J. A.; Zhou, G.; Tagat, J. R.; Lin, S.-I.; McCombie, S. W.; Ruperto, V. B.; Duffy, R. A.; McQuade, R. A.; Crosby, G.; Taylor, L. A., Substituted 2-(R)-methyl piperazines as muscarinic M_2 selective ligands. *Bioorg. Med. Chem. Lett.* **2002,** *12* (5), 791-794.
62. Sheardown, M. J., Muscarinic M_1 receptor agonists and M_2 receptor antagonists as therapeutic targets in Alzheimer's disease. *Expert Opin. Ther. Pat.* **2002,** *12* (6), 863-870.
63. Leaf, R. C.; Muller, S. A., Effects of scopolamine on operant avoidance acquisition and retention. *Psychopharmacologia* **1966,** *9* (2), 101-109.
64. Hulme, E.; Birdsall, N.; Buckley, N., Muscarinic receptor subtypes. *Annu. Rev. Pharmacol. Toxicol.* **1990,** *30* (1), 633-673.
65. Caulfield, M. P., Muscarinic receptors-characterization, coupling and function. *Pharmacol. Ther.* **1993,** *58* (3), 319-379.
66. Eglen, R. M.; Hegde, S. S.; Watson, N., Muscarinic receptor subtypes and smooth muscle function. *Pharmacol. Rev.* **1996,** *48* (4), 531-565.
67. Buckley, N. J.; Bonner, T.; Brann, M., Localization of a family of muscarinic receptor mRNAs in rat brain. *The Journal of neuroscience* **1988,** *8* (12), 4646-4652.
68. Gautam, D.; Gavrilova, O.; Jeon, J.; Pack, S.; Jou, W.; Cui, Y.; Li, J. H.; Wess, J., Beneficial metabolic effects of M_3 muscarinic acetylcholine receptor deficiency. *Cell Metab.* **2006,** *4* (5), 363-375.
69. Gautam, D.; Jeon, J.; Starost, M. F.; Han, S.-J.; Hamdan, F. F.; Cui, Y.; Parlow, A. F.; Gavrilova, O.; Szalayova, I.; Mezey, E., Neuronal M_3 muscarinic acetylcholine receptors are essential for somatotroph proliferation and normal somatic growth. *Proc. Natl. Acad. Sci. USA* **2009,** *106* (15), 6398-6403.
70. Ikeda, K.; Kobayashi, S.; Suzuki, M.; Miyata, K.; Takeuchi, M.; Yamada, T.; Honda, K., M_3 receptor antagonism by the novel antimuscarinic agent solifenacin in the urinary bladder and salivary gland. *Naunyn-Schmiedeberg's Arch. Pharmacol.* **2002,** *366* (2), 97-103.
71. Betz, A. J.; McLaughlin, P. J.; Burgos, M.; Weber, S. M.; Salamone, J. D., The muscarinic receptor antagonist tropicamide suppresses tremulous jaw movements in a rodent model of parkinsonian tremor: possible role of M_4 receptors. *Psychopharmacology* **2007,** *194* (3), 347-359.
72. Wall, S. J.; Yasuda, R. P.; Li, M.; Ciesla, W.; Wolfe, B. B., The ontogeny of M_1-M_5 muscarinic receptor subtypes in rat forebrain. *Dev. Brain Res.* **1992,** *66* (2), 181-185.
73. Weiner, D. M.; Levey, A. I.; Brann, M. R., Expression of muscarinic acetylcholine and dopamine receptor mRNAs in rat basal ganglia. *Proc. Natl. Acad. Sci. USA* **1990,** *87* (18), 7050-7054.
74. Wess, J.; Lambrecht, G.; Mutschler, E.; Brann, M.; Dörje, F., Selectivity profile of the

novel muscarinic antagonist UH-AH 37 determined by the use of cloned receptors and isolated tissue preparations. *Br. J. Pharmacol.* **1991,** *102* (1), 246-250.
75. Maggio, R.; Barbier, P.; Bolognesi, M. L.; Minarini, A.; Tedeschi, D.; Melchiorre, C., Binding profile of the selective muscarinic receptor antagonist tripitramine. *Eur. J. Pharmacol., Mol. Pharmacol. Sect.* **1994,** *268* (3), 459-462.
76. Dörje, F.; Wess, J.; Lambrecht, G.; Tacke, R.; Mutschler, E.; Brann, M., Antagonist binding profiles of five cloned human muscarinic receptor subtypes. *J. Pharmacol. Exp. Ther.* **1991,** *256* (2), 727-733.
77. Buckley, N. J.; Bonner, T. I.; Buckley, C. M.; Brann, M. R., Antagonist binding properties of five cloned muscarinic receptors expressed in CHO-K1 cells. *Mol. Pharmacol.* **1989,** *35* (4), 469-476.
78. Gillberg, P.-G.; Sundquist, S.; Nilvebrant, L., Comparison of the in vitro and in vivo profiles of tolterodine with those of subtype-selective muscarinic receptor antagonists. *Eur. J. Pharmacol.* **1998,** *349* (2), 285-292.
79. Böhme, T. M.; Augelli-Szafran, C. E.; Hallak, H.; Pugsley, T.; Serpa, K.; Schwarz, R. D., Synthesis and pharmacology of benzoxazines as highly selective antagonists at M_4 muscarinic receptors. *J. Med. Chem.* **2002,** *45* (14), 3094-3102.
80. Shekhar, A.; Potter, W. Z.; Lightfoot, J.; Lienemann D Pharm, J.; Dubé, S.; Mallinckrodt, C.; Bymaster, F. P.; McKinzie, D. L.; Felder, C. C., Selective muscarinic receptor agonist xanomeline as a novel treatment approach for schizophrenia. *Am. J. Psychiatry.* **2008,** *165* (8), 1033-1039.
81. Shekhar, A.; Potter, W. Z.; Lightfoot, J.; Lienemann, J.; Pharm, D.; Dubé, S.; Mallinckrodt, C.; Bymaster, F. P.; McKinzie, D. L.; Felder, C. C., Selective muscarinic receptor agonist xanomeline as a novel treatment approach for schizophrenia. *Am. J. Psychiatry.* **2008**.
82. Bodick, N. C.; Offen, W. W.; Levey, A. I.; Cutler, N. R.; Gauthier, S. G.; Satlin, A.; Shannon, H. E.; Tollefson, G. D.; Rasmussen, K.; Bymaster, F. P., Effects of xanomeline, a selective muscarinic receptor agonist, on cognitive function and behavioral symptoms in Alzheimer disease. *Arch. Neurol.* **1997,** *54* (4), 465-473.
83. Christopoulos, A.; Pierce, T. L.; Sorman, J. L.; El-Fakahany, E. E., On the unique binding and activating properties of xanomeline at the M_1 muscarinic acetylcholine receptor. *Mol. Pharmacol.* **1998,** *53* (6), 1120-1130.
84. Kane, B. E.; Grant, M. K.; El-Fakahany, E. E.; Ferguson, D. M., Synthesis and evaluation of xanomeline analogs-Probing the wash-resistant phenomenon at the M_1 muscarinic acetylcholine receptor. *Bioorg. Med. Chem.* **2008,** *16* (3), 1376-1392.
85. Jakubík, J.; Tuček, S.; El-Fakahany, E. E., Role of receptor protein and membrane lipids in xanomeline wash-resistant binding to muscarinic M_1 receptors. *J. Pharmacol. Exp. Ther.* **2004,** *308* (1), 105-110.
86. Sauerberg, P.; Jeppesen, L.; Olesen, P. H.; Sheardown, M. J.; Fink-Jensen, A.; Rasmussen, T.; Rimvall, K.; Shannon, H. E.; Bymaster, F. P.; DeLapp, N. W., Identification of side chains on 1, 2, 5-thiadiazole-azacycles optimal for muscarinic M_1 receptor activation. *Bioorg. Med. Chem. Lett.* **1998,** *8* (20), 2897-2902.
87. Ensinger, H.; Doods, H.; Immel-Sehr, A.; Kuhn, F.; Lambrecht, G.; Mendla, K.; Müller, R.; Mutschler, E.; Sagrada, A.; Walther, G., WAL 2014-a muscarinic agonist with preferential neuron-stimulating properties. *Life Sci.* **1993,** *52* (5-6), 473-480.
88. Walland, A.; Pieper, M., Central activation of the sympathetic nervous system including the adrenals in anaesthetized guinea pigs by the muscarinic agonist talsaclidine. *Naunyn-Schmiedeberg's Arch. Pharmacol.* **1998,** *357* (4), 426-430.
89. Bromidge, S. M.; Brown, F.; Cassidy, F.; Clark, M. S.; Dabbs, S.; Hadley, M. S.; Hawkins, J.; Loudon, J. M.; Naylor, C. B.; Orlek, B. S., Design of [R-(Z)]-(+)-α-(methoxyimino)-1-azabicyclo [2.2. 2] octane-3-acetonitrile (SB 202026), a functionally selective azabicyclic muscarinic M_1 agonist incorporating the N-methoxy imidoyl nitrile group as a novel ester Bioisostere. *J. Med. Chem.* **1997,** *40* (26), 4265-4280.
90. TSUKAMOTO, S.-i.; FUJII, M.; YASUNAGA, T.; MATSUDA, K., Synthesis and Structure-Activity Studies of a Series of 1-Oxa-8-azaspiro [4.5] decanes as M_1

Muscarinic Agonists. *Chem. Pharm. Bull.* **1995,** *43* (5), 842-852.
91. Jakubík, J.; Bačáková, L.; El-Fakahany, E. E.; Tuček, S., Positive cooperativity of acetylcholine and other agonists with allosteric ligands on muscarinic acetylcholine receptors. *Mol. Pharmacol.* **1997,** *52* (1), 172-179.
92. Conti, P.; Dallanoce, C.; De Amici, M.; De Micheli, C.; Ebert, B., Synthesis and binding affinity of new muscarinic ligands structurally related to oxotremorine. *Bioorg. Med. Chem. Lett.* **1997,** *7* (8), 1033-1036.
93. Ellis, J.; Huyler, J.; Brann, M. R., Allosteric regulation of cloned M_1- M_5 muscarinic receptor subtypes. *Biochem. Pharmacol.* **1991,** *42* (10), 1927-1932.
94. Lazareno, S.; Gharagozloo, P.; Kuonen, D.; Popham, A.; Birdsall, N., Subtype-selective positive cooperative interactions between brucine analogues and acetylcholine at muscarinic receptors: radioligand binding studies. *Mol. Pharmacol.* **1998,** *53* (3), 573-589.
95. Lüllmann, H.; Ohnesorge, F.; Schauwecker, G.-C.; Wassermann, O., Inhibition of the actions of carbachol and DFP on guinea pig isolated atria by alkane-bis-ammonium compounds. *Eur. J. Pharmacol.* **1969,** *6* (3), 241-247.
96. Clark, A.; Mitchelson, F., The inhibitory effect of gallamine on muscarinic receptors. *Br. J. Pharmacol.* **1976,** *58* (3), 323-331.
97. Jakubik, J.; Bacáková, L.; El-Fakahany, E. E.; Tucek, S., Subtype selectivity of the positive allosteric action of alcuronium at cloned M_1-M_5 muscarinic acetylcholine receptors. *J. Pharmacol. Exp. Ther.* **1995,** *274* (3), 1077-1083.
98. Lanzafame, A. A.; Sexton, P. M.; Christopoulos, A., Interaction studies of multiple binding sites on M_4 muscarinic acetylcholine receptors. *Mol. Pharmacol.* **2006,** *70* (2), 736-746.
99. Proška, J.; Tuček, S., Positive allosteric action of eburnamonine on cardiac muscarinic acetylcholine receptors. *Eur. J. Pharmacol.* **1996,** *305* (1), 201-205.
100. Lazareno, S.; Popham, A.; Birdsall, N. J., Allosteric Interactions of Staurosporine and Other Indolocarbazoles with N-[methyl-^{3}H] Scopolamine and Acetylcholine at Muscarinic Receptor Subtypes: Identification of a Second Allosteric Site. *Mol. Pharmacol.* **2000,** *58* (1), 194-207.
101. Roszkowski, A. P., An unusual type of sympathetic ganglionic stimulant. *J. Pharmacol. Exp. Ther.* **1961,** *132* (2), 156-170.
102. Birdsall, N.; Burgen, A.; Hulme, E.; Stockton, J.; Zigmond, M., The effect of McN-A-343 on muscarinic receptors in the cerebral cortex and heart. *Br. J. Pharmacol.* **1983,** *78* (2), 257-259.
103. Langmead, C.; Austin, N.; Branch, C.; Brown, J.; Buchanan, K.; Davies, C.; Forbes, I.; Fry, V.; Hagan, J.; Herdon, H., Characterization of a CNS penetrant, selective M_1 muscarinic receptor agonist, 77-LH-28-1. *Br. J. Pharmacol.* **2008,** *154* (5), 1104-1115.
104. Jones, C. K.; Brady, A. E.; Davis, A. A.; Xiang, Z.; Bubser, M.; Tantawy, M. N.; Kane, A. S.; Bridges, T. M.; Kennedy, J. P.; Bradley, S. R., Novel selective allosteric activator of the M_1 muscarinic acetylcholine receptor regulates amyloid processing and produces antipsychotic-like activity in rats. *The Journal of Neuroscience* **2008,** *28* (41), 10422-10433.
105. Conn, P. J.; Jones, C. K.; Lindsley, C. W., Subtype-selective allosteric modulators of muscarinic receptors for the treatment of CNS disorders. *Trends Pharmacol. Sci.* **2009,** *30* (3), 148-155.
106. Sur, C.; Mallorga, P. J.; Wittmann, M.; Jacobson, M. A.; Pascarella, D.; Williams, J. B.; Brandish, P. E.; Pettibone, D. J.; Scolnick, E. M.; Conn, P. J., *N*-desmethylclozapine, an allosteric agonist at muscarinic 1 receptor, potentiates *N*-methyl-D-aspartate receptor activity. *Proc. Natl. Acad. Sci. USA* **2003,** *100* (23), 13674-13679.
107. Haga, K.; Kruse, A. C.; Asada, H.; Yurugi-Kobayashi, T.; Shiroishi, M.; Zhang, C.; Weis, W. I.; Okada, T.; Kobilka, B. K.; Haga, T., Structure of the human M_2 muscarinic acetylcholine receptor bound to an antagonist. *Nature* **2012,** *482* (7386), 547-551.
108. Kruse, A. C.; Hu, J.; Pan, A. C.; Arlow, D. H.; Rosenbaum, D. M.; Rosemond, E.; Green, H. F.; Liu, T.; Chae, P. S.; Dror, R. O., Structure and dynamics of the M_3 muscarinic

acetylcholine receptor. *Nature* **2012,** *482* (7386), 552-556.
109. Thal, D. M.; Sun, B.; Feng, D.; Nawaratne, V.; Leach, K.; Felder, C. C.; Bures, M. G.; Evans, D. A.; Weis, W. I.; Bachhawat, P., Crystal structures of the M_1 and M_4 muscarinic acetylcholine receptors. *Nature* **2016,** *531* (7594), 335-340.
110. Kruse, A. C.; Ring, A. M.; Manglik, A.; Hu, J.; Hu, K.; Eitel, K.; Hübner, H.; Pardon, E.; Valant, C.; Sexton, P. M., Activation and allosteric modulation of a muscarinic acetylcholine receptor. *Nature* **2013,** *504* (7478), 101-106.
111. Pettersen, E. F.; Goddard, T. D.; Huang, C. C.; Couch, G. S.; Greenblatt, D. M.; Meng, E. C.; Ferrin, T. E., UCSF Chimera-a visualization system for exploratory research and analysis. *J. Comput. Chem.* **2004,** *25* (13), 1605-1612.
112. Portoghese, P. S., From models to molecules: opioid receptor dimers, bivalent ligands, and selective opioid receptor probes. *J. Med. Chem.* **2001,** *44* (14), 2259-2269.
113. Bhushan, R. G.; Sharma, S. K.; Xie, Z.; Daniels, D. J.; Portoghese, P. S., A Bivalent Ligand (KDN-21) Reveals Spinal δ and κ Opioid Receptors Are Organized as Heterodimers That Give Rise to δ1 and κ 2 Phenotypes. Selective Targeting of δ-κ Heterodimers. *J. Med. Chem.* **2004,** *47* (12), 2969-2972.
114. Daniels, D. J.; Kulkarni, A.; Xie, Z.; Bhushan, R. G.; Portoghese, P. S., A bivalent ligand (KDAN-18) containing δ-antagonist and κ-agonist pharmacophores bridges δ2 and κ1 opioid receptor phenotypes. *J. Med. Chem.* **2005,** *48* (6), 1713-1716.
115. Zhang, S.; Yekkirala, A.; Tang, Y.; Portoghese, P. S., A bivalent ligand (KMN-21) antagonist for μ/κ heterodimeric opioid receptors. *Bioorg. Med. Chem. Lett.* **2009,** *19* (24), 6978-6980.
116. Portoghese, P.; Larson, D.; Sayre, L.; Yim, C.; Ronsisvalle, G.; Tam, S.; Takemori, A., Opioid agonist and antagonist bivalent ligands. The relationship between spacer length and selectivity at multiple opioid receptors. *J. Med. Chem.* **1986,** *29* (10), 1855-1861.
117. Perez, M.; Jorand-Lebrun, C.; Pauwels, P. J.; Pallard, I.; Halazy, S., Dimers of $5HT_1$ ligands preferentially bind to $5HT_{1b1d}$ receptor subtypes. *Bioorg. Med. Chem. Lett.* **1998,** *8* (11), 1407-1412.
118. Birnkammer, T.; Spickenreither, A.; Brunskole, I.; Lopuch, M.; Kagermeier, N.; Bernhardt, G. n.; Dove, S.; Seifert, R.; Elz, S.; Buschauer, A., The bivalent ligand approach leads to highly potent and selective acylguanidine-type histamine H_2 receptor agonists. *J. Med. Chem.* **2012,** *55* (3), 1147-1160.
119. Kagermeier, N.; Werner, K.; Keller, M.; Baumeister, P.; Bernhardt, G.; Seifert, R.; Buschauer, A., Dimeric carbamoylguanidine-type histamine H_2 receptor ligands: A new class of potent and selective agonists. *Bioorg. Med. Chem.* **2015,** *23* (14), 3957-3969.
120. Soriano, A.; Ventura, R.; Molero, A.; Hoen, R.; Casadó, V.; Cortés, A.; Fanelli, F.; Albericio, F.; Lluís, C.; Franco, R., Adenosine A_2A receptor-antagonist/dopamine D_2 receptor-agonist bivalent ligands as pharmacological tools to detect A_2A-D_2 receptor heteromers. *J. Med. Chem* **2009,** *52* (18), 5590-5602.
121. Abadi, A. H.; Lankow, S.; Hoefgen, B.; Decker, M.; Kassack, M. U.; Lehmann, J., Dopamine/Serotonin Receptor Ligands, Part III [1]: Synthesis and Biological Activities of 7, 7'-Alkylene-bis-6, 7, 8, 9, 14, 15-hexahydro-5*H*-benz [*d*] indolo [2, 3-g] azecines-Application of the Bivalent Ligand Approach to a Novel Type of Dopamine Receptor Antagonist. *Arch. Pharm. (Weinheim)* **2002,** *335* (8), 367-373.
122. Huber, D.; Hubner, H.; Gmeiner, P., 1, 1'-Disubstituted ferrocenes as molecular hinges in mono-and bivalent dopamine receptor ligands. *J. Med. Chem.* **2009,** *52* (21), 6860-6870.
123. Kühhorn, J.; Hübner, H.; Gmeiner, P., Bivalent dopamine D_2 receptor ligands: synthesis and binding properties. *J. Med. Chem.* **2011,** *54* (13), 4896-4903.
124. Melchiorre, C.; Angeli, P.; Lambrecht, G.; Mutschler, E.; Picchio, M. T.; Wess, J., Antimuscarinic action of methoctramine, a new cardioselective M_2 muscarinic receptor antagonist, alone and in combination with atropine and gallamine. *Eur. J. Pharmacol.* **1987,** *144* (2), 117-124.
125. Christopoulos, A.; Grant, M. K.; Ayoubzadeh, N.; Kim, O. N.; Sauerberg, P.; Jeppesen, L.; El-Fakahany, E. E., Synthesis and pharmacological evaluation of dimeric

muscarinic acetylcholine receptor agonists. *J. Pharmacol. Exp. Ther.* **2001,** *298* (3), 1260-1268.
126. Karellas, P.; McNaughton, M.; Baker, S. P.; Scammells, P. J., Synthesis of bivalent β_2-adrenergic and adenosine A_1 receptor ligands. *J. Med. Chem.* **2008,** *51* (19), 6128-6137.
127. Jacobson, K. A.; Xie, R.; Young, L.; Chang, L.; Liang, B. T., A novel pharmacological approach to treating cardiac ischemia binary conjugates of A_1 and A_3 adenosine receptor agonists. *J. Biol. Chem.* **2000,** *275* (39), 30272-30279.
128. Halazy, S.; Perez, M.; Fourrier, C.; Pallard, I.; Pauwels, P. J.; Palmier, C.; John, G. W.; Valentin, J.-P.; Bonnafous, R.; Martinez, J., Serotonin dimers: application of the bivalent ligand approach to the design of new potent and selective 5-$HT_{1B/1D}$ agonists. *J. Med. Chem.* **1996,** *39* (25), 4920-4927.
129. Russo, O.; Berthouze, M.; Giner, M.; Soulier, J.-L.; Rivail, L.; Sicsic, S.; Lezoualc'h, F.; Jockers, R.; Berque-Bestel, I., Synthesis of specific bivalent probes that functionally interact with 5-HT_4 receptor dimers. *J. Med. Chem.* **2007,** *50* (18), 4482-4492.
130. Bonger, K. M.; van den Berg, R. J.; Heitman, L. H.; IJzerman, A. P.; Oosterom, J.; Timmers, C. M.; Overkleeft, H. S.; van der Marel, G. A., Synthesis and evaluation of homo-bivalent GnRHR ligands. *Bioorg. Med. Chem.* **2007,** *15* (14), 4841-4856.
131. Mohr, K.; Tränkle, C.; Kostenis, E.; Barocelli, E.; De Amici, M.; Holzgrabe, U., Rational design of dualsteric GPCR ligands: quests and promise. *Br. J. Pharmacol.* **2010,** *159* (5), 997-1008.
132. Valant, C.; Sexton, P. M.; Christopoulos, A., Orthosteric/allosteric bitopic ligands. *Mol. Interventions* **2009,** *9* (3), 125.
133. Lane, J. R.; Sexton, P. M.; Christopoulos, A., Bridging the gap: bitopic ligands of G-protein-coupled receptors. *Trends Pharmacol. Sci.* **2013,** *34* (1), 59-66.
134. Disingrini, T.; Muth, M.; Dallanoce, C.; Barocelli, E.; Bertoni, S.; Kellershohn, K.; Mohr, K.; De Amici, M.; Holzgrabe, U., Design, synthesis, and action of oxotremorine-related hybrid-type allosteric modulators of muscarinic acetylcholine receptors. *J. Med. Chem.* **2006,** *49* (1), 366-372.
135. Antony, J.; Kellershohn, K.; Mohr-Andrä, M.; Kebig, A.; Prilla, S.; Muth, M.; Heller, E.; Disingrini, T.; Dallanoce, C.; Bertoni, S., Dualsteric GPCR targeting: a novel route to binding and signaling pathway selectivity. *The FASEB Journal* **2009,** *23* (2), 442-450.
136. Narlawar, R.; Lane, J. R.; Doddareddy, M.; Lin, J.; Brussee, J.; IJzerman, A. P., Hybrid ortho/allosteric ligands for the adenosine A_1 receptor. *J. Med. Chem.* **2010,** *53* (8), 3028-3037.
137. Valant, C.; May, L. T.; Aurelio, L.; Chuo, C. H.; White, P. J.; Baltos, J.-A.; Sexton, P. M.; Scammells, P. J.; Christopoulos, A., Separation of on-target efficacy from adverse effects through rational design of a bitopic adenosine receptor agonist. *Proc. Natl. Acad. Sci. USA* **2014,** *111* (12), 4614-4619.
138. Peralta, E. G.; Ashkenazi, A.; Winslow, J.; Smith, D.; Ramachandran, J.; Capon, D. J., Distinct primary structures, ligand-binding properties and tissue-specific expression of four human muscarinic acetylcholine receptors. *The EMBO Journal* **1987,** *6* (13), 3923.
139. Sharif, N.; Williams, G.; DeSantis, L., Affinities of muscarinic drugs for [^{3}H] *N*-methylscopolamine (NMS) and [^{3}H] oxotremorine (OXO) binding to a mixture of M_1−M_4 muscarinic receptors: Use of NMS/OXO-M ratios to group compounds into potential agonist, partial agonist, and antagonist classes. *Neurochem. Res.* **1995,** *20* (6), 669-674.
140. Watson, M.; Roeske, W. R.; Johnson, P. C.; Yamamura, H. I., [^{3}H] Pirenzepine identifies putative M_1 muscarinic receptors in human stellate ganglia. *Brain Res.* **1984,** *290* (1), 179-182.
141. Salmon, M.; Luttmann, M. A.; Foley, J. J.; Buckley, P. T.; Schmidt, D. B.; Burman, M.; Webb, E. F.; DeHaas, C. J.; Kotzer, C. J.; Barrett, V. J., Pharmacological characterization of GSK573719 (umeclidinium): a novel, long-acting, inhaled antagonist of the muscarinic cholinergic receptors for treatment of pulmonary diseases. *J. Pharmacol. Exp. Ther.* **2013,** *345* (2), 260-270.

142. Lazareno, S.; Doležal, V.; Popham, A.; Birdsall, N., Thiochrome enhances acetylcholine affinity at muscarinic M_4 receptors: receptor subtype selectivity via cooperativity rather than affinity. *Mol. Pharmacol.* **2004,** *65* (1), 257-266.
143. Berrie, C. P.; Birdsall, N. J.; Hulme, E. C.; Keen, M.; Stockton, J. M., Solubilization and characterization of guanine nucleotide-sensitive muscarinic agonist binding sites from rat myocardium. *Br. J. Pharmacol.* **1984,** *82* (4), 853-861.
144. Tränkle, C.; Kostenis, E.; Burgmer, U.; Mohr, K., Search for lead structures to develop new allosteric modulators of muscarinic receptors. *J. Pharmacol. Exp. Ther.* **1996,** *279* (2), 926-933.
145. Lazareno, S.; Birdsall, N., Detection, quantitation, and verification of allosteric interactions of agents with labeled and unlabeled ligands at G protein-coupled receptors: interactions of strychnine and acetylcholine at muscarinic receptors. *Mol. Pharmacol.* **1995,** *48* (2), 362-378.
146. Tränkle, C.; Mohr, K., Divergent modes of action among cationic allosteric modulators of muscarinic M_2 receptors. *Mol. Pharmacol.* **1997,** *51* (4), 674-682.
147. Tränkle, C.; Mies-Klomfass, E.; Cid, M. H. B.; Holzgrabe, U.; Mohr, K., Identification of a [^{3}H] ligand for the common allosteric site of muscarinic acetylcholine M_2 receptors. *Mol. Pharmacol.* **1998,** *54* (1), 139-145.
148. Jonker, N.; Kool, J.; Irth, H.; Niessen, W. M., Recent developments in protein-ligand affinity mass spectrometry. *Anal. Bioanal. Chem.* **2011,** *399* (8), 2669-2681.
149. Lepre, C. A.; Moore, J. M.; Peng, J. W., Theory and applications of NMR-based screening in pharmaceutical research. *Chem. Rev.* **2004,** *104* (8), 3641-3676.
150. Cottet, M.; Faklaris, O.; Zwier, J. M.; Trinquet, E.; Pin, J.-P.; Durroux, T., Original fluorescent ligand-based assays open new perspectives in G-protein coupled receptor drug screening. *Pharmaceuticals* **2011,** *4* (1), 202-214.
151. Iturrioz, X.; Alvear-Perez, R.; De Mota, N.; Franchet, C.; Guillier, F.; Leroux, V.; Dabire, H.; Le Jouan, M.; Chabane, H.; Gerbier, R., Identification and pharmacological properties of E339-3D6, the first nonpeptidic apelin receptor agonist. *The FASEB Journal* **2010,** *24* (5), 1506-1517.
152. Young, S. M.; Bologa, C.; Prossnitz, E. R.; Oprea, T. I.; Sklar, L. A.; Edwards, B. S., High-throughput screening with HyperCyt® flow cytometry to detect small molecule formylpeptide receptor ligands. *J. Biomol. Screen.* **2005,** *10* (4), 374-382.
153. Arttamangkul, S.; Alvarez-Maubecin, V.; Thomas, G.; Williams, J. T.; Grandy, D. K., Binding and internalization of fluorescent opioid peptide conjugates in living cells. *Mol. Pharmacol.* **2000,** *58* (6), 1570-1580.
154. Hunyady, L.; Baukal, A. J.; Gáborik, Z.; Olivares-Reyes, J. A.; Bor, M.; Szaszák, M.; Lodge, R.; Catt, K. J.; Balla, T., Differential PI 3-kinase dependence of early and late phases of recycling of the internalized AT_1 angiotensin receptor. *J. Cell Biol.* **2002,** *157* (7), 1211-1222.
155. May, L. T.; Self, T. J.; Briddon, S. J.; Hill, S. J., The effect of allosteric modulators on the kinetics of agonist-G protein-coupled receptor interactions in single living cells. *Mol. Pharmacol.* **2010,** *78* (3), 511-523.
156. May, L. T.; Bridge, L. J.; Stoddart, L. A.; Briddon, S. J.; Hill, S. J., Allosteric interactions across native adenosine-A_3 receptor homodimers: quantification using single-cell ligand-binding kinetics. *The FASEB Journal* **2011,** *25* (10), 3465-3476.
157. Maurel, D.; Comps-Agrar, L.; Brock, C.; Rives, M.-L.; Bourrier, E.; Ayoub, M. A.; Bazin, H.; Tinel, N.; Durroux, T.; Prézeau, L., Cell-surface protein-protein interaction analysis with time-resolved FRET and snap-tag technologies: application to GPCR oligomerization. *Nat. Methods* **2008,** *5* (6), 561-567.
158. Hern, J. A.; Baig, A. H.; Mashanov, G. I.; Birdsall, B.; Corrie, J. E.; Lazareno, S.; Molloy, J. E.; Birdsall, N. J., Formation and dissociation of M_1 muscarinic receptor dimers seen by total internal reflection fluorescence imaging of single molecules. *Proc. Natl. Acad. Sci. USA* **2010,** *107* (6), 2693-2698.
159. Bonnet, D.; Ilien, B.; Galzi, J.-L.; Riché, S.; Antheaune, C.; Hibert, M., A rapid and versatile method to label receptor ligands using “click” chemistry: Validation with the

muscarinic M_1 antagonist pirenzepine. *Bioconjugate Chem.* **2006,** *17* (6), 1618-1623.
160. Ilien, B.; Glasser, N.; Clamme, J.-P.; Didier, P.; Piemont, E.; Chinnappan, R.; Daval, S. B.; Galzi, J.-L.; Mely, Y., Pirenzepine promotes the dimerization of muscarinic M_1 receptors through a three-step binding process. *J. Biol. Chem.* **2009,** *284* (29), 19533-19543.
161. Jones, L. H.; Randall, A.; Napier, C.; Trevethick, M.; Sreckovic, S.; Watson, J., Design and synthesis of a fluorescent muscarinic antagonist. *Bioorg. Med. Chem. Lett.* **2008,** *18* (2), 825-827.
162. Daval, S. B.; Kellenberger, E.; Bonnet, D.; Utard, V.; Galzi, J.-L.; Ilien, B., Exploration of the orthosteric/allosteric interface in human M_1 muscarinic receptors by bitopic fluorescent ligands. *Mol. Pharmacol.* **2013,** *84* (1), 71-85.
163. Tahtaoui, C.; Parrot, I.; Klotz, P.; Guillier, F.; Galzi, J.-L.; Hibert, M.; Ilien, B., Fluorescent pirenzepine derivatives as potential bitopic ligands of the human M_1 muscarinic receptor. *J. Med. Chem.* **2004,** *47* (17), 4300-4315.
164. Daval, S. B.; Valant, C. I.; Bonnet, D.; Kellenberger, E.; Hibert, M.; Galzi, J.-L.; Ilien, B., Fluorescent derivatives of AC-42 to probe bitopic orthosteric/allosteric binding mechanisms on muscarinic M_1 receptors. *J. Med. Chem.* **2012,** *55* (5), 2125-2143.

Chapter 2

Scope and objectives

2. Scope and objectives

Muscarinic acetylcholine receptors (MRs) were identified as targets for the treatment of disorders such as Alzheimer's and Parkinson's disease. The family of MRs comprises five subtypes and due to the high conservation of the orthosteric binding pocket, highly subtype selective ligands are lacking. As the MRs' 'vestibule' or 'common' allosteric site is less conserved, the dualsteric ligand approach was considered a promising strategy to develop ligands with high subtype selectivity. The design of subtype selective MR ligands is supposed to benefit from the structural information provided by the recently reported crystal structures of the M_1R-M_4R[1-4].

The recent study on a series of dibenzodiazepinone-type MR ligands revealed that the replacement of the terminal basic diethylamino moiety of the M_2R preferring antagonist DIBA (*cf*. Figure 1A) by various bulky groups afforded derivatives with high M_2R affinity[5]. Based on these results, this doctoral thesis aimed at the synthesis and characterization of DIBA-derived heterodimeric MR ligands by conjugation of the DIBA pharmacophore to different reported orthosteric and allosteric MR ligands (the agonist xanomeline, the antagonists 4-DAMP and propantheline, and the allosteric modulators TBPB and 77-LH-28-1) using different linker types (*cf*. Figure 1B). In addition, monomeric and homodimeric ligands had to be prepared as reference compounds.

The heterodimeric ligands had to be investigated with respect to M_1R-M_5R affinity using the orthosteric radioligand [^{3}H]NMS to obtain the MR selectivity profiles. Furthermore, the preparation and characterization of radio- and fluorescence labeled compounds had been envisaged. For this purpose, amino-functionalized branched linker elements (*cf*. Figure 1B) had to be incorporated into the dimeric ligands.

M_2R saturation binding studies (including experiments in the presence of allosteric MR modulators) as well as competition binding experiments with various kinds of MR ligands (orthosteric, dualsteric, allosteric) had to be performed aiming at an elucidation of the binding mode of the heterodimeric ligands at the M_2R.

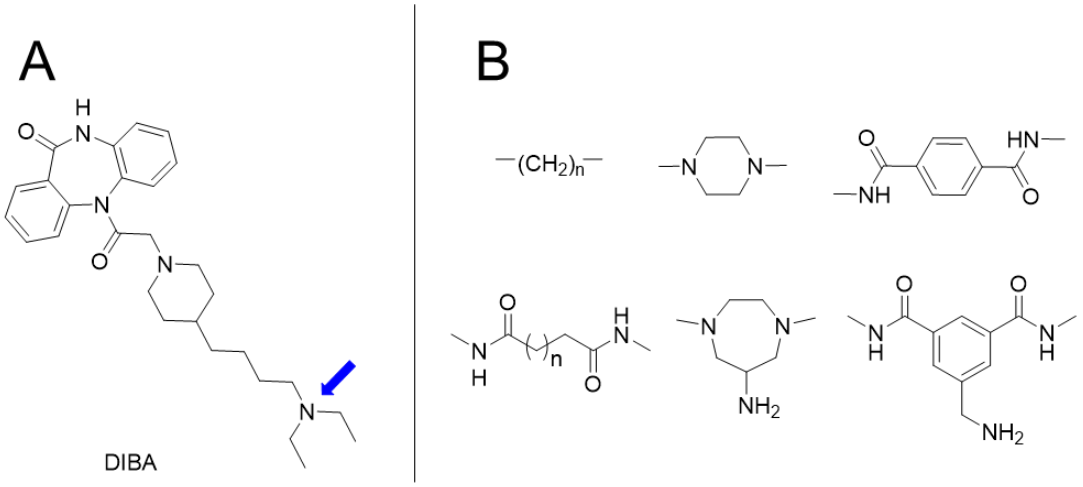

Figure 1. (A) Structure of DIBA and proposed site of attachment (blue arrow) for the conjugation to various MR ligands. (B) Moieties to be implemented in the linkers of dimeric MR ligands.

The characterization of selected fluorescently labeled ligands had to be substantiated by flow cytometry, high content analysis and fluorescence microscopy. From such investigations it was expected to get information on the binding mode at the M_2R and the suitability of the fluorescent ligands with respect to the characterization of unlabeled MR ligands as well as cellular imaging.

2.1. References

1. Kruse, A. C.; Hu, J.; Pan, A. C.; Arlow, D. H.; Rosenbaum, D. M.; Rosemond, E.; Green, H. F.; Liu, T.; Chae, P. S.; Dror, R. O., Structure and dynamics of the M_3 muscarinic acetylcholine receptor. *Nature* **2012,** *482* (7386), 552-556.
2. Haga, K.; Kruse, A. C.; Asada, H.; Yurugi-Kobayashi, T.; Shiroishi, M.; Zhang, C.; Weis, W. I.; Okada, T.; Kobilka, B. K.; Haga, T., Structure of the human M_2 muscarinic acetylcholine receptor bound to an antagonist. *Nature* **2012,** *482* (7386), 547-551.
3. Thal, D. M.; Sun, B.; Feng, D.; Nawaratne, V.; Leach, K.; Felder, C. C.; Bures, M. G.; Evans, D. A.; Weis, W. I.; Bachhawat, P., Crystal structures of the M_1 and M_4 muscarinic acetylcholine receptors. *Nature* **2016,** *531* (7594), 335-340.
4. Kruse, A. C.; Ring, A. M.; Manglik, A.; Hu, J.; Hu, K.; Eitel, K.; Hübner, H.; Pardon, E.; Valant, C.; Sexton, P. M., Activation and allosteric modulation of a muscarinic acetylcholine receptor. *Nature* **2013,** *504* (7478), 101-106.
5. Keller, M.; Tränkle, C.; She, X.; Pegoli, A.; Bernhardt, G.; Buschauer, A.; Read, R. W., M_2 Subtype preferring dibenzodiazepinone-type muscarinic receptor ligands: Effect of chemical homo-dimerization on orthosteric (and allosteric?) binding. *Bioorg. Med. Chem.* **2015,** *23* (14), 3970-3990.

Chapter 3

Synthesis and pharmacological characterization of dibenzodiazepinone-type heterodimeric muscarinic receptor ligands

3. Synthesis and pharmacological characterization of dibenzodiazepinone-type heterodimeric muscarinic receptor ligands

3.1. Introduction

GPCRs constitute a large superfamily of cell surface receptors, which are classified into more than 100 subfamilies[1]. GPCRs are the most frequently addressed drug targets. Around 30 % of all marketed prescription drugs act on GPCRs[2-3]. Muscarinic acetylcholine receptors (mAChRs or MRs) belong to the class A GPCRs and comprise five receptor subtypes in humans, designated M_1R to M_5R. M_1R, M_3R, M_5R receptors couple to G proteins of the G_q class, M_2R, M_4R receptors interact with G proteins of the G_i family[4]. MRs have been identified as targets for the treatment of various diseases such as Alzheimer's disease and Parkinson's disease, but due to the high conservation within the orthosteric binding site across all five mAChR subtypes, the development of subtype selective orthosteric ligands is challenging[5]. Besides the ACh binding pocket (the "orthosteric site"), muscarinic receptors contain additional "allosteric binding sites"[6-8], which are less conserved than the orthosteric region and can potentially be exploited to develop subtype selective ligands[9-10]. The M_2 subtype was the first GPCR to be found as being sensitive to allosteric modulation[11] and numerous allosteric MR modulators were identified, such as compounds **14**[12], **15**[13] and **16**[14-15] (*cf*. Figure 1B).

Homo- and heterobivalent ligands have been emerged at GPCRs field in recent years, like histamine[16-17], dopamine[18-19], and adenosine[20-21] and NPY[22-23] receptors. Benefits of bivalent ligands can include increased ligand affinity and improved selectivity[24-25]. As a variation of bivalent ligands, the concept of dualsteric[11, 26-28] (bitopic orthosteric/allosteric) ligands of GPCRs led to novel chemical tools. The first examples of rationally designed bitopic ligands targeting mAChRs were derived from the orthosteric agonist oxotremorine (**3**) and hexamethonium-like allosteric modulators. This series of hybrid molecules showed a gain in subtype selectivity compared to **3** (e.g. compound **17**, *cf*. Figure 1C)[29]. Another example of a designed bitopic MR ligand is THRX-160209 (compound **18**, *cf*. Figure 1C), which is reported to exhibit higher affinity and subtype selectivity than the corresponding monovalent ligands and was suggested to bind in a multivalent manner to the M_2 receptor[30].

AF-DX 384[31] (**8**) (*cf*. Figure 1A) was developed from the M_1 preferring M receptor antagonist pirenzepine[32] as M_2R preferring pyridobenzodiazepinone-type M receptor antagonist. Likewise, the dibenzodiazepinone-type M receptor antagonist DIBA (**9**) showed high affinity for the M_2 receptor (K_i value: 0.3 nM)[33]. Moreover, Tränkle et. al suggested a dualsteric binding

mode of **8** at the M_2 receptor[34]. A hybrid MR ligand formed of **8** and the allosteric modulator W84 (**15**) was reported to exhibit a pronounced positive cooperativity with NMS, pointing a new way for the development of allosteric enhancers[35-36].

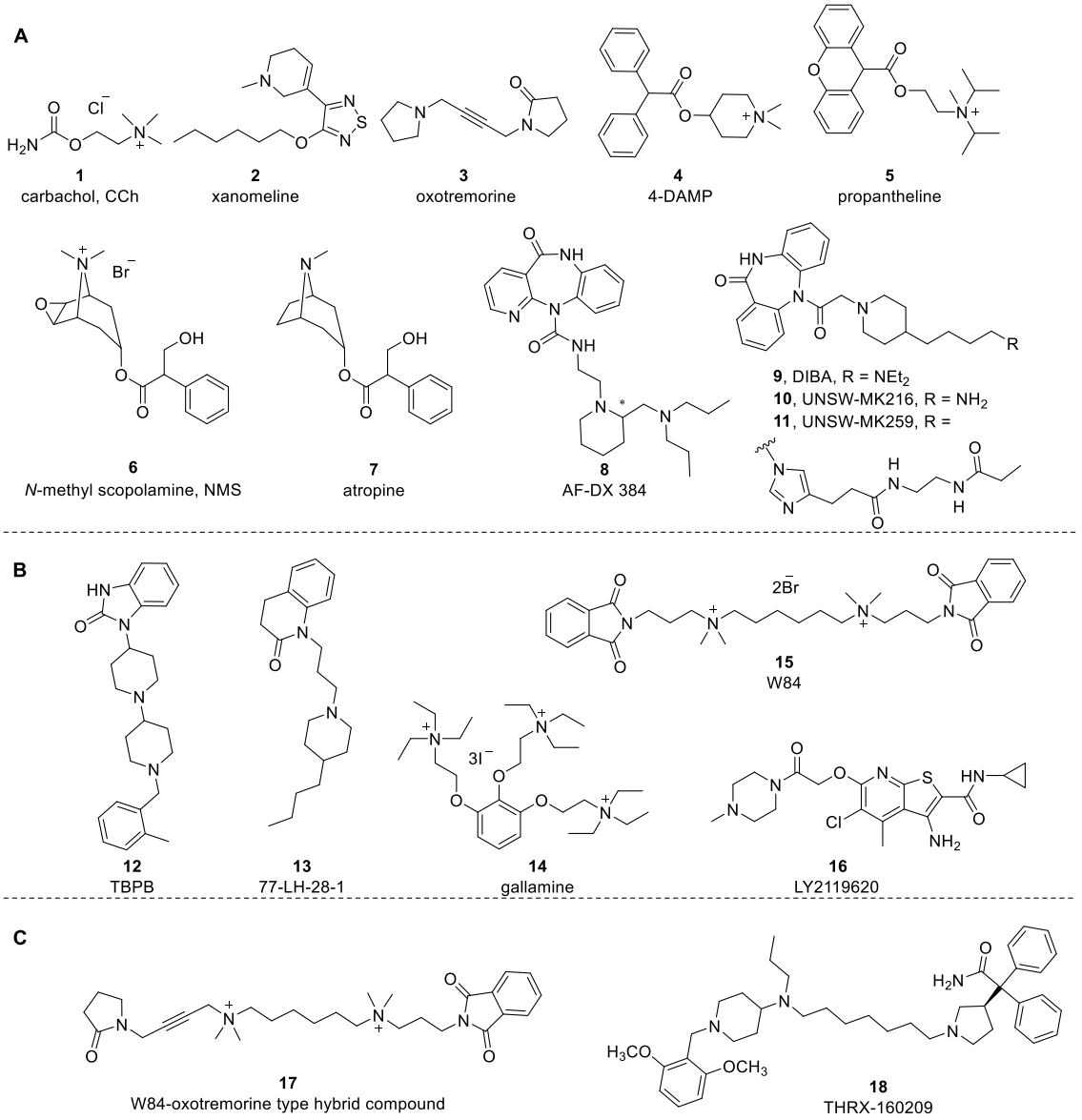

Figure 1. (A) Chemical structures of reported MR agonists (**1**-**3**) and antagonists (**4**-**11**). (B) Chemical structures of the allosteric MR ligands **12**-**16**. (C) Structures of the hybrid ligands **17** and **18**, which were suggested to bind dualsterically at the M_2R[29-30].

This study was directed towards the design, synthesis, and pharmacological evaluation of DIBA-derived heterodimeric MR ligands comprising five combinations of DIBA with reported orthosteric or allosteric MR ligands: 'DIBA-xanomeline', 'DIBA-TBPB', 'DIBA-77-LH-28-1', 'DIBA-4-DAMP' and 'DIBA-propantheline' (in total nineteen heterodimeric ligands). Xanomeline (*cf*. Figure 1A) is a M_1 selective MR agonist (see general introduction). TBPB (*cf*. Figure 1B) was reported to selectively activate M_1 receptors through an allosteric mechanism as shown by mutagenesis and molecular pharmacology studies[37-39]. And TBPB was proposed

as a bitopic ligand, interacting with both the orthosteric site and an allosteric site at the M_1R[40]. Similarly, the competitive mechanism or with a strong negative cooperativity between [^{3}H]NMS and 77-LH-28-1 (*cf*. Figure 1B) was reported at M_1R, and 77-LH-28-1 was also suggested to bind allosterically to [^{3}H]NMS-occupied M_1 receptor, and competed with the prototypical allosteric modulator (C_7/$_3$-phth)[41]. 4-DAMP and propantheline (*cf*. Figure 1A) are non-selective orthosteric MR antagonists with high affinities (K_i (4-DAMP, M_1R-M_5R): 0.52-3.80 nM, K_i (propantheline, M_1R-M_4R): 0.057-0.33 nM)[31, 42].

In addition to the heterodimeric ligands, four homodimeric ligands derived from xanomeline, two homodimeric ligand derived from DIBA, a monomeric DIBA derivative, a monomeric xanomeline derivative and a monomeric TBPB derivative were prepared as reference compounds. Furthermore, two radiolabeled heterodimeric ligands ('DIBA-TBPB' type and 'DIBA-xanomeline' type) were prepared as molecular tools and characterized by saturation binding (including experiments in the presence of allosteric modulators "Schild-like analysis"), kinetic investigations and equilibrium competition binding studies.

3.2. Results and discussion

3.2.1. Chemistry

3.2.1.1. Synthesis of the diazepane derivative 28

Treatment of diethyl oxalate (**19**) with one equivalent of benzylamine (**20**) afforded the N-substituted ethyl oxamate **21**. The subsequent reaction with methylamine converted compound **21** to the unsymmetrical *N*,*N*'-disubstituted oxamide **22**. Reduction of **22**, using lithium aluminum hydride, resulted in compound **23** as reported[43]. Homopiperazine **25** was obtained from **23** by nitro-Mannich reaction using nitroethanol and paraformaldehyde. Compound **25** was treated with an excess of *tert*-C_4H_9OK in methanol resulted compound **26**[44-46]. Reduction of the nitro group in **26** to an amino group using Raney nickel, and subsequent Boc-protection gave compound **27**. Debenzylation of **27** applying palladium-catalyzed hydrogenolysis yielded compound **28** (*cf*. Scheme 1).

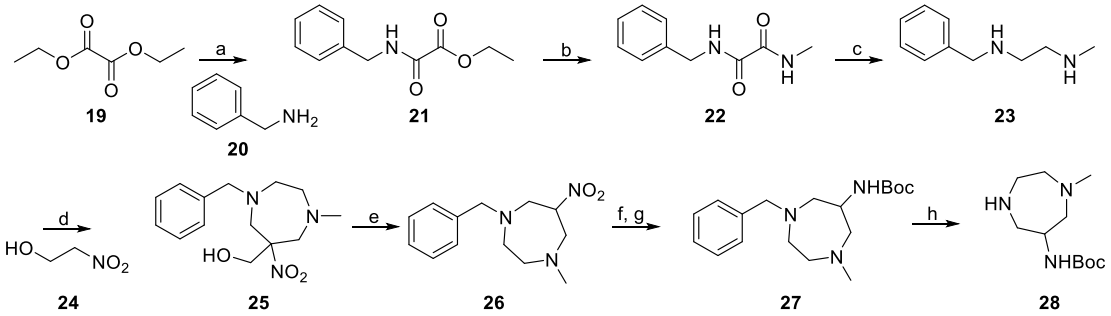

Scheme 1. Synthesis of the diazepane derivative **28**. Reagents and conditions: (a) $CHCl_3$, reflux, overnight, 65%; (b) CH_3NH_2 (2M in THF), EtOH, rt, 8 h, 97%; (c) $LiAlH_4$, abs. THF, 0 °C/reflux, overnight,

60%; (d) paraformaldehyde, toluene/EtOH 1:1 (v/v), reflux, 6 h, 88%; (e) potassium *tert*-butoxide, MeOH, 40 °C, 30 min, 67%; (f) H_2, Ni-Raney, EtOH, rt, overnight, 98%; (g) di-*tert*-butyl dicarbonate, $CHCl_3$, rt, overnight, 54%; (h) 10% Pd/C, H_2, THF/H_2O 1:4 (V/V), rt, overnight, 77%.

3.2.1.2. Synthesis of the piperazine derivative 32

The synthesis of piperazine derivative **32** started with commercially available 2-bromoethan-1-amine hydrobromide (**29**), which was Boc-protected to obtain compound **30**. This intermediate was treated with an excess of piperazine (**31**) to afford building block **32** (*cf*. Scheme 2).

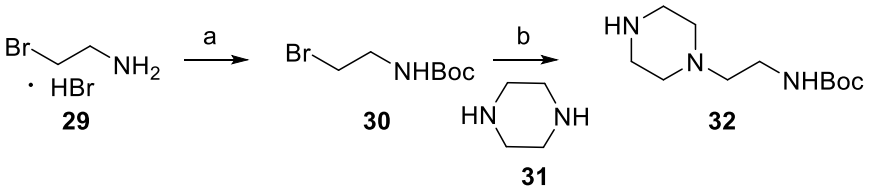

Scheme 2. Synthesis of the piperazine derivative **32**. Reagents and conditions: (a) di-*tert*-butyl dicarbonate, triethylamine, CH_2Cl_2, rt, overnight, 80%; (b) K_2CO_3, MeCN, reflux, 3 h, 91%.

3.2.1.3. Synthesis of xanomeline derivatives 40, 41, 46 and 52-55

Hydroxy- or amino-functionalized xanomeline derivatives (**38** and **50**) were required as key intermediates for the synthesis of heterodimeric ligands (*cf*. Scheme 3). The intermediate **34** was synthesized from 3-pyridinecarbaldehyde (**33**) according a slightly modified Strecker synthesis from the literature[47-48]. Initially, **33** was treated with potassium cyanide yielding the cyanohydrin, after isolation, the cyanohydrin was immediately reacted with ammonium chloride under basic aqueous conditions to give **34**. The intermediate **34** was cyclized with sulfur monochloride in DMF to give 3-(3-chloro-1,2,5-thiadiazol-4-yl)pyridine (**35**). Propane-1,3-diol (**36**) or pentane-1,5-diol (**42**) were treated with sodium hydride and **35** to give the hydroxylated derivatives **37** and **43**. This procedure is different from the described nucleophilic displacement of the chlorine of **35**, where one of the hydroxyl groups was protected with *tert*-butylchlorodiphenylsilane (TBDPSCl)[49]. **37** and **43** were quaternized with excess methyl iodide in acetone and then reduced to the tetrahydropyridine product **38** or **44** with the help of sodium borohydride in methanol (*cf*. Scheme 3). In order to convert the primary hydroxy groups of **38** and **44** to bromide, an Apple reaction was applied using tetrabromomethane and triphenylphosphine in dichloromethane to yield compounds **39**[50] and **45**. Alkylation of piperazine using the bromides **39** or **45** gave the intermediate **40** and the homodimeric ligand **46**. When compound **28** alkylated with compound **39**, followed by removal of the Boc group, afforded the monomeric ligand **41**, which was prepared for comparative purposes in pharmacological assays.

The synthesis of amino-functionalized derivatives of xanomeline is shown in Scheme 3,

deprotonation of *tert*-butyl (5-hydroxypentyl)carbamate (**47**) with excess of sodium hydride in anhydrous tetrahydrofuran followed by refluxing in the presence of intermediate **35** afforded compound **48**. Reduction and methylation of **48** led to the 1,2,5,6-tetrahydropyridine derivative **49**. Cleavage of the Boc group using trifluoroacetic acid (TFA) in dichloromethane afforded compound **50**, which was coupled with compound **51** by using coupling reagents TBTU and HOBt in the presence of DIPEA to obtain intermediate **52** after subsequent removal of the Boc group. Furthermore, compound **50** was treated with octanedioyl dichloride or decanedioyl dichloride in the presence of triethylamine to yield the homodimeric compounds **53** or **54**. Amidation of terephthalic acid with amine **50** using coupling reagents EDC and HOBt afforded the homodimeric ligand **55**, containing a rigid central linker moiety (*cf*. Scheme 3).

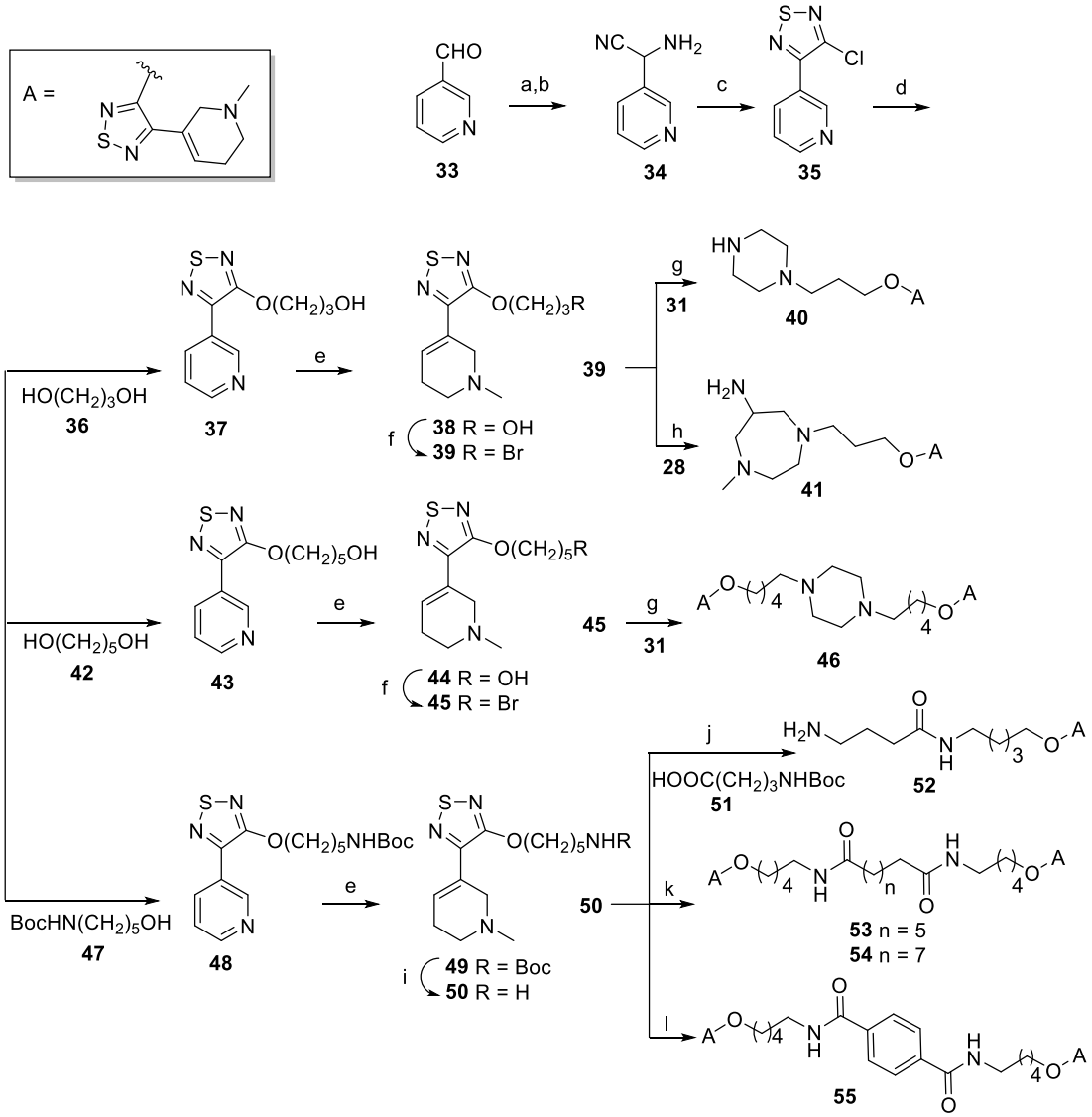

Scheme 3. Synthesis of the xanomeline derivatives **39**, **40**, **41**, **46** and **52**-**55**. Reagents and conditions: (a) KCN, H_2O, AcOH, 5 °C/rt, 2 h, 98%; (b) NH_4Cl, 25% aq NH_3, rt, 20 h, 67%; (c) S_2Cl_2, DMF, 5-10 °C, 45 min, 69%; (d) NaH, abs. THF, reflux, 2-8 h, 52% for **37**, 48% for **43**, 27% for **48**; (e) (1) methyl iodide, acetone, rt, 24-36 h; (2) $NaBH_4$, MeOH, 0 °C/rt, overnight, 41% for **38**, 92% for **44**, 79% for **49**; (f) CBr_4, PPh_3, CH_2Cl_2, -5 °C/rt, 24 h, 50% for **39**, 82% for **45**; (g) K_2CO_3, MeCN, microwave, 110 °C (30 min) or reflux (2 h), 66% for **40**, 22% for **46**; (h) (1) **28**, K_2CO_3, MeCN, microwave, 110 °C (30 min); (2) TFA/CH_2Cl_2 1:4 v/v, rt, 8 h, 66%; (i) TFA/CH_2Cl_2 1:4 v/v, rt, 8 h, 56%; (j) (1) **51**, TBTU, HOBt, DIPEA,

DMF, rt/60 °C, 3 h; (2) TFA/CH_2Cl_2 1:4 v/v, rt, 8 h, 89%; (k) octanedioyl dichloride or decanedioyl dichloride, triethylamine, abs. THF, 0 °C/rt, overnight, 39% for **53**, 65% for **54**; (l) terephthalic acid, EDC, HOBt, DMF, rt, overnight, 26%.

3.2.1.4. Synthesis of TBPB derivatives 63, 64, 66, 67

The synthesis of TBPB derivatives is outlined in Scheme 4. Beginning with commercially available 1-fluoro-2-nitrobenzene (**56**), an aromatic nucleophilic substitution with ethyl 4-aminopiperidine-1-carboxylate (**57**) under microwave irradiation yielded nitroaniline **58**, which was reduced by palladium-catalyzed hydrogenation to provide o-phenylendiamine derivative **59**. The benzimidazolone formation from **59** using triphosgene afforded **60** (*cf*. Scheme 4). Subsequent removal of the ethyl carbamate group by alkaline hydrolysis gave **61**[51]. Reductive amination of the N-Boc protected piperidinone (**62**) with the secondary amine **61**, using sodium cyanoborohydride, followed by removal of the Boc group afforded compound **63**. Alkylation of **63** with *tert*-butyl (2-bromoethyl)carbamate (**30**) and Boc-deprotection yielded **64** as a building block for the synthesis of heterodimeric ligands. Acylation of **63** with 2-bromoacetyl bromide (**65**) afforded amide **66** (*cf*. Scheme 4). Finally, N-alkylation of the homopiperazine derivative **28** with bromide **66** followed by removal of Boc group afforded the TBPB derivative **67**.

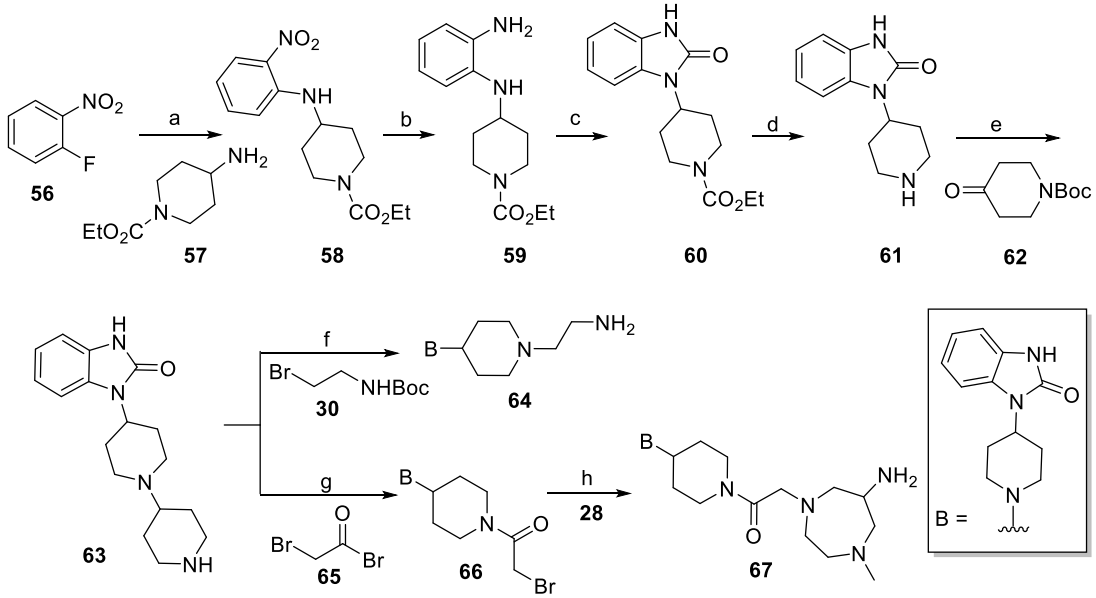

Scheme 4. Synthesis of the TBPB derivatives **63**, **64**, **66**, **67**. Reagents and conditions: (a) K_2CO_3, NaI, DMF, microwave, 180 °C, 10 min, 72%; (b) 10% Pd/C, H_2, rt, overnight, 89%; (c) triphosgene, $NaHCO_3$, CH_2Cl_2, 0 °C/rt, 2 h, 73%; (d) 10% aq NaOH, reflux, 5 h, 81%; (e) (1) **62**, $NaBH_3CN$, acetic acid, MeOH, 0 °C/rt, overnight; (2) TFA/CH_2Cl_2 1:4 v/v, rt, 8 h, 75%; (f) (1) **30**, K_2CO_3, MeCN, reflux, 8 h; (2) TFA/CH_2Cl_2 1:4 v/v, rt, 8 h, 86%; (g) 2-bromoacetyl bromide, pyridine, $CHCl_3$, 0 °C/rt, overnight, 91%; (h) (1) **28**, K_2CO_3, MeCN, microwave, 110 °C, 30 min; (2) TFA/CH_2Cl_2 1:4 v/v, rt, 8 h, 43%.

3.2.1.5. Synthesis of 4-DAMP derivatives 71 and 73

The synthesis of the building blocks **71** and **73**, required for the preparation of 'DIBA-4-DAMP'-type heterodimeric ligands, started from diphenylacetic acid (**68**) and Boc protected piperidin-4-ol (**69**) (*cf*. Scheme 5). Unlike a reported procedure, which transformed the carboxylic acid **68** into the corresponding acid chloride prior to esterification with alcohol **69**[52], the ester **70** was formed from **68** and **69** using *N*,*N*'-dicyclohexylcarbodiimide (DCC) and 4-dimethylaminopyridine (DMAP) as coupling reagents. Treatment of **70** with TFA gave **71** as the bisdesmethyl analogue of 4-DAMP. Alkylation of **71** with bromide **30** afforded compound **72**, which was converted to **73** by removal of the Boc group (*cf*. Scheme 5).

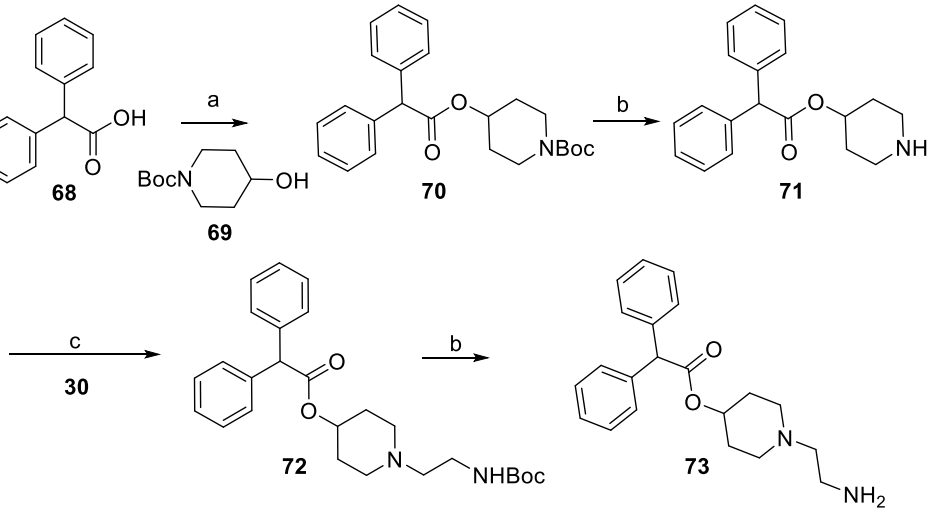

Scheme 5. Synthesis of the 4-DAMP derivatives **71** and **73**. Reagents and conditions: (a) DCC, DMAP, CH_2Cl_2, 0 °C/rt, overnight, 97%; (b) TFA/CH_2Cl_2 1:4 v/v, rt, 8 h, 56% for **42**, 83% for **44**; (c) K_2CO_3, MeCN, reflux, 3 h, 67%.

3.2.1.6. Synthesis of propantheline derivatives 77, 78 and 80

Scheme 6 depicts the synthesis of the propantheline building blocks **77**, **78** and **80**, which were used for the synthesis of the 'DIBA-propantheline'-type heterodimeric ligands. Xanthene-9-carboxylic acid (**74**) was condensed with 2-bromoethan-1-ol or 4-bromobutan-1-ol to yield compound **75** and **76**, respectively. Treatment of **75** and **76** with an excess of piperazine afforded the alkylation products **77** and **78** in moderate yield (*cf*. Scheme 6). Alkylation of **77** with bromide **30** gave compound **79**, which was converted to the propantheline-derived compound **80** by Boc-deprotection using TFA.

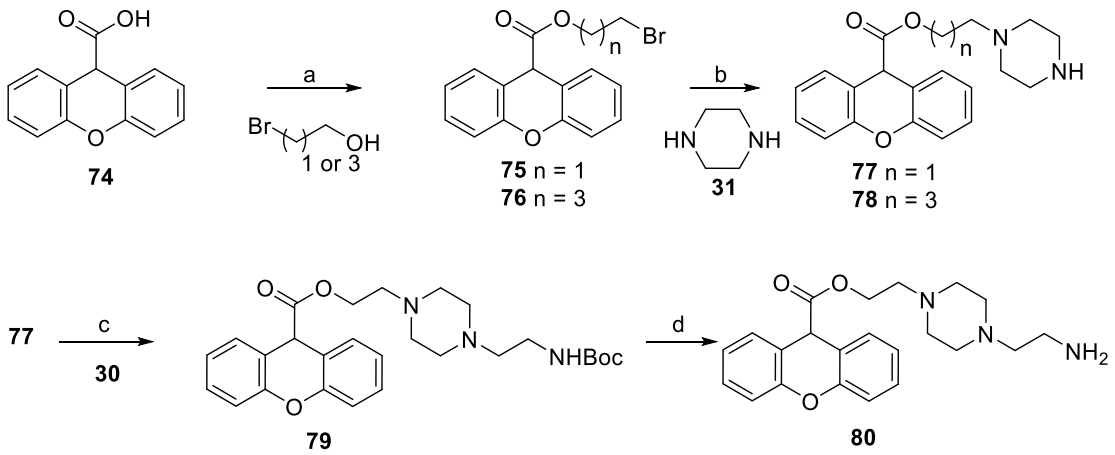

Scheme 6. Synthesis of the propantheline derivatives **77**, **78** and **80**. Reagents and conditions: (a) 2-bromoethan-1-ol or 4-bromobutan-1-ol, DCC, DMAP, CH_2Cl_2, 0 °C/rt, overnight, 68% for **75**, 56% for **76**; (b) K_2CO_3, MeCN, reflux, 1.5 h or overnight, 59% for **77**, 46% for **78**; (c) K_2CO_3, MeCN, reflux, 2 h, 57%; (d) TFA/CH_2Cl_2 1:4 v/v, rt, overnight, 88%.

3.2.1.7. Synthesis of 77-LH-28-1 derivatives 86 and 88

The synthesis of the 77-LH-28-1-derived intermediates **86** and **88** is shown in Scheme 7. Treatment of commercially available 3,4-dihydro-2(1*H*)-quinolinone (**81**) with 1-chloro-3-iodopropane (**82**) in the presence of caesium carbonate in acetonitrile afforded compound **83** as described in the literature[53]. Alkylation of piperidine **84** with chloride **83** in the presence of potassium carbonate and sodium iodide yielded compound **85**. The alcohol **85** was converted to the corresponding bromide (**86**) under Apple reaction condition using tetrabromomethane and triphenylphosphine (*cf*. Scheme 7). Compound **86** was treated with piperazine **32** to afford the alkylation product **87**, which was Boc-deprotected to yield the 77-LH-28-1 derivative **88**.

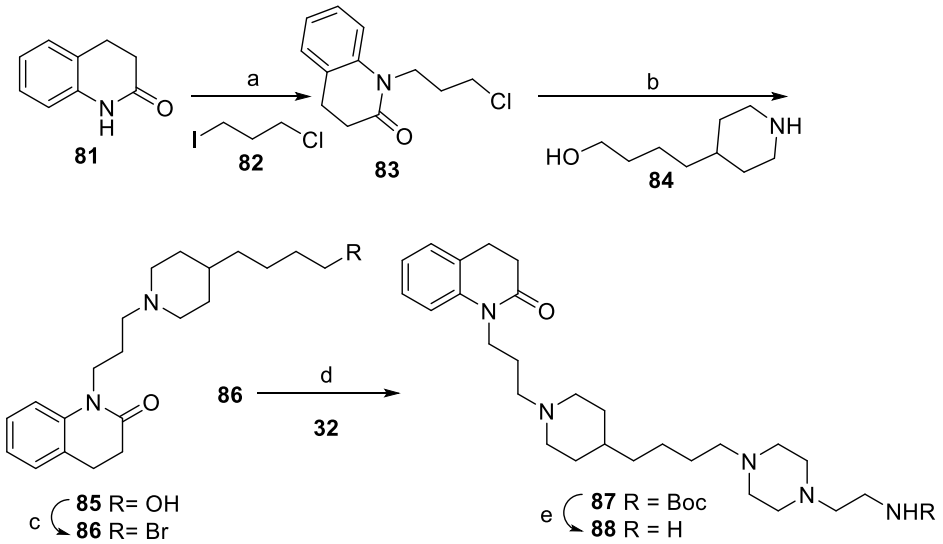

Scheme 7. Synthesis of the 77-LH-28-1 derivatives **86** and **88**. Reagents and conditions: (a) Cs_2CO_3, MeCN, 50 °C, 12 h, 69%; (b) K_2CO_3, NaI, MeCN, 50 °C, 24 h, 53%; (c) CBr_4, PPh_3, CH_2Cl_2, -5 °C/rt, overnight, 31%; (d) K_2CO_3, MeCN, reflux, 2 h, 62%; (e) TFA/CH_2Cl_2 1:4 v/v, rt, 8 h, 97%.

3.2.1.8. Synthesis of DIBA derivatives 94, 95 and 96

The preparation of the dibenzodiazepinone derivatives **94**, **95**, and **96** is illustrated in Scheme 8. The dibenzodiazepinone moiety **91** was obtained by heating 2-chlorobenzoic acid (**89**) and o-phenylenediamine (**90**) in chlorobenzene in the presence of copper[54-55]. Compound **91** was treated with chloroacetyl chloride to give the acylated derivative **92** (*cf*. Scheme 8). Nucleophilic substitution of the chlorine in **92** by 4-(piperidin-4-yl)butan-1-ol (**84**) gave compound **93**. The alcohol **93** was converted to the respective bromide (compound **94**) by using the Apple reaction conditions described above. Alkylation of compound **28** using bromide **94** and subsequent Boc-deprotection yielded the monomeric DIBA derivative **95** (*cf*. Scheme 8). Aiming at dimeric ligands with extended linkers, compound **32** was alkylated using again bromide **94**, followed by Boc-deprotection with TFA to obtain compound **96**.

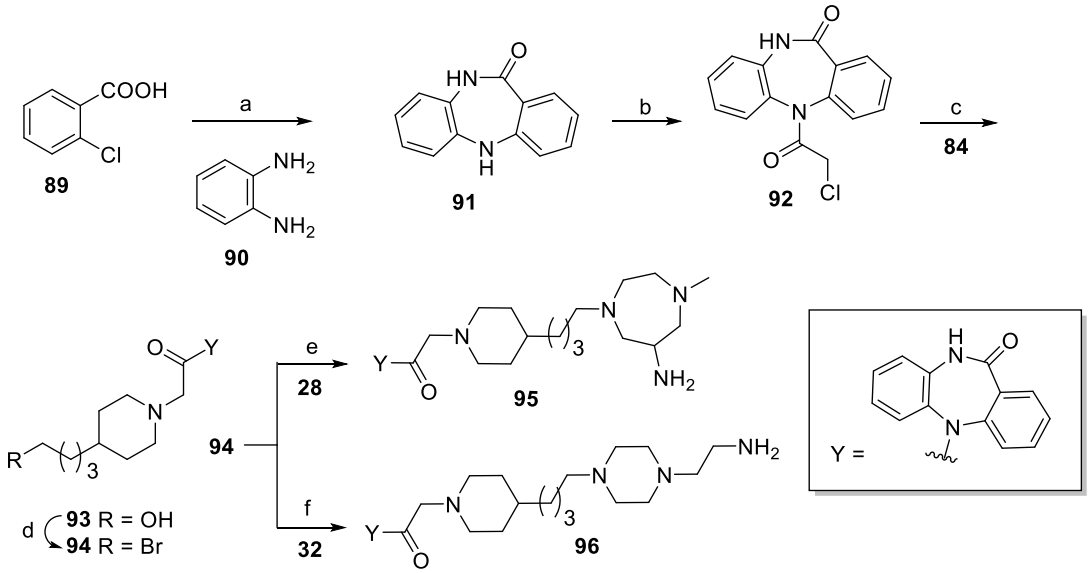

Scheme 8. Synthesis of the DIBA derivatives **94**, **95** and **96**. Reagents and conditions: (a) copper powder, chlorobenzene, reflux, 6 h, 13%; (b) 2-chloroacetyl chloride, *N*,*N*-dimethylaniline, THF, overnight, 84%; (c) K_2CO_3, MeCN, reflux, 8 h, 62%; (d) CBr_4, PPh_3, CH_2Cl_2, -5°C/rt, overnight, 78%; (e) (1) **28**, K_2CO_3, MeCN, reflux, 3 h; (2) TFA/CH_2Cl_2/H_2O 10:10:1 v/v/v, rt, 2 h, 17%; (f) (1) **32**, K_2CO_3, MeCN, reflux, 3 h; (2) TFA/CH_2Cl_2 1:4 v/v, rt, 8 h, 66%.

3.2.1.9. Synthesis of dibenzodiazepinone-derived heterodimeric ligands 97-102, 105a, 106-108, 110, 111 and 114-120

The synthesis of the dibenzodiazepinone-derived heterodimeric ligands is outlined in Scheme 9 (**97**-**102**, **105a, 106**-**108**) and Scheme 10 (**110, 111**, **114**-**120**). The heterodimeric ligands **97**-**101** were prepared through alkylation of compounds **40**, **63**, **71**, **77** and **78**, respectively, using bromide **94**. The heterodimeric ligand **102** was prepared by alkylation of compound **10**[55] (*cf*. Figure 1A) with bromide **86** (*cf*. Scheme 9). Alkylation of the homopiperazine derivative **103** applying a mixture of the bromides **39** and **94**, followed by Boc-deprotection, yielded the heterodimeric ligand **105a**, which was propionylated to give the congener **106**. Likewise,

alkylation of **103** applying a mixture of the bromides **66** and **94**, followed by Boc-deprotection, gave the heterodimeric ligand **107**, which was propionylated yielding the congener **108**. The DIBA type homodimeric ligand **105b** was isolated during the preparation of compound **105a** and **107**, and the non-DIBA type homodimeric ligands formed by double alkylation of **103** with bromides **39** and **66** were not isolated (*cf*. Scheme 9).

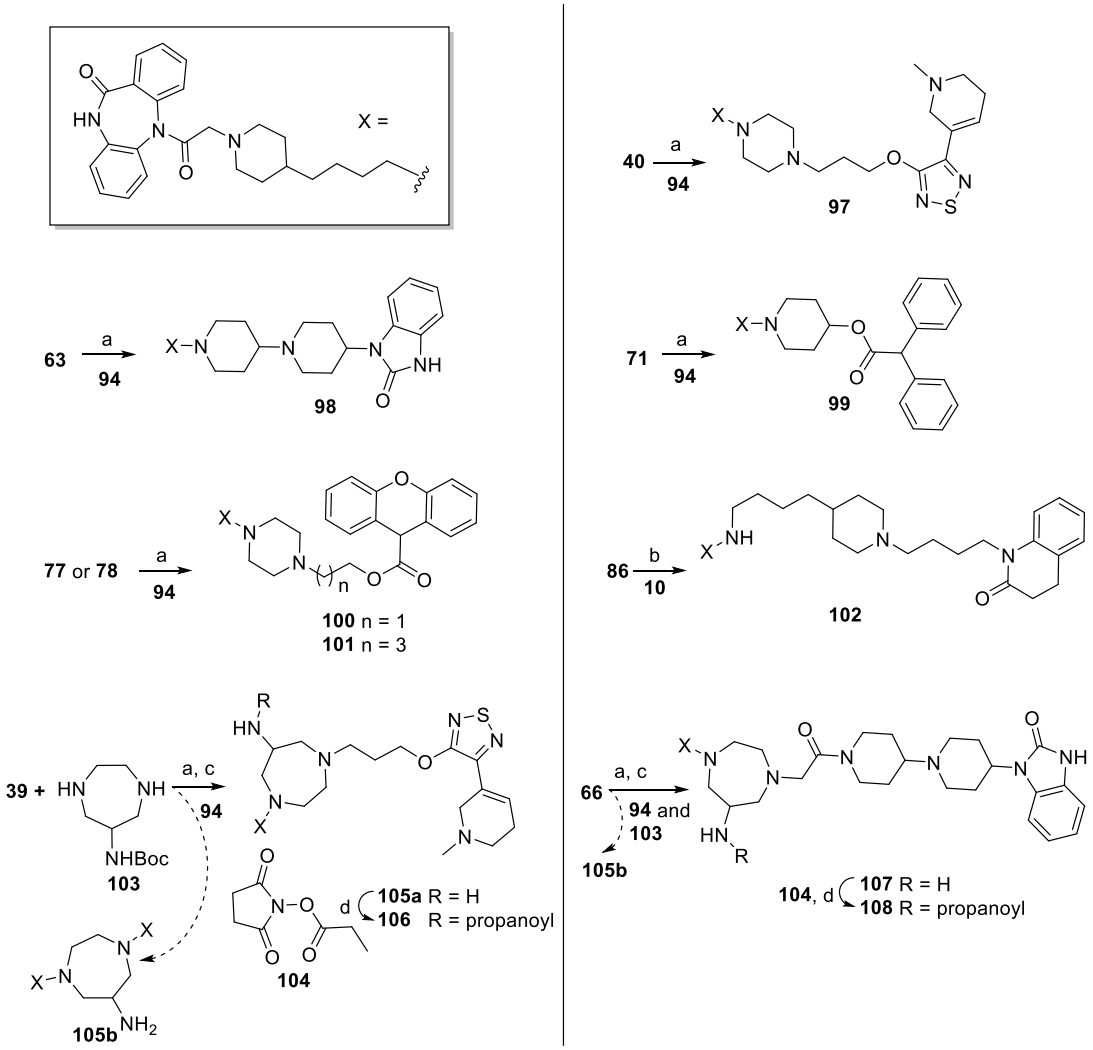

Scheme 9. Synthesis of the DIBA-derived heterodimeric ligands **97**-**102**, **105**-**108**. Reagents and conditions: (a) K_2CO_3, MeCN, microwave, 110 °C, 30 min or reflux, 3 h to overnight, 41% for **97**, 57% for **98**, 27% for **99**, 51% for **100**, 38% for **101**; (b) NaI, K_2CO_3, MeCN, reflux, 3 h, 52% for **102**; (c) TFA/CH_2Cl_2/H_2O 10:10:1 v/v/v, rt, 2 h, 17% for **105a** (two steps), 12% for **107** (two steps); (d) DIPEA, DMF, rt, 2 h, 95% for **106**, 96% for **108**.

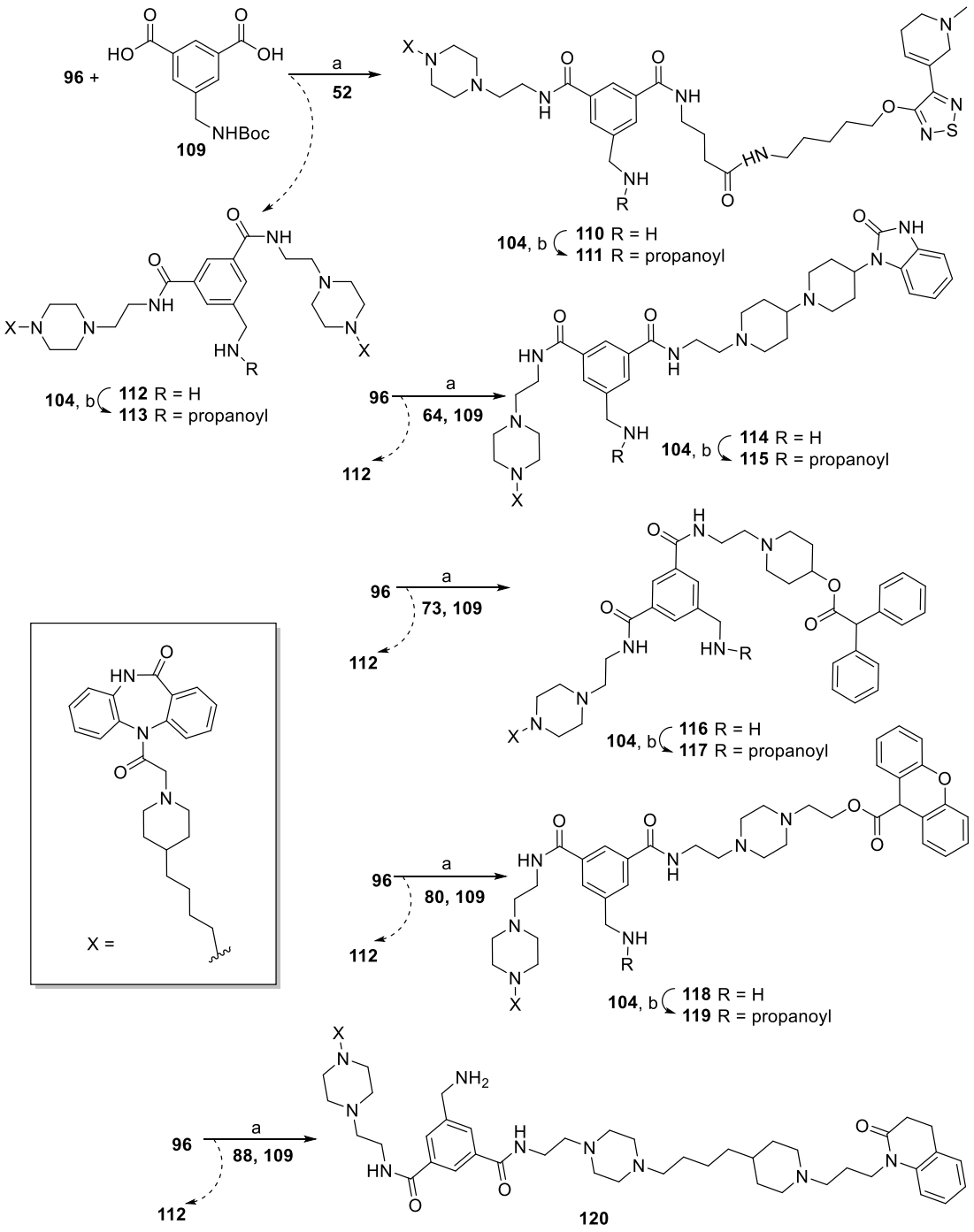

Scheme 10. Synthesis of the dibenzodiazepinone-type homo- or heterodimeric ligands **110**-**120**. Reagents and conditions: (a) (1) TBTU, HOBt, diisopropylethylamine, DMF, 3 h; (2) TFA/CH_2Cl_2/H_2O 10:10:1 v/v/v, rt, 2 h, 14% for **110**, 10% for **114**, 28% for **116**, 15% for **118**, 4% for **120**; (b) DIPEA, DMF, rt, 2 h, 89% for **111**, 79% for **113**, 88% for **115**, 83% for **117**, for 86% **119**.

Amidation of the isophthalic acid derivative **109** applying a mixture of amines **96** and **52**, followed by Boc-deprotection, afforded the heterodimeric ligand **110** and the homodimeric ligand **112**. Propionylation of **110** and **112** gave the congeners **111** and **113**, respectively (*cf*. Scheme 10). Likewise, the heterodimeric ligands **114**, **116**, **118** and **120** were obtained by amidation of **109** using the amine mixtures **96**/**64**, **96**/**73**, **96**/**80** and **96**/**88**, respectively, and subsequent Boc-deprotection (*cf*. Scheme 10). Propionylation of **114**, **116** and **118** at the

central linker moiety afforded the propionamide congeners **115**, **117** and **119**. It should be noted that the respective non-DIBA type homodimeric ligands generated by double amidation of **109** with amines **52**, **64**, **73**, **80** and **88** were formed, but were not isolated (*cf*. Scheme 10).

3.2.2. Equilibrium competition binding studies with [^{3}H]NMS

The receptor binding affinities of twenty eight new MR ligands, comprising the monomeric xanomeline derivative **41**, TBPB derivative **67**, DIBA derivative **95**, the 'DIBA-DIBA' type homodimeric ligands **112** and **113**, the 'xanomeline-xanomeline' type homodimeric ligands **46** and **53**-**55**, as well as the 'DIBA-xanomeline' type heterodimeric ligands **97**, **105a**, **106**, **110** and **111**, the 'DIBA-TBPB' type heterodimeric ligands **98**, **107**, **108**, **114** and **115**, the 'DIBA-77-LH-28-1' type heterodimeric compounds **102** and **120**, the 'DIBA-propantheline' type dimeric ligands **100**, **101**, **118** and **119**, and the 'DIBA-4-DAMP' type heterodimeric ligands **99**, **116** and **117**, were investigated in equilibrium binding experiments using the orthosteric antagonist radioligand [^{3}H]N-methylscopolamine ([^{3}H]**6**) at live CHO cells stably expressing the human muscarinic receptor subtypes M_1-M_5. M_1-M_5 receptor saturation binding experiments with [^{3}H]**6** were performed in our lab[55]. The pK_d values amounted to 9.85 (M_1R), 10.1 (M_2R), 10.1 (M_3R), 10.5 (M_4R) and 9.63 (M_5R) were in good agreement with previously reported data[31, 56].

Figure 2A shows the sigmoidal curves of a subset of the xanomeline-type homodimeric ligands **46** and **53**-**55**, the monomeric ligand **41** derived from xanomeline, the monomeric ligand **95** derived from DIBA, and five 'DIBA-xanomeline' type heterodimeric ligands (**97**, **105a**, **106**, **110** and **111**) at M_2R. For the homobivalent ligands of xanomeline, we observed a gradual, spacer-length-dependent (not counting the xanomeline O atom) increase in affinity at the M_2R for the 14- (**46**), 18- (**55**), 20- (**53**), and 22-atom (**54**) spacers (K_i values: 21, 4.6, 4.0 nM and 2.3 nM, respectively) compared to the parent compound xanomeline (K_i = 210 nM) (data not shown in Table 1), the covalent tethering of two xanomeline pharmacophores caused 10-100 fold higher affinities at M_2R compared with xanomeline (**2**). A similar phenomenon was observed for M_1R, compared with the parent compound xanomeline (K_i = 160 nM, data not showed in Table 1), ligands **46**, **55**, **53** and **54** showed increasing M_1R affinities (K_i values: 53, 24, 5.9 and 4.5 nM, respectively) depending on the length of the linker, and showed 3-35 fold higher affinities at M_1R than xanomeline (**2**). In contrast, the monomeric ligand derived from xanomeline (compound **41**) obtained from replacing xanomeline's O-hexyl chain by the amino-functionalized moiety showed a decrease in affinity at M_2R.

All of the tested DIBA derivatives (including monomeric (**95**) and heterodimeric (**97**, **105a**, **106**,

110 and **111**) ligands) exhibited K_i values in the low nanomolar range at M_2R, and showed higher affinities at M_2R than xanomeline derived monomeric (**41**) or homodimeric (**46**, **53**-**55**) ligands (*cf*. Table 1). Compound **97**, containing a xanomeline and a DIBA moiety linked by piperazine, showed a remarkably high M_2R affinity with a K_i value of 0.08 nM. Compound **105a**, containing 1,4-diazepane ring between DIBA and xanomeline moieties, showed low nanomolar range affinity with a K_i value of 0.51 nM. With a K_i value of 0.46 nM, the propionamide congener **106** had a comparable affinity. Remarkably, though compound **110** and its propionamide derivative **111** comprise complex linker moieties, these two heterodimeric ligands had high affinity at the M_2R with K_i values of 0.26 nM and 0.35 nM, respectively. This means that, although the linkers in compounds **97**, **105a**, **106**, **110** and **111** differ in the chemical nature and vary in length, these compounds showed comparable high M_2R affinities (*cf*. Table 1). Moreover, all 'DIBA-xanomeline' type heterodimeric ligands showed slightly higher M_2R affinities than the DIBA-derived monomeric ligand **95** (K_i 2.2 nM), indicating that conjugation to the second pharmacophore (xanomeline) is favorable with respect to M_2 receptor binding.

The effect on [^{3}H]NMS M_2R equilibrium binding of the second subset of compounds, comprising the monomeric ligand **67** derived from TBPB, the 'DIBA-TBPB' type ligands **98**, **107**, **108**, **114** and **115**, as well as the 'DIBA-77-LH-28-1' type heterodimeric compounds **102** and **120** is depicted in Figure 2B. The heterodimeric ligands (**98**, **102**, **107**, **108**, **114**, **115** and **120**) all exhibited slightly higher M_2 affinities (K_i values: 0.20 to 0.82 nM) than the DIBA derived monomeric ligand **95** (K_i value: 2.2 nM). The TBPB-like monomeric ligand **67** displayed low M_2R affinity (K_i 1800 nM). This phenomenon suggested that chemical dimerization of DIBA and TBPB, as well as DIBA and 77-LH-28-1 leads to increased affinity at M_2R. Interestingly, the heterodimeric ligands containing a piperazine moiety in the spacer (**114**, **115**, **120**) showed slightly increased affinities with K_i values in the range of 0.20-0.37 nM, compared to other heterodimeric ligands (**98**, **102**, **107** and **108**) without a piperazine moiety in the spacer (K_i values from 0.60 to 0.82 nM), indicating that the involvement of piperazine moiety in the linker favors the interaction with the M_2 receptor in this set of compounds.

The effect on [^{3}H]NMS M_2R equilibrium binding of the third subset of compounds, comprising the 'DIBA-4-DAMP' type heterodimeric ligands **99**, **116** and **117**, the 'DIBA-propantheline' type heterodimeric ligands **100**, **101**, **118** and **119** as well as the 'DIBA-DIBA' homodimeric ligands **112** and **113** are depicted in Figure 2C. The homo- or heterodimeric ligands, which contain long and basic spacers (**118**, K_i = 0.80 nM; **119**, K_i = 1.1 nM; **116**, K_i = 0.84 nM; **117**, K_i = 1.2 nM), had higher M_2 affinity compared to compounds with a short spacer (**99**, K_i = 2.2 nM; **100**, K_i = 2.1 nM; **101**, K_i = 5.8 nM). Moreover, the DIBA-derived homodimeric ligands **112** and **113**,

showed comparable affinities at M_2R (K_i value: 0.15 nM or 0.58 nM) with the heterodimeric ligands **116**-**119**, which also contained complex spacer moieties. This suggested that the ligands with bulky spacer moieties are even better tolerated by the M_2R than ligands containing the sample linkers in the sets of 'DIBA-4-DAMP' or 'DIBA-propantheline' type heterodimeric ligands.

A selection of the new dibenzodiazepinone heterodimeric ligands (compounds **97**, **98**, **99**, **100**, **101**, **102**, **106**, **108**, **111**, **115**, **117**, **119**, **120**) as well as the dibenzodiazepinone-type monomeric ligand **95** were also studied in equilibrium binding experiments with [^{3}H]NMS at the M receptor subtypes M_1, M_3, M_4 and M_5. The K_i values and hill slopes are included in Table 1. The [^{3}H]NMS displacement curves of ligand **97**, **106** and **115** at intact CHO-hMx cells (x = 1-5) are showed in Figure 2D-2F. All of these compounds showed a preference for the M_2 receptor, but high M_2R selectivity toward all of the other four subtypes wasn't found for any of the MR ligands. Affinities obtained for the subtypes M_1 and M_4 were higher than affinities for the subtypes M_3 and M_5. There was one exception, compound **100**, which showed the affinity pattern $M_2>M_1\approx M_5>M_3>M_4$. For the rest of compounds, the selectivity pattern can be concluded as $M_2>M_1\approx M_4>M_3\approx M_5$ (**98**, **99**, **101**, **102**, **106**, **111**, **117**); $M_2>M_1\approx M_4>M_3>M_5$ (**97**, **115**, **119**, **120**) and $M_2>M_1\approx M_4>M_5>M_3$ (**95**, **108**). With the excellent K_i value of 0.08 nM at the M_2R, compound **97** showed the best M_2R selectivity among the investigated ligands, the K_i value of **97** at the M_1R was 23-fold higher, at the M_4R 31-fold higher and the affinity to M_3R and M_5R was considerably lower with K_i ratios of 175 and 425, respectively. Compared to **97**, the MR antagonist tripitramine[57], containing three pyridobenzodiazepinone moieties, and the monomeric pyridobenzodiazepinone derivative AF-DX 384 (compound **8**, *cf*. Figure 1A)[31] exhibit lower M_2R selectivities according to published data (K_i ratios $M_1R/M_2R/M_3R/M_4R/M_5R$: 6:1:142:24:125 and 5:1:11:1.5:90, respectively).

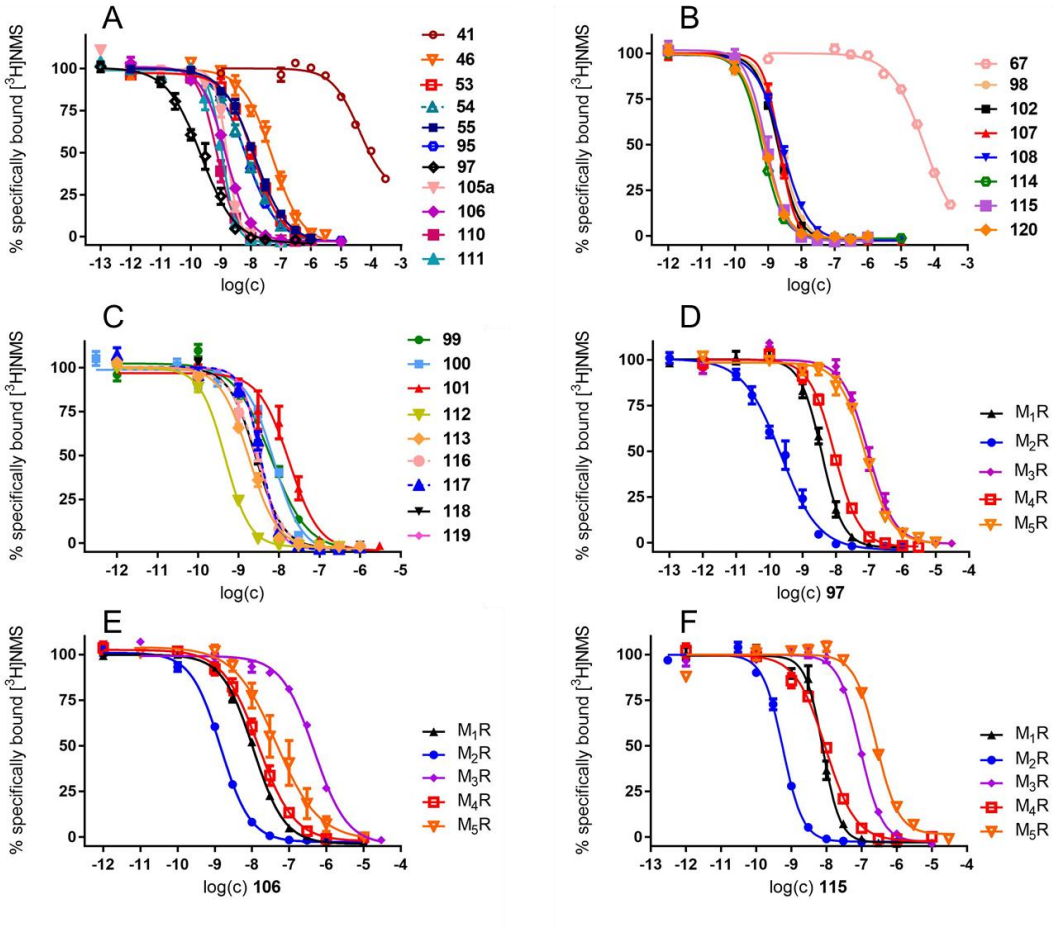

Figure 2. (A-C) Concentration-dependent effects of compounds **41**, **46**, **53**-**55**, **67**, **95**, **97**-**102**, **105a**, **106**-**108**, **110**-**120** on [^{3}H]NMS (c = 0.2 nM) equilibrium binding at intact CHO-hM_2 cells. (D-F) Concentration-dependent effects of the heterodimeric ligands **97** (D), **106** (E) and **115** (F) on equilibrium binding of [^{3}H]NMS (c = 0.2 nM (M_1, M_2, M_3), 0.1 nM (M_4) or 0.3 nM (M_5)) at intact CHO-hM_x cells (x = 1-5). Data analyzed by four-parameter logistic fits, represent mean values ± SEM from at least three independent experiments (performed in triplicate

Table 1. MR affinities (K_i values) of the monomeric xanomeline derivative **41**, TBPB derivative **67**, DIBA derivative **95**, the homodimeric ligands **112** and **113** ('DIBA-DIBA') and **46**, **53**-**55** ('xanomeline-xanomeline'), as well as the heterodimeric ligands **97**, **105a**, **106**, **110** and **111** ('DIBA-xanomeline'), **98**, **107**, **108**, **114** and **115** ('DIBA-TBPB'), **102** and **120** ('DIBA-77-LH-28-1'), **100**, **101**, **118** and **119** ('DIBA-propantheline') and **99**, **116** and **117** ('DIBA-4-DAMP') obtained from equilibrium competition binding studies with [^{3}H]NMS at live CHO-hMx cells (x = 1-5).

No.	M_1R		M_2R		M_3R		M_4R		M_5R	
	K_i (nM)	slope[a]	K_i (nM)	slope[a]	K_i (nM)	slope[a]	K_i (nM)	slope[a]	K_i (nM)	slope[a]
41	n.d.	n.d.	14000 ± 480	-1.0 ± 0.09	n.d.	n.d.	n.d.	n.d.	n.d.	n.d
46	53 ± 11	-1.0 ± 0.07	21 ± 6.6	-0.92 ± 0.18	50 ± 2.3	-0.95 ± 0.04	n.d.	n.d.	n.d.	n.d.
53	5.9 ± 1.0	-0.89 ± 0.10	4.0 ± 1.4	-0.94 ± 0.08	7.3 ± 0.69	-1.1 ± 0.03	n.d.	n.d.	n.d.	n.d.
54	4.5 ± 0.55	-1.3 ± 0.05	2.3 ± 0.05	-0.84 ± 0.07	n.d.	n.d.	n.d.	n.d.	n.d.	n.d.
55	24 ± 6.8	-1.2 ± 0.18	4.6 ± 1.3	-0.82 ± 0.10	n.d.	n.d.	n.d.	n.d.	n.d.	n.d.
67	n.d.	n.d.	1800 ± 810	-0.87 ± 0.04	n.d.	n.d.	n.d.	n.d.	n.d.	n.d.
95	67 ± 16	0.92 ± 0.08	2.2 ± 0.16	-0.87 ± 0.08	570 ± 75	-0.93 ± 0.20	9.2 ± 0.29	-0.8 ± 0.02	160 ± 66	-1.1 ± 0.15
97	1.8 ± 0.48	-1.5 ± 0.02	0.08 ± 0.02	-1.0 ± 0.05	14 ± 1.9	-1.2 ± 0.07	2.5 ± 0.02	-1.2 ± 0.05	34 ± 2.5	-1.1 ± 0.22
98	3.1 ± 0.32	-1.1 ± 0.05	0.77 ± 0.02	-1.4 ± 0.20	110 ± 26	-1.1 ± 0.07	3.2 ± 0.30	-1.2 ± 0.08	83 ± 13	-1.1 ± 0.20
99	26 ± 6.1	-1.0 ± 0.22	2.2 ± 0.12	-1.2 ± 0.17	38 ± 11	-1.35 ± 0.06	9.3 ± 4.2	-1.2 ± 0.13	54 ± 6.3	-1.1 ± 0.13
100	4.0 ± 0.78	-1.0 ± 0.12	2.1 ± 0.37	-1.1 ± 0.22	7.8 ± 1.0	-1.4 ± 0.09	14 ± 8.1	-1.0 ± 0.14	3.4 ± 0.51	-1.2 ± 0.10
101	33 ± 12	-1.4 ± 0.30	5.8 ± 2.3	-1.5 ± 0.22	100 ± 27	-0.85 ± 0.03	13 ± 4.4	-1.3 ± 0.13	92 ± 6.1	-1.1 ± 0.11
102	4.7 ± 0.83	-1.0 ± 0.05	0.60 ± 0.13	-1.4 ± 0.22	140 ± 11	-1.0 ± 0.09	3.0 ± 0.23	-1.4 ± 0.07	95 ± 16	-1.0 ± 0.25
105a	5.2 ± 0.89	-1.5 ± 0.17	0.51 ± 0.06	-2.2 ± 0.05	63 ± 5.5	-1.3 ± 0.16	n.d.	n.d.	n.d.	n.d.
106	4.7 ± 0.36	-1.1 ± 0.05	0.46 ± 0.03	-1.1 ± 0.06	140 ± 10	-0.93 ± 0.04	3.5 ± 1.8	-0.94 ± 0.07	100 ± 22	-1.2 ± 0.19
107	4.9 ± 0.33	-1.5 ± 0.05	0.71 ± 0.11	-1.9 ± 0.05	61 ± 9.0	-1.0 ± 0.09	n.d.	n.d.	n.d.	n.d.
108	19 ± 3.1	-1.2 ± 0.23	0.82 ± 0.17	-1.1 ± 0.13	610 ± 120	-1.01 ± 0.03	7.7 ± 1.8	-0.85 ± 0.08	140 ± 33	-1.3 ± 0.10
110	1.8 ± 0.47	-1.3 ± 0.31	0.26 ± 0.08	-1.8 ± 0.09	19 ± 6.3	-1.28 ± 0.04	n.d.	n.d.	n.d.	n.d.
111	1.6 ± 0.29	-1.6 ± 0.03	0.35 ± 0.03	-2.4 ± 0.15	14 ± 0.71	-0.99 ± 0.04	1.3 ± 0.19	-1.1 ± 0.14	7.4 ± 0.26	-1.0 ± 0.11
112	2.5 ± 0.56	-2.1 ± 0.19	0.15 ± 0.02	-1.5 ± 0.13	17 ± 2.0	-1.3 ± 0.10	n.d.	n.d.	n.d.	n.d.
113	3.5 ± 0.59	-1.7 ± 0.34	0.58 ± 0.07	-1.3 ± 0.07	13 ± 2.1	-1.2 ± 0.08	n.d.	n.d.	n.d.	n.d.
114	1.9 ± 0.37	-1.2 ± 0.07	0.20 ± 0.03	-1.4 ± 0.12	17 ± 1.1	-1.2 ± 0.05	n.d.	n.d.	n.d.	n.d.
115	3.3 ± 0.90	-1.6 ± 0.15	0.37 ± 0.05	-1.8 ± 0.15	28 ± 2.4	-1.4 ± 0.10	2.4 ± 0.12	-1.0 ± 0.05	110 ± 8.9	-1.3 ± 0.14
116	6.0 ± 0.66	-1.3 ± 0.19	0.84 ± 0.35	-1.6 ± 0.23	77 ± 36	-1.3 ± 0.08	n.d.	n.d.	n.d.	n.d.
117	4.8 ± 0.69	-1.5 ± 0.14	1.2 ± 0.19	-2.1 ± 0.16	30 ± 2.9	-1.3 ± 0.09	2.9 ± 0.52	-1.5 ± 0.32	24 ± 3.1	-1.5 ± 0.12
118	5.2 ± 1.8	-1.7 ± 0.19	0.80 ± 0.35	-1.5 ± 0.31	29 ± 4.1	-1.2 ± 0.12	n.d.	n.d.	n.d.	n.d.
119	3.9 ± 1.3	-1.1 ± 0.07	1.1 ± 0.19	-2.3 ± 0.17	19 ± 2.6	-1.2 ± 0.13	4.7 ± 0.22	-1.4 ± 0.06	43 ± 8.6	-1.0 ± 0.12
120	3.6 ± 0.69	-1.7 ± 0.20	0.24 ± 0.02	-1.3 ± 0.13	13 ± 0.76	-1.42 ± 0.09	3.8 ± 0.72	-1.5 ± 0.20	42 ± 1.0	-1.1 ± 0.22

[a]Curve slope of the four-parameter logistic fit. Mean values ± SEM from 3-5 independent experiments (each performed in triplicate). K_d values[55] / applied concentrations of [^{3}H]NMS: M_1: 0.12 / 0.2 nM; M_2: 0.090 / 0.2 nM; M_3: 0.089 / 0.2 nM; M_4: 0.040 / 0.1 nM; M_5: 0.24 / 0.3 nM.

3.2.3. Functional studies

The heterodimeric dibenzodiazepinone derivatives **106** and **115** were investigated in an IP accumulation assay using HEK-293 cells transiently transfected with the human M_2R and the hybrid G-protein $G\alpha q_{i5\text{-}HA}$. Compound **1** caused a concentration-dependent increase in IP1 accumulation with a pEC_{50} of 6.93 ± 0.09 (n = 8). By contrast, **106** and **115** did not induce an IP1 accumulation when studied in agonist mode (*cf*. Figure 3A), that is, both compounds were not capable of stabilizing a G-protein activating conformation of the M_2R. To allow an estimation of the inhibitory potency of **106** and **115**, we tested the ability of compounds **7**, **106** and **115** to antagonize the effect of **1** at a concentration corresponding to EC_{80} (0.3 µM). Compounds **7**, **106** and **115** completely inhibited the IP1 accumulation elicited by **1** proving that these compounds are M_2R antagonists as previously reported for **8**[34] (*cf*. Figure 3B).

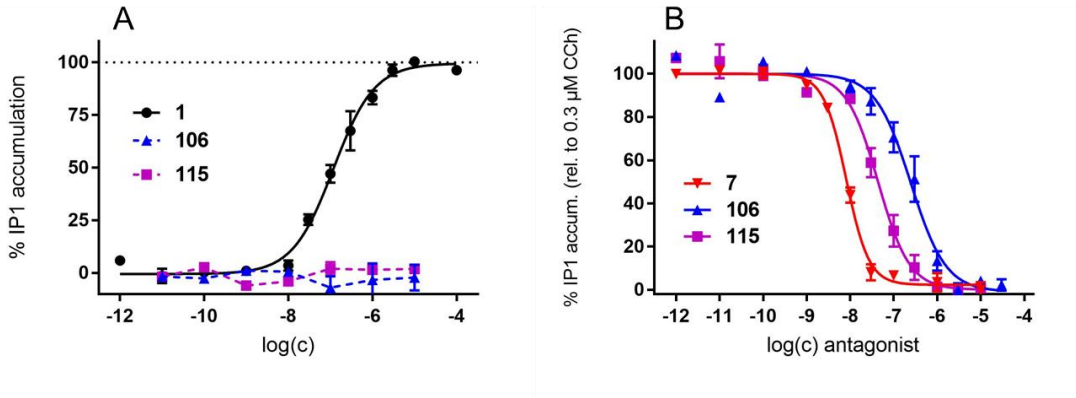

Figure 3. Investigation of M_2R agonism and antagonism of compounds **106** and **115** in an IP1 accumulation assay using HEK-hM_2-G_{qi} cells. (A) Concentration-dependent effect of **1**, **106** and **115** on the accumulation of IP1. **106** and **115** elicited no response. pEC_{50} of **1**: 6.93 ± 0.09 (mean ± SEM from eight independent experiments performed in triplicate). (B) Concentration-dependent inhibition of the IP1 accumulation (induced by **1**, 0.3 µM) by **7**, **106** and **115**. Corresponding pK_b values: **7**: 8.63, **106**: 7.16, **115**: 7.91. Data represent the means ± SEM from at least five independent experiments (each performed in triplicate).

3.2.4. Synthesis and characterization of the radiolabeled ligands [^{3}H]106 and [^{3}H]115

Aiming at the preparation of the high-affinity propionamides **106** and **115** in their tritiated form, the stabilities of **106** and **115** in aqueous solution were investigated at pH 7.4 in PBS over 48 h. The compounds proved to be stable under these conditions (*cf*. Figure 4). For the synthesis of [^{3}H]**106** and [^{3}H]**115** an excess of the precursor amines **105a** or **114** was treated with succinimidyl [^{3}H]propionate to afford [^{3}H]**106** with a radiochemical yield of 36% and a specific activity of 2.420 TBq/mmol, and [^{3}H]**115** with a radiochemical yield of 35% and a specific activity of 1.815 TBq/mmol. The radioligands were obtained in high radiochemical purities (98% and 99%, respectively; *cf*. Figure 5B and 5D). Quality controls by RP-HPLC after ten months

of storage as solution in ethanol at -20 °C revealed an excellent stability of [^{3}H]**115** and approximately 10% decomposition of [^{3}H]**106** (*cf*. Figure 5C and 5E).

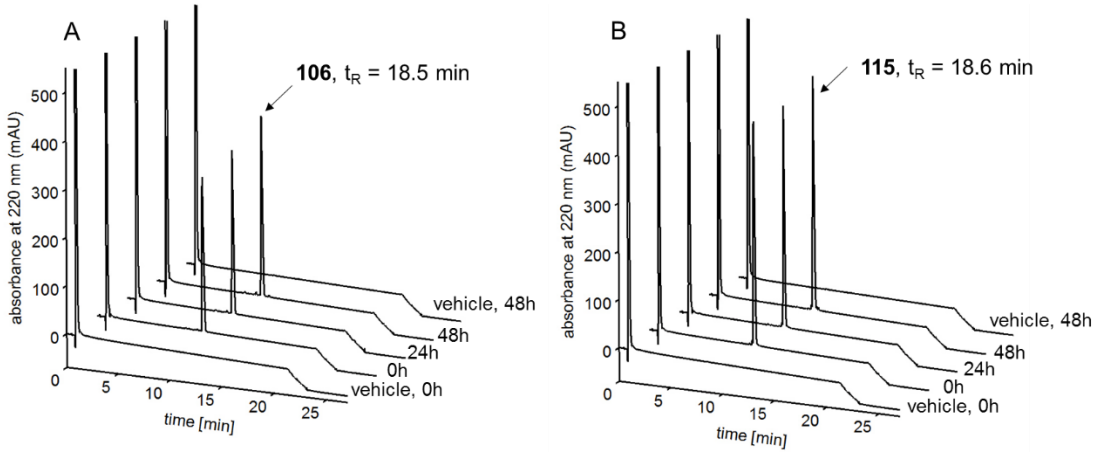

Figure 4. HPLC analysis of **106** (A) and **115** (B) after incubation in PBS (pH = 7.4) at 23 °C for up to 48 h. **106** and **115** showed no decomposition. HPLC conditions see experimental section.

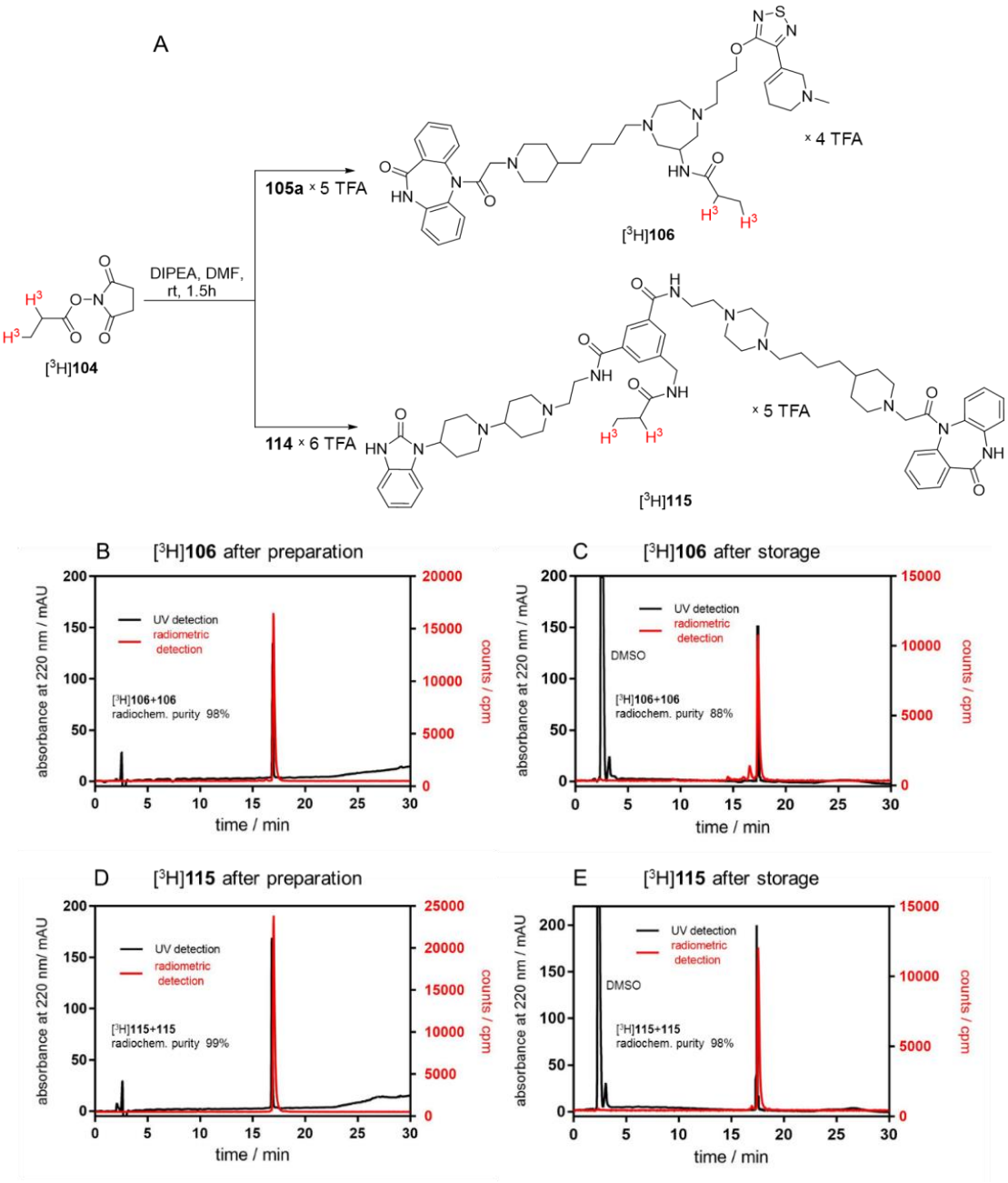

Figure 5. Preparation, purity and identity control of the radiolabeled dibenzodiazepinone derivatives [^{3}H]**106** and [^{3}H]**115**. (A) Synthesis of [^{3}H]**106** and [^{3}H]**115** by [^{3}H]propionylation of the amine precursors **105a** and **114**, respectively, using succinimidyl [^{3}H]propionate ([^{3}H]**104**). (B, C) HPLC analysis of [^{3}H]**106** (B: 0.18 µM, C: 0.17 µM) spiked with "cold" **106** (3 µM), analyzed 3 days after synthesis and after 10 months of storage at -20 °C in EtOH/H_2O (1:1). (D, E) HPLC analysis of [^{3}H]**115** (D: 0.23 µM, E: 0.23 µM) spiked with "cold" **115** (3 µM), analyzed 3 days after synthesis and after 10 months of storage at -20 °C in EtOH/H_2O (1:1). HPLC conditions see experimental section.

3.2.5. Characterization of [^{3}H]106 and [^{3}H]115

Initially, saturation binding experiments with the tritiated radioligands [^{3}H]**106** and [^{3}H]**115** were performed on intact adherent CHO-hM_2 cells in white-transparent 96-wells plates revealing K_d values of 1.5 and 0.37 nM, respectively (mean values from at least three independent

experiments performed in triplicate) (*cf*. Figure 6B and 6D). At concentrations around the K_d value, unspecific binding amounted to approx. 40% ([^{3}H]**106**) and 30% ([^{3}H]**115**) of total binding. Saturation binding studies with [^{3}H]**106** and [^{3}H]**115** performed at CHO-hM_2 cell homogenates, precluding the detection of unspecific binding of the radioligand to the microplate, resulted in lower unspecific binding (< 25% of total binding at K_d) and yielded binding constants of 1.1 and 0.12 nM, respectively (*cf*. Figure 6A and 6C). Because of the higher ratio of specific over unspecific binding when using cell homogenates, further studies (association and dissociation kinetics, competition binding experiments and saturation binding of [^{3}H]**115** in the presence of the allosteric modulator (**15**) were performed with CHO-hM_2 cell homogenates.

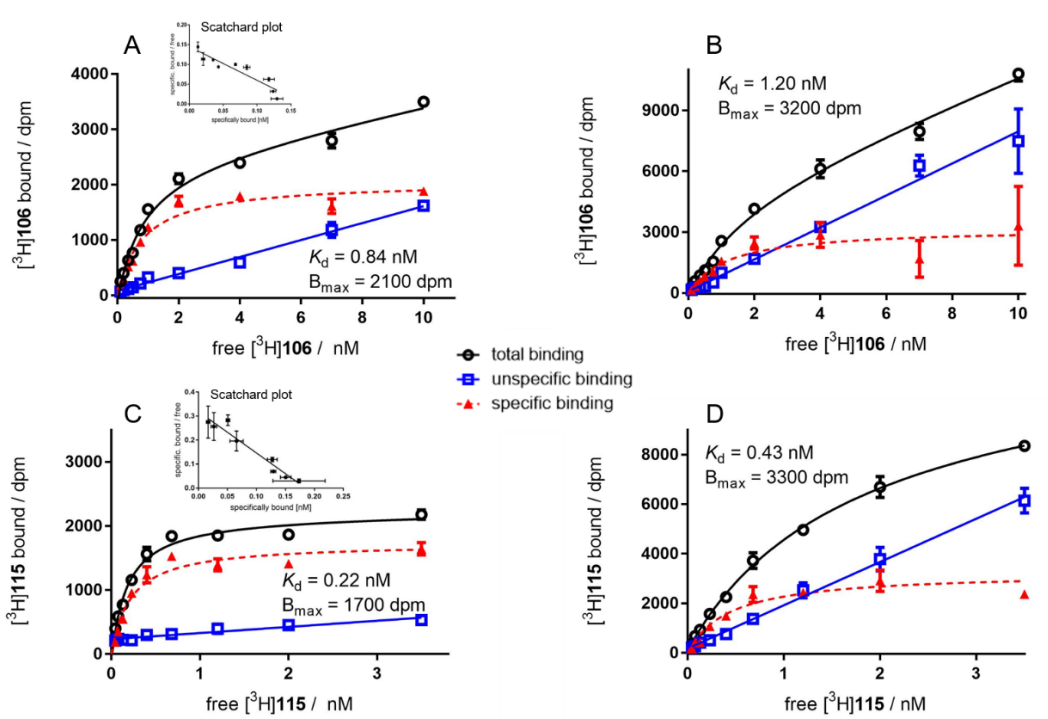

Figure 6. Representative saturation isotherms of specific M_2R binding (shown in dashed line) of [^{3}H]**106** (A, B) and [^{3}H]**115** (C, D) obtained from experiments either performed with CHO-hM_2 cell homogenates (A, C) or live adherent CHO-hM_2 cells (B, D). Non-specific binding (shown in blue) was determined in the presence of the orthosterically binding MR antagonist atropine (500-fold excess). Experiments were performed in triplicate. Specific binding data were analyzed by an equation describing a one-site binding. Error bars of specific binding and error bars in the Scatchard plots represent propagated errors calculated according to the Gaussian law of errors. Error bars of total and nonspecific binding represent the SEM.

To be noticed, as the orthosteric antagonist **7**, used to determine unspecific binding in saturation binding studies, was able to completely prevent one-site (monophasic) specific binding of [^{3}H]**106** and [^{3}H]**115** to the M_2R, these data strongly suggest that the heterodimeric dibenzodiazepinone-type MR ligands **106** and **115** address the orthosteric binding site of the M_2R.

The association of both, [^{3}H]**106** and [^{3}H]**115**, to the M_2R was monophasic and resulted in

comparable k_{on} values (*cf*. Figure 7A and 7C, Table 2). Plateaus were reached after approximately 40 min and 20 min, respectively. With a half-life of 53 min, [^{3}H]**106** completely dissociated from the M_2R. By contrast, the dissociation of [^{3}H]**115** was incomplete, reaching a plateau at 48% of initially bound radioligand, with a half-life of 32 min (*cf*. Figure 7B and 7D). This result suggests in part a (pseudo)irreversible (long lasting) binding of [^{3}H]**115**. One reason could be conformational adjustments of the receptor upon ligand binding[58], another reason might be an enhanced rebinding capability of the dimeric ligand by a simultaneous interaction with two or more binding sites[59]. The kinetically derived dissociation constants K_d(kin), calculated according to K_d(kin) = k_{off}/k_{on}, amounted to 0.33 nM for [^{3}H]**106** and 0.057 nM for [^{3}H]**115** and were in good agreement with the K_d values obtained from saturation binding experiments ([^{3}H]**106**: K_d = 1.1 nM, [^{3}H]**115**: K_d = 0.12 nM), indicating that both radioligands follow (in part) the law of mass action[60]. An overview of the M_2R binding characteristics of [^{3}H]**106** and [^{3}H]**115** is provided in Table 2.

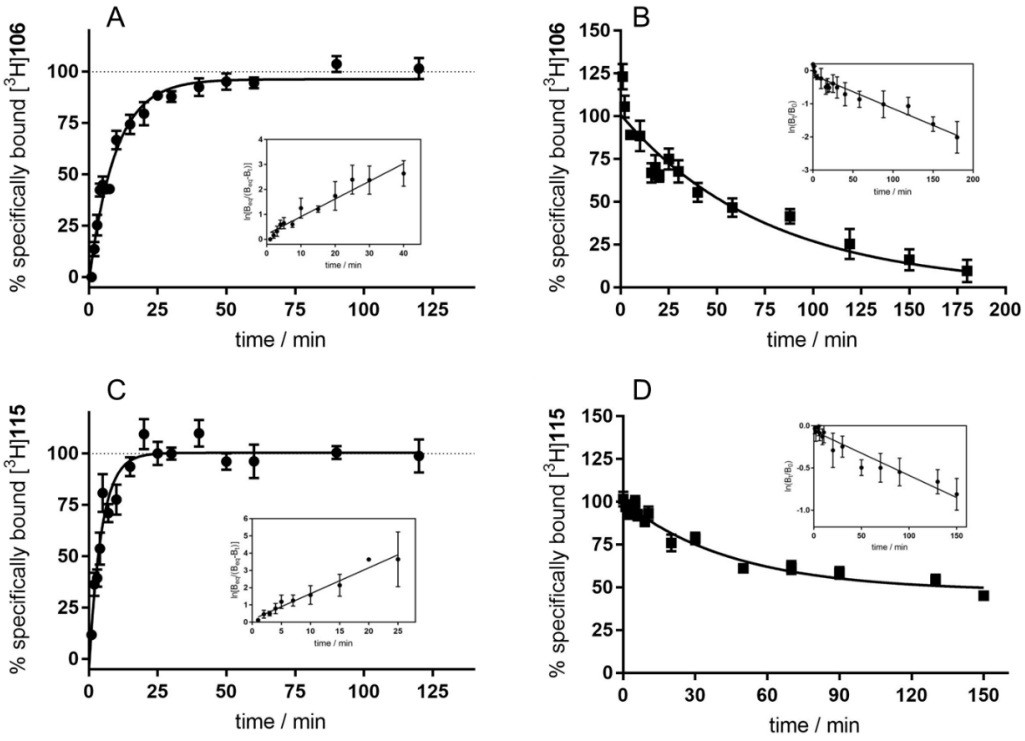

Figure 7. Association and dissociation kinetics of [^{3}H]**106** (A, B) and [^{3}H]**115** (C, D) determined at CHO-hM_2 cell homogenates at 23 °C. (A) Association of [^{3}H]**106** (c = 2.0 nM) to the M_2R. Inset: ln[$B_{eq}/(B_{eq}-B_t)$] versus time, k_{obs} = slope = 0.071 min^{-1}. (B) Dissociation of [^{3}H]**106** (preincubation: 4 nM, 1 h) from the M_2R determined in the presence of atropine (1000-fold excess); monophasic exponential decline, $t_{1/2}$ = 53 min. Inset: ln[B_t/B_0] versus time. Slope·(−1) = k_{off} = 0.010 min^{-1}. (C) Association of [^{3}H]**115** (c = 0.6 nM) to the M_2R. Inset: ln[$B_{eq}/(B_{eq}-B_t)$] versus time, k_{obs} = slope = 0.15 min^{-1}. (D) Dissociation of [^{3}H]**115** (preincubation: 0.6 nM, 1 h) from the M_2R determined in the presence of atropine (1000-fold excess), monophasic exponential decline, $t_{1/2}$ = 32 min. Inset: ln[B_t/B_0] versus time. Slope·(−1) = k_{off} = 0.005 min^{-1}. Data represent the mean ± SEM from three (A, B, D) or two (C) independent experiments (each performed in triplicate).

Table 2. M_2R binding characteristics of [^{3}H]**106** and [^{3}H]**115**.

radio-ligands	Saturation binding		Binding kinetics		
	K_d [nM][a]	K_d [nM][b]	K_d(kin) [nM][c]	k_{on} [$min^{-1}nM^{-1}$][d]	k_{off} [min^{-1}][e] $t_{1/2}$ [min][e]
[^{3}H]**106**	1.5 ± 0.26	1.1 ± 0.20	0.33 ± 0.08	0.044 ± 0.009	0.013 ± 0.001 53 ± 6
[^{3}H]**115**	0.37 ± 0.03	0.12 ± 0.02	0.057 ± 0.0004	0.32 ± 0.03	0.019 ± 0.0008 32 ± 2

[a]Dissociation constant determined by saturation binding at live CHO-hM_2R cells; mean ± SEM from three independent experiments (performed in triplicate). [b]Dissociation constant determined by saturation binding at CHO-hM_2 cell homogenates; mean ± SEM from at least three independent experiments (performed in triplicate). [c]Kinetically derived dissociation constant ± propagated error (K_d(kin) = k_{off}/k_{on}). [d]Association rate constant ± propagated error, calculated from k_{obs}, k_{off} and the applied radioligand concentration (*cf*. experimental section). [e]Dissociation rate constant and half-life; mean ± SEM from three independent experiments (performed in triplicate).

3.2.6. M_2R equilibrium competition binding with [^{3}H]106 and [^{3}H]115

Figure 8A shows the concentration-dependent effects of the orthosteric MR antagonists **7** and **11** as well as of the allosteric modulator **15** on M_2R equilibrium binding of [^{3}H]**106**, and Figure 8B presents the concentration-dependent effects of various reported orthosteric (**2**, **7**), allosteric (**14**, **15**, **16**) and dualsteric (**8**, **11**) MR ligands as well as **115** on M_2R equilibrium binding of [^{3}H]**115**. All investigated compounds were capable of totally inhibiting (displacing) specific M_2R binding of [^{3}H]**106** or [^{3}H]**115**, suggesting either a competitive mechanism or a strongly negative cooperativity between the studied compounds and the radiolabeled dibenzodiazepinone derivatives[61]. Generally, K_i values obtained from equilibrium competition binding experiments with [^{3}H]**106** and [^{3}H]**115** were in good agreement with reported K_i values (*cf*. Table 3). However, K_i values determined with [^{3}H]**106** and [^{3}H]**115** were consistently higher than K_i values from competition binding experiments with [^{3}H]NMS (compounds **2**, **7**, **8**, **11**, *cf*. Table 3). The reason for this discrepancy might be due to a multivalent binding mode of the heterodimeric radioligand (reflected by an in part long-lasting binding), therefore, higher competitor concentrations were required for the displacement of [^{3}H]**115**. Equilibrium competition binding experiments with [^{3}H]**115** and **8**, as well as with [^{3}H]**115** and **11**, were also performed after preincubation of CHO-hM_2 cell homogenates with **8** or **11** for 90 min. However, incubation with the competitors prior to the addition of [^{3}H]**115** did not result in an increase in the apparent affinities of **8** and **11** (*cf*. Figure 9).

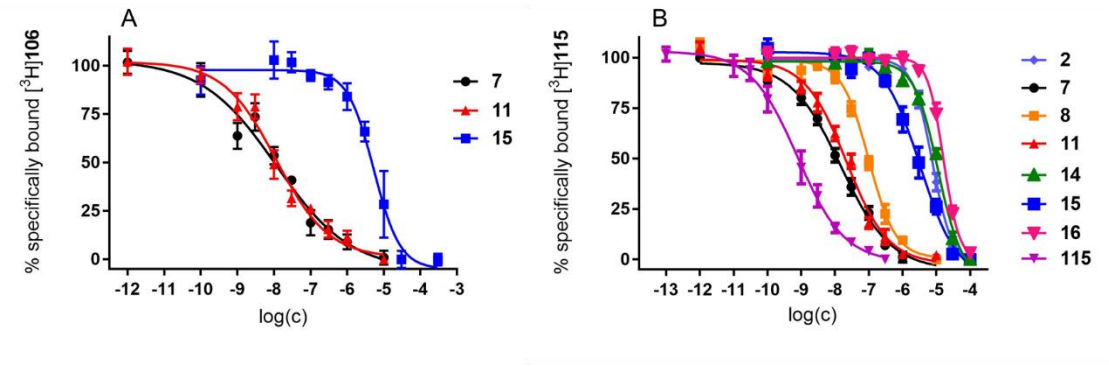

Figure 8. Concentration-dependent effects of various reported orthosteric (**2**, **7**), dualsteric (**8**, **11**), allosteric (**14**, **15** and **16**) MR ligands and **115** on M_2R equilibrium binding of [^{3}H]**106** (c = 2.0 nM, K_d = 1.1 nM) (A) and [^{3}H]**115** (c = 0.3 nM, K_d = 0.12 nM) (B) determined at CHO-hM_2 cell homogenates at 22 °C. Data analyzed by four-parameter logistic fits, represent mean values ± SEM from at least three independent experiments (performed in triplicate).

Table 3. Comparison of M_2R binding data (K_i or IC_{50} values) of various orthosteric (**2**, **7**), allosteric (**14**, **15** and **16**), dualsteric (**8**, **11**) MR ligands and **115** determined with [^{3}H]**106**, [^{3}H]**115** or [^{3}H]NMS

ligand	[^{3}H]**106** K_i [nM][a]	[^{3}H]**115** K_i [nM][a]	[^{3}H]NMS K_i* or IC_{50}** [nM]
2	-	2300 ± 260	210 ± 59*[b]
7	2.8 ± 0.60	4.6 ± 1.6	0.94 ± 0.19*[b]
8	-	29 ± 9.6	2.0 ± 0.21*[b]
11	5.2 ± 2.9	6.3 ± 1.3	0.79 ± 0.10*[b]
14	-	3500 ± 570	2200 ± 410**[c]
15	1800 ± 900	1200 ± 530	460 ± 130**[c]
16	-	4900 ± 210	>10000**[c]
115	-	0.34 ± 0.15	0.37 ± 0.05*[b]

[a]Determined by equilibrium competition binding with [^{3}H]**106** (c = 2 nM) or [^{3}H]**115** (c = 0.3 nM) at CHO-hM_2 cell homogenates; mean values ± SEM from at least three independent experiments (performed in triplicate). [b]Determined by equilibrium competition binding with [^{3}H]NMS (c = 0.2 nM) at live CHO-hM_2 cells; mean ± SEM from at least three independent experiments (performed in triplicate). [c]IC_{50} values obtained from nonlinear four-parameter logistic curve analyses of data characterizing the inhibition of [^{3}H]NMS (c = 0.2 nM) equilibrium binding at live CHO-hM_2 cells; mean ± SEM from at least three independent experiments (performed in triplicate).

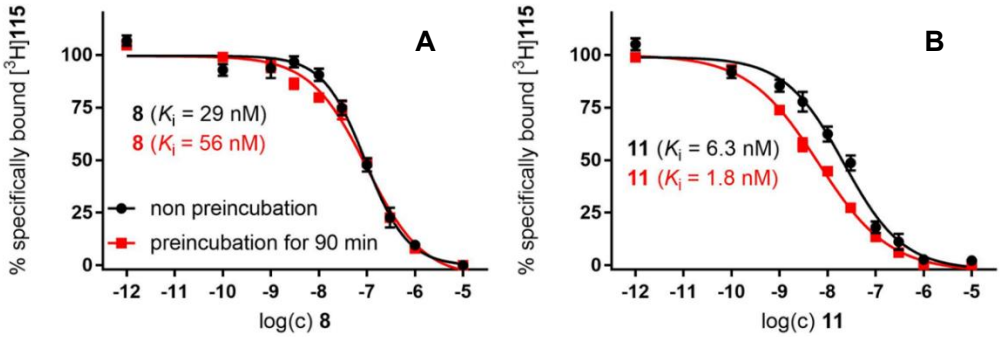

Figure 9. Concentration-dependent effects of MR ligands **8** (A) and **11** (B) on M_2R equilibrium binding of [^{3}H]**115** (c = 0.3 nM, K_d = 0.12 nM) determined at CHO-hM_2 cell homogenates at 22 °C, **8** or **11** was preincubated with the M_2R for 90 min before the addition of [^{3}H]**115**. Data analyzed by four-parameter logistic fits, represent mean values ± SEM from three independent experiments (performed in triplicate).

3.2.7. Schild-like analysis with allosteric modulator 15 at the M_2R using [^{3}H]115

Competition binding studies with [^{3}H]NMS and **106**, and [^{3}H]NMS and **115** at the M_2R, as well as M_2R saturation binding experiments with [^{3}H]**106** and [^{3}H]**115** (see above) suggested that the dibenzodiazepinone-type heterodimeric ligands **106** and **115** bind to the orthosteric site of the M_2R. Furthermore, competition binding experiments with [^{3}H]**106** or [^{3}H]**115** at the M_2R, for instance with the allosteric modulator **15**, resulting in sigmoidal curves which reached 0% specific binding of the dimeric radioligands, indicated binding of [^{3}H]**106** and [^{3}H]**115** to the allosteric vestibule of the M_2R. In order to substantiate the hypothesis of dualsteric binding of dibenzodiazepinone-type heterodimeric ligands such as **115** at the M_2R, saturation binding studies with [^{3}H]**115** were performed in the presence of the allosteric modulator **15** (*cf*. Figure 10). This kind of experiment is equivalent to the Schild analysis used to investigate the inhibiting effect of a receptor antagonist on the response elicited by an agonist and is considered the experiment of choice to unveil competitive or non-competitive mechanisms[62-65]. For instance, it was used to prove the competitive interplay between the allosteric modulator brucine and the pirenzepine derived fluorescent tracer Bo(22)Pz at M_1R[62]. As becomes obvious from Figure 10A the presence of **15** led to a parallel rightward shift of the saturation isotherms of [^{3}H]**115**. A plot of log(affinity shift - 1) versus log(concentration of **15**) yielded a straight line ('Schild' regression, *cf*. Figure 10B) with a slope not different from unity (slope = 0.97 ± 0.06, P > 0.5), indicating a competitive interaction between [^{3}H]**115** and the allosteric modulator **15**, and thus suggesting again a dualsteric binding of **115** at the M_2R. The 'pA_2' value (7.05 ± 0.23) derived from the 'Schild' regression was in accordance with the pK_i value (6.06 ± 0.27) from equilibrium competition binding studies with [^{3}H]**115** and **15** as well as with reported M_2R binding data of **15** (pK_A 6.00/6.53[35]).

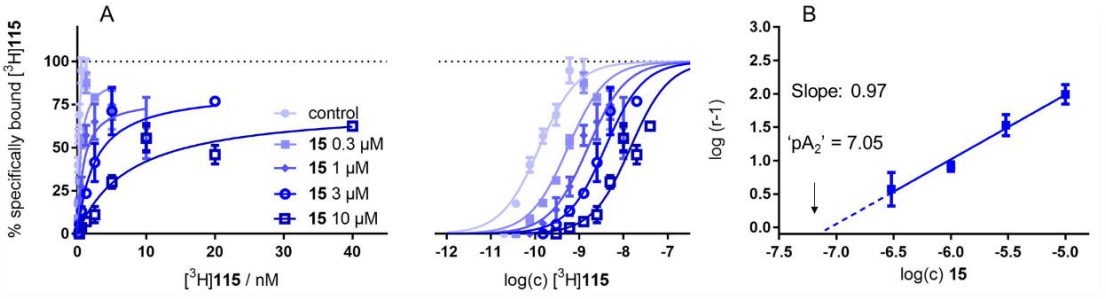

Figure 10. Effect of the allosteric modulator **15** on saturation binding of [^{3}H]**115** determined at CHO-hM_2 cell homogenates at 22 °C. (A) Saturation isotherm of specific radioligand binding plotted in linear and in semi-logarithmic scale. (B) "Schild" regression resulting from the rightward shifts (ΔpK_d) of the saturation isotherms (log(r-1) plotted vs. log(concentration **15**), where r = $10^{\Delta pKd}$). The presence of compound **15** led to a parallel rightward shift of the saturation isotherms of [^{3}H]**115**. The slope of the linear "Schild" regression was not different from unity (P > 0.5, based on the slope mean value ± SEM (0.97 ± 0.06) from three sets of independent saturation binding experiments (performed in triplicate))

indicating a competitive interaction between [^{3}H]**115** and **15**. Data represent mean values ± SEM from three independent experiments (each performed in triplicate).

3.3. Conclusion

The present study focused on the synthesis and characterization of a series of dibenzodiazepinone-type dimeric MR ligands comprising two homodimeric ligands ('DIBA-DIBA') and nineteen heterodimeric ligands (5 × 'DIBA-xanomeline', 5 × 'DIBA-TBPB', 2 × 'DIBA-77-LH-28-1', 4 × 'DIBA-propantheline' and 3 × 'DIBA-4-DAMP'). The most interesting finding was that all of these DIBA-derived dimeric ligands exhibited high M_2R affinities (K_i values: 0.08-5.8 nM, *cf*. Table 1), i.e. variation of the type of the linker (short vs. long, basic vs. non-basic, etc.) and the second pharmacophoric group had almost no impact on M_2R binding. In other words, it was surprising that the bulky 'side chain' attached to the dibenzodiazepinone moiety did hardly influence or disturb M_2R binding. As the monomeric and dimeric reference compounds (**41**, **46**, **53**-**55**, **67**), devoid of the dibenzodiazepinone moiety, exhibited considerably lower M_2R affinity compared with the DIBA-derived ligands, the high M_2R affinity of the heterodimeric dibenzodiazepinone-type ligands is most likely mediated by the 'dibenzodiazepinone' pharmacophore, which presumably binds to the orthosteric site of the M_2R. The 'DIBA-xanomeline' type heterodimeric ligand **97** displayed the highest M_2R affinity (K_i 0.08 nM) and exhibited the highest M_2 subtype preference within the series of presented MR ligands. Two tritium-labeled heterodimeric M_2R ligands ([^{3}H]**106** and [^{3}H]**115**) were prepared and characterized by saturation binding experiments, kinetic studies and equilibrium competition binding with various MR ligands. With a K_d value of 0.12 nM and high chemical stability, [^{3}H]**115** proved to be an interesting new molecular tool for studying muscarinic receptors and MR ligands. The results from various M_2R binding experiments with [^{3}H]**115**, in particular saturation binding studies in the absence or presence of the allosteric MR ligand W84 (**15**), strongly indicated a simultaneous interaction of **115** with the orthosteric and the 'common' allosteric binding site, i.e a dualsteric binding mode at the M_2R. This work suggests dibenzodiazepinone-type MR ligands as an interesting compound class to develop highly selective M_2R ligands according to the dualsteric (bitopic) ligand approach.

3.4. Experimental section

3.4.1. Chemistry

3.4.1.1. General experimental conditions

Commercial reagents and chemicals were purchased from Acros Organics (Geel, Belgium), IRIS Biotech GmbH (Marktredwitz, Germany), Alfa Aesar GmbH & Co. KG (Karlsruhe,

Germany), Merck KGaA (Darmstadt, Germany), Sigma-Aldrich Chemie GmbH (Munich, Germany), TCI Europe (Zwijndrecht, Belgium), MP Biomedicals (Eschwege, Germany), Absource Diagnostic (Munich, Germany) or Abcam (Cambridge, UK) and used without further purification. Technical grade solvents (acetone, ethyl acetate, light petroleum (40-60 °C) and dichloromethane) were distilled before use. Deuterated solvents for NMR spectroscopy were from Deutero GmbH (Kastellaun, Germany). Acetonitrile for HPLC (gradient grade) was obtained from Merck (Darmstadt, Germany). Anhydrous DMF was purchased from Sigma-Aldrich Chemie GmbH. The radiolabeled MR antagonist [^{3}H]NMS (specific activity = 80 Ci/mmol) was purchased from American Radiolabeled Chemicals Inc. (St. Louis, MO) via Hartman Analytics GmbH (Braunschweig, Germany). Millipore water was used throughout for the preparation of buffers and HPLC eluents. If moisture-free conditions were required, reactions were performed in dried glassware under inert atmosphere (argon). Anhydrous THF was obtained by distillation over sodium, and anhydrous CH_2Cl_2 was prepared by distillation over P_2O_5 after predrying over $CaCl_2$. Reactions were monitored by TLC using aluminum plates coated with silica gel (Merck silica gel 60 F254, thickness 0.2 mm). Spots were detected by UV light (254 nm or 366 nm) or by staining using a 0.3% solution of ninhydrine in n-butanol (amines) or iodine. Flash chromatography was performed in glass columns on silica gel (Merck silica gel 60, 40-63 µm). Polypropylene reaction vessels (1.5 or 2 mL) with screw cap (Süd-Laborbedarf, Gauting, Germany) were used for the synthesis of radioligands ([^{3}H]**106** and [^{3}H]**115**), for small scale reactions, for the investigation of chemical stabilities (**106**, **115**) and for the preparation and storage of stock solutions. All melting points are uncorrected and were measured with a Büchi 530 (Büchi GmbH, Essen, Germany) apparatus. Microwave assisted reactions were performed with an Initiator 2.0 synthesizer (Biotage, Uppsala, Sweden).

NMR spectra were recorded on a Bruker Avance 300 (7.05 T, 1H: 300.1 MHz, 13C: 75.5 MHz), Bruker Avance III HD 400 (9.40 T, 1H: 400 MHz, 13C: 100 MHz) or a Bruker Avance III HD 600 equipped with a cryogenic probe (14.1 T 1H: 600.1 MHz, 13C: 150.9 MHz) (Bruker, Karlsruhe, Germany) with TMS as external standard. Abbreviations for the multiplicities of the signals: s (singlet), d (doublet), t (triplet), dd (doublet of doublet), q (quartet), m (multiplet), brs (broad singlet). For compound **97**, **106** and **115**, 2D-NMR techniques (^{1}H-COSY, HSQC, HMBC) were used to assign ^{1}H and ^{13}C chemical shifts. IR spectra were measured with a NICOLET 380 FT-IR spectrophotometer (Thermo Electron Corporation). Low-resolution mass spectrometry (MS) was performed on a Finnigan SSQ 710A instrument (CI-MS) (Thermo Finnigan, San Jose, CA). High-resolution mass spectrometry (HRMS) analysis was performed on an Agilent 6540 UHD Accurate-Mass Q-TOF LC/MS system (Agilent Technologies, Santa Clara, CA) using an ESI source. Preparative HPLC was performed on a system from Knauer (Berlin, Germany) consisting of two K-1800 pumps and a K-2001 detector. A Kinetex-XB C18, 5 µm, 250 mm × 21 mm (Phenomenex, Aschaffenburg, Germany) served as stationary phase

at a flow-rate of 15 mL/min using mixtures of acetonitrile and 0.1% aq TFA as mobile phase. A detection wavelength of 220 nm was used throughout. Lyophilisation of the collected fractions was performed with an Alpha 2-4 LD apparatus (Martin Christ, Osterode am Harz, Germany) equipped with a RZ 6 rotary vane vacuum pump (Vacuubrand, Wertheim, Germany). Elemental analysis was performed with a Vario MICRO Cube elemental analyzer (Elementar Analysensysteme, Hanau, Germany). Analytical HPLC analysis was performed on a system from Merck-Hitachi (Hitachi, Düsseldorf, Germany) composed of a L-6200-A pump, an AS-2000A autosampler, a L-4000A UV detector, a D-6000 interface. A Kinetex-XB C18, 5 µm, 250 mm × 4.6 mm (Phenomenex, Aschaffenburg, Germany) was used as stationary phase at a flow rate of 0.8 mL/min. Mixtures of acetonitrile (A) and 0.1% aq TFA (B) were used as mobile phase (degassed by Helium purging). The following linear gradient was applied: 0-30 min: A/B 5:95-85:15, 30-32 min: 85:15-95:5, 32-40 min: 95:5. Detection was performed at 220 nm throughout. The oven temperature was 30 °C. The HPLC purity of all analyzed compounds was >95%.

Annotation concerning the NMR spectra (^{1}H, ^{13}C) of the dibenzodiazepinone derivatives (**92-102**, **105a, 106-108** and **110-120**): due to a slow rotation about the exocyclic amide group on the NMR time scale, two isomers (ratios provided in the experimental protocols) were evident in the ^{1}H- and ^{13}C-NMR spectra. The isolated DIBA-type homodimeric ligand **105b** was handed to Andrea Pegoli in our research group for further processing. In addition, the number of the TFA salts of the piperazine derivatives was identified by elemental analysis (compounds **97** and **117**).

3.4.1.2. Experimental protocols and analytical data

Ethyl 2-(benzylamino)-2-oxoacetate (21)[43]

Diethyl oxalate (**19**) (2.0 g, 13.68 mmol) was mixed in chloroform (100 mL) in a 250-mL three-necked round bottom flask. A solution of benzylamine (**20**) (1.3 g, 13.68 mmol) in chloroform (50 mL) was added slowly to the reaction mixture. The reaction mixture was refluxed overnight. The solid formed during the reaction was removed by filtration and discarded. The combined filtrate and washings were concentrated under reduced pressure to give compound **21** as yellow oil (1.8 g, 65%). After cooling in the refrigerator (ca. -20 °C) overnight the oil crystallized to form a yellow solid, m.p. 45-48 °C (Lit[43] m.p. 50-51 °C). R_f = 0.2 (light petroleum/ethyl acetate 6:1 v/v). ^{1}H-NMR (300 MHz, $CDCl_3$): δ (ppm) 1.38 (t, *J* 7.1 Hz, 3H), 4.34 (q, *J* 7.1 Hz, 2H), 4.52 (d, *J* 6.0 Hz, 2H), 7.27-7.39 (m, 5H), 7.41 (brs, 1H). ^{13}C-NMR (75 MHz, $CDCl_3$): 14.0, 43.9, 63.3, 127.9, 128.0, 128.9, 136.8, 156.5, 160.7. HRMS (ESI): *m/z* $[M+H]^+$ calcd. for $[C_{11}H_{14}NO_3]^+$ 208.0968, found: 208.0971. $C_{11}H_{13}NO_3$ (207.23).

***N*^{1}-Benzyl-*N*^{2}-methyloxalamide (22)[43]**

To a solution of compound **21** (1.0 g, 4.83 mmol) in abs. ethanol (20 mL) was added a 2 M solution of methylamine (3.62 mL, 7.24 mmol) in THF. A white solid was formed instantly. After 8 h, collected the solid by filtration, evaporation of the filtrate provided a second portion of product. Combined two portions of product to yield compound **22** as white powder (900 mg, 97%), m.p. 160-163 °C (Lit[43]. m.p. 184-185 °C), which was used without further purification. R_f = 0.3 (light petroleum/ethyl acetate 3:1 v/v).^{1}H-NMR (300 MHz, $CDCl_3$): δ (ppm) 2.91 (d, *J* 6.0 Hz, 3H), 4.49 (d, *J* 6.0 Hz, 2H), 7.25-7.38 (m, 5H), 7.55 (brs, 1H), 7.83 (brs, 1H). ^{13}C-NMR (75 MHz, $CDCl_3$): 26.2, 43.7, 127.8, 127.9, 128.8, 136.8, 159.7, 160.4. HRMS (ESI): *m/z* [*M*+H]$^+$ calcd. for $[C_{10}H_{13}N_2O_2]^+$ 193.0972, found: 193.0976. $C_{10}H_{12}N_2O_2$ (192.22).

***N*^{1}-Benzyl-*N*^{2}-methylethane-1,2-diamine (23)[43]**

Lithium aluminum hydride (143 mg, 3.77 mmol) was placed in a 50 mL three-necked round bottom flask with abs. THF (15 mL) under an atmosphere of argon. The suspension was immersed in an ice bath and compound **22** (290 mg, 1.51 mmol) dissolved in abs. THF (10 mL) was added to the solution dropwise. The reaction mixture was refluxed overnight. The flask was immersed in an ice bath for quenching, water (0.15 mL), 15% aq NaOH (0.45 mL) and water (0.15 mL) were added dropwise. The suspension was stirred at 0 °C for 30 min. Filtered the white solid, washed the white solid with chloroform (3 × 10 mL). The filtrate was concentrated under reduced pressure to give the crude product, which was subjected to flash column chromatography (eluent: CH_2Cl_2/MeOH/25% aq NH_3 90:3:1 v/v/v) to provide compound **23** as colorless oil (150 mg, 60%). R_f = 0.3 (CH_2Cl_2/MeOH/25% aq NH_3 90:9:1 v/v/v). ^{1}H-NMR (300 MHz, $CDCl_3$): δ (ppm) 1.91 (s, 2H), 2.39 (s, 3H), 2.64-2.71 (m, 2H), 2.72-2.74 (m, 2H), 3.77 (s, 2H), 7.18-7.24 (m, 1H), 7.27-7.29 (m, 4H). ^{13}C-NMR (75 MHz, $CDCl_3$): δ (ppm) 36.3, 48.4, 51.4, 53.9, 126.9, 128.1, 128.4, 140.4. HRMS (ESI): *m/z* [*M*+H]$^+$ calcd. for $[C_{10}H_{17}N_2]^+$ 165.1386, found: 165.1387. $C_{10}H_{16}N_2$ (164.25).

(1- Benzyl-4-methyl-6-nitro-1,4-diazepan-6-yl) methanol (25)

Compound **23** (4.6 g, 28.04 mmol) and 2-nitroethanol (compound **24**) (1985 µL, 27.70 mmol) were dissolved in toluene/ethanol (1:1 v/v) (60 mL). Paraformaldehyde (2.5 g, 83.33 mmol) was added in small portions under stirring, and the suspension was heated to reflux for 6 h. The solvent was evaporated, and the crude product was dissolved in CH_2Cl_2 (20 mL) and washed with H_2O (3 x 20 mL). The organic phase was dried over Na_2SO_4. The product was purified by flash column chromatography (eluent: light petroleum/ethyl acetate 4:1 to 2:1 v/v) to provide compound **25** as yellow oil (6.9 g, 88%). R_f = 0.3 (light petroleum/ethyl acetate 2:1 v/v). ^{1}H-NMR (300 MHz, $CDCl_3$): δ (ppm) 2.45 (s, 3H), 2.53-2.76 (m, 4H), 2.96-3.16 (m, 2H), 3.42-3.50 (m, 2H), 3.54-3.76 (m, 3H), 3.76-3.88 (m, 2H), 7.22-7.37 (m, 5H). ^{13}C-NMR (75 MHz,

$CDCl_3$): δ (ppm) 48.3, 57.9, 59.0, 61.2, 61.6, 63.8, 66.2, 93.9, 127.6, 128.5, 129.1, 138.6. HRMS (ESI): *m/z* [*M*+H]$^+$ calcd. for $[C_{14}H_{22}N_3O_3]^+$ 280.1656, found: 280.1661. $C_{14}H_{21}N_3O_3$ (279.34)

1-Benzyl-4-methyl-6-nitro-1,4-diazepane (26)

Potassium *tert*-butoxide (2.2 g, 19.61 mmol) was added portionwise to a solution of compound **25** (3.7 g, 13.25 mmol) in MeOH (50 mL). The mixture was heated at 40 °C for 30 min and cooled slowly to room temperature. The solvent was evaporated and the residue dissolved in a solution of $NH_2OH{\cdot}HCl$ (1.4 g, 20.15 mmol) in water (100 mL) followed by extraction with CH_2Cl_2 (3 x 20 mL). The combined extracts were washed with brine and dried over Na_2SO_4. The solvent was evaporated at ca 25 °C to afford compound **26** as yellow oil (2.2 g, 67%). R_f = 0.7 (CH_2Cl_2/MeOH/25% aq NH_3 95:5:1 v/v/v). ^{1}H-NMR (300 MHz, $CDCl_3$): δ (ppm) 2.45 (s, 3H), 2.54-2.77 (m, 4H), 3.09-3.26 (m, 2H), 3.32-3.42 (m, 2H), 3.67-3.78 (m, 2H), 4.53-4.69 (m, 1H), 7.21-7.39 (m, 5H). ^{13}C-NMR (75 MHz, $CDCl_3$): δ (ppm) 47.4, 56.7, 56.9, 58.9, 59.9, 62.9, 84.6, 127.4, 128.5, 128.8, 138.8. HRMS (ESI): *m/z* [*M*+H]$^+$ calcd. for $[C_{13}H_{20}N_3O_2]^+$ 250.1550, found: 250.1552. $C_{13}H_{19}N_3O_2$ (249.31).

***tert*-Butyl (1-benzyl-4-methyl-1,4-diazepan-6-yl)carbamate (27)**

A mixture of compound **26** (4.3 g, 17.25 mmol) was dissolved in 95% ethanol (65 mL), Raney 2800 (slurry in H_2O, ca 6 mL) was carefully added to the solution, the suspension was stirred in an autoclave (1 L) under an atmosphere of hydrogen at 10 atm at room temperature overnight. The catalyst was filtered off and the filtrate was concentrated to afford the compound 1-benzyl-4-methyl-1,4-diazepan-6-amine as a brown oily residue (3.7 g, 98%). This material (3.7 g, 16.87 mmol) was dissolved in $CHCl_3$ (50 mL) and di-*tert*-butyl dicarbonate (4.5 g, 20.64 mmol) in $CHCl_3$ (50 mL) was slowly added to this solution. The mixture was stirred at room temperature overnight. H_2O (50 mL) was added followed by extraction with CH_2Cl_2 (3 × 50 mL). The combined extracts were dried over Na_2SO_4 and the volatiles were evaporated to afford the crude product, which was subjected to flash column chromatography (eluent: CH_2Cl_2/MeOH/25% aq NH_3 90:3:1 v/v/v) to yield compound **27** as yellow oil (2.9 g, 54%). R_f = 0.8 (CH_2Cl_2/MeOH/25% aq NH_3 90:9:1 v/v/v). ^{1}H-NMR (300 MHz, $CDCl_3$): δ (ppm) 1.40 (s, 9H), 2.35 (s, 3H), 2.39-2.69 (m, 5H), 2.71-2.91 (m, 3H), 3.55 (d, *J* 13 Hz, 1H), 3.67 (d, *J* 13 Hz, 1H), 3.72-3.79 (m, 1H), 5.50 (br. s, 1H), 7.18-7.39 (m, 5H). ^{13}C-NMR (75 MHz, $CDCl_3$): δ (ppm) 28.5, 48.2, 48.8, 56.5, 58.9, 59.5, 62.2, 63.5, 78.9, 127.2, 128.4, 128.9, 139.3, 155.4. HRMS (ESI): *m/z* [*M*+H]$^+$ calcd. for $[C_{18}H_{30}N_3O_2]^+$ 320.2333, found: 320.2342. $C_{18}H_{29}N_3O_2$ (319.45).

***tert*-Butyl (1-methyl-1,4-diazepan-6-yl)carbamate (28)**

Compound **27** (200 mg, 0.626 mmol) was suspended in THF/H_2O (1:4 v/v) (5 mL) followed by the addition of 10% Pd/C (40 mg). The mixture was stirred in an autoclave (1 L) under an atmosphere of hydrogen at 10 atm at room temperature overnight. Filtered the reaction mixture through a pad of celite, the filtrate was concentrated under reduced pressure to give compound **28** as colorless oil (110 mg, 77%), which was used without further purification. R_f = 0.2 (CH_2Cl_2/MeOH/25% aq NH_3 90:9:1 v/v/v). ^{1}H-NMR (300 MHz, [D_6]DMSO): δ (ppm) 1.36 (s, 9H), 2.27 (s, 3H), 2.35-2.49 (m, 4H), 2.58-2.69 (m, 2H), 2.59-2.68 (m, 2H), 2.85-2.91 (m, 1H), 3.49-3.66 (m, 1H), 6.58 (brs, 1H). ^{13}C-NMR (75 MHz, [D_6]DMSO): δ (ppm) 28.3, 47.2, 49.1, 50.7, 52.7, 60.4, 61.3, 77.7, 154.9. HRMS (ESI): *m/z* [*M*+H]$^+$ calcd. for [$C_{11}H_{24}N_3O_2$]$^+$ 230.1863, found: 230.1868. $C_{11}H_{23}N_3O_2$ (229.32).

***tert*-Butyl (2-bromoethyl)carbamate (30)**

2-bromoethan-1-amine hydrobromide (compound **29**) (3.0 g, 14.63 mmol) and di-*tert*-butyl dicarbonate (3.2 g, 14.67 mmol) were dissolved in CH_2Cl_2 (80 mL). Triethylamine (2.05 mL, 14.71 mmol) was added dropwise and the reaction mixture was stirred at room temperature overnight. CH_2Cl_2 (20 mL) was added, the mixture was washed with brine, and the organic phase was dried over Na_2SO_4 followed by removal of the solvent under reduced pressure. The product was purified by flash column chromatography (eluent: light petroleum/ethyl acetate 8:2 v/v) to give compound **30** as yellow oil (2.6 g, 80%). R_f = 0.7 (light petroleum/ethyl acetate 2:1 v/v). ^{1}H-NMR (400 MHz, $CDCl_3$): δ (ppm) 1.44 (s, 9H), 3.44 (t, *J* 5.5 Hz, 2H), 3.47-3.57 (m, 2H), 4.98 (s, 1H). ^{13}C-NMR (100 MHz, $CDCl_3$): 28.4, 32.8, 42.4, 79.8, 155.5. $C_7H_{14}BrNO_2$ (224.10).

***tert*-Butyl (2-(piperazin-1-yl)ethyl)carbamate (32)**

Compound **30** (1.0 g, 4.46 mmol), piperazine (compound **31**) (1.5 g, 17.44 mmol) and K_2CO_3 (1.2 g, 8.70 mmol) were added to MeCN (50 mL) and the mixture was kept under reflux for 3 h. The mixture was filtered and the filtrate was concentrated to afford a yellow oily residue, which was dissolved in CH_2Cl_2 (20 mL) followed by washing with water. The aqueous phase was treated with CH_2Cl_2 (3 × 20 mL) and the organic extracts were collected. All organic phases were combined and dried over Na_2SO_4. Removal of the volatiles under reduced pressure gave the crude product, which was subjected to flash column chromatography (eluent: CH_2Cl_2/MeOH/25% aq NH_3 90:3:1 v/v/v) to yield compound **32** as yellow oil (0.93 g, 91%). R_f = 0.4 (CH_2Cl_2/MeOH/25% aq NH_3 90:9:1 v/v/v). ^{1}H-NMR (300 MHz, $CDCl_3$): δ (ppm)1.45 (s, 9H), 2.42-2.46 (m, 6H), 2.57 (brs, 1H), 2.83-3.01 (m, 4H), 3.19-3.27 (m, 2H), 4.97 (brs, 1H). ^{13}C-NMR (75 MHz, $CDCl_3$): 28.5, 36.9, 45.7, 53.6, 57.7, 82.6, 160.0. HRMS (ESI): *m/z* [*M*+H]$^+$ calcd. for [$C_{11}H_{24}N_3O_2$]$^+$ 230.1863, found: 230.1869. $C_{11}H_{23}N_3O_2$ (229.32).

2-Amino-2-(pyridin-3-yl)acetonitrile (34)[47]

To a cooled (5 °C) solution of potassium cyanide (10.4 g, 159.7 mmol) in water (100 mL) was added 3-pyridinecarbaldehyde (compound **33**) (11.4 g, 106.5 mmol) dropwise. Afterwards, acetic acid (9.1 mL, 159.7 mmol) was added over a period of 30 min. The mixture was stirred at room temperature for 2 h followed by extraction with ethyl acetate (3 × 50 mL). The combined organic phases were dried over Na_2SO_4 and the solvent was removed under reduced pressure to give the intermediate 2-hydroxy-2-(pyridin-3-yl)acetonitrile as yellow solid (14.0 g, 98%), which was used without further purification. R_f = 0.4 (CH_2Cl_2/MeOH 10:1 v/v). ^{1}H-NMR (300 MHz, $CDCl_3$): δ (ppm) 5.65 (s, 1H), 7.38 (dd, *J* 7.9, 4.9 Hz, 1H), 7.93 (d, *J* 9.5 Hz, 1H), 8.45 (dd, *J* 4.9, 1.3 Hz, 1H), 8.58 (d, *J* 1.9 Hz, 1H). ^{13}C-NMR (75 MHz, $CDCl_3$) δ (ppm) 60.7, 118.9, 124.6, 133.2, 135.7, 146.8, 149.4. The intermediate (14.0 g, 104.4 mmol) was added to a solution of NH_4Cl (33.9 g, 633.7 mmol) in H_2O (100 mL) followed by the addition of 25% aq NH_4OH (10 mL). The mixture was stirred at room temperature for 20 h. Extracted the mixture with ethyl acetate (10 × 30 mL), the combined organic phases were dried over Na_2SO_4. Removal of the volatiles under reduced pressure gave compound **34** as brown oil (9.3 g, 67%). R_f = 0.3 (CH_2Cl_2/MeOH 10:1 v/v). ^{1}H-NMR (300 MHz, $CDCl_3$): δ (ppm) 2.09 (brs, 2H), 4.91 (s, 1H), 7.24-7.34 (m, 1H), 7.78-7.87 (m, 1H), 8.54 (dd, *J* 4.8, 1.5 Hz, 1H), 8.65-8.77 (m, 1H). ^{13}C-NMR (75 MHz, $CDCl_3$): δ (ppm) 45.2, 120.2, 123.8, 132.2, 134.5, 148.3, 150.3. HRMS (ESI): *m/z* $[M+H]^+$ calcd. for $[C_7H_8N_3]^+$ 134.0713, found: 134.0713. $C_7H_7N_3$ (133.15).

3-Chloro-4-(pyridin-3-yl)-1,2,5-thiadiazole (35)[47]

To a cooled (5-10 °C) solution of S_2Cl_2 (10.8 mL, 137.2 mmol) in DMF (50 mL) was added a solution of compound **34** (9.1 g, 68.34 mmol) in DMF (65 mL) over a period of 1 h. The mixture was stirred at 5-10 °C for additional 45 min and ice water (30 mL) was added. The formed precipitate was removed by filtration. To the filtrate was added 20% NaOH solution to adjust a pH of 8, thereby keeping the temperature below 20 °C. Extracted the mixture with ethyl acetate (3 × 20 mL). The combined organic phases were dried over Na_2SO_4 and the volatiles were removed under reduced pressure to give the crude product, which was subjected to flash column chromatography (eluent: light petroleum/ethyl acetate 3:2 v/v) to afford compound **35** as a white solid (9.4 g, 69%), m.p. 40-42 °C (Lit[47]. m.p. 48-49 °C). R_f = 0.7 (light petroleum/acetone 1:1 v/v). ^{1}H-NMR (300 MHz, $CDCl_3$): δ (ppm) 7.41-7.46 (m, 1H), 8.24-8.28 (m, 1H), 8.72 (dd, *J* 4.9, 1.6 Hz, 1H), 9.20 (dd, *J* 2.2, 0.6 Hz, 1H). ^{13}C-NMR (75 MHz, $CDCl_3$): δ (ppm) 123.4, 126.9, 135.7, 143.6, 149.4, 150.9, 155.2. HRMS (ESI): *m/z* $[M+H]^+$ calcd. for $[C_7H_5ClN_3S]^+$ 197.9887, found: 197.9893. $C_7H_4ClN_3S$ (197.64).

3-((4-(Pyridin-3-yl)-1,2,5-thiadiazol-3-yl)oxy)propan-1-ol (37)[50]

A suspension of 60% NaH in mineral oil (363 mg, 9.47 mmol) was added to abs. THF (10 mL)

under an atmosphere of argon. The mixture was cooled to 0 °C and propane-1,3-diol (compound **36**) (460 mg, 6.04 mmol) was added under stirring. The mixture was then kept under reflux for 1 h. A solution of compound **35** (600 mg, 3.03 mmol) in abs. THF (10 mL) was added and reflux was continued for 8 h. The solvent was removed under reduced pressure and ice-cold water was added dropwise to the residue. Extracted the mixture with ethyl acetate (3 × 20 mL). The combined organic phases were dried over Na_2SO_4 and concentrated under reduced pressure to give the crude product, which was subjected to flash column chromatography (eluent: light petroleum/acetone 2:1 v/v) to afford compound **37** as yellow oil (370 mg, 52%). R_f = 0.3 (light petroleum/acetone 2:1 v/v). ^{1}H-NMR (300 MHz, $CDCl_3$): δ (ppm) 2.08-2.20 (m, 2H), 2.19 (brs, 1H), 3.87 (t, *J* 6.0 Hz, 2H), 4.69 (t, *J* 6.1 Hz, 2H), 7.36-7.40 (m, 1H), 8.30-8.54 (m, 1H), 8.62 (dd, *J* 4.8, 1.6 Hz, 1H), 9.36 (dd, *J* 2.1, 0.7 Hz, 1H). ^{13}C-NMR (75 MHz, $CDCl_3$): δ (ppm) 31.9, 59.0, 68.2, 123.6, 127.7, 134.9, 144.8, 148.4, 149.9, 162.7. HRMS (ESI): *m/z* [M+*H*]$^+$ calcd. for $[C_{10}H_{12}N_3O_2S]^+$ 238.0645, found: 238.0651. $C_{10}H_{11}N_3O_2S$ (237.28).

3-((4-(1-Methyl-1,2,5,6-tetrahydropyridin-3-yl)-1,2,5-thiadiazol-3-yl)oxy)propan-1-ol (38)[50]

To a solution of compound **37** (370 mg, 1.56 mmol) in acetone (5 mL) was added methyliodide (0.97 mL, 15.6 mmol) and the mixture was stirred at room temperature for 24 h. The formed precipitate was collected by filtration and washed with acetone (5 mL). Drying *in vacuo* gave the N-methylated, but non-reduced intermediate as yellow solid (480 mg, 81%). R_f = 0.1 (CH_2Cl_2/MeOH 10:1 v/v). ^{1}H-NMR (300 MHz, [D_4]MeOH): δ (ppm) 1.99-2.06 (m, 2H), 3.59-3.65 (m, 2H), 4.45 (s, 3H), 4.62 (t, *J* 6.3 Hz, 2H), 8.28 (dd, *J* 8.2, 6.2 Hz, 1H), 9.07 (dd, *J* 12, 7.3 Hz, 2H), 9.54 (s, 1H). The intermediate (470 mg, 1.24 mmol) was dissolved in MeOH (10 mL). The solution was cooled to -5 °C and $NaBH_4$ (143 mg, 3.76 mmol) was added carefully. The mixture was stirred at room temperature overnight. The solvent was removed under reduced pressure. The residue was dissolved in CH_2Cl_2 (10 mL) followed by washing with water. The aqueous phase was treated with CH_2Cl_2 (3 × 10 mL) and the organic extracts were collected. All organic phases were combined and dried over Na_2SO_4. Removal of the volatiles reduced pressure gave the crude product, which was subjected to flash column chromatography (eluent: CH_2Cl_2/MeOH/25% aq NH_3 90:9:1 v/v/v) to afford compound **38** as brown oil (130 mg, 41%). R_f = 0.3 (CH_2Cl_2/MeOH/25% aq NH_3 85:15:1 v/v/v). ^{1}H-NMR (300 MHz, $CDCl_3$): δ (ppm) 2.03-2.11 (m, 2H), 2.38-2.51 (m, 5H), 2.56 (brs, 1H), 2.59 (t, *J* 5.6 Hz, 2H), 3.40-3.54 (m, 2H), 3.78 (t, *J* 6.1 Hz, 2H), 4.59 (t, *J* 6.1 Hz, 2H), 6.87-7.13 (m, 1H). ^{13}C-NMR (75 MHz, $CDCl_3$): δ (ppm) 26.5, 32.0, 45.9, 51.2, 54.9, 59.3, 67.9, 128.4, 129.2, 146.7, 162.5. HRMS (ESI): *m/z* [*M*+H]$^+$ calcd. for $[C_{11}H_{18}N_3O_2S]^+$ 256.1114, found: 256.1115. $C_{11}H_{17}N_3O_2S$ (255.34).

3-(3-Bromopropoxy)-4-(1-methyl-1,2,5,6-tetrahydropyridin-3-yl)-1,2,5-thiadiazole (39)[50]

Compound **38** (400 mg, 1.57 mmol) and PPh_3 (1.2 g, 4.57 mmol) were dissolved in CH_2Cl_2 (30 mL) and the solution was cooled to -5 °C under an atmosphere of argon. A solution of CBr_4 (3.4 g, 10.25 mmol) in CH_2Cl_2 (20 mL) was slowly dropped into the stirred mixture, thereby keeping the temperature of the mixture below 5 °C. After completed addition, stirring was continued at room temperature for 24 h. The solvent was removed under reduced pressure to give a brown residue, and subjected to flash column chromatography (eluent: light petroleum/acetone/25% aq NH_3 85:15:1 v/v/v) to afford compound **39** as a brown oil (300 mg, 50%). R_f = 0.6 (light petroleum/acetone/25% aq NH_3 65:35:1 v/v/v). ^{1}H-NMR (300 MHz, $CDCl_3$): δ (ppm) 2.26-2.36 (m, 2H), 2.41-2.49 (m, 5H), 2.58 (t, *J* 5.8 Hz, 2H), 3.45 (dd, *J* 4.4, 2.5 Hz, 2H), 3.71 (t, *J* 6.4 Hz, 2H), 4.61 (t, *J* 6.0, 2H), 6.91-7.08 (m, 1H). ^{13}C-NMR (75 MHz, $CDCl_3$): δ (ppm) 26.5, 29.4, 31.8, 45.8, 51.1, 54.9, 68.4, 128.4, 129.1, 146.7, 161.9. HRMS (ESI): *m/z* [*M*+H]$^+$ calcd. for $[C_{11}H_{17}BrN_3OS]^+$ 318.0270, found: 318.0271. $C_{11}H_{16}BrN_3OS$ (318.23).

3-(1-Methyl-1,2,5,6-tetrahydropyridin-3-yl)-4-(3-(piperazin-1-yl)propoxy)-1,2,5 thiadiazole (40)

Compound **39** (600 mg, 1.89 mmol) and piperazine (1.3 g, 15.09 mmol) were suspended in MeCN (12 mL) followed by the addition of potassium carbonate (523 mg, 3.78 mmol). The mixture was refluxed for 2 h. Insoluble material was separated by filtration and washed with CH_2Cl_2 (2 × 10 mL). The filtrate and washings were combined and the volatiles were evaporated to yield a brown oil-like residue, which was dissolved in CH_2Cl_2 (20 mL) followed by washing with brine. The aqueous phase was treated with CH_2Cl_2 (3 × 10 mL) and the organic extracts were collected. All organic phases were combined and dried over Na_2SO_4. The solvent was removed under reduced pressure to yield the crude product, which was subjected to column chromatography (eluent: CH_2Cl_2/MeOH/25% aq NH_3 90:6:1 v/v/v) to obtain compound **40** as yellow oil (405 mg, 66%). R_f = 0.4 (CH_2Cl_2/MeOH/25% aq NH_3 90:9:1 v/v/v). ^{1}H-NMR (300 MHz, [D$_4$]MeOH): δ (ppm) 1.92-2.13 (m, 2H), 2.30-2.43 (m, 4H), 2.44 (s, 3H), 2.45-2.52 (m, 4H), 2.55 (t, *J* 5.7 Hz, 2H), 2.90 (t, *J* 4.7 Hz, 4H), 3.43 (s, 2H), 4.49 (t, *J* 6.4 Hz, 2H), 7.02-7.04 (m, 1H). ^{13}C-NMR (75 MHz, [D$_4$]MeOH): δ (ppm) 26.2, 26.6, 45.90, 45.92, 51.2, 54.3, 55.0, 55.7, 69.2, 128.3, 129.3, 146.8, 162.4. HRMS (ESI): *m/z* [*M*+H]$^+$ calcd. for $[C_{15}H_{26}N_5OS]^+$ 324.1853, found: 324.1854. $C_{15}H_{25}N_5OS$ (323.46).

1-Methyl-4-(3-((4-(1-methyl-1,2,5,6-tetrahydropyridin-3-yl)-1,2,5-thiadiazol-3-yl)oxy)propyl)-1,4-diazepan-6-amine tetrakis(hydrotrifluoroacetate) (41)

Compound **39** (490 mg, 1.52 mmol) and compound **28** (354 mg, 1.54 mmol) were suspended in MeCN (20 mL) followed by the addition of potassium carbonate (427 mg, 3.09 mmol). The mixture was stirred at 110 °C under microwave irradiation for 30 min. Solids were separated

by filtration and washed with CH_2Cl_2 (2 × 10 mL). The combined filtrate and washings were concentrated under reduced pressure yielding a yellow oily residue, which was dissolved in CH_2Cl_2 (10 mL) followed by washing with brine. The aqueous phase was treated with CH_2Cl_2 (3 × 10 mL) and the organic extracts were collected. All organic phases were combined and dried over Na_2SO_4. Removal of the volatiles under reduced pressure yielded the Boc-protected intermediate as yellow oily residue, which was dissolved in CH_2Cl_2/TFA (4:1 v/v) (5 mL). The mixture was stirred at room temperature overnight. CH_2Cl_2 (10 mL) was added, the volatiles were evaporated and the residue was subjected to purification by preparative HPLC (column: Kinetex XB-C18 5 µm 250 × 21 mm; gradient: 0-30 min: MeCN/0.1% aq TFA 5:95-62:38, t_R = 11 min), which afforded compound **41** as white fluffy solid (830 mg, 66%). ^{1}H-NMR (400 MHz, [D$_4$]MeOH): δ (ppm) 2.09-2.16 (m, 2H), 2.66-2.86 (m, 2H), 2.93 (t, *J* 7.3 Hz, 2H), 2.97 (s, 3H), 2.96-3.02 (m, 1H), 3.05 (s, 3H), 3.09-3.14 (m, 1H), 3.15-3.29 (m, 2H), 3.32-3.39 (m, 1H), 3.47 (t, *J* 5.5 Hz, 2H), 3.52-3.68 (m, 3H), 3.83-3.93 (m, 1H), 4.00-4.05 (m, 1H), 4.49-4.54 (m, 1H), 4.57 (t, *J* 6.4 Hz, 2H), 7.22 (t, *J* 4.1 Hz, 1H). ^{13}C-NMR (100 MHz, [D$_4$]MeOH): δ (ppm) 23.8, 27.1, 43.3, 46.5, 48.7, 50.9, 51.7, 53.1, 55.3, 56.2, 57.8, 58.8, 70.2, 114.6 (TFA), 116.3 (TFA), 117.4 (TFA), 119.3 (TFA), 125.3, 128.3, 145.6, 162.1 (TFA), 162.4 (TFA), 163.8 (TFA), 163.1 (TFA), 163.6. RP-HPLC (220 nm): 97% (t_R = 10.7 min, k = 2.7). HRMS (ESI): *m/z* [*M*+H]$^+$ calcd. for $[C_{17}H_{31}N_6OS]^+$ 367.2275, found: 367.2273. $C_{17}H_{30}N_6OS \cdot C_8H_4F_{12}O_8$ (366.53 + 456.09).

5-((4-(Pyridin-3-yl)-1,2,5-thiadiazol-3-yl)oxy)pentan-1-ol (43)

A suspension of 60% NaH in mineral oil (908 mg, 23.69 mmol) was added to abs. THF (40 mL) under an atmosphere of argon. The suspension was cooled to 0 °C, 1,5-pentanediol (compound **42**) (2.0 g, 19.20 mmol) was added under stirring, and the mixture was refluxed for 1 h. A solution of compound **35** (1.5 g, 7.58 mmol) in abs. THF (10 mL) was added and reflux was continued for 8 h. The solvent was removed under reduced pressure and ice-cold water was added dropwise to the residue. Extracted the mixture with ethyl acetate (3 × 30 mL), the combined organic phases were dried over Na_2SO_4 and concentrated under reduced pressure to give the crude product, which was subjected to flash column chromatography (eluent: light petroleum/acetone 2:1 v/v) to afford compound **43** as colorless oil (960 mg, 48%). R_f = 0.3 (light petroleum/acetone 2:1 v/v). ^{1}H-NMR (300 MHz, $CDCl_3$): δ (ppm) 1.50-1.76 (m, 4H), 1.86 (brs, 1H), 1.89-1.98 (m, 2H), 3.69 (t, *J* 6.2 Hz, 2H), 4.54 (t, *J* 6.5 Hz, 2H), 7.40 (dd, *J* 8.0, 4.9 Hz, 1H), 8.42 (d, *J* 8.0 Hz, 1H), 8.64 (d, *J* 4.8 Hz, 1H), 9.40 (s, 1H). ^{13}C-NMR (75 MHz, $CDCl_3$): δ (ppm) 21.6, 28.2, 32.6, 62.2, 71.4, 123.4, 127.4, 134.7, 144.5, 147.9, 150.4, 162.7. HRMS (ESI): *m/z* [*M*+H]$^+$ calcd. for $[C_{12}H_{16}N_3O_2S]^+$ 266.0958, found: 266.0966. $C_{12}H_{15}N_3O_2S$ (265.33).

5-((4-(1-Methyl-1,2,5,6-tetrahydropyridin-3-yl)-1,2,5-thiadiazol-3-yl)oxy)pentan-1-ol (44)

To a solution of compound **43** (0.96 g, 3.62 mmol) in acetone (15 mL) was added methyliodide (2.3 mL, 36.2 mmol) and the mixture was stirred at room temperature for 24 h. The formed precipitate was collected by filtration, washed with acetone and dried under vacuum to yield the N-methylated, but non-reduced intermediate as yellow solid (1.4 g, 95%). R_f = 0.1 (CH_2Cl_2/MeOH 6:1 v/v). ^{1}H-NMR (300 MHz, [D$_4$]MeOH): δ (ppm) 1.51-1.73 (m, 4H), 1.87-2.07 (m, 2H), 3.60 (t, *J* 5.9 Hz, 2H), 4.52 (s, 3H), 4.65 (t, *J* 6.5 Hz, 2H), 8.22 (dd, *J* 8.1, 6.2 Hz, 1H), 8.96 (d, *J* 6.1 Hz, 1H), 9.24 (d, *J* 8.3 Hz, 1H), 9.57 (s, 1H). The intermediate (1.4 g, 3.44 mmol) was dissolved in MeOH (20 mL) and the solution was cooled to -5 °C. $NaBH_4$ (519 mg, 13.66 mmol) was added carefully. The mixture was stirred at room temperature overnight. The solvent was removed under reduced pressure. The residue was dissolved in CH_2Cl_2 (20 mL) followed by washing with water. The aqueous phase was treated with CH_2Cl_2 (3 × 20 mL) and the organic extracts were collected. All organic phases were combined and dried over Na_2SO_4. Removal of the volatiles under reduced pressure gave the crude product, which was subjected to flash column chromatography (eluent: CH_2Cl_2/MeOH/25% aq NH_3 97:3:1 v/v/v) to afford compound **44** as brown oil (900 mg, 92%). R_f = 0.3 (CH_2Cl_2/MeOH/25% aq NH_3 85:15:1 v/v/v). ^{1}H-NMR (300 MHz, $CDCl_3$): δ (ppm) 1.47-1.59 (m, 2H), 1.59-1.69 (m, 2H), 1.78-1.98 (m, 2H), 2.39- 2.49 (m, 5H), 2.57 (t, *J* 5.6 Hz, 2H), 3.44 (dd, *J* 4.4, 2.4 Hz, 2H), 3.66 (t, *J* 6.3 Hz, 2H), 4.44 (t, *J* 6.6 Hz, 2H), 7.00-7.09 (m, 1H). ^{13}C-NMR (75 MHz, $CDCl_3$): δ (ppm) 22.3, 26.6, 28.6, 32.3, 45.9, 51.2, 54.9, 62.6, 70.8, 128.4, 129.2, 146.8, 162.5. HRMS (ESI): *m/z* [*M*+H]$^+$ calcd. for $[C_{13}H_{22}N_3O_2S]^+$ 284.1427, found: 284.1430. $C_{13}H_{21}N_3O_2S$ (283.39).

3-((5-Bromopentyl)oxy)-4-(1-methyl-1,2,5,6-tetrahydropyridin-3-yl)-1,2,5-thiadiazole (45)

Compound **44** (850 mg, 3.0 mmol) and PPh_3 (2.4 g, 9.15 mmol) were dissolved in CH_2Cl_2 (30 mL) and the solution was cooled to -5 °C under an atmosphere of argon. A solution of CBr_4 (6.5 g, 19.59 mmol) in CH_2Cl_2 (15 mL) was slowly dropped into the stirred mixture, thereby keeping the temperature of the mixture below 5 °C. Stirring was continued at room temperature for 24 h. The solvent was removed under reduced pressure and the residue subjected to column chromatography (eluent: light petroleum/acetone/25% aq NH_3 65:35:1 v/v/v) to afford compound **45** as brown oil (740 mg, 71%). R_f = 0.4 (light petroleum/acetone/25% aq NH_3 65:35:1 v/v/v). ^{1}H-NMR (300 MHz, $CDCl_3$): δ (ppm) 1.56-1.71 (m, 2H), 1.81-2.01 (m, 4H), 2.39-2.50 (m, 5H), 2.57 (t, *J* 5.5 Hz, 2H), 3.36-3.52 (m, 4H), 4.46 (t, *J* 6.4 Hz, 2H), 6.97-7.13 (m, 1H). ^{13}C-NMR (75 MHz, $CDCl_3$): δ (ppm) 24.7, 26.7, 28.0, 32.2, 33.5, 45.9, 51.2, 55.0, 70.4, 128.5, 129.3, 146.8, 162.3. HRMS (ESI): *m/z* [*M*+H]$^+$ calcd. for $[C_{13}H_{21}BrN_3OS]^+$ 346.0583, found: 346.0585. $C_{13}H_{20}BrN_3OS$ (346.29).

1,4-Bis(5-((4-(1-methyl-1,2,5,6-tetrahydropyridin-3-yl)-1,2,5-thiadiazol-3-yl)oxy)pentyl)piperazine (46)

Compound **45** (730 mg, 2.11 mmol), potassium carbonate (193 mg, 1.39 mmol), and piperazine (60 mg, 0.70 mmol) were added to MeCN (5 mL). The mixture was stirred at 110 °C under microwave irradiation for 30 min, and cooled to room temperature. Insoluble material was removed by filtration and the filtrate was concentrated under reduced pressure to give the crude product, which was dissolved in CH_2Cl_2 (10 mL) followed by washing with H_2O (3 x 10 mL). The organic phase was dried over Na_2SO_4 and the solvent was removed under reduced pressure. The product was purified by flash column chromatography (eluent: CH_2Cl_2/MeOH/25% aq NH_3 97:3:1 v/v/v) to afford compound **46** as white solid (96 mg, 22%), m.p. 41-42 °C. R_f = 0.7 (CH_2Cl_2/MeOH/25% aq NH_3 90:9:1 v/v/v). ^{1}H-NMR (300 MHz, $CDCl_3$): δ (ppm) 1.31-1.61 (m, 8H), 1.71-1.90 (m, 4H), 2.26-2.33 (m, 5H), 2.34-2.38 (m, 4H), 2.39 (s, 6H), 2.41-2.52 (m, 11H), 3.38 (dd, *J* 4.3, 2.4 Hz, 4H), 4.38 (t, *J* 6.5 Hz, 4H), 6.85-7.15 (m, 2H). ^{13}C-NMR (75 MHz, $CDCl_3$): δ (ppm) 24.0, 26.5, 26.6, 28.8, 45.9, 51.1, 53.1, 55.0, 58.5, 70.7, 128.3, 129.3, 146.8, 162.5. RP-HPLC (220 nm): 97% (t_R = 13.9 min, k = 3.8). HRMS (ESI): *m/z* $[M+H]^+$ calcd. for $[C_{30}H_{49}N_8O_2S_2]^+$ 617.3414, found: 617.3407. $C_{30}H_{48}N_8O_2S_2$ (616.89).

***tert*-Butyl (5-((4-(pyridin-3-yl)-1,2,5-thiadiazol-3-yl)oxy)pentyl)carbamate (48)**

To a cooled (0 °C) solution of 5-amino-1-pentanol (1.0 g, 9.67 mmol) and triethylamine (1.2 mL, 8.89 mmol) in CH_2Cl_2 (50 mL) was slowly added di-*tert*-butyl dicarbonate (1.9 g, 8.71 mmol) in CH_2Cl_2 (20 mL). The mixture was stirred at 0 °C for 30 min and stirring was continued at room temperature for additional 12 h. Saturated aq NH_4Cl (20 mL) was added followed by extraction with CH_2Cl_2 (3 x 20 mL). The combined organic extracts was washed with brine, dried over Na_2SO_4 and concentrated under reduced pressure to give the intermediate *tert*-butyl (5-hydroxypentyl)carbamate (compound **47**)[66] as colorless oil (1.9 g, 97%) without purification. R_f = 0.5 (light petroleum/acetone 2:1 v/v). ^{1}H-NMR (300 MHz, $CDCl_3$): δ (ppm) 1.42 (s, 9H), 1.46-1.61 (m, 6H), 1.63 (brs, 1H), 3.12 (t, *J* 6.9 Hz, 2H), 3.64 (t, *J* 6.4 Hz, 2H), 4.53 (brs, 1H). ^{13}C-NMR (75 MHz, $CDCl_3$): δ (ppm) 22.9, 28.4, 29.8, 32.2, 40.4, 62.5, 79.2, 156.0. HRMS (ESI): *m/z* $[M+H]^+$ calcd. for $[C_{10}H_{22}NO_3]^+$ 204.1594, found: 204.1595. To a stirred and cooled (0 °C) solution of compound **47** (307 mg, 1.51 mmol) in abs. THF (5 mL) was added the suspension of 60% NaH in mineral oil (73 mg, 1.90 mmol) in portions under an atmosphere of argon, followed by the addition of **35** (200 mg, 1.01 mmol) dissolved in abs. THF (2 mL). The mixture was stirred at 0 °C for 5 min and slowly warmed up until reflux. Reflux was continued for 2 h. The solvent was removed under reduced pressure and ice-cold water was added dropwise to the residue. Extracted the mixture with ethyl acetate (3 × 5 mL), the combined organic phases were dried over Na_2SO_4 and concentrated under reduced pressure to give the crude product, which was subjected to flash column chromatography (eluent: light petroleum/acetone 5:1 v/v) to afford compound **48** as colorless oil (100 mg, 27%). R_f = 0.4 (light petroleum/acetone 2:1 v/v). ^{1}H-NMR (300 MHz, $CDCl_3$): δ (ppm) 1.43 (s, 9H), 1.47-1.67

(m, 4H), 1.82-1.99 (m, 2H), 3.12-3.18 (m, 2H), 4.52 (t, *J* 6.5 Hz, 2H), 4.70 (brs, 1H), 7.33-7.51 (m, 1H), 8.33-8.51 (m, 1H), 8.65 (dd, *J* 4.8, 1.5 Hz, 1H), 9.39 (d, *J* 1.6 Hz, 1H). ^{13}C-NMR (75 MHz, $CDCl_3$): δ (ppm) 23.3, 28.4, 28.6, 29.8, 40.4, 71.1, 79.1, 123.5, 127.6, 134.7, 144.9, 148.5, 150.1, 156.0, 162.7. HRMS (ESI): *m/z* $[M+H]^+$ calcd. for $[C_{17}H_{25}N_4O_3S]^+$ 365.1642, found: 365.1644. $C_{17}H_{24}N_4O_3S$ (364.46).

tert-Butyl (5-((4-(1-methyl-1,2,5,6-tetrahydropyridin-3-yl)-1,2,5-thiadiazol-3-yl)oxy)pentyl)carbamate (49)

To a solution of compound **48** (3.3 g, 9.05 mmol) in acetone (10 mL) was added methyliodide (5.7 mL, 91.2 mmol) and the mixture was stirred at room temperature for 24 h. The formed precipitated was collected, washed with acetone and dried under vacuum to afford the N-methylated, but non-reduced intermediate as yellow solid (3.3 g, 96%). R_f = 0.1 (CH_2Cl_2/MeOH 6:1 v/v). This intermediate (3.0 g, 7.91 mmol) was dissolved in MeOH (50 mL) and the solution was cooled to -5 °C followed by the careful addition of $NaBH_4$ (2.1 g, 55.26 mmol). The mixture was stirred at room temperature overnight. The solvent was removed under reduced pressure. The residue was dissolved in CH_2Cl_2 (20 mL) followed by washing with brine. The aqueous phase was treated with CH_2Cl_2 (3 × 20 mL) and the organic extracts were collected. All organic phases were combined and dried over Na_2SO_4. Removal of the solvent under reduced pressure gave the crude product, which was subjected to flash column chromatography (eluent: CH_2Cl_2/MeOH/25% aq NH_3 97:3:1 v/v/v) to afford compound **49** as brown oil (2.4 g, 79%). R_f = 0.7 (CH_2Cl_2/MeOH/25% aq NH_3 90:9:1 v/v/v). ^{1}H-NMR (300 MHz, $CDCl_3$): δ (ppm) 1.37 (s, 9H), 1.38-1.62 (m, 4H), 1.76-1.94 (m, 2H), 2.49 (s, 3H), 2.41-2.52 (m, 2H), 2.60 (t, *J* 5.6 Hz, 2H), 3.14 (dd, *J* 13, 6.3 Hz, 2H), 3.46-3.48 (m, 2H), 4.44 (t, *J* 6.6 Hz, 2H), 4.57 (brs, 1H), 7.00-7.08 (m, 1H). ^{13}C-NMR (75 MHz, $CDCl_3$): δ (ppm) 23.3, 26.4, 28.4, 28.5, 29.8, 40.4, 45.8, 51.2, 54.8, 70.7, 79.1, 128.3, 129.0, 146.6, 156.0, 162.4. HRMS (ESI): *m/z* $[M+H]^+$ calcd. for $[C_{18}H_{31}N_4O_3S]^+$ 383.2111, found: 383.2103. $C_{18}H_{30}N_4O_3S$ (382.52).

5-((4-(1-Methyl-1,2,5,6-tetrahydropyridin-3-yl)-1,2,5-thiadiazol-3-yl)oxy)pentan-1-amine (50)

Compound **49** (50 mg, 0.13 mmol) was dissolved in CH_2Cl_2 (4 mL) and TFA (1 mL) was added. The mixture was stirred at room temperature overnight and cooled to 0 °C followed by the addition of 25% aq NH_3 to adjust the pH to 10. The product was extracted with CH_2Cl_2 (5 × 5 mL). The combined organic phases were dried over Na_2SO_4 and concentrated under reduced pressure to afford compound **50** as colorless oil (20 mg, 56%), which was used without further purification. R_f = 0.3 (CH_2Cl_2/MeOH/25% aq NH_3 90:9:1 v/v/v). ^{1}H-NMR (300 MHz, $CDCl_3$): δ (ppm) 1.34-1.55 (m, 4H), 1.73-1.87 (m, 4H), 2.32-2.43 (m, 5H), 2.50 (t, *J* 5.5 Hz, 2H), 2.66 (t, *J* 6.7 Hz, 2H), 3.36-3.38 (m, 2H), 4.38 (t, *J* 6.6 Hz, 2H), 6.92-7.05 (m, 1H). ^{13}C-NMR (75 MHz,

$CDCl_3$): δ (ppm) 23.3, 26.6, 28.7, 33.1, 41.9, 45.9, 51.2, 55.0, 70.7, 128.4, 129.3, 146.7, 162.3. HRMS (ESI): *m/z* [*M*+H]$^+$ calcd. for [$C_{13}H_{23}N_4OS$]$^+$ 283.1587, found: 283.1586. $C_{13}H_{22}N_4OS$ (282.41).

4-Amino-*N*-(5-((4-(1-methyl-1,2,5,6-tetrahydropyridin-3-yl)-1,2,5-thiadiazol-3-yl)oxy)pentyl)butanamide (52)

4-aminobutanoic acid (200 mg, 1.93 mmol) was dissolved in H_2O/THF (1:1 v/v) (10 mL) and di-*tert*-butyl dicarbonate (507 mg, 2.32 mmol) was slowly added followed by the addition of triethylamine (810 µL, 5.82 mmol). The mixture was stirred at room temperature overnight. THF was removed under reduced pressure and 0.1 M aq $KHSO_4$ solution was slowly added to adjust the pH to 3. The product was extracted with ethyl acetate (3 × 10 mL), the combined extracts were dried over Na_2SO_4 and concentrated under reduced pressure to yield the intermediate 4-((*tert*-butoxycarbonyl)amino)butanoic acid (compound **51**) as colorless oil (270 mg, 69%), which was used without further purification. R_f = 0.8 (CH_2Cl_2/MeOH/acetic acid 90:9:1 v/v/v). ^{1}H-NMR (300 MHz, $CDCl_3$): δ (ppm) 1.43 (s, 9H), 1.75-1.86 (m, 2H), 2.38 (t, *J* 7.2 Hz, 2H), 3.16 (t, *J* 6.7 Hz, 2H), 4.75 (brs, 1H), 10.06 (brs, 1H). ^{13}C-NMR (75 MHz, $CDCl_3$): δ (ppm) 25.1, 28.4, 31.3, 39.8, 60.5, 171.4, 178.4. HRMS (ESI): *m/z* [*M*+H]$^+$ calcd. for [$C_9H_{16}NO_4$]$^+$ 202.1085, found: 202.1090. To a solution of the intermediate **51** (51 mg, 0.25 mmol) in DMF (1 mL) were added HOBt (34 mg, 0.25 mmol), TBTU (80 mg, 0.25 mmol) and DIPEA (86 µL, 0.49 mmol) and the mixture was stirred at room temperature for 30 min. Compound **50** (70 mg, 0.25 mmol) dissolved in DMF (1 mL) was added and the mixture was stirred at 60 °C for 3 h. H_2O (5 mL) was added, followed by extraction with ethyl acetate (3 × 5 mL). The combined extracts were dried over Na_2SO_4 and concentrated under reduced pressure to yield the crude product, which was subjected to flash column chromatography (eluent: CH_2Cl_2/MeOH/25% aq NH_3 90:3:1 v/v/v) to yield the intermediate *tert*-butyl (4-((5-((4-(1-methyl-1,2,5,6-tetrahydropyridin-3-yl)-1,2,5-thiadiazol-3-yl)oxy)pentyl)amino)-4-oxobutyl)carbamate as yellow oil (80 mg, 67%). R_f = 0.5 (CH_2Cl_2/MeOH/25% aq NH_3 90:9:1 v/v/v). ^{1}H-NMR (300 MHz, $CDCl_3$): δ (ppm) 1.42 (s, 9H), 1.46-1.57 (m, 4H), 1.73-1.80 (m, 2H), 1.82-1.91 (m, 2H), 2.19 (t, *J* 6.9 Hz, 2H), 2.49-2.55 (m, 5H), 2.63-2.81 (m, 2H), 3.12-3.18 (m, 2H), 3.23-3.29 (m, 2H), 3.51-3.73 (m, 2H), 4.45 (t, *J* 6.4 Hz, 2H), 4.90 (brs, 1H), 6.37 (brs, 1H), 7.07-7.09 (m, 1H). ^{13}C-NMR (75 MHz, $CDCl_3$): δ (ppm) 23.4, 26.4, 26.6, 28.4, 28.5, 29.2, 33.6, 39.3, 39.6, 45.8, 51.1, 54.8, 70.7, 79.3, 128.3, 129.0, 146.6, 156.7, 162.4, 172.7. HRMS (ESI): *m/z* [*M*+H]$^+$ calcd. for [$C_{22}H_{38}N_5O_4S$]$^+$ 468.2639, found: 468.2650. This intermediate (80 mg, 0.17 mmol) was dissolved in CH_2Cl_2/TFA (4:1 v/v) (5 mL) and the mixture was stirred at room temperature overnight. CH_2Cl_2 (5 mL) was added followed by the addition of 25% aq NH_3 to adjust the pH of the aqueous phase to 11. The product was extracted with CH_2Cl_2 (5 × 10 mL). The combined organic phases were dried over Na_2SO_4 and concentrated under reduced

pressure to give compound **52** as yellow oil (55 mg, 89%), which was used without further purification. R_f = 0.4 (CH_2Cl_2/MeOH/25% aq NH_3 80:16:1 v/v/v). ^{1}H-NMR (300 MHz, $CDCl_3$): δ (ppm) 1.38-1.64 (m, 4H), 1.70-1.92 (m, 4H), 1.96 (brs, 2H), 2.22-2.28 (m, 2H), 2.35-2.48 (m, 5H), 2.52-2.56 (m, 2H), 3.00-3.37 (m, 4H), 3.39-3.42 (m, 2H), 4.41 (t, *J* 6.5 Hz, 2H), 6.88-7.13 (m, 1H), 8.56 (brs, 1H). ^{13}C-NMR (75 MHz, $CDCl_3$): δ (ppm) 23.5, 26.6, 28.5, 29.3, 31.0, 34.1, 39.3, 41.1, 45.9, 51.2, 55.0, 70.6, 128.4, 129.3, 146.8, 162.4, 172.8. HRMS (ESI): *m/z* [*M*+H]$^+$ calcd. for $[C_{17}H_{30}N_5O_2S]^+$ 368.2115, found: 368.2116. $C_{17}H_{29}N_5O_2S$ (367.51)

N^1,*N*^{8}-Bis(5-((4-(1-methyl-1,2,5,6-tetrahydropyridin-3-yl)-1,2,5-thiadiazol-3-yl) oxy)pentyl)octanediamide (53)

To a cooled (0 °C) solution of compound **50** (300 mg, 1.06 mmol) and triethylamine (322 mg, 3.18 mmol) in abs. THF (2 mL) was added dropwise octanedioyl dichloride (76 µL, 0.43 mmol) dissolved in abs. THF (1 mL) under an atmosphere of argon. The mixture was stirred at room temperature overnight. The solvent was evaporated. The residue was dissolved in ethyl acetate (5 mL) followed by washing with water. The aqueous phase was treated with ethyl acetate (3 × 10 mL) and the organic extracts were collected. All organic phases were combined and dried over Na_2SO_4. Removal of the solvent under reduced pressure gave the crude product, which was subjected to flash column chromatography (eluent: CH_2Cl_2/MeOH/25% aq NH_3 97:3:1 v/v/v) to afford compound **53** as white solid (118 mg, 39%), m.p. 55-57 °C. R_f = 0.6 (CH_2Cl_2/MeOH/25% aq NH_3 90:9:1 v/v/v). ^{1}H-NMR (300 MHz, $CDCl_3$): δ (ppm) 1.26-1.37 (m, 4H), 1.48-1.65 (m, 10H), 1.78-1.96 (m, 6H), 2.14 (t, *J* 7.5 Hz, 4H), 2.40-2.50 (m, 10H), 2.57-2.61 (m, 4H), 3.23-3.29 (m, 4H), 3.42-3.49 (m, 4H), 4.44 (t, *J* 6.5 Hz, 4H), 5.58 (brs, 2H), 7.02-7.05 (m, 2H). ^{13}C-NMR (75 MHz, $CDCl_3$): δ (ppm) 23.4, 25.8, 26.6, 28.5, 28.7, 29.4, 36.6, 39.3, 45.9, 51.2, 55.0, 70.6, 128.4, 129.3, 146.8, 162.4, 173.0. RP-HPLC (220 nm): 96% (t_R = 18.1 min, *k* = 5.3). HRMS (ESI): *m/z* [*M*+H]$^+$ calcd. for $[C_{34}H_{55}N_8O_4S_2]^+$ 703.3782, found: 703.3786. $C_{34}H_{54}N_8O_4S_2$ (702.98).

N^1,*N*^{10}-Bis(5-((4-(1-methyl-1,2,5,6-tetrahydropyridin-3-yl)-1,2,5-thiadiazol-3-yl)oxy)pentyl)decanediamide (54)

To a cooled (0 °C) solution of compound **50** (400 mg, 1.42 mmol) and triethylamine (430 mg, 4.25 mmol) in abs. THF (5 mL) was added dropwise decanedioyl dichloride (92 µL, 0.57 mmol) dissolved in abs. THF (1 mL) under an atmosphere of argon. The mixture was stirred at room temperature overnight. The solvent was evaporated. The residue was dissolved in ethyl acetate (5 mL) followed by washing with brine. The aqueous phase was treated with ethyl acetate (3 × 10 mL) and the organic extracts were collected. All organic phases were combined and dried over Na_2SO_4. Removal of the solvent under reduced pressure gave the crude product, which was subjected to flash column chromatography (eluent: CH_2Cl_2/MeOH/25% aq

NH_3 97:3:1 v/v/v) to afford compound **54** as white solid (270 mg, 65%), m.p. 45-49 °C. R_f = 0.5 (CH_2Cl_2/MeOH/25% aq NH_3 90:9:1 v/v/v). ^{1}H-NMR (300 MHz, $CDCl_3$): δ (ppm) 1.25-1.33 (m, 8H), 1.41-1.63 (m, 10H), 1.81-1.94 (m, 4H), 2.06 -2.23 (m, 4H), 2.12-2.17 (m, 4H), 2.46-2.53 (m, 8H), 2.63-2.67 (m, 4H), 3.27 (dd, *J* 13, 6.8 Hz, 4H), 3.49-3.54 (m, 4H), 4.44 (t, *J* 6.5 Hz, 4H), 5.54 (brs, 2H), 7.03-7.07 (m, 2H). ^{13}C-NMR (75 MHz, CDCl3): δ (ppm) 23.4, 25.7, 26.6, 28.5, 29.1, 29.2, 29.4, 36.8, 39.3, 45.9, 51.2, 55.0, 70.6, 128.4, 129.3, 146.8, 162.4, 173.1. RP-HPLC (220 nm): 98% (t_R = 19.5 min, *k* = 5.8). HRMS (ESI): *m/z* $[M+H]^+$ calcd. for $[C_{36}H_{59}N_8O_4S_2]^+$ 731.4095, found: 731.4097. $C_{36}H_{58}N_8O_4S_2$ (731.0320).

N^1,N^4-Bis(5-((4-(1-methyl-1,2,5,6-tetrahydropyridin-3-yl)-1,2,5-thiadiazol-3-yl)oxy)pentyl)terephthalamide (55)

To a solution of terephthalic acid (117 mg, 0.71 mmol) in DMF (3 mL) were added EDC (271 mg, 1.41 mmol), HOBt (216 mg, 1.41 mmol) and DIPEA (183 mg, 1.42 mmol) and the mixture was stirred at room temperature for 30 min. Compound **50** (400 mg, 1.42 mmol) in DMF (2 mL) was added and stirring was continued at room temperature overnight. H_2O (10 mL) was added followed by extraction with ethyl acetate (3 × 10 mL). The combined extracts were washed with brine, dried over Na_2SO_4 and concentrated under reduced pressure to give the crude product, which was subjected to flash column chromatography (eluent: CH_2Cl_2/MeOH/25% aq NH_3 95:5:1 v/v/v) to afford compound **55** as white solid (130 mg, 26%), m.p. 50-53 °C. R_f = 0.5 (CH_2Cl_2/MeOH/25% aq NH_3 95:5:1 v/v/v). ^{1}H-NMR (300 MHz, $CDCl_3$): δ (ppm) 1.52-1.61 (m, 4H), 1.67-1.78 (m, 4H), 1.83-1.96 (m, 4H), 2.42-2.52 (m, 4H), 2.62 (s, 6H), 2.78 (t, *J* 5.8 Hz, 4H), 3.46-3.54 (m, 4H), 3.65-3.70 (m, 4H), 4.47 (t, *J* 6.2 Hz, 4H), 6.94 (brs, 2H), 7.01-7.09 (m, 2H), 7.85 (s, 4H). ^{13}C-NMR (75 MHz, $CDCl_3$): δ (ppm) 23.6, 25.0, 28.5, 29.3, 39.9, 44.9, 50.7, 53.8, 70.9, 127.0, 127.3, 127.8, 137.2, 145.7, 162.4, 166.9. RP-HPLC (220 nm): 96% (t_R = 18.3 min, *k* = 5.4). HRMS (ESI): *m/z* $[M+H]^+$ calcd. for $[C_{34}H_{47}N_8O_4S_2]^+$ 695.3156, found: 695.3158. $C_{34}H_{46}N_8O_4S_2$ (694.91).

Ethyl 4-((2-nitrophenyl)amino)piperidine-1-carboxylate (58)[67]

Ethyl 4-aminopiperidine-1-carboxylate (compound **57**) (244 mg, 1.42 mmol) and potassium carbonate (587 mg, 4.25 mmol) were added to a stirred solution of 1-fluoro-2-nitrobenzene (compound **56**) (200 mg, 1.42 mmol) in DMF (1.5 mL) followed by the addition of sodium iodide (106 mg, 0.71 mmol). The mixture was stirred at 180 °C under microwave irradiation for 10 min, cooled to room temperature and diluted with water (50 mL). The product was extracted with ethyl acetate (3 × 10 mL). The combined extracts were washed with brine and dried over Na_2SO_4. Removal of the volatiles under reduced pressure gave compound **58** as yellow solid (300 mg, 72%), which was used without further purification. R_f = 0.2 (light petroleum/ethyl acetate 5:1 v/v), m.p. 80-82 °C. ^{1}H-NMR (300 MHz, $CDCl_3$): δ (ppm) 1.28 (t, *J* 7.1 Hz, 3H),

1.51-1.63 (m, 2H), 1.70 (brs, 1H), 2.05-2.11 (m, 2H), 3.04-3.20 (m, 2H), 3.66-3.74 (m, 1H), 4.05-4.19 (m, 4H), 6.63-6.68 (m, 1H), 6.87 (d, *J* 8.4 Hz, 1H), 7.37-7.50 (m, 1H), 8.19 (dd, *J* 8.6, 1.6 Hz, 1H). ^{13}C-NMR (75 MHz, $CDCl_3$): δ (ppm) 14.7, 31.7, 42.2, 49.1, 61.6, 113.9, 115.5, 127.3, 132.0, 136.3, 144.3, 155.5. HRMS (ESI): *m/z* [*M*+H]$^+$ calcd. for $[C_{14}H_{20}N_3O_4]^+$ 294.1448, found: 294.1453. $C_{14}H_{19}N_3O_4$ (293.32).

Ethyl 4-((2-aminophenyl)amino)piperidine-1-carboxylate (59)

A mixture of compound **58** (200 mg, 0.68 mmol), 10% Pd/C (20 mg) and MeOH (10 mL) was stirred in an autoclave (1 L) under an atmosphere of hydrogen at 10 atm at room temperature overnight. The catalyst was removed by filtation through a pad of celite, which was washed with MeOH (2 × 5 mL). The combined filtrates were concentrated under reduced pressure to give compound **59** as purple solid (160 mg, 89%), which was used without further purification. R_f = 0.4 (light petroleum/acetone = 4:1), m.p. 138-140 °C. ^{1}H-NMR (300 MHz, $CDCl_3$): δ (ppm) 1.27 (t, *J* 7.1 Hz, 3H), 1.35-1.48 (m, 2H), 1.98-2.12 (m, 2H), 2.90-3.09 (m, 3H), 3.20 (brs, 1H), 3.34-3.51 (m, 2H), 4.07 (brs, 2H), 4.15 (q, *J* 12 Hz, 2H), 6.64-6.89 (m, 4H). ^{13}C-NMR (75 MHz, $CDCl_3$): δ (ppm) 14.7, 32.3, 42.6, 50.3, 61.4, 113.9, 117.1, 119.6, 120.6, 135.2, 135.3, 155.6. HRMS (ESI): *m/z* [*M*+H]$^+$ calcd. for $[C_{14}H_{22}N_3O_2]^+$ 264.1707, found: 264.1718. $C_{14}H_{21}N_3O_2$ (263.34).

Ethyl 4-(2-oxo-2,3-dihydro-1*H*-benzo[*d*]imidazol-1-yl)piperidine-1-carboxylate (60)

A solution of triphosgene (85 mg, 0.28 mmol) in anhydrous CH_2Cl_2 (5 mL) was added dropwise over 10 min to a stirred and cooled (0 °C) mixture of compound **59** (50 mg, 0.19 mmol), sodium bicarbonate (24 mg, 0.28 mmol) in CH_2Cl_2 (10 mL). The mixture was slowly warmed up to room temperature and stirred for additional 2 h. Water (5 mL) was added slowly and the organic phase was separated followed by additional extraction with CH_2Cl_2 (2 x 10 mL). The combined organic phases were washed with brine, dried over Na_2SO_4 and evaporated under reduced pressure to give the crude product, which was subjected to column chromatography (eluent: light petroleum/acetone 2:1 v/v) to give compound **60** as white solid (40 mg, 73%). R_f = 0.3 (light petroleum/ethyl acetate 1:1 v/v), m.p. 173-176 °C. ^{1}H-NMR (300 MHz, $CDCl_3$): δ (ppm) 1.30 (t, *J* 7.1 Hz, 3H), 1.84-1.95 (m, 2H), 2.30-2.41 (m, 2H), 2.89-2.98 (m, 2H), 4.19 (q, *J* 7.1 Hz, 2H), 4.37-4.41 (m, 2H), 4.46-4.57 (m, 1H), 7.05-7.16 (m, 4H), 10.25 (brs, 1H). ^{13}C-NMR (75 MHz, $CDCl_3$): δ (ppm) 14.7, 30.9, 43.6, 50.8, 61.6, 109.4, 110.0, 121.2, 121.5, 128.1, 128.9, 155.5, 206.9. HRMS (ESI): *m/z* [*M*+H]+ calcd. for $[C_{15}H_{20}N_3O_3]^+$ 290.1499, found: 290.1515. $C_{15}H_{19}N_3O_3$ (289.34).

1-(Piperidin-4-yl)-1,3-dihydro-2*H*-benzo[*d*]imidazol-2-one (61)

Compound **60** (200 mg, 0.69 mmol) was suspended in 10% aq NaOH (16 mL), the mixture

was kept under reflux for 5 h, and cooled to room temperature and acidified by the addition of 10% HCl solution until the evolution of gas had ceased (pH around 2). Afterwards, the pH was carefully adjusted to 9 using 15% NaOH solution, followed by extraction with CH_2Cl_2 (4 x 10 mL). The combined extracts were dried over Na_2SO_4 and the solvent was evaporated under reduced pressure to give compound **61** as white solid (120 mg, 81%), m.p. 112-115 °C, which was used without further purification. R_f = 0.4 (CH_2Cl_2/MeOH/25% aq NH_3 90:9:1 v/v/v). ^{1}H-NMR (300 MHz, [D_6]DMSO): δ (ppm) 1.56-1.60 (m, 2H), 2.08-2.30 (m, 2H), 2.53-2.61 (m, 2H), 3.04-3.08 (m, 2H), 3.29 (brs, 1H), 4.17-4.28 (m, 1H), 6.92-7.03 (m, 3H), 7.28 (dd, *J* 7.1, 2.4 Hz, 1H), 10.83 (brs, 1H). ^{13}C-NMR (75 MHz, [D_6]DMSO): δ (ppm) 29.8, 45.6, 50.1, 108.7, 108.8, 120.1, 120.3, 128.2, 129.0, 153.5. HRMS (ESI): *m/z* [*M*+H]$^+$ calcd. for [$C_{12}H_{16}N_3O$]$^+$ 218.1288, found: 218.1289. $C_{12}H_{15}N_3O$ (217.27).

1-([1,4'-Bipiperidin]-4-yl)-1,3-dihydro-2*H*-benzo[*d*]imidazol-2-one (63)

4-piperidine hydrochloride (5.0 g, 32.55 mmol) and sodium bicarbonate (5.5 g, 65.49 mmol) were added to THF/H_2O (1:1 v/v) (150 mL) followed by the slow addition of di-*tert*-butyl dicarbonate (5.7 g, 26.12 mmol) in THF (20 mL). The mixture was stirred at room temperature overnight. THF was evaporated and the product was extracted with CH_2Cl_2 (3 x 50 mL). The combined extracts were washed with brine and dried over Na_2SO_4. The solvent was removed under reduced pressure and the product was purified by column chromatography (eluent: light petroleum/ethyl acetate 7:1 v/v) to yield the intermediate *tert*-butyl 4-oxopiperidine-1-carboxylate (compound **62**) as white solid (6.4 g, 98%). R_f = 0.8 (CH_2Cl_2/MeOH 30:1 v/v). ^{1}H-NMR (300 MHz, $CDCl_3$): δ (ppm) 1.49 (s, 9H), 2.43 (t, *J* 6.0 Hz, 4H), 3.73 (t, *J* 6.0 Hz, 4H). ^{13}C-NMR (75 MHz, $CDCl_3$): δ (ppm) 28.4, 41.2, 43.1, 80.5, 154.6, 208.1. HRMS (ESI): *m/z* [*M*+H]$^+$ calcd. for [$C_{10}H_{18}NO_3$]$^+$ 200.1281, found: 200.1279. The intermediate **62** (1.6 g, 8.03 mmol) and acetic acid (0.16 mL, 2.74 mmol) were added to a stirred and cooled (0 °C) solution of compound **61** (1.2 g, 5.53 mmol) in MeOH (50 mL) and the mixture was stirred at 0 °C for 15 min. Sodium cyanoborohydride (688 mg, 10.95 mmol) was added and the stirred mixture was allowed to warm up to room temperature, followed by stirring overnight. 5% aq $KHCO_3$ (16 mL) was added prior to extraction with CH_2Cl_2 (3 x 20 mL). The combined organic phases were washed with brine and dried over Na_2SO_4. The volatiles were removed under reduced pressure and the product was purified by flash column chromatography (eluent: CH_2Cl_2/MeOH/25% aq NH_3 97:2:1 to 95:4:1 v/v/v) to yield the intermediate *tert*-butyl 4-(2-oxo-2,3-dihydro-1*H*-benzo[*d*]imidazol-1-yl)-[1,4'-bipiperidine]-1'-carboxylate (1.15 g, 52%) as white solid. R_f = 0.7 (CH_2Cl_2/MeOH/25% aq NH_3 90:9:1 v/v/v). The Boc-protected intermediate (1.1 g, 2.75 mmol) was dissolved in TFA/CH_2Cl_2 (1:4 v/v) (15 mL) and the mixture was stirred at room temperature overnight. The pH was carefully adjusted to 11 by adding 25% aq NH_3. The two phases were separated and the aqueous phase was treated with CH_2Cl_2 (5 x 20 mL).

The combined organic phases were dried over Na_2SO_4 and the solvent was removed under reduced pressure. The product was purified by flash column chromatography with (eluent: CH_2Cl_2/MeOH/25% aq NH_3 90:9:1 v/v/v) to afford compound **63** as white solid (620 mg, 75%), m.p. 180-182 °C. R_f = 0.4 (CH_2Cl_2/MeOH/25% aq NH_3 90:9:1 v/v/v). ^{1}H-NMR (300 MHz, [D_4]MeOH): δ (ppm) 1.63-1.88 (m, 4H), 2.05-2.09 (m, 2H), 2.36-2.58 (m, 4H), 2.65-2.74 (m, 1H), 2.84-3.02 (m, 2H), 3.12-3.15 (m, 2H), 3.34-3.42 (m, 2H), 4.24-4.33 (m, 1H), 6.95-7.17 (m, 3H), 7.33-7.39 (m, 1H). ^{13}C-NMR (75 MHz, [D_4]MeOH): δ (ppm) 27.1, 29.9, 45.1, 49.9, 52.0, 60.7, 110.5, 110.6, 122.2, 122.5, 129.6, 130.3, 156.2. HRMS (ESI): *m/z* [*M*+H]$^+$ calcd. for [$C_{17}H_{25}N_4O$]$^+$ 301.2023, found: 301.2025. $C_{17}H_{24}N_4O$ (300.41).

1-(1'-(2-Aminoethyl)-[1,4'-bipiperidin]-4-yl)-1,3-dihydro-2*H*-benzo[*d*]imidazol-2-one (64)

Compound **63** (570 mg, 1.89 mmol), *tert*-butyl (2-bromoethyl) carbamate (compound **30**) (508 mg, 2.27 mmol) and potassium carbonate (525 mg, 3.80 mmol) were added to MeCN (60 mL) and the mixture was stirred under reflux overnight. Insoluble material was removed by filtration. The filtrate was concentrated under reduced pressure to yield a yellow oily residue, which was dissolved in CH_2Cl_2 (10 mL) followed by washing with water. The aqueous phase was treated with CH_2Cl_2 (3 × 10 mL) and the organic extracts were collected. All organic phases were combined and dried over Na_2SO_4. Removal of the solvent under reduced pressure yielded a yellow oil, which was subjected to flash column chromatography (eluent: CH_2Cl_2/MeOH/25% aq NH_3 90:3:1 to 90:9:1 v/v/v) to afford the Boc-protected intermediate as colorless oil (350 mg, 42%). R_f = 0.6 (CH_2Cl_2/MeOH/25% aq NH_3 90:9:1 v/v/v). ^{1}H-NMR (300 MHz, [D_4]MeOH): δ (ppm) 1.43 (s, 9H), 1.54-1.67 (m, 2H), 1.72-1.84 (m, 2H), 1.87-1.91 (m, 2H), 2.01-2.10 (m, 2H), 2.27-2.60 (m, 7H), 3.01-3.05 (m, 2H), 3.08-3.24 (m, 4H), 4.20-4.43 (m, 1H), 6.89-7.16 (m, 3H), 7.24-7.57 (m, 1H). ^{13}C-NMR (75 MHz, [D_4]MeOH): δ (ppm) 28.8, 28.9, 29.9, 38.7, 50.1, 52.0, 54.4, 58.7, 63.1, 80.2, 110.7, 110.9, 122.3, 122.6, 129.7, 130.3, 156.3, 158.4. HRMS (ESI): *m/z* [*M*+H]$^+$ calcd. for [$C_{24}H_{38}N_5O_3$]$^+$ 444.2969, found: 444.2966. The intermediate (150 mg, 0.34 mmol) was dissolved in CH_2Cl_2/TFA (4:1 v/v) (5 mL) and the mixture was stirred at room temperature overnight. 25% aq NH_3 was added to adjust the pH to 11 followed by extraction with CH_2Cl_2/MeOH (9:1 v/v) (5 × 10 mL). Removal of the volatiles from the combined extracts *in vacuo* gave compound **64** as colorless oil (100 mg, 86%), which was used without further purification. R_f = 0.1 (CH_2Cl_2/MeOH/25% aq NH_3 90:9:1 v/v/v). ^{1}H-NMR (300 MHz, [D_4]MeOH): δ (ppm) 1.50-1.71 (m, 2H), 1.76-1.79 (m, 2H), 1.89-1.94 (m, 2H), 2.00-2.11 (m, 2H), 2.32-2.52 (m, 7H), 2.74-2.78 (m, 1H), 3.00-3.17 (m, 4H), 3.39-3.45 (m, 1H), 4.18-4.44 (m, 1H), 6.95-7.16 (m, 3H), 7.34-7.52 (m, 1H). ^{13}C-NMR (75 MHz, [D_4]MeOH): δ (ppm) 28.9, 29.8, 39.3, 50.2, 52.1, 54.5, 61.2, 63.2, 110.6, 110.9, 122.3, 122.6, 129.7, 130.3, 156.3. HRMS (ESI): *m/z* [*M*+H]$^+$ calcd. for [$C_{19}H_{30}N_5O$]$^+$ 344.2445, found: 344.2443. $C_{19}H_{29}N_5O$ (343.48).

1-(1'-(2-Bromoacetyl)-[1,4'-bipiperidin]-4-yl)-1,3-dihydro-2*H*-benzo[*d*]imidazol-2-one (66)

To a solution of compound **63** (630 mg, 2.09 mmol) in $CHCl_3$ (50 mL) was added pyridine (762 µL, 9.45 mmol) and the mixture was cooled in an ice bath. 2-Bromoacetyl bromide (compound **65**) (820 µL, 9.45 mmol) was added dropwise and stirring was continued at room temperature overnight. H_2O (10 mL) was added and the phases were separated. The organic phase was washed with brine, dried over Na_2SO_4 and the solvent was evaporated to obtain the crude product, which was subjected to flash column chromatography (eluent: CH_2Cl_2/MeOH/25% aq NH_3 90:3:1 v/v/v) to yield compound **66** as colorless oil (800 mg, 91%). R_f = 0.7 (CH_2Cl_2/MeOH/25% aq NH_3 95:5:1 v/v/v). ^{1}H-NMR (300 MHz, [D$_4$]MeOH): δ (ppm) 1.35-1.73 (m, 2H), 1.78-1.92 (m, 2H), 2.01 (t, *J* 11 Hz, 2H), 2.36-2.61 (m, 4H), 2.72 (t, *J* 13 Hz, 2H), 3.14-3.22 (m, 3H), 3.99-4.10 (m, 3H), 4.26-4.33 (m, 1H), 4.55-4.57 (m, 1H), 7.02-7.09 (m, 3H), 7.33-7.48 (m, 1H). ^{13}C-NMR (75 MHz, [D$_4$]MeOH): δ (ppm) 28.8, 29.5, 29.9, 42.9, 47.4, 52.0, 62.7, 110.6, 110.8, 122.2, 122.6, 129.7, 130.4, 156.3, 167.7. HRMS (ESI): *m/z* $[M+H]^+$ calcd. for $[C_{19}H_{26}BrN_4O_2]^+$ 421.1234, found: found: 421.1244. $C_{19}H_{25}BrN_4O_2$ (421.34).

1-(1'-(2-(6-Amino-4-methyl-1,4-diazepan-1-yl)acetyl)-[1,4'-bipiperidin]-4-yl)-1,3-dihydro-2*H*-benzo[*d*]imidazol-2-one tetrakis(hydrotrifluoroacetate) (67)

Potassium carbonate (53 mg, 0.38 mmol) was added to a suspension of compound **66** (80 mg, 0.19 mmol) and compound **28** (48 mg, 0.21 mmol) in MeCN (2 mL). The mixture was stirred at 110 °C under microwave irradiation for 30 min and cooled to room temperature. Insoluble material was separated by filtration and washed with CH_2Cl_2 (2 × 10 mL). The combined filtrate and washings were concentrated under reduced pressure yielding a yellow residue, which was dissolved in CH_2Cl_2 (5 mL) followed by washing with water. The aqueous phase was treated with CH_2Cl_2 (3 × 10 mL) and the organic extracts were collected. All organic phases were combined and dried over Na_2SO_4. Removal of the volatiles under reduced pressure gave the Boc-protected intermediate (50 mg, 46%), which was dissolved in CH_2Cl_2/TFA (4:1 v/v) (5 mL). The mixture was stirred at room temperature for 8 h. CH_2Cl_2 (10 mL) was added and the volatiles were evaporated. Purification by preparative HPLC (column: Kinetex XB-C18 5 µm 250 × 21 mm; gradient: 0-30 min: MeCN/0.1% aq TFA 5:95-62:38, t_R = 12 min) afforded compound **67** as white fluffy solid (35 mg, 43%). ^{1}H-NMR (600 MHz, [D$_4$]MeOH): δ (ppm) 1.63-1.90 (m, 2H), 2.09-2.11 (m, 2H), 2.21-2.22 (m, 2H), 2.68-2.72 (m, 1H), 2.82-2.91 (m, 2H), 3.02 (s, 3H), 3.05-3.21 (m, 4H), 3.25-3.29 (m, 1H), 3.32-3.37 (m, 2H), 3.47-3.58 (m, 3H), 3.59-3.66 (m, 2H), 3.65-3.74 (m, 4H), 3.77-3.82 (m, 1H), 3.96-3.97 (m, 1H), 4.57-4.63 (m, 1H), 4.72-4.75 (m, 1H), 7.03-7.09 (m, 3H), 7.32 (d, *J* 3.4 Hz, 1H). ^{13}C-NMR (150 MHz, [D$_4$]MeOH): δ (ppm) 27.3, 27.5, 27.9, 41.6, 43.9, 46.7, 50.2, 50.4, 51.9, 58.5, 58.6, 60.6, 64.7, 110.0, 110.7, 115.1 (TFA), 117.0 (TFA), 118.9 (TFA), 120.9 (TFA), 122.4, 122.9, 129.7, 130.1, 156.1, 162.3 (TFA), 162.6 (TFA), 162.8 (TFA), 163.0 (TFA), 170.8. RP-HPLC (220 nm):

98% (t_R = 11.6 min, k = 3.0). HRMS (ESI): *m/z* [*M*+H]$^+$ calcd. for $[C_{25}H_{40}N_7O_2]^+$ 470.3238, found: 470.3241. $C_{25}H_{39}N_7O_2 \cdot C_8H_4F_{12}O_8$ (469.63 + 456.09).

***tert*-Butyl 4-(2,2-diphenylacetoxy)piperidine-1-carboxylate (70)**

Di-*tert*-butyl dicarbonate (5.6 g, 25.68 mmol) in THF (20 mL) was slowly added to a solution of piperidin-4-ol (2.0 g, 19.77 mmol) and triethylamine (3.6 mL, 25.70 mmol) in THF/H_2O (1:7 v/v) (200 mL) and the mixture was stirred at room temperature overnight. THF was removed by evaporation followed by extraction with CH_2Cl_2 (3 × 50 mL). The combined extracts were dried over Na_2SO_4 and concentrated under reduced pressure. The residue was subjected to column chromatography (eluent: CH_2Cl_2/MeOH 30:1 to 15:1 v/v) to yield the Boc-protected intermediate (compound **69**) as white solid (3.7 g, 93%). Compound **69** (2.9 g, 14.41 mmol) and 2,2-diphenylacetic acid (compound **68**) (2.7 g, 12.74 mmol) were dissolved in CH_2Cl_2 (100 mL) and the solution was cooled to 0 °C. DMAP (173 mg, 1.42 mmol) was added and the mixture was allowed to clear up before the slow addition of *N*,*N'*-dicyclohexylcarbodiimide (3.2 g, 15.51 mmol) under stirring at 0 °C. The mixture was slowly warmed up to room temperature and kept under stirring overnight. H_2O (50 mL) was added, the phases were separated and the aqueous phase was treated with CH_2Cl_2 (3 × 20 mL). The combined organic phases were washed with brine, dried over Na_2SO_4 and concentrated under reduced pressure to give the crude product, which was subjected to column chromatography (eluent: light petroleum/acetone 3:1 v/v) to afford compound **70** as yellow oil (4.9 g, 97%). R_f = 0.8 (light petroleum/acetone 3:1 v/v). ^{1}H-NMR (300 MHz, $CDCl_3$): δ (ppm) 1.40 (s, 9H), 1.49-1.59 (m, 2H), 1.72-1.82 (m, 2H), 3.15-3.24 (m, 2H), 3.15-3.24 (m, 2H), 4.93-5.00 (m, 2H), 7.18-7.29 (m, 10H). ^{13}C-NMR (75 MHz, $CDCl_3$): δ (ppm) 28.4, 30.3, 57.3, 65.9, 70.4, 79.7, 127.3, 128.5, 128.6, 138.6, 154.7, 171.8. HRMS (ESI): *m/z* [*M*+Na]$^+$ calcd. for $[C_{24}H_{29}NNaO_4]^+$ 418.1989, found: 418.1988. $C_{24}H_{29}NO_4$ (395.50).

Piperidin-4-yl 2, 2-diphenylacetate (71)

Compound **70** (860 mg, 2.17 mmol) was dissolved in CH_2Cl_2 (40 mL) and the solution was cooled to 0 °C. TFA (10 mL) was added dropwise, the mixture was allowed to warm up to room temperature and stirring was continued for 8 h. Ice water (10 mL) was added followed by the slow addition of 25% aq NH_3 to adjust the pH value to 11. The product was extracted with CH_2Cl_2 (3 × 15 mL), the combined organic phases were dried over Na_2SO_4 and concentrated under reduced pressure to give compound **71** as white solid (360 mg, 56%), m.p. 75-77 °C. R_f = 0.6 (CH_2Cl_2/MeOH/25% aq NH_3 90:9:1 v/v/v/). ^{1}H-NMR (300 MHz, $CDCl_3$): δ (ppm) 1.45-1.65 (m, 2H), 1.82 (brs, 1H), 1.84-1.93 (m, 2H), 2.64-2.73 (m, 2H), 2.89-3.03 (m, 2H), 4.90-4.99 (m, 1H), 5.01 (s, 1H), 7.21-7.35 (m, 10H). ^{13}C-NMR (75 MHz, $CDCl_3$): δ (ppm) 31.9, 43.9, 57.4, 71.4, 127.3, 128.6, 128.7, 138.9, 171.9. HRMS (ESI): *m/z* [*M*+H]$^+$ calcd. for $[C_{19}H_{22}NO_2]^+$

296.1645, found: 296.1666. $C_{19}H_{21}NO_2$ (295.38).

1-(2-((*tert*-Butoxycarbonyl)amino)ethyl)piperidin-4-yl 2,2-diphenylacetate (72)

Compound **71** (150 mg, 0.51 mmol), *tert*-butyl (2-bromoethyl) carbamate (compound **30**) (136 mg, 0.61 mmol) and potassium carbonate (140 mg, 1.01 mmol) were added to MeCN (50 mL) and the mixture was refluxed for 3 h. Insoluble material was separated by filtration and washed with CH_2Cl_2 (2 × 5 mL). The combined filtrate and washings were concentrated under reduced pressure to yield a brown residue, which was dissolved in CH_2Cl_2 (10 mL) followed by washing with water. The aqueous phase was treated with CH_2Cl_2 (3 × 5 mL) and the organic extracts were collected. All organic phases were combined and dried over Na_2SO_4. Removal of the solvent under reduced pressure gave the crude product, which was subjected to flash column chromatography (eluent: CH_2Cl_2/MeOH/25% aq NH_3 90:3:1 v/v/v) to yield compound **72** as colorless oil (150 mg, 67%). R_f = 0.6 (CH_2Cl_2/MeOH/25% aq NH_3 90:10:1 v/v/v). ^{1}H-NMR (300 MHz, $CDCl_3$): δ (ppm) 1.40 (s, 9H), 1.58-1.70 (m, 2H), 1.81-1.95 (m, 2H), 2.21-2.30 (m, 2H), 2.39 (t, *J* 12 Hz, 2H), 2.49-2.59 (m, 2H), 3.16-3.18 (m, 2H), 4.82-4.89 (m, 1H), 4.96 (s, 1H), 5.03 (brs, 1H), 7.18-7.28 (m, 10H). ^{13}C-NMR (75 MHz, $CDCl_3$): δ (ppm) 28.5, 30.2, 37.1, 50.2, 57.1, 57.3, 70.3, 79.3, 127.3, 128.59, 128.60, 138.7, 155.9, 171.8. HRMS (ESI): *m/z* [*M*+H]$^+$ calcd. for $[C_{26}H_{35}N_2O_4]^+$ 439.2591, found: 439.2619. $C_{26}H_{34}N_2O_4$ (438.57).

1-(2-Aminoethyl)piperidin-4-yl 2,2-diphenylacetate (73)

Compound **72** (500 mg, 1.14 mmol) was dissolved in CH_2Cl_2 (4 mL), TFA (1 mL) was added slowly and the mixture was stirred at room temperature for 8 h. 25% aq NH_3 was added slowly to adjust the pH to 11, followed by extraction with CH_2Cl_2/MeOH (9:1 v/v) (5 × 10 mL). The combined extracts were dried over Na_2SO_4 and the volatiles were evaporated to afford compound **73** as colorless oil (320 mg, 83%), which was used without further purification. R_f = 0.3 (CH_2Cl_2/MeOH/25% aq NH_3 90:10:1 v/v/v). ^{1}H-NMR (300 MHz, $CDCl_3$): δ (ppm) 1.59-1.77 (m, 2H), 1.84-1.93 (m, 2H), 2.26 (t, *J* 8.5 Hz, 2H), 2.38-2.47 (m, 2H), 2.55 (brs, 2H), 2.79 (t, *J* 6.0 Hz, 4H), 4.84-4.92 (m, 1H), 5.00 (s, 1H), 7.23-7.26 (m, 2H), 7.28-7.37 (m, 8H). ^{13}C-NMR (75 MHz, $CDCl_3$): δ (ppm) 30.6, 38.5, 50.5, 57.3, 59.5, 70.7, 127.2, 128.57, 128.62, 138.7, 171.9. HRMS (ESI): *m/z* [*M*+H]$^+$ calcd. for $[C_{21}H_{27}N_2O_2]^+$ 339.2067, found: 339.2072. $C_{21}H_{26}N_2O_2$ (338.45).

2-Bromoethyl 9*H*-xanthene-9-carboxylate (75)

9*H*-xanthene-9-carboxylic acid (compound **74**) (1.0 g, 4.42 mmol) and 2-bromoethan-1-ol (1.1 g, 8.87 mmol) were dissolved in CH_2Cl_2 (30 mL) and the solution was cooled to 0 °C. *N*,*N*′-Dicyclohexylcarbodiimide (1.1 g, 5.34 mmol) dissolved in CH_2Cl_2 (5 mL) was added dropwise followed by the addition of DMAP (270 mg, 2.21 mmol). The mixture was allowed to warm up

to room temperature and stirring was continued overnight. H_2O (50 mL) was added, the phases were separated and the aqueous phase was treated with CH_2Cl_2 (3 × 30 mL). The combined organic phases were washed with brine, dried over Na_2SO_4 and concentrated under reduced pressure. Purification by column chromatography (eluent: light petroleum/acetone 7:1 v/v) afforded compound **75** as colorless oil (1.0 g, 68%). R_f = 0.7 (light petroleum/acetone 3:1 v/v). ^{1}H-NMR (300 MHz, $CDCl_3$): δ (ppm) 3.40 (t, *J* 6.1 Hz, 2H), 4.35 (t, *J* 6.1 Hz, 2H), 5.06 (s, 1H), 7.06-7.19 (m, 4H), 7.27-7.36 (m, 4H). ^{13}C-NMR (75 MHz, CDCl3): δ (ppm) 28.3, 45.2, 64.5, 117.1, 117.9, 123.4, 129.1, 129.3, 151.4, 171.4. HRMS (ESI): *m/z* $[M+H]^+$ calcd. for $[C_{16}H_{14}BrO_3]^+$ 333.0121, found: 333.0124. $C_{16}H_{13}BrO_3$ (333.18).

4-Bromobutyl 9*H*-xanthene-9-carboxylate (76)

9*H*-Xanthene-9-carboxylic acid (compound **74**) (2.0 g, 8.84 mmol) and 4-bromobutan-1-ol (1.6 g, 10.61 mmol) were dissolved in CH_2Cl_2 (30 mL) and the mixture was cooled to 0 °C. A solution of *N*, *N'*-dicyclohexylcarbodiimide (2.2 g, 10.61 mmol) in CH_2Cl_2 (5 mL) was added dropwise followed by the addition of DMAP (270 mg, 2.21 mmol). The mixture was allowed to warm up to room temperature and stirring was continued overnight. H_2O (20 mL) was added, the phases were separated and the aqueous phase was treated with CH_2Cl_2 (3 × 15 mL). The combined organic phases were washed with brine, dried over Na_2SO_4 and concentrated under reduced pressure. Purification by column chromatography (eluent: light petroleum/acetone 7:1 v/v) yielded compound **76** as colorless oil (1.8 g, 56%). R_f = 0.7 (light petroleum/acetone 4:1 v/v). ^{1}H-NMR (300 MHz, $CDCl_3$): δ (ppm) 1.59-1.74 (m, 4H), 3.23 (t, *J* 9.0 Hz, 2H), 4.06 (t, *J* 6.0 Hz, 2H), 4.99 (s, 1H), 7.04-7.18 (m, 4H), 7.26-7.34 (m, 4H). ^{13}C-NMR (75 MHz, $CDCl_3$): δ (ppm) 27.1, 29.0, 33.0, 45.7, 64.5, 117.1, 118.5, 123.4, 128.9, 129.3, 151.4, 171.9. HRMS (ESI): *m/z* $[M+H]^+$ calcd. for $[C_{18}H_{18}BrO_3]^+$ 361.0434, found: 361.0435. $C_{18}H_{17}BrO_3$ (361.24).

2-(Piperazin-1-yl)ethyl 9*H*-xanthene-9-carboxylate (77)

Compound **75** (500 mg, 1.50 mmol), piperazine (1.04 g, 12.08 mmol) and potassium carbonate (416 mg, 3.01 mmol) were added to MeCN (18 mL) and the mixture was refluxed overnight. Insoluble material was separated by filtration and washed with CH_2Cl_2 (2 × 10 mL). The combined filtrate and washings were concentrated under reduced pressure yielding a yellow oil, which was dissolved in CH_2Cl_2 (10 mL) followed by washing with brine. The aqueous phase was treated with CH_2Cl_2 (3 × 15 mL) and the organic extracts were collected. All organic phases were combined and dried over Na_2SO_4. Removal of the solvent under reduced pressure gave the crude product, which was subjected to column chromatography (eluent: CH_2Cl_2/MeOH/25% aq NH_3 96:3:1 v/v/v) to yield compound **77** as yellow solid (300 mg, 59%). R_f = 0.5 (CH_2Cl_2/MeOH/25% aq NH_3 90:9:1 v/v/v), m.p. 77-79 °C. ^{1}H-NMR (300 MHz, $CDCl_3$): δ (ppm) 2.36-2.54 (m, 6H), 2.82-2.92 (m, 4H), 4.61 (brs, 1H), 4.13 (t, *J* 10 Hz, 2H), 5.00 (s,

1H), 7.05-7.17 (m, 4H), 7.27-7.35 (m, 4H). ^{13}C-NMR (75 MHz, $CDCl_3$): δ (ppm) 44.2, 45.6, 50.9, 56.3, 62.7, 117.0, 118.4, 123.3, 128.9, 129.2, 151.4, 171.5. HRMS (ESI): *m/z* $[M+H]^+$ calcd. for $[C_{20}H_{23}N_2O_3]^+$ 339.1703, found: 339.1707. $C_{20}H_{22}N_2O_3$ (338.41).

4-(Piperazin-1-yl)butyl 9*H*-xanthene-9-carboxylate (78)

Compound **76** (1.0 g, 2.77 mmol), piperazine (1.9 g, 22.07 mmol) and potassium carbonate (1.2 g, 8.70 mmol) were added to MeCN (50 mL) and the stirred mixture was kept under reflux for 1.5 h. Insoluble material was separated by filtration and washed with CH_2Cl_2 (2 × 20 mL). The combined filtrate and washings were concentrated under reduced pressure to give a yellow oil, which was dissolved in CH_2Cl_2 (20 mL) followed by washing with water. The aqueous phase was treated with CH_2Cl_2 (3 × 30 mL) and the organic extracts were collected. All organic phases were combined and dried over Na_2SO_4. Removal of the volatiles under reduced pressure gave the crude product, which was subjected to column chromatography (eluent: CH_2Cl_2/MeOH/25% aq NH_3 94:5:1 v/v/v) to afford compound **78** as colorless oil (470 mg, 46%). R_f = 0.5 (CH_2Cl_2/MeOH/25% aq NH_3 90:9:1 v/v/v). ^{1}H-NMR (300 MHz, $CDCl_3$): δ (ppm) 1.19-1.42 (m, 2H), 1.43-1.60 (m, 2H), 2.12-2.26 (m, 4H), 2.26-2.32 (m, 2H), 2.36 (brs, 1H), 2.81-2.94 (m, 4H), 4.04 (t, *J* 6.3 Hz, 2H), 4.98 (s, 1H), 7.00-7.17 (m, 4H), 7.23-7.35 (m, 4H). ^{13}C-NMR (75 MHz, $CDCl_3$): δ (ppm) 22.6, 26.5, 45.6, 45.8, 54.1, 58.4, 65.3, 116.9, 118.5, 123.3, 128.9, 129.1, 151.3, 171.9. HRMS (ESI): *m/z* $[M+H]^+$ calcd. for $[C_{22}H_{27}N_2O_3]^+$ 367.2016, found: 367.2027. $C_{22}H_{26}N_2O_3$ (366.46).

2-(4-(2-((*tert*-Butoxycarbonyl)amino)ethyl)piperazin-1-yl)ethyl-9*H*-xanthene-9-carboxylate (79)

Compound **77** (1.27 g, 3.76 mmol), *tert*-butyl (2-bromoethyl) carbamate (compound **30**) (921 mg, 4.13 mmol) and potassium carbonate (1.3 g, 9.41 mmol) were added to MeCN (30 mL) and the mixture was kept under reflux for 2 h. Insoluble material was separated by filtration and washed with CH_2Cl_2 (2 × 10 mL). The filtrate and washings were combined and the volatiles were removed under reduced pressure yielding a yellow oily residue, which was dissolved in CH_2Cl_2 (20 mL) followed by washing with water. The aqueous phase was treated with CH_2Cl_2 (3 × 20 mL) and the organic extracts were collected. All organic phases were combined and dried over Na_2SO_4. Removal of the solvent under reduced pressure gave the crude product, which was subjected to column chromatography (eluent: CH_2Cl_2/MeOH/25% aq NH_3 90:3:1 v/v/v) to afford compound **79** as yellow oil (1.03 g, 57%). R_f = 0.5 (CH_2Cl_2/MeOH/25% aq NH_3 90:10:1 v/v/v). ^{1}H-NMR (300 MHz, $CDCl_3$): δ (ppm) 1.45 (d, *J* 5.3 Hz, 9H), 2.13-2.38 (m, 8H), 2.42 (t, *J* 5.9 Hz, 2H), 2.45-2.55 (m, 2H), 3.19-3.27 (m, 2H), 4.08-4.19 (m, 2H), 4.99 (s, 1H), 5.04 (brs, 1H), 7.04-7.11 (m, 2H), 7.04-7.13 (m, 2H), 7.23-7.31 (m, 4H). ^{13}C-NMR (75 MHz, $CDCl_3$): δ (ppm) 28.5, 37.0, 45.5, 52.8, 53.5, 56.3, 57.0, 63.3, 79.2,

116.9, 118.4, 123.3, 129.0, 129.1, 151.3, 155.9, 171.6. HRMS (ESI): *m/z* $[M+H]^+$ calcd. for $[C_{27}H_{36}N_3O_5]^+$ 482.2649, found: 482.2645. $C_{27}H_{35}N_3O_5$ (481.59).

2-(4-(2-Aminoethyl)piperazin-1-yl)ethyl 9*H*-xanthene-9-carboxylate (80)

Compound **79** (1.0 g, 2.08 mmol) was dissolved in CH_2Cl_2 (8 mL), TFA (2 mL) was added slowly, and the mixture was stirred at room temperature overnight. 25% aq NH_3 was added to adjust the pH to 11, followed by extraction with CH_2Cl_2/MeOH (9:1 v/v) (5 × 15 mL). The combined extracts were dried over Na_2SO_4. Removal of the solvent *in vacuo* gave compound **80** as colorless oil (700 mg, 88%), which was used without further purification. R_f = 0.2 (CH_2Cl_2/MeOH/25% aq NH_3 90:10:1 v/v/v). ^{1}H-NMR (300 MHz, [D$_4$]MeOH): δ (ppm) 2.20-2.42 (m, 8H), 2.41-2.61 (m, 4H), 2.67-2.79 (m, 2H), 4.05-4.23 (m, 2H), 4.90 (s, 1H), 7.01-7.21 (m, 4H), 7.23-7.44 (m, 4H). ^{13}C-NMR (75 MHz, [D$_4$]MeOH): δ (ppm) 38.9, 46.1, 53.9, 54.0, 57.4, 60.9, 64.4, 117.8, 119.9, 124.6, 130.32, 130.34, 152.9, 173.2. HRMS (ESI): *m/z* $[M+H]^+$ calcd. for $[C_{22}H_{28}N_3O_3]^+$ 382.2125, found: 382.2123. $C_{22}H_{27}N_3O_3$ (381.48).

1-(3-Chloropropyl)-3,4-dihydroquinolin-2(1*H*)-one (83)[53]

3,4-dihydroquinolin-2(1*H*)-one (compound **81**) (1.0 g, 6.80 mmol), 1-chloro-3-iodopropane (compound **82**) (1.7 mg, 8.32 mmol) and caesium carbonate (4.4 g, 13.51 mmol) were added to MeCN (50 mL) and the mixture was stirred and heated to 50 °C for 12 h. Insoluble material was separated by filtration and washed with CH_2Cl_2 (2 × 20 mL). The filtrate and washings were combined and the volatiles were removed under reduced pressure yielding a yellow solid, which was dissolved in CH_2Cl_2 (20 mL). This solution was washed with brine, the phases were separated and the aqueous phase was treated with CH_2Cl_2 (3 × 20 mL). The combined organic phases were dried over Na_2SO_4 and concentrated under reduced pressure to yield a yellow oil, which was subjected to column chromatography (eluent: CH_2Cl_2/MeOH/25% aq NH_3 90:3:1 v/v/v) to afford compound **83** as yellow oil (1.05 g, 69%). R_f = 0.7 (CH_2Cl_2/MeOH/25% aq NH_3 90:3:1). ^{1}H-NMR (300 MHz, [D$_4$]MeOH): δ (ppm) 2.07-2.21 (m, 2H), 2.59-2.70 (m, 2H), 2.81-2.98 (m, 2H), 3.56-3.71 (m, 2H), 4.00-4.20 (m, 2H), 6.97-7.10 (m, 2H), 7.15-7.31 (m, 2H). ^{13}C-NMR (75 MHz, [D$_4$]MeOH): δ (ppm) 25.5, 30.2, 31.8, 40.1, 42.8, 114.6, 122.9, 126.5, 127.6, 128.1, 139.4, 170.4. HRMS (ESI): *m/z* $[M+H]^+$ calcd. for $[C_{12}H_{15}ClNO]^+$ 224.0837, found: 224.0846. $C_{12}H_{14}ClNO$ (223.70).

1-(3-(4-(4-Hydroxybutyl)piperidin-1-yl)propyl)-3,4-dihydroquinolin-2(1*H*)-one (85)

4-(Piperidin-4-yl)butanoic acid hydrochloride (1.0 g, 4.81 mmol) was suspended in anhydrous THF (20 mL) under an atmosphere of argon. The suspension was immersed in an ice bath and lithium aluminium hydride (456 mg, 12.01 mmol) was added in portions under stirring. The mixture was slowly warmed up to room temperature, then kept under reflux overnight, and

cooled in an ice bath. For quenching, water (5 mL), 15% NaOH solution (10 mL) and water (10 mL) were added dropwise to reaction mixture. Insoluble material was separated by filtration and washed with chloroform (3 × 20 mL). The combined filtrate and washings were dried over Na_2SO_4 and concentrated under reduced pressure to give the intermediate 4-(piperidin-4-yl)butan-1-ol[68] (compound **84**) as colorless oil-like residue (510 mg, 68%), which was used without further purification. R_f = 0.1 (CH_2Cl_2/MeOH/25% aq NH_3 66:33:1 v/v/v). ^{1}H-NMR (300 MHz, [D$_4$]MeOH): δ (ppm) 1.04-1.18 (m, 2H), 1.20-1.31 (m, 2H), 1.31-1.44 (m, 3H), 1.47-1.57 (m, 2H), 1.70 (d, *J* 12 Hz, 2H), 2.55-2.57 (m, 2H), 2.99-3.01 (m, 2H), 3.54 (t, *J* 6.5 Hz, 2H). ^{13}C-NMR (75 MHz, [D$_4$]MeOH): δ (ppm) 23.9, 33.8, 33.9, 37.2, 38.2, 47.1, 62.9. HRMS (ESI): *m/z* [*M*+H]$^+$ calcd. for $[C_9H_{20}NO]^+$ 158.1539, found: 158.1541. The intermediate **84** (867 mg, 5.52 mmol) and compound **83** (1.1 g, 4.92 mmol) were dissolved in MeCN (30 mL), followed by the addition of potassium carbonate (1.4 g, 10.14 mmol) and sodium iodide (376 mg, 2.51 mmol). The mixture was kept at 50 °C for 24 h. Insoluble material was separated by filtration and washed with CH_2Cl_2 (2 × 10 mL). The filtrate and washings were combined and the solvent was removed under reduced pressure to yield a yellow residue, which was dissolved in CH_2Cl_2 (20 mL) followed by washing with water. The aqueous phase was treated with CH_2Cl_2 (3 × 20 mL) and the organic extracts were collected. All organic phases were combined and dried over Na_2SO_4. Removal of the solvent under reduced pressure gave crude product, which was subjected to column chromatography (eluent: CH_2Cl_2/MeOH/25% aq NH_3 90:9:1 v/v/v) to afford compound **85** as colorless oil (900 mg, 53%). R_f = 0.4 (CH_2Cl_2/MeOH/25% aq NH_3 90:10:1 v/v/v). ^{1}H-NMR (300 MHz, $CDCl_3$): δ (ppm) 1.26-1.42 (m, 7H), 1.45-1.59 (m, 2H), 1.68 (brs, 1H), 1.68-1.72 (m, 2H), 1.84-2.12 (m, 4H), 2.45-2.56 (m, 2H), 2.59-2.65 (m, 2H), 2.77-2.94 (m, 2H), 2.99-3.03 (m, 2H), 3.62 (t, *J* 6.4 Hz, 2H), 3.90-4.00 (m, 2H), 6.96-7.01 (m, 1H), 7.07 (d, *J* 7.7 Hz, 1H), 7.13-7.16 (m, 1H), 7.20-7.26 (m, 1H). ^{13}C NMR (75 MHz, $CDCl_3$): δ (ppm) 18.4, 22.9, 24.4, 25.4, 31.8, 32.9, 36.0, 40.5, 50.8, 53.9, 55.9, 62.8, 114.9, 122.9, 126.4, 127.6, 128.0, 139.4, 170.4. HRMS (ESI): *m/z* [*M*+H]$^+$ calcd. for $[C_{21}H_{33}N_2O_2]^+$ 345.2537, found: 345.2565. $C_{21}H_{32}N_2O_2$ (344.50).

1-(3-(4-(4-Bromobutyl)piperidin-1-yl)propyl)-3,4-dihydroquinolin-2(1*H*)-one (86)

Compound **85** (900 mg, 2.61 mmol) and PPh_3 (2.06 g, 7.86 mmol) were dissolved in anhydrous CH_2Cl_2 (30 mL) and the solution was cooled to -5 °C. A solution of CBr_4 (3.03 g, 9.14 mmol) in anhydrous CH_2Cl_2 (15 mL) was slowly dropped into the stirred mixture, thereby keeping the temperature of the mixture below 5 °C. Stirring was continued at room temperature overnight. The solvent was evaporated yielding a yellow residue, which was subjected to column chromatography (eluent: light petroleum/acetone/25% aq NH_3 80:20:1 v/v/v) to yield compound **86** as colorless oil (330 mg, 31%). R_f = 0.3 (light petroleum/acetone/25% aq NH_3 80:20:1 v/v/v). ^{1}H-NMR (300 MHz, CDCl3): δ (ppm) 1.26-1.31 (m, 5H), 1.35-1.52 (m, 2H), 1.68

(d, *J* 9.3 Hz, 2H), 1.76-2.03 (m, 6H), 2.42 (t, *J* 6.1 Hz, 2H), 2.60-2.65 (m, 2H), 2.80-3.01 (m, 4H), 3.40 (t, *J* 6.8 Hz, 2H), 3.96 (t, *J* 7.5Hz, 2H), 6.96-7.01 (m, 1H), 7.08 (d, *J* 8.1 Hz, 1H), 7.15 (dd, *J* 7.3, 1.1 Hz, 1H), 7.22 (dd, *J* 11, 4.6 Hz, 1H). ^{13}C-NMR (75 MHz, $CDCl_3$): δ (ppm) 24.8, 25.5, 25.7, 32.0, 32.2, 33.0, 34.1, 35.6, 35.7, 40.7, 54.1, 56.1, 115.1, 122.9, 126.6, 127.6, 128.1, 139.7, 170.4. HRMS (ESI): *m/z* [*M*+H]$^+$ calcd. for $[C_{21}H_{32}BrN_2O]^+$ 407.1693, found: 407.1695. $C_{21}H_{31}BrN_2O$ (407.40).

tert-Butyl (2-(4-(4-(1-(3-(2-oxo-3,4-dihydroquinolin-1(2*H*)-yl)propyl)piperidin-4-yl)butyl)piperazin-1-yl)ethyl)carbamate (87)

Compound **86** (1.21 g, 2.97 mmol), *tert*-butyl (2-(piperazin-1-yl) ethyl)carbamate (compound **32**) (1.5 g, 6.55 mmol) and potassium carbonate (1.24 g, 8.99 mmol) were added to MeCN (60 mL) and the stirred mixture was kept under reflux for 2 h. Insoluble material was removed by filtration and the filtrate was concentrated under reduced pressure yielding a yellow oily residue, which was dissolved in CH_2Cl_2 (20 mL) followed by washing with water. The aqueous phase was treated with CH_2Cl_2 (3 × 30 mL) and the organic extracts were collected. All organic phases were combined and dried over Na_2SO_4. Removal of the solvent under reduced pressure gave the crude product, which was subjected to column chromatography (eluent: CH_2Cl_2/MeOH/25% aq NH_3 90:3:1 v/v/v) to afford compound **87** as yellow oil (1.02 g, 62%). R_f = 0.5 (CH_2Cl_2/MeOH/25% aq NH_3 90:9:1 v/v/v). ^{1}H-NMR (300 MHz, $CDCl_3$): δ (ppm) 1.13-1.18 (m, 7H), 1.38 (s, 9H), 1.39-1.44 (m, 2H), 1.53-1.62 (m, 2H), 1.71-1.94 (m, 4H), 2.19-2.29 (m, 2H), 2.30-2.51 (m, 10H), 2.54-2.59 (m, 3H), 2.74-2.94 (m, 4H), 3.08-3.21 (m, 2H), 3.90 (t, *J* 6.0 Hz, 2H), 6.89-6.95 (m, 1H), 7.02-7.09 (m, 2H), 7.05-7.11 (m, 1H), 7.12-7.20 (m, 1H). ^{13}C-NMR (75 MHz, $CDCl_3$): δ (ppm) 24.7, 25.6, 27.1, 28.5, 31.9, 32.2, 35.6, 36.4, 37.1, 40.5, 52.9, 53.2, 54.1, 56.1, 57.1, 58.8, 65.9, 79.1, 114.9, 122.7, 126.5, 127.5, 127.9, 139.6, 155.9, 170.2. HRMS (ESI): *m/z* [*M*+H]$^+$ calcd. for $[C_{32}H_{54}N_5O_3]^+$ 556.4221, found: 556.4227. $C_{32}H_{53}N_5O_3$ (555.81)

1-(3-(4-(4-(4-(2-Aminoethyl)piperazin-1-yl)butyl)piperidin-1-yl)propyl)-3,4-dihydroquinolin-2(1*H*)-one (88)

Compound **87** (300 mg, 0.54 mmol) was dissolved in CH_2Cl_2/TFA (4:1 v/v) (5 mL) and the mixture was stirred at room temperature for 8 h. 25% aq NH_3 was added to adjust the pH to 11, followed by extraction with CH_2Cl_2/MeOH (9:1 v/v) (5 × 10 mL). The combined extracts were dried over Na_2SO_4. Removal of the volatiles *in vacuo* yielded compound **88** as yellow oil (240 mg, 97%), which was used without further purification. R_f = 0.1 (CH_2Cl_2/MeOH/25% aq NH_3 90:9:1 v/v/v). ^{1}H-NMR (300 MHz, [D_4]MeOH): δ (ppm) 1.16-1.32 (m, 7H), 1.44-1.54 (m, 2H), 1.62-1.70 (m, 2H), 1.76-1.86 (m, 2H), 1.89-1.98 (m, 2H), 2.32-2.40 (m, 6H), 2.42-2.67 (m, 10H), 2.78-2.82 (m, 2H), 2.81-2.98 (m, 4H), 3.86-4.09 (m, 2H), 6.89-7.08 (m, 1H), 7.08-7.31(m,

3H). ^{13}C-NMR (75 MHz, [D$_4$]MeOH): δ (ppm) 25.5, 25.8, 26.3, 27.7, 32.8, 33.0, 36.8, 37.6, 38.7, 41.3, 53.9, 55.1, 55.0, 57.1, 59.8, 60.1, 116.5, 124.4, 128.3, 128.7, 129.2, 140.4, 170.5. HRMS (ESI): *m/z* [*M*+H]$^+$ calcd. for [$C_{27}H_{46}N_5O$]$^+$ 456.3697, found: 456.3700. $C_{27}H_{45}N_5O$ (455.69).

5,10-Dihydro-11*H*-dibenzo[*b*,*e*][1,4]diazepin-11-one (91)[54]

A mixture of 2-chlorobenzoic acid (compound **89**) (20 g, 127.7 mmol), 1,2-benzenediamine (compound **90**) (13.8 g, 127.6 mmol) and copper powder (8.1 g, 127.5 mmol) in chlorobenzene (300 mL) was kept under reflux in a round bottom flask, equipped with a Dean-stark apparatus, for 6 h. The hot mixture was filtered and the solid was washed with a small amount of chlorobenzene. The combined filtrates were concentrated under reduced pressure to reach a volume of approx. 400 mL. After storage at -20 °C for 12 h the crystalline product was collected and recrystallized from ethanol/ethyl acetate (1:1 v/v) to yield **91** as yellow-green crystals (3.5 g, 13%). R_f = 0.6 (light petroleum/ethyl acetate 1:1 v/v), m.p. 247-249 °C (Lit[54]. m.p. 256-257 °C). ^{1}H-NMR (300 MHz, [D$_6$]DMSO): (ppm) 6.85-7.02 (m, 6H), 7.26-7.40 (m, 1H), 7.67 (dd, *J* 7.9, 1.6 Hz, 1H), 7.85 (s, 1H), 9.85 (s, 1H). ^{13}C-NMR (75 MHz, [D$_6$]DMSO): δ (ppm) 118.9, 119.7, 120.6, 121.2, 122.6, 122.7, 124.4, 129.7, 131.9, 133.1, 139.9, 150.3, 167.8. HRMS (ESI): *m/z* [*M*+H]$^+$ calcd. for [$C_{13}H_{11}N_2O$]$^+$ 211.0866, found: 211.0862. $C_{13}H_{10}N_2O$ (210.24).

5-(2-Chloroacetyl)-5,10-dihydro-11*H*-dibenzo[*b*,*e*][1,4]diazepin-11-one (92)[69]

Under an atmosphere of argon compound **91** (3.5 g, 16.65 mmol), *N*,*N*-dimethylaniline (1.61 g, 13.28 mmol) and 2-chloroacetyl chloride (6.59 g, 58.35 mmol) were added to abs. THF (50 mL) and the mixture was kept under reflux overnight. 5% aq $KHCO_3$ (40 mL) was added slowly, resulting in the formation of a greyish solid, which was collected by filtration. The filtrate was concentrated under reduced pressure yielding a white-pink solid, which was washed with light petroleum/ethyl acetate (1:1 v/v) until the color of the solid turned to grey. The grey solids were combined and dried under vacuum (4.02 g, 84%). R_f = 0.4 (light petroleum/ethyl acetate 1:1 v/v), m.p. 231-233 °C (Lit[69]. m.p. 241-242 °C). Ratio of configurational isomers evident in the NMR spectra: ca 1.5:1. ^{1}H-NMR (300 MHz, [D$_6$]DMSO) δ (ppm) 4.10 (d, *J* 14 Hz, 0.6H), 4.19 (d, *J* 13 Hz, 0.4H), 4.40 (d, *J* 12 Hz, 1H), 7.17-7.33 (m, 2H), 7.34-7.61 (m, 3H), 7.61-7.89 (m, 3H), 10.70 (s, 0.4 H), 10.76 (s, 0.6H). ^{13}C-NMR (75 MHz, [D$_6$]DMSO) δ (ppm) 41.7, 121.3, 121.6, 124.3, 124.9, 126.3, 126.9, 127.2, 127.8, 127.9, 128.1, 128.7, 129.1, 129.3, 130.3, 130.6, 132.4, 132.7, 133.1, 134.3, 135.3, 141.3, 164.9, 165.5, 165.7. HRMS (ESI): *m/z* [*M*+H]$^+$ calcd. for [$C_{15}H_{12}ClN_2O_2$]$^+$ 287.0582, found: 287.0581. $C_{15}H_{11}ClN_2O_2$ (286.72).

5-(2-(4-(4-Hydroxybutyl)piperidin-1-yl)acetyl)-5,10-dihydro-11*H*-dibenzo[*b*,*e*][1,4]diazepin-11-one (93)

4-(Piperidin-4-yl)butan-1-ol (compound **84**) (1.81 g, 11.53 mmol), compound **92** (3.0 g, 10.46 mmol) and potassium carbonate (5.8 g, 42.03 mmol) were added to MeCN (80 mL) and the mixture was kept under reflux for 8 h. Insoluble material was separated by filtration and washed with CH_2Cl_2 (2 × 20 mL). The filtrate and washings were combined and the volatiles were removed under reduced pressure yielding a yellow oil, which was dissolved in CH_2Cl_2 (20 mL) followed by washing with brine. The aqueous phase was treated with CH_2Cl_2 (3 × 20 mL) and the organic extracts were collected. All organic phases were combined and dried over Na_2SO_4. Removal of the volatiles under reduced pressure gave the crude product, which was subjected to column chromatography (eluent: CH_2Cl_2/MeOH/25% aq NH_3 96:3:1 v/v/v) to afford compound **93** as white solid (2.9 g, 62%), m.p. 143-145 °C. R_f = 0.8 (CH_2Cl_2/MeOH/25% aq NH_3 90:9:1 v/v/v). Ratio of configurational isomers evident in the NMR spectra: ca 1.2:1. ^{1}H-NMR (300 MHz, [D$_4$]MeOH): δ (ppm) 0.86-1.13 (m, 2H), 1.13-1.21 (m, 3H), 1.27-1.38 (m, 2H), 1.40-1.64 (m, 4H), 1.78-2.04 (m, 2H), 2.48-2.65 (m, 1H), 2.74-2.85 (m, 1H), 3.02 (d, *J* 15 Hz, 0.55H), 3.11-3.16 (m, 1H), 3.22 (d, *J* 15 Hz, 0.45H), 3.51 (t, *J* 6.5 Hz, 2H), 7.18-7.30 (m, 2H), 7.30-7.39 (m, 1H), 7.40-7.56 (m, 3H), 7.61-7.66 (m, 1H), 7.80-7.94 (m, 1H). ^{13}C-NMR (75 MHz, [D$_4$]MeOH): δ (ppm) 24.0, 32.7, 32.9, 33.9, 36.4, 37.4, 54.8, 54.9, 62.9, 123.0, 123.1, 126.6, 127.0, 127.8, 128.9, 129.0, 129.5, 129.9, 130.6, 131.1, 132.1, 132.3, 134.3, 134.7, 135.9, 136.9, 143.7, 169.2, 169.4, 171.2, 171.5. HRMS (ESI): *m/z* [*M*+H]$^+$ calcd. for [$C_{24}H_{30}N_3O_3$]$^+$ 408.2282, found: 408.2299. $C_{24}H_{29}N_3O_3$ (407.22).

5-(2-(4-(4-Bromobutyl)piperidin-1-yl)acetyl)-5,10-dihydro-11*H*-dibenzo[*b*,*e*][1,4]diazepin-11-one (94)

Under an atmosphere of argon compound **93** (200 mg, 0.49 mmol) and PPh_3 (386 mg, 1.47 mmol) were dissolved in CH_2Cl_2 (5 mL) in a three-necked round bottom flask and the solution was cooled to -5 °C. A solution of CBr_4 (1.06 g, 3.20 mmol) in CH_2Cl_2 (10 mL) was added dropwise, thereby keeping the temperature of the mixture below 5 °C. Stirring was continued at room temperature overnight. The solvent was evaporated and the residue subjected to column chromatography to column chromatography (eluent: light petroleum/acetone/25% aq NH_3 83:16:1 v/v/v) to afford compound **94** as white solid (180 mg, 78%). R_f = 0.5 (light petroleum/acetone/25% aq NH_3 66:33:1 v/v/v), m.p. 68-70 °C. Ratio of configurational isomers evident in the NMR spectra: ca 1.2:1. ^{1}H-NMR (300 MHz, [D$_4$]MeOH): δ (ppm) 1.03-1.27 (m, 5H), 1.31-1.46 (m, 2H), 1.46-1.62 (m, 2H), 1.73-1.82 (m, 2H), 1.82-2.03 (m, 2H), 2.47-2.64 (m, 1H), 2.77-2.85 (m, 1H), 3.01 (d, *J* 18 Hz, 0.55H), 3.10-3.18 (m, 1H), 3.21 (d, *J* 18 Hz, 0.45H), 3.41 (t, *J* 6.7 Hz, 2H), 7.17-7.40 (m, 3H), 7.40-7.59 (m, 3H), 7.61-7.66 (m, 1H), 7.84-7.90 (m, 1H). ^{13}C-NMR (75 MHz, [D$_4$]MeOH): δ (ppm) 26.3, 32.8, 34.1, 34.4, 36.3, 36.6, 54.8, 54.9, 61.0, 122.9, 126.6, 126.9, 127.8, 128.9, 129.0, 129.5, 129.9, 130.1, 130.6, 133.0, 132.1, 134.3, 134.7, 135.9, 143.9, 169.3, 171.4. HRMS (ESI): *m/z* [*M*+H]$^+$ calcd. for [$C_{24}H_{29}BrN_3O_2$]$^+$

470.1438, found: 470.1437. $C_{24}H_{28}BrN_3O_2$ (470.41).

5-(2-(4-(4-(6-Amino-4-methyl-1,4-diazepan-1-yl)butyl)piperidin-1-yl)acetyl)-5,10-dihydro-11*H*-dibenzo[*b*,*e*][1,4]diazepin-11-one tetrakis(hydrotrifluoroacetate) (95)

Potassium carbonate (70 mg, 0.51 mmol) was added to a solution of compound **94** (120 mg, 0.26 mmol) and compound **28** (65 mg, 0.28 mmol) in MeCN (5 mL), and the mixture was kept under reflux for 3 h. Insoluble material was removed by filtration. The filtrate was concentrated under reduced pressure to yield a yellow oil, which was dissolved in CH_2Cl_2 (5 mL) followed by washing with brine. The aqueous phase was treated with CH_2Cl_2 (3 × 10 mL) and the organic extracts were collected. All organic phases were combined and dried over Na_2SO_4. Removal of the solvent under reduced pressure gave the Boc-protected intermediate as yellow oil (110 mg, 69%), which was dissolved in CH_2Cl_2/TFA/H_2O (10:10:1 v/v/v) (5 mL). The mixture was stirred at room temperature for 2 h. CH_2Cl_2 (10 mL) was added and the volatiles were evaporated. Purification by preparative HPLC (column: Kinetex XB-C18 5 µm 250 × 21 mm; gradient: 0-30 min: MeCN/0.1% aq TFA 5:95-62:38, t_R = 14 min) afforded compound **95** as white fluffy solid (30 mg, 17%). Ratio of configurational isomers evident in the NMR spectra: ca 1.5:1. ^{1}H-NMR (600 MHz, [D$_4$]MeOH): δ (ppm) 1.27-1.37 (m, 4H), 1.40-1.55 (m, 3H), 1.56-1.66 (m, 2H), 1.87-1.95 (m, 2H), 2.83 (s, 3H), 2.88 (t, *J* 7.9 Hz, 2H), 2.90-2.96 (m, 1H), 3.01-3.05 (m, 1H), 3.08-3.15 (m, 1H), 3.21-3.24 (m, 1H), 3.26-3.28 (m, 2H), 3.32-3.39 (m, 3H), 3.43-3.48 (m, 2H), 3.69-3.79 (m, 2H), 3.82-3.86 (m, 1H), 4.39 (d, *J* 17 Hz, 0.6H), 4.43 (d, *J* 17 Hz, 0.4H), 7.23-7.29 (m, 1H), 7.31-7.40 (m, 2H), 7.45-7.52 (m, 2H), 7.60-7.75 (m, 2H), 7.89 (d, *J* 8.0 Hz, 0.6H), 7.96 (d, *J* 8.0 Hz, 0.4H). ^{13}C-NMR (150 MHz, [D$_4$]MeOH): δ (ppm) 24.8, 26.7, 30.4, 34.3, 36.4, 46.5, 52.7, 54.9, 55.3, 55.6, 56.4, 57.9, 58.0, 58.2, 59.6, 123.1, 123.7, 126.9, 127.5, 127.9, 128.5, 128.9, 129.4, 130.1, 130.5, 130.9, 131.2, 131.7, 131.9, 132.3, 132.9, 133.4, 134.6, 134.9, 135.5, 135.7, 136.9, 140.9, 142.7, 164.9, 165.5, 168.9, 168.8. RP-HPLC (220 nm): 99% (t_R = 13.7 min, *k* = 3.8). HRMS (ESI): *m/z* [*M*+H]$^+$ calcd. for $[C_{30}H_{43}N_6O_2]^+$ 519.3442, found: 519.3441. $C_{30}H_{42}N_6O_2 \cdot C_8H_4F_{12}O_8$ (518.71 + 456.09).

5-(2-(4-(4-(4-(2-Aminoethyl)piperazin-1-yl)butyl)piperidin-1-yl)acetyl)-5,10-dihydro-11*H*-dibenzo[*b*,*e*][1,4]diazepin-11-one tetrakis(hydrotrifluoroacetate) (96)

Compound **94** (280 mg, 0.60 mmol), *tert*-butyl (2-(piperazin-1-yl)ethyl)carbamate (**32**) (164 mg, 0.72 mmol) and potassium carbonate (247 mg, 1.79 mmol) were added to MeCN (20 mL) and the mixture was kept under reflux for 3 h. Insoluble material was separated by filtration and washed with CH_2Cl_2 (2 × 5 mL). The filtrate and washings were combined and the solvent was evaporated. The residue was dissolved in CH_2Cl_2 (10 mL) followed by washing with brine. The aqueous phase was treated with CH_2Cl_2 (3 × 10 mL) and the organic extracts were collected. All organic phases were combined and dried over Na_2SO_4. The volatiles were removed under

reduced pressure and the residue was subjected to flash column chromatography (eluent: CH_2Cl_2/MeOH/25% aq NH_3 90:3:1 v/v/v) to afford the Boc-protected intermediate as white solid (270 mg, 73%). R_f = 0.6 (CH_2Cl_2/MeOH/25% aq NH_3 90:10:1 v/v/v). The intermediate (270mg, 0.436 mmol) was dissolved in CH_2Cl_2 (5mL), TFA (1 mL) was added slowly, and the mixture was stirred at room temperature for 8 h. CH_2Cl_2 (10 mL) was added and the volatiles were evaporated. Purification by preparative HPLC (column: Kinetex XB-C18 5 µm 250 × 21 mm; gradient: 0-30 min: MeCN/0.1% aq TFA 20:80-64:36, t_R = 8 min) afforded compound **96** as white fluffy solid (280 mg, 66%). Ratio of configurational isomers evident in the NMR spectra: ca 1.8:1. ^{1}H-NMR (600 MHz, [D$_4$]MeOH): δ (ppm) 1.29-1.42 (m, 4H), 1.42-1.60 (m, 3H), 1.69-1.74 (m, 2H), 1.83 -2.04 (m, 2H), 2.51 (s, 2H), 2.69 (t, *J* 5.7 Hz, 2H), 2.84-2.99 (m, 1H), 3.00-3.24 (m, 9H), 3.38-3.60 (m, 3H), 3.70-3.80 (m, 2H), 4.39 (d, *J* 17 Hz, 0.65H), 4.44 (d, *J* 17 Hz, 0.35H), 7.24-7.29 (m, 1H), 7.31-7.38 (m, 2H), 7.45-7.52 (m, 2H), 7.60-7.75 (m, 2H), 7.89 (d, *J* 7.8 Hz, 0.65H), 7.96 (d, *J* 7.8 Hz, 0.35H). ^{13}C-NMR (150 MHz, [D$_4$]MeOH): δ (ppm) 24.5, 24.9, 30.4, 34.3, 36.1, 37.3, 50.6, 53.0, 54.6, 54.9, 55.3, 57.7, 58.0, 123.1, 123.6, 126.8, 127.5, 127.9, 128.5, 128.9, 129.5, 130.1, 130.5, 130.9, 131.2, 131.7, 131.9, 132.3, 132.9, 133.4, 134.6, 134.9, 135.5, 135.7, 137.0, 141.0, 142.7, 164.9, 165.4, 168.6, 168.8. RP-HPLC (220 nm): 99% (t_R = 13.4 min, *k* = 3.7). HRMS (ESI): *m/z* [*M*+H]$^+$ calcd. for $[C_{30}H_{43}N_6O_2]^+$ 519.3442, found: 519.3447. $C_{30}H_{42}N_6O_2 \cdot C_8H_4F_{12}O_8$ (518.71 + 456.09).

5-(2-(4-(4-(4-(3-((4-(1-Methyl-1,2,5,6-tetrahydropyridin-3-yl)-1,2,5-thiadiazol-3-yl)oxy)propyl)piperazin-1-yl)butyl)piperidin-1-yl)acetyl)-5,10-dihydro-11*H*-dibenzo[*b*,*e*][1,4]diazepin-11-one tetrakis(hydrotrifluoroacetate) (97)

Compound **94** (100 mg, 0.21 mmol), compound **40** (76 mg, 0.23 mmol) and potassium carbonate (88 mg, 0.64 mmol) were added to MeCN (5 mL) and the mixture was refluxed for 6 h. Insoluble material was separated by filtration and washed with CH_2Cl_2 (2 × 10 mL). The filtrate and washings were combined and the solvent was evaporated yielding a yellow oil, which was dissolved in CH_2Cl_2 (5 mL) followed by washing with brine. The aqueous phase was treated with CH_2Cl_2 (3 × 10 mL) and the organic extracts were collected. All organic phases were combined, dried over Na_2SO_4, and the volatiles were removed under reduced pressure. Purification by preparative HPLC (column: Kinetex XB-C18 5 µm 250 × 21 mm; gradient: 0-30 min: MeCN/0.1% aq TFA 20:80-62:38, t_R = 8 min) afforded **97** as white fluffy solid (100 mg, 41%). Anal. calcd. for $C_{39}H_{52}N_8O_3S \cdot C_8H_4F_{12}O_8 \cdot H_{13}O_{6.5}$: C 43.89, H 5.41, N 8.71, S 2.49; found: C 43.77, H 4.63, N 8.27, S 2.35. Ratio of configurational isomers evident in the NMR spectra: ca 1.5:1. ^{1}H-NMR (600 MHz, [D$_4$]MeOH): δ (ppm) 1.29-1.36 (m, 2H), 1.38-1.43 (m, 2H), 1.44-1.59 (m, 3H), 1.69-1.75 (m, 2H), 1.89-1.97 (m, 2H), 2.20-2.28 (m, 2H), 2.68-2.78 (m, 2H), 2.92-2.96 (m, 1H), 3.06 (s, 3H), 2.98-3.09 (m, 3H), 3.09-3.14 (m, 2H), 3.17-

3.30 (m, 5H), 3.42-3.45 (m, 5H), 3.63 (brs, 1H), 3.71-3.81 (m, 2H), 4.04 (d, *J* 14.3 Hz, 1H), 4.40 (d, *J* 17 Hz, 0.6H), 4.44 (d, *J* 17 Hz, 0.4H), 4.48-4.58 (m, 1H), 4.61 (t, *J* 6.2 Hz, 2H), 7.22-7.24 (m, 1H), 7.26-7.32 (m, 1H), 7.34-7.39 (m, 1H), 7.46-7.51 (m, 1H), 7.52-7.54 (m, 1H), 7.62-7.77 (m, 3H), 7.89-7.91 (m, 0.6H), 7.95-8.00 (m, 0.4H). ^{13}C-NMR (150 MHz, [D$_4$]MeOH): δ (ppm) 23.9, 24.5, 25.1, 25.8, 30.4, 34.3, 36.1, 43.3, 50.6, 50.9, 51.4, 53.1, 54.9, 55.3, 57.8, 57.9, 58.0, 69.7, 115.1, 116.9, 123.1, 123.6, 125.3, 126.9, 127.5, 127.9, 128.4, 128.5, 128.9, 129.4, 130.1, 130.5, 130.9, 131.2, 131.9, 132.3, 132.9, 133.4, 134.6, 134.9, 135.5, 135.7, 137.0, 142.7, 145.6, 158.8, 159.1, 163.4, 164.9, 165.4. RP-HPLC (220 nm): 99% (t_R = 14.2 min, *k* = 3.9). HRMS (ESI): *m/z* [*M*+H]$^+$ calcd. for [$C_{39}H_{53}N_8O_3S$]$^+$ 713.3956, found: 713.3951. $C_{39}H_{52}N_8O_3S \cdot C_8H_4F_{12}O_8$ (712.96 + 456.09).

5-(2-(4-(4-(4-(2-Oxo-2,3-dihydro-1*H*-benzo[d]imidazol-1-yl)-[1,4'-bipiperidin]-1'-yl)butyl)piperidin-1-yl)acetyl)-5,10-dihydro-11*H*-dibenzo[*b*,*e*][1,4]diazepin-11-one tris(hydrotrifluoroacetate) (98)

Compound **98** was prepared from **94** (80 mg, 0.17 mmol), potassium carbonate (71 mg, 0.51 mmol) and **63** (56 mg, 0.19 mmol) according to the procedure for the synthesis of **97**, but the reflux period was 3 h instead of 6 h. Purification by preparative HPLC (column: Kinetex XB-C18 5 µm 250 × 21 mm; gradient: 0-30 min: MeCN/0.1% aq TFA 20:80-62:38, t_R = 11 min) afforded **98** as white fluffy solid (100 mg, 57%). Ratio of configurational isomers evident in the NMR spectra: ca 1.5:1. ^{1}H-NMR (300 MHz, [D$_4$]MeOH): δ (ppm) 1.24-1.45 (m, 6H), 1.44-1.58 (m, 4H), 1.69-1.77 (m, 2H), 1.88-1.98 (m, 3H), 2.09-2.26 (m, 3H), 2.44-2.48 (m, 1H), 2.80-2.99 (m, 3H), 3.02-3.14 (m, 4H), 3.34-3.48 (m, 2H), 3.54 (t, *J* 6.3 Hz, 1H), 3.62-3.82 (m, 6H), 4.38-4.40 (m, 0.4H), 4.42-4.45 (m, 0.6H), 4.58-4.67(m, 1H), 7.02-7.07 (m, 2H), 7.24-7.34 (m, 2H), 7.34-7.38 (m, 1H), 7.44-7.55 (m, 3H), 7.60-7.78 (m, 3H), 7.89-7.91 (m, 0.6H), 7.96-7.98 (m, 0.4H). ^{13}C-NMR (75 MHz, [D$_4$]MeOH): δ (ppm) 25.8, 27.8, 28.5, 29.8, 32.9, 36.4, 37.4, 52.0, 54.1, 54.9, 59.5, 61.0, 61.3, 62.8, 68.8, 110.6, 110.8, 122.2, 122.5, 123.0, 126.6, 127.0, 127.7, 128.9, 129.0, 129.4, 129.6, 129.9, 130.2, 130.5, 131.1, 132.1, 132.2, 134.3, 134.7, 136.0, 136.9, 143.7, 143.8, 156.2, 169.1, 169.3, 171.2, 171.4. RP-HPLC (220 nm): 99% (t_R = 14.9 min, *k* = 4.2). HRMS (ESI): *m/z* [*M*+H]$^+$ calcd. for [$C_{41}H_{52}N_7O_3$]$^+$ 690.4126, found: 690.4128. $C_{41}H_{51}N_7O_3 \cdot C_6H_3F_9O_6$ (689.91 + 342.07).

1-(4-(1-(2-Oxo-2-(11-oxo-10,11-dihydro-5*H*-dibenzo[*b*,*e*][1,4]diazepin-5-yl)ethyl)piperidin-4-yl)butyl)piperidin-4-yl 2,2-diphenylacetate (99)

Compound **99** was prepared from **94** (100 mg, 0.21 mmol) and **71** (69 mg, 0.23 mmol) according to the procedure for the synthesis of **97**, but the reflux period was 5 h instead of 6 h. Potassium carbonate: 88 mg, 0.64 mmol. Purification by column chromatography (eluent: CH_2Cl_2/MeOH/25% aq NH_3 90:3:1 v/v/v) afforded compound **99** as white solid (40 mg, 27%),

m. p. 47-49 °C. R_f = 0.6 (CH_2Cl_2/MeOH/25% aq NH_3 90:9:1 v/v/v). Ratio of configurational isomers evident in the NMR spectra: ca 1.5:1. ^{1}H-NMR (300 MHz, [D_4]MeOH): δ (ppm) 0.97-1.31 (m, 8H), 1.39-1.42 (m, 2H), 1.48-1.58 (m, 1H), 1.61-1.71 (m, 2H), 1.79-2.01 (m, 4H), 2.20-2.36 (m, 4H), 2.36-2.51 (m, 2H), 2.55-2.70 (m, 1H), 2.78-2.85 (m, 1H), 2.99-3.04 (m, 0.6H), 3.11-3.26 (m, 1.4H), 4.84-4.87 (m, 1H), 5.07 (s, 1H), 7.21-7.25 (m, 3H), 7.28-7.32 (m, 9H), 7.36-7.40 (m, 1H), 7.41-7.51 (m, 2H), 7.53-7.56 (m, 1H), 7.61-7.66 (m, 1H), 7.84-7.90 (m, 1H). ^{13}C-NMR (75 MHz, [D_4]MeOH): δ (ppm) 25.8, 27.7, 31.0, 32.9, 33.0, 36.4, 37.4, 51.2, 54.8, 55.0, 58.4, 59.6, 71.5, 123.0, 126.6, 126.9, 127.8, 128.3, 128.9, 129.0, 129.6, 129.7, 129.9, 130.6, 132.0, 132.2, 134.3, 134.7, 136.0, 136.9, 140.3, 143.8, 143.9, 169.4, 171.2, 171.5, 173.5. RP-HPLC (220 nm): 99% (t_R = 21.1 min, k = 6.4). HRMS (ESI): *m/z* [*M*+H]$^+$ calcd. for [$C_{43}H_{49}N_4O_4$]$^+$ 685.3748, found: 685.3752. $C_{43}H_{48}N_4O_4$ (684.88).

2-(4-(4-(1-(2-Oxo-2-(11-oxo-10,11-dihydro-5*H*-dibenzo[*b*,*e*][1,4]diazepin-5-yl)ethyl)piperidin-4-yl)butyl)piperazin-1-yl)ethyl 9*H*-xanthene-9-carboxylate tris(hydrotrifluoroacetate) (100)

Compound **100** was prepared from **94** (80 mg, 0.17 mmol) and **77** (58 mg, 0.17 mmol) according to the procedure for the synthesis of **97**, but the reflux period was 3 h instead of 6 h. Potassium carbonate: 94 mg, 0.68 mmol. Purification by preparative HPLC (column: Kinetex XB-C18 5 µm 250 × 21 mm; gradient: 0-30 min: MeCN/0.1% aq TFA 20:80-64:36, t_R = 16 min) afforded compound **100** as white fluffy solid (93 mg, 51%). Ratio of configurational isomers evident in the NMR spectra: ca 1.5:1. ^{1}H-NMR (300 MHz, [D_4]MeOH): δ (ppm) 1.25-1.42 (m, 4H), 1.44-1.56 (m, 3H), 1.63-1.70 (m, 2H), 1.87-2.04 (m, 2H), 2.57-2.75 (m, 5H), 2.86-3.19 (m, 8H), 3.33-3.61 (m, 2H), 3.71-3.84 (m, 2H), 4.20 (t, *J* 5.1 Hz, 2H), 4.41 (d, *J* 12 Hz, 0.6H), 4.47 (d, *J* 12 Hz, 0.4H), 5.10 (s, 1H), 7.07-7.17 (m, 4H), 7/25-7.46 (m, 7H), 7.47-7.55 (m, 2H), 7.61-7.79 (m, 2H), 7.89-7.92 (m, 0.6 H), 7.96-7.98 (m, 0.4H). ^{13}C-NMR (75 MHz, [D_4]MeOH): δ (ppm) 19.1, 24.6, 25.1, 30.5, 34.4, 36.2, 46.6, 50.9, 42.7, 55.3, 56.7, 57.7, 58.1, 63.3, 117.9, 120.2, 122.2, 123.7, 124.6, 126.9, 127.6, 127.9, 128.6, 128.9, 130.2, 130.4, 130.5, 130.9, 131.8, 132.4, 133.5, 134.6, 136.5, 137.1, 152.9, 162.8, 165.0, 165.5, 172.9. RP-HPLC (220 nm): 99% (t_R = 20.3 min, k = 6.1). HRMS (ESI): *m/z* [*M*+H]$^+$ calcd. for [$C_{44}H_{50}N_5O_5$]$^+$ 728.3806, found: 728.3805. $C_{44}H_{49}N_5O_5 \cdot C_6H_3F_9O_6$ (727.91 + 342.07).

4-(4-(4-(1-(2-Oxo-2-(11-oxo-10,11-dihydro-5*H*-dibenzo[*b*,*e*][1,4]diazepin-5-yl)ethyl)piperidin-4-yl)butyl)piperazin-1-yl)butyl 9*H*-xanthene-9-carboxylate (101)

Compound **101** was prepared from **94** (50 mg, 0.11 mmol) and **78** (39 mg, 0.11 mmol) according to the procedure for the synthesis of **97**, but the reflux period was 5 h instead of 6 h. Potassium carbonate: 59 mg, 0.43 mmol. Purification by column chromatography (eluent: CH_2Cl_2/MeOH/25% aq NH_3 90:3:1 v/v/v) yielded compound **101** as white solid (32 mg, 38%),

m.p. 43-45 °C. R_f = 0.5 (CH_2Cl_2/MeOH/25% aq NH_3 90:9:1 v/v/v). Ratio of configurational isomers evident in the NMR spectra: ca 1.5:1. ^{1}H-NMR (300 MHz, [D_4]MeOH): δ (ppm) 0.98-1.11 (m, 2H), 1.24-1.37 (m, 8H), 1.41-1.64 (m, 6H), 1.84-2.00 (m, 2H), 2.15-2.25 (m, 3H), 2.26-2.38 (m, 4H), 2.38-2.51 (m, 4H), 2.61-2.65 (m, 1H), 2.78-2.85 (m, 1H), 2.99-3.04 (m, 0.6H), 3.12-3.26 (m, 1.4H), 4.04 (t, *J* 6.0 Hz, 2H), 5.05 (s, 1H), 7.07-7.13 (m, 4H), 7.19-7.26 (m, 2H), 7.27 (d, *J* 1.5 Hz, 1H), 7.30-7.38 (m, 4H), 7.41-7.49 (m, 1.6H), 7.50-7.58 (m, 1.4H), 7.62-7.67 (m, 1H), 7.84-7.91 (m, 1H). ^{13}C-NMR (75 MHz, [D_4]MeOH): δ (ppm) 23.6, 25.8, 27.6, 32.9, 33.1, 36.5, 37.5, 46.7, 53.7, 53.8, 54.9, 55.0, 58.9, 59.8, 61.1, 66.2, 117.9, 120.2, 123.1, 124.6, 126.6, 127.0, 127.8, 129.0, 129.5, 129.9, 130.2, 130.3, 132.1, 134.3, 134.7, 136.0, 136.9, 143.8, 152.8, 169.2, 169.4, 171.3, 171.5, 173.4. RP-HPLC (220 nm): 95% (t_R = 19.4 min, *k* = 5.8). HRMS (ESI): *m/z* [*M*+H]$^+$ calcd. for [$C_{46}H_{54}N_5O_5$]$^+$ 756.4119, found: 756.4117. $C_{46}H_{53}N_5O_5$ (755.96).

5-(2-(4-(4-(4-((1-(3-(2-Oxo-3,4-dihydroquinolin-1(2*H*)-yl)propyl)piperidin-4-yl)butyl)amino)butyl)piperidin-1-yl)acetyl)-5,10-dihydro-11*H*-dibenzo[*b*,*e*][1,4]diazepin-11-one (102)

Compound **86** (50 mg, 0.12 mmol), compound **10** (50 mg, 0.12 mmol), potassium carbonate (71 mg, 0.51 mmol) and sodium iodide (9 mg, 0.06 mmol) were added to MeCN (5 mL) and the mixture was kept under reflux for 3 h. Insoluble material was separated by filtration and washed with CH_2Cl_2 (2 × 10 mL). The filtrate and washings were combined and the solvent was removed under reduced pressure yielding a yellow oily residue, which was dissolved in CH_2Cl_2 (5 mL) followed by washing with brine. The aqueous phase was treated with CH_2Cl_2 (3 × 10 mL) and the organic extracts were collected. All organic phases were combined, dried over Na_2SO_4, and the volatiles were removed under reduced pressure. Purification by column chromatography (eluent: CH_2Cl_2/MeOH/25% aq NH_3 90:3:1 v/v/v) afforded compound **102** as yellow solid (46 mg, 52%), m.p. 141-143 °C. R_f = 0.5 (CH_2Cl_2/MeOH/25% aq NH_3 90:9:1 v/v/v). Ratio of configurational isomers evident in the NMR spectra: ca 1.5:1. ^{1}H-NMR (300 MHz, [D_4]MeOH): δ (ppm) 0.98-1.17 (m, 3H), 1.17-1.35 (m, 12H), 1.42-1.51 (m, 5H), 1.55-1.58 (m, 1H), 1.63-1.69 (m, 2H), 1.78-1.86 (m, 2H), 1.87-2.02 (m, 4H), 2.32-2.43 (m, 2H), 2.48-2.58 (m, 5H), 2.58-2.66 (m, 2H), 2.78-2.81 (m, 0.6H), 2.83-2.95 (m, 4H), 2.99-3.04 (m, 0.4H), 3.10-3.25 (m, 1H), 3.99 (t, *J* 7.3 Hz, 2H), 7.00-7.05 (m, 1H), 7.13-7.28 (m, 5H), 7.28-7.38 (m, 1H), 7.39-7.51 (m, 2H), 7.54-7.57 (m, 1H), 7.62-7.67 (m, 1H), 7.84-7.90 (m, 1H). ^{13}C-NMR (75 MHz, [D_4]MeOH): δ (ppm) 25.1, 25.4, 25.5, 26.2, 30.4, 30.7, 32.7, 32.8, 32.9, 33.0, 34.0, 36.4, 36.8, 37.4, 37.5, 41.3, 50.5, 50.6, 54.8, 55.0, 57.1, 116.4, 123.0, 124.4, 126.6, 127.0, 127.8, 128.2, 128.6, 129.0, 129.1, 129.5, 129.9, 130.6, 131.1, 131.9, 132.0, 132.2, 134.3, 135.9, 140.2, 143.8, 144.9, 169.1, 169.3, 171.2, 171.4, 172.7. RP-HPLC (220 nm): 95% (t_R = 16.7 min, *k* = 4.8). HRMS (ESI): *m/z* [*M*+H]$^+$ calcd. for [$C_{45}H_{61}N_6O_3$]$^+$ 733.4800, found: 733.4805. $C_{45}H_{60}N_6O_3$

(733.01).

5-(2-(4-(4-(6-Amino-4-(3-((4-(1-methyl-1,2,5,6-tetrahydropyridin-3-yl)-1,2,5-thiadiazol-3-yl)oxy)propyl)-1,4-diazepan-1-yl)butyl)piperidin-1-yl)acetyl)-5,10-dihydro-11*H*-dibenzo[*b*,*e*][1,4]diazepin-11-one pentakis(hydrotrifluoroacetate) (105a)

Compound **94** (196 mg, 0.42 mmol), *tert*-butyl (1,4-diazepan-6-yl)carbamate (compound **103**) (90 mg, 0.42 mmol) and compound **39** (134 mg, 0.42 mmol) were added to MeCN (10 mL), followed by the addition of potassium carbonate (116 mg, 0.84 mmol). The mixture was stirred under reflux overnight. Insoluble material was separated by filtration and washed with CH_2Cl_2 (2 × 10 mL). The filtrate and washings were combined and the solvent was evaporated to yield a yellow residue, which was dissolved in CH_2Cl_2 (5 mL) followed by washing with brine. The aqueous phase was treated with CH_2Cl_2 (3 × 10 mL) and the organic extracts were collected. All organic phases were combined, dried over Na_2SO_4, and the volatiles were removed under reduced pressure. The residue was subjected to column chromatography (eluent: CH_2Cl_2/MeOH/25% aq NH_3 90:3:1) to afford the Boc-protected intermediate as colorless oil, which was dissolved in CH_2Cl_2/TFA/H_2O (10:10:1 v/v/v) (5 mL). The mixture was stirred at room temperature for 2 h. CH_2Cl_2 (10 mL) was added and the volatiles were evaporated. Purification by preparative HPLC (column: Kinetex XB-C18 5 µm 250 × 21 mm; gradient: 0-30 min: MeCN/0.1% aq TFA 5:95-62:48, t_R = 15 min) afforded compound **105a** as white fluffy solid (92 mg, 17%). Ratio of configurational isomers evident in the NMR spectra: ca 1.5:1. ^{1}H-NMR (600 MHz, [D$_4$]MeOH): δ (ppm) 1.27-1.41 (m, 4H), 1.41-1.47 (m, 1H), 1.49-1.58 (m, 2H), 1.65-1.79 (m, 2H), 1.84-2.01 (m, 2H), 2.07-2.20 (m, 2H), 2.64-2.85 (m, 2H), 2.92 (t, *J* 7.4 Hz, 3H), 3.05 (s, 3H), 2.98-3.09 (m, 3H), 3.14 (t, *J* 16 Hz, 2H), 3.17-3.19 (m, 1H), 3.23-3.28 (m, 1H), 3.31-3.33 (m, 1H), 3.34-3.40 (m, 1H), 3.40-3.48 (m, 2H), 3.48-3.56 (m, 2H), 3.59-3.66 (m, 1H), 3.69-3.80 (m, 2H), 3.82-3.89 (m, 1H), 3.97-4.09 (m, 1H), 4.39 (d, *J* 17 Hz, 0.6H), 4.43 (d, *J* 17 Hz, 0.4H), 4.46-4.54 (m, 1H), 4.57 (t, *J* 6.5 Hz, 2H), 7.20-7.23 (m, 1H), 7.23-7.30 (m, 1H), 7.29-7.42 (m, 2H), 7.44-7.56 (m, 2H), 7.61-7.76 (m, 2H), 7.89-7.90 (m, 0.6H), 7.96-7.97 (m, 0.4H). ^{13}C-NMR (150 MHz, [D$_4$]MeOH): δ (ppm) 23.9, 24.6, 25.5, 27.1, 30.4, 34.3, 36.2, 43.3, 49.6, 50.9, 52.1, 53.1, 54.9, 55.3, 55.6, 56.2, 56.5, 57.9, 58.0, 59.9, 70.3, 117.0 (TFA), 118.9 (TFA), 123.1, 123.6, 125.4, 126.8, 127.5, 127.9, 128.3, 128.5, 128.9, 129.4, 130.1, 130.6, 130.9, 131.2, 131.7, 131.9, 132.4, 133.0, 133.4, 134.6, 134.9, 135.5, 135.7, 137.0, 141.0, 142.7, 145.6, 162.4 (TFA), 162.6 (TFA), 163.6, 164.9, 165.4, 168.6, 168.8. RP-HPLC (220 nm): 98% (t_R = 14.3 min, k = 4.0). HRMS (ESI): *m/z* [*M*+H]$^+$ calcd. for $[C_{40}H_{56}N_9O_3S]^+$ 742.4221, found: 742.42210. $C_{40}H_{55}N_9O_3S \cdot C_{10}H_5F_{15}O_{10}$ (742.00 + 570.12).

***N*-(1-(3-((4-(1-Methyl-1,2,5,6-tetrahydropyridin-3-yl)-1,2,5-thiadiazol-3-yl)oxy)propyl)-4-(4-(1-(2-oxo-2-(11-oxo-10,11-dihydro-5*H*-dibenzo[*b*,*e*][1,4]diazepin-5-yl)ethyl)piperidin-**

4-yl)butyl)-1,4-diazepan-6-yl)propionamide tetrakis(hydrotrifluoroacetate) (106)

Compound **105** (12.5 mg, 9.53 µmol) was dissolved in DMF (100 µL) in a 1.5-mL polypropylene reaction vessel, followed by the addition of DIPEA (17 µL, 98 µmol) and a solution of succinimidyl propionate (compound **104**) (2.5 mg, 14.6 µmol) in DMF (20 µL). Stirring of the mixture was continued at room temperature for 2 h. 10% aq TFA (100 µL) was added. Purification by preparative HPLC (column: Kinetex XB-C18 5 µm 250 × 21 mm; gradient: 0-30 min: MeCN/0.1% aq TFA 5:95-62:48, t_R = 16 min) afforded compound **106** as white fluffy solid (11.4 mg, 95%). IR (KBr): 3430, 3050, 2605, 1680, 1455, 1365, 1210, 1135, 840, 725. Ratio of configurational isomers evident in the NMR spectra: ca 1.5:1. ^{1}H-NMR (600 MHz, [D$_4$]MeOH): δ (ppm) 1.10 (t, *J* 7.6 Hz, 3H), 1.26-1.42 (m, 4H), 1.43-1.59 (m, 3H), 1.64-1.76 (m, 2H), 1.88-1.96 (m, 2H), 2.13-2.17 (m, 2H), 2.23 (q, *J* 7.6 Hz, 2H), 2.65-2.83 (m, 2H), 2.89-2.95 (m, 1H), 3.05 (s, 3H), 2.98-3.08 (m, 3H), 3.12-3.15 (m, 2H), 3.16-3.28 (m, 5H), 3.41-3.44 (m, 5H), 3.63 (d, *J* 4.5 Hz, 1H), 3.70-3.74 (m, 1.5H), 3.79 (d, *J* 17 Hz, 0.5H), 4.03 (d, *J* 15 Hz, 1H), 4.25- 4.32(m, 1H), 4.39 (d, *J* 17 Hz, 0.6H), 4.43 (d, *J* 17 Hz, 0.4H), 4.46-4.55 (m, 1H), 4.60 (t, *J* 6.4 Hz, 2H), 7.21-7.23 (m, 1H), 7.24-7.30 (m, 1H), 7.30-7.39 (m, 2H), 7.46-7.49 (m, 1H), 7.51-7.53 (m, 1H), 7.60-7.76 (m, 2H), 7.88-7.92 (m, 0.6H), 7.96-7.97 (m, 0.4H). ^{13}C-NMR (150 MHz, [D$_4$]MeOH): δ (ppm) 10.1, 23.9, 24.5, 25.6, 26.9, 29.9, 30.4, 34.3, 36.2, 43.2, 46.9, 49.6, 50.9, 52.4, 53.1, 54.9, 55.2, 56.2, 57.5, 58.0, 58.4, 59.2, 70.1, 116.9, 123.1, 123.6, 125.4, 126.9, 127.5, 127.9, 128.4, 128.5, 128.9, 129.4, 130.1, 130.6, 130.9, 131.2, 131.7, 132.4, 133.0, 133.4, 134.6, 134.9, 135.5, 135.7, 137.1, 141.0, 142.7, 145.6, 162.1 (TFA), 162.3 (TFA), 163.6, 164.9, 165.4, 168.6, 168.8, 176.9. RP-HPLC (220 nm): 98% (t_R = 14.8 min, *k* = 4.2). HRMS (ESI): *m/z* [*M*+H]$^+$ calcd. for [$C_{43}H_{60}N_9O_4S$]$^+$ 798.4483, found: 798.4487. $C_{43}H_{59}N_9O_4S \cdot C_8H_4F_{12}O_8$ (798.06 + 456.09).

5-(2-(4-(4-(6-Amino-4-(2-oxo-2-(4-(2-oxo-2,3-dihydro-1*H*-benzo[*d*]imidazol-1-yl)-[1,4'-bipiperidin]-1'-yl)ethyl)-1,4-diazepan-1-yl)butyl)piperidin-1-yl)acetyl)-5,10-dihydro-11*H*-dibenzo[*b*,*e*][1,4]diazepin-11-one pentakis(hydrotrifluoroacetate) (107)

Potassium carbonate (44 mg, 0.32 mmol) was added to a mixture of compound **66** (45 mg, 0.11 mmol), compound **94** (50 mg, 0.11 mmol), *tert*-butyl (1,4-diazepan-6-yl)carbamate (compound **103**) (23 mg, 0.11 mmol) in MeCN (2 mL). The mixture was stirred at 110 °C under microwave irradiation for 30 min, and cooled to room temperature. Insoluble material was separated by filtration and washed with CH_2Cl_2 (2 × 5 mL). The filtrate and the washings were combined and the solvent was evaporated. The residue was dissolved in CH_2Cl_2 (5 mL) followed by washing with brine. The aqueous phase was treated with CH_2Cl_2 (3 × 5 mL) and the organic extracts were collected. All organic phases were combined and dried over Na_2SO_4. Removal of the volatiles under reduced pressure gave the Boc-protected intermediate, which was dissolved in CH_2Cl_2/TFA/H_2O (10:10:1 v/v/v) (4 mL). The mixture was stirred at room

temperature for 2 h. CH_2Cl_2 (10 mL) was added and the volatiles were evaporated. Purification by preparative HPLC (column: Kinetex XB-C18 5 µm 250 × 21 mm; gradient: 0-30 min: MeCN/0.1% aq TFA 5:95-62:38, t_R = 16 min) afforded compound **107** as white fluffy solid (19 mg, 12%). ^{1}H-NMR (600 MHz, [D$_4$]MeOH): δ (ppm) 1.36-1.42 (m, 4H), 1.42-1.59 (m, 3H), 1.64-1.72 (m, 1H), 1.73-1.87 (m, 3H), 1.89-1.97 (m, 2H), 2.09-2.22 (m, 4H), 2.69 (t, *J* 13 Hz, 1H), 2.80-2.89 (m, 2H), 2.91-2.97 (m, 1H), 3.00-3.07 (m, 2H), 3.07-3.22 (m, 4H), 3.24-3.27 (m, 3H), 3.33-3.41 (m, 1H), 3.41-3.49 (m, 2H), 3.50-3.68 (m, 4H), 3.69-3.76 (m, 5H), 3.76-3.83 (m, 2H), 3.96-3.98 (m, 1H), 4.39 (d, *J* 17 Hz, 0.6H), 4.43 (d, *J* 17 Hz, 0.4H), 4.57-4.62 (m, 1H), 4.72-4.74 (m, 1H), 7.04-7.07 (m, 3H), 7.22-7.30 (m, 1H), 7.29-7.38 (m, 3H), 7.46-7.49 (m, 1H), 7.50-7.54 (m, 1H), 7.61-7.64 (m, 1H), 7.66-7.76 (m, 1H), 7.89 (d, *J* 7.7 Hz 0.6H), 7.96 (d, *J* 7.7 Hz, 0.4H). ^{13}C-NMR (150 MHz, [D$_4$]MeOH): δ (ppm) 24.5, 25.0, 27.3, 27.5, 27.8, 27.9, 30.4, 34.3, 36.1, 41.6, 43.9, 50.2, 50.4, 51.8, 54.9, 55.3, 56.1, 58.0, 58.5, 59.9, 64.7, 109.9, 110.7, 115.0 (TFA), 116.9 (TFA), 118.9 (TFA), 120.9 (TFA), 122.4, 122.9, 123.1, 123.6, 126.8, 127.5, 127.9, 128.5, 128.9, 129.4, 129.7, 130.1, 130.5, 130.9, 131.2, 131.7, 131.9, 132.3, 133.0, 133.4, 134.6, 134.9, 135.5, 135.7, 137.0, 141.0, 142.7, 156.1, 162.3 (TFA), 162.5 (TFA), 162.8 (TFA), 162.9 (TFA), 164.9, 165.4, 168.6, 168.8, 170.8. RP-HPLC (220 nm): 99% (t_R = 14.9 min, *k* = 4.2). HRMS (ESI): *m/z* [*M*+2H]$^{2+}$ calcd. for [$C_{48}H_{66}N_{10}O_4$]$^{2+}$ 423.2629, found: 423.2613. $C_{48}H_{64}N_{10}O_4 \cdot C_{10}H_5F_{15}O_{10}$ (845.11 + 570.12).

_N_-(1-(4-(1-(2-Oxo-2-(11-oxo-10,11-dihydro-5_H_-dibenzo[_b_,_e_][1,4]diazepin-5-yl)ethyl)piperidin-4-yl)butyl)-4-(2-oxo-2-(4-(2-oxo-2,3-dihydro-1_H_-benzo[_d_]imidazol-1-yl)-[1,4'-bipiperidin]-1'-yl)ethyl)-1,4-diazepan-6-yl)propionamide tetrakis(hydrotrifluoroacetate) (108)

Compound **108** was prepared from **107** (7.6 mg, 5.37 µmol) and **104** (1.4 mg, 8.18 µmol) according to the procedure for the synthesis of **106**. DIPEA: 10 µL, 58 µmol. Purification by preparative HPLC (column: Kinetex XB-C18 5 µm 250 × 21 mm; gradient: 0-30 min: MeCN/0.1% aq TFA 5:95-62:48, t_R = 16 min) yielded compound **108** as hygroscopic white fluffy solid (7 mg, 96%). Ratio of isomers evident in the NMR spectra: ca 1.5:1. ^{1}H-NMR (600 MHz, [D$_4$]MeOH): δ (ppm) 1.14 (t, *J* 7.6 Hz, 3H), 1.32-1.45 (m, 4H), 1.45-1.59 (m, 3H), 1.60-1.80 (m, 4H), 1.80-1.89 (m, 1H), 1.91-1.99 (m, 2H), 2.09-2.12 (m, 2H), 2.19-2.24 (m, 2H), 2.27 (q, *J* 12 Hz, 2H), 2.68-2.76 (m, 1H), 2.81-2.89 (m, 2H), 2.89-3.00 (m, 2H), 3.03-3.17 (m, 4H), 3.16-3.23 (m, 3H), 3.33-3.51 (m, 5H), 3.51-3.60 (m, 2H), 3.69-3.85 (m, 6H), 3.98-4.06 (m, 1H), 4.12-4.19 (m, 1H), 4.41 (d, *J* 17 Hz, 0.6H), 4.45 (d, *J* 17 Hz, 0.4H), 4.58-4.62 (m, 1H), 4.74-4.76 (m, 1H), 7.05-7.08 (m, 3H), 7.19-7.40 (m, 4H), 7.47-7.51 (m, 1H), 7.51-7.53 (m, 1H), 7.63 (dd, *J* 15, 7.1 Hz, 1H), 7.66-7.76 (m, 1H), 7.90 (d, *J* 8.0 Hz, 0.6H), 7.97 (d, *J* 8.0 Hz, 0.4H). ^{13}C-NMR (150 MHz, [D$_4$]MeOH): δ (ppm) 10.2, 24.5, 25.4, 27.3, 27.5, 27.9, 30.1, 30.4, 34.3, 36.2, 41.7, 44.1, 50.2, 50.4, 54.9, 55.3, 56.7, 57.2, 58.0, 59.2, 59.6, 61.0, 64.8, 109.9, 110.7, 116.9 (TFA), 118.9

(TFA), 122.4, 122.9, 123.1, 123.6, 126.9, 127.5, 127.9, 128.5, 128.9, 129.4, 129.7, 130.1, 130.6, 130.9, 131.2, 131.7, 131.9, 132.4, 133.0, 133.4, 134.6, 134.9, 135.5, 135.7, 137.0, 141.0, 142.7, 156.1, 162.6 (TFA), 162.8 (TFA), 164.9, 165.5, 168.6, 168.8, 177.1. RP-HPLC (220 nm): 99% (t_R = 15.6 min, k = 4.4). HRMS (ESI): *m/z* [*M*+2H]$^{2+}$ calcd. for [$C_{51}H_{70}N_{10}O_5$]$^{2+}$ 451.2760, found: 451.2764. $C_{51}H_{68}N_{10}O_5 \cdot C_8H_4F_{12}O_8$ (901.17 + 456.09).

5-(Aminomethyl)-*N*^{1}-(4-((5-((4-(1-methyl-1,2,5,6-tetrahydropyridin-3-yl)-1,2,5-thiadiazol-3-yl)oxy)pentyl)amino)-4-oxobutyl)-*N*^{3}-(2-(4-(4-(1-(2-oxo-2-(11-oxo-10,11-dihydro-5*H*-dibenzo[*b*,*e*][1,4]diazepin-5-yl)ethyl)piperidin-4-yl)butyl)piperazin-1-yl)ethyl)isophthalamide pentakis(hydrotrifluoroacetate) (110)

and **5-(Aminomethyl)-*N*^{1},*N*^{3}-bis(2-(4-(4-(1-(2-oxo-2-(11-oxo-10,11-dihydro-5*H*-dibenzo[*b*,*e*][1,4]diazepin-5-yl)ethyl)piperidin-4-yl)butyl)piperazin-1-yl)ethyl)isophthalamide heptakis(hydrotrifluoroacetate) (112)**

TBTU (244 mg, 0.76 mmol) and DIPEA (131 µL, 0.76 mmol) were added to a solution of **109** (113 mg, 0.38 mmol) and HOBt (103 mg, 0.76 mmol) in DMF (2 mL) and the mixture was stirred at room temperature for 20 min. A solution of **52** (140 mg, 0.38 mmol), **96** (370 mg, 0.38 mmol) and DIPEA (131 µL, 0.76 mmol) in DMF (2 mL) was added dropwise and stirring was continued at 60 °C for 3 h. H_2O (10 mL) was added followed by extraction with ethyl acetate (3 × 5 mL). The combined extracts were dried over Na_2SO_4 and concentrated under reduced pressure to yield the Boc-protected intermediate as yellow oil, which was dissolved in CH_2Cl_2/TFA/H_2O (10:10:1 v/v/v) (5 mL). The mixture was stirred at room temperature for 2 h. CH_2Cl_2 (10 mL) was added and the volatiles were evaporated. Purification by preparative HPLC (column: Kinetex XB-C18 5 µm 250 × 21 mm; gradient: 0-25 min: MeCN/0.1% aq TFA 12:88-64:36, t_R (**112**) = 11 min, t_R (**110**) = 12 min) afforded compound **110** (101 mg, 14%) and compound **112** (60 mg, 8%) as white fluffy solids. **110**: ratio of isomers evident in the NMR spectra: ca 1.5:1. ^{1}H-NMR (600 MHz, [D$_4$]MeOH): δ (ppm) 1.23-1.43 (m, 5H), 1.43-1.54 (m, 5H), 1.54-1.63 (m, 3H), 1.68-1.73 (m, 2H), 1.82-2.01 (m, 7H), 2.28 (t, *J* 7.5 Hz, 2H), 2.69-2.81 (m, 2H), 2.89-2.95 (m, 4H), 3.02-3.05 (m, 1H), 3.05 (s, 3H), 3.06-3.11 (m, 3H), 3.15-3.22 (m, 3H), 3.31-3.39 (m, 3H), 3.39-3.47 (m, 4H), 3.58-3.68 (m, 3H), 3.70-3.73 (m, 1.5H), 3.78 (d, *J* 18 Hz, 0.5H), 4.02-4.05 (m, 1H), 4.23 (s, 2H), 4.39 (d, *J* 17 Hz, 0.6H), 4.43 (d, *J* 17 Hz, 0.4H), 4.51 (t, *J* 6.5 Hz, 2H), 7.23-7.26 (m, 1H), 7.27-7.39 (m, 2H), 7.46-7.53 (m, 2H), 7.59-7.76 (m, 3H), 7.89-7.90 (m, 0.6 H), 7.95-7.96 (m, 0.4H), 8.04-8.10 (m, 2H), 8.29-8.30 (m, 1H). ^{13}C-NMR (150 MHz, [D$_4$]MeOH): δ (ppm) 22.5, 23.0, 23.1, 23.8, 25.4, 28.1, 28.7, 29.0, 32.9, 33.2, 34.7, 36.1, 38.8, 39.3, 41.9, 42.4, 48.2, 49.6, 50.9, 51.8, 53.5, 53.9, 55.7, 56.3, 56.6, 70.9, 121.7, 122.2, 124.1, 125.5, 126.1, 126.3, 126.5, 126.8, 127.1, 127.5, 127.5, 128.0, 128.7, 129.2, 129.5, 129.8, 130.3, 130.6, 130.9, 131.6, 132.0, 133.2, 133.5, 134.1, 134.2, 134.3, 135.4, 135.6, 135.8, 139.5, 139.6, 141.3, 144.2, 160.2 (TFA), 160.4 (TFA), 160.6 (TFA), 160.8 (TFA),

162.4, 163.6, 164.0, 167.1, 167.2, 167.4, 167.6, 174.0. RP-HPLC (220 nm): 96% (t_R = 14.9 min, k = 4.2). HRMS (ESI): *m/z* $[M+H]^+$ calcd. for $[C_{56}H_{77}N_{12}O_6S]^+$ 1045.5810, found: 1045.5803. $C_{56}H_{76}N_{12}O_6S \cdot C_{10}H_5F_{15}O_{10}$ (1045.36 + 570.12).

112: Ratio of isomers evident in the NMR spectra: ca 1.5:1. ^{1}H-NMR (600 MHz, [D$_4$]MeOH): δ (ppm) 1.29-1.42 (m, 8H), 1.41-1.60 (m, 6H), 1.63-1.77 (m, 4H), 1.88-1.96 (m, 4H), 2.83-2.97 (m, 2H), 2.98-3.10 (m, 6H), 3.11-3.14 (m, 4H), 3.16-3.28 (m, 4H), 3.30-3.36 (m, 4H), 3.26-3.60 (m, 10H), 3.69-3.72 (m, 6H), 3.77-3.89 (m, 2H), 4.23 (s, 2H), 4.40 (d, *J* 17 Hz, 1.2H), 4.44 (d, *J* 17 Hz, 0.8H), 7.21-7.35 (m, 4H), 7.36-7.38 (m, 1H), 7.44-7.54 (m, 4H), 7.58-7.71 (m, 4H), 7.55-7.73 (m, 1H), 7.86-7.91 (m, 1.2H), 7.95-7.96 (m, 0.8H), 8.10 (s, 2H), 8.34 (s, 1H). ^{13}C-NMR (150 MHz, [D$_4$]MeOH): δ (ppm) 23.1, 23.7, 29.0, 32.9, 34.7, 35.6, 42.4, 49.3, 50.1, 53.5, 53.9, 56.0, 56.3, 56.6, 113.7 (TFA), 115.6 (TFA), 117.6 (TFA), 119.5 (TFA), 121.7, 122.3, 125.5, 126.1, 126.5, 127.1, 127.5, 128.1, 128.7, 129.1, 129.5, 129.8, 130.3, 130.6, 130.8, 130.9, 131.6, 132.0, 133.2, 133.5, 134.1, 134.3, 135.2, 135.6, 139.6, 141.3, 161.0 (TFA), 161.4 (TFA), 163.6, 164.1, 167.2, 167.4, 167.7. RP-HPLC (220 nm): 98% (t_R = 14.4 min, k = 4.1). HRMS (ESI): *m/z* $[M+H]^+$ calcd. for $[C_{69}H_{91}N_{13}O_6]^{2+}$ 589.8602, found: 589.8601. $C_{69}H_{89}N_{13}O_6 \cdot C_{14}H_7F_{21}O_{14}$ (1196.56 + 798.16).

N^1-(4-((5-((4-(1-Methyl-1,2,5,6-tetrahydropyridin-3-yl)-1,2,5-thiadiazol-3-yl)oxy)pentyl)amino)-4-oxobutyl)-*N*^{3}-(2-(4-(4-(1-(2-oxo-2-(11-oxo-10,11-dihydro-5H-dibenzo[*b*,*e*][1,4]diazepin-5-yl)ethyl)piperidin-4-yl)butyl)piperazin-1-yl)ethyl)-5-(propionamidomethyl)isophthalamide tetrakis(hydrotrifluoroacetate) (111)

Compound **111** was prepared from **110** (16 mg, 8.7 µmol) and **104** (2.3 mg, 13 µmol) according to the procedure for the synthesis of **106**. DIPEA: 17 µL, 98 µmol. Purification by preparative HPLC (column: Kinetex XB-C18 5 µm 250 × 21 mm; gradient: 0-25 min: MeCN/0.1% aq TFA 20:80-95:5, t_R = 9 min), yielded compound **111** as white fluffy solid (12 mg, 89%). Ratio of isomers evident in the NMR spectra: ca 1.5:1. ^{1}H-NMR (600 MHz, [D$_4$]MeOH): δ (ppm) 1.14 (t, *J* 7.6 Hz, 3H), 1.31-1.43 (m, 6H), 1.43-1.61 (m, 7H), 1.64-1.79 (m, 2H), 1.84-1.94 (m, 6H), 1.92-1.99 (m, 1H), 2.24-2.30 (m, 4H), 2.61-2.68 (m, 1H), 2.69-2.83 (m, 3H), 2.85-2.97 (m, 4H), 2.99-3.14 (m, 9H), 3.18 (t, *J* 6.6 Hz, 2H), 3.39-3.41 (m, 3H), 3.42-3.53 (m, 1H), 3.61 (t, *J* 6.2 Hz, 3H), 3.70-3.80 (m, 2H), 4.03 (d, *J* 15 Hz, 1H), 4.39 (d, *J* 17 Hz, 0.6H), 4.41 (d, *J* 17 Hz, 0.4H), 4.44 (d, *J* 4.5 Hz, 2H), 4.50 (t, *J* 6.5 Hz, 2H), 7.23-7.24 (m, 1H), 7.26-7.40 (m, 2H), 7.46-7.48 (m, 1H), 7.50-7.53 (m, 1H), 7.59-7.68 (m, 2H), 7.68-7.76 (m, 1H), 7.88 (s, 2H), 7.89-7.90 (m, 0.6H), 7.96-7.97 (m, 0.4H), 8.14-8.15 (m, 1H). ^{13}C-NMR (150 MHz, [D$_4$]MeOH): δ (ppm) 10.4, 23.9, 24.4, 24.5, 25.2, 26.5, 26.8, 29.5, 30.0, 30.1, 30.4, 34.3, 34.6, 36.1, 37.5, 40.2, 40.6, 43.3, 43.7, 51.0, 52.3, 53.2, 54.9, 55.3, 57.4, 57.8, 58.0, 72.4, 115.1 (TFA), 116.4 (TFA), 117.0 (TFA), 118.9 (TFA), 123.1, 123.6, 125.4, 126.1, 126.9, 127.5, 127.9, 128.2, 128.5, 128.9, 129.4, 130.1, 130.3, 130.6, 130.9, 131.2, 131.7, 132.3, 133.0, 133.4, 134.6, 134.9, 135.5,

136.7, 136.2, 136.5, 137.0, 141.0, 141.5, 142.7, 145.6, 163.8, 164.9, 165.4, 168.6, 168.8, 169.2, 169.6, 171.1, 171.9, 175.4, 177.1. RP-HPLC (220 nm): 98% (t_R = 15.9 min, k = 4.5). HRMS (ESI): *m/z* $[M+H]^+$ calcd. for $[C_{59}H_{81}N_{12}O_7S]^+$ 1101.6072, found: 1101.6066. $C_{59}H_{80}N_{12}O_7S \cdot C_8H_4F_{12}O_8$ (1101.43 + 456.09).

N^1,N^3-Bis(2-(4-(4-(1-(2-oxo-2-(11-oxo-10,11-dihydro-5*H*-dibenzo[*b*,*e*][1,4]diazepin-5-yl)ethyl)piperidin-4-yl)butyl)piperazin-1-yl)ethyl)-5-(propionamidomethyl)isophthalamide hexakis(hydrotrifluoroacetate) (113)

Compound **113** was prepared from **112** (17 mg, 8.52 µmol) and **104** (2.3 mg, 13 µmol) according to the procedure for the synthesis of **106**. DIPEA: 16 µL, 93 µmol. Purification by preparative HPLC (column: Kinetex XB-C18 5 µm 250 × 21 mm; gradient: 0-25 min: MeCN/0.1% aq TFA 20:80-64:36, t_R = 11 min), yielded compound **113** as white fluffy solid (13 mg, 79%). Ratio of isomers evident in the NMR spectra: ca 1.5:1. ^{1}H-NMR (600 MHz, [D$_4$]MeOH): δ (ppm) 1.14 (t, *J* 7.6 Hz, 3H), 1.30-1.48 (m, 10H), 1.48-1.61 (m, 4H), 1.68-1.79 (m, 4H), 1.85-2.01 (m, 4H), 2.28 (q, *J* 7.6 Hz, 2H), 2.81-2.99 (m, 4H), 2.99-3.08 (m, 6H), 3.08-3.17 (m, 6H), 3.17-3.26 (m, 4H), 3.34-3.48 (m, 8H), 3.48-3.65 (m, 4H), 3.38-3.83 (m, 6H), 4.36-4.51 (m, 4H), 7.20-7.31 (m, 2H), 7.32-7.35 (m, 2H), 7.36-7.39 (m, 1H), 7.44-7.51 (m, 2H), 7.51-7.53 (m, 2H), 7.61-7.69 (m, 4H), 7.72-7.78 (m, 1H), 7.89 (d, *J* 7.7 Hz, 1.2H), 7.93 (s, 2H), 7.96 (d, *J* 7.7 Hz, 0.8H), 8.25 (s, 1H). ^{13}C-NMR (150 MHz, [D$_4$]MeOH): δ (ppm) 10.4, 24.5, 25.1, 30.1, 30.4, 34.2, 36.1, 37.2, 43.5, 50.8, 52.0, 54.9, 55.3, 57.5, 57.8, 58.1, 116.9 (TFA), 118.9 (TFA), 123.1, 123.7, 126.3, 126.9, 127.5, 127.9, 128.5, 128.9, 129.5, 130.1, 130.5, 130.7, 130.9, 131.2, 131.7, 131.9, 132.3, 133.0, 133.4, 134.6, 134.9, 135.5, 135.7, 136.0, 137.0, 141.0, 141.6, 142.7, 162.4 (TFA), 162.6 (TFA), 165.0, 165.5, 168.6, 168.8, 169.6, 177.1. RP-HPLC (220 nm): 95% (t_R = 15.3 min, k = 4.3). HRMS (ESI): *m/z* $[M+H]^+$ calcd. for $[C_{72}H_{94}N_{13}O_7]^+$ 1252.7394, found: 1252.7375. $C_{72}H_{93}N_{13}O_7 \cdot C_{12}H_6F_{18}O_{12}$ (1252.62 + 684.14).

5-(Aminomethyl)-N^1-(2-(4-(2-oxo-2,3-dihydro-1*H*-benzo[*d*]imidazol-1-yl)-[1,4'-bipiperidin]-1'-yl)ethyl)-N^3-(2-(4-(4-(1-(2-oxo-2-(11-oxo-10,11-dihydro-5*H*-dibenzo[*b*,*e*][1,4]diazepin-5-yl)ethyl)piperidin-4-yl)butyl)piperazin-1-yl)ethyl)isophthalamide hexakis(hydrotrifluoroacetate) (114)

Compound **114** was prepared from **109** (80 mg, 0.27 mmol), **96** (263 mg, 0.27 mmol) and **64** (93 mg, 0.27 mmol) according to the procedure for the synthesis of **110** and **112**. TBTU: 173 mg, 0.54 mmol; HOBt: 73 mg, 0.54 mmol; DIPEA: 189 + 189 µL, 1.1 + 1.1 mmol. Purification by preparative HPLC (column: Kinetex XB-C18 5 µm 250 × 21 mm; gradient: 0-25 min: MeCN/0.1% aq TFA 15:85-64:36, t_R (**112**) = 10 min, t_R (**114**) = 12 min) yielded compounds **112** (25 mg, 5%) and **114** (45 mg, 10%) as white fluffy solids. **114**: ratio of isomers evident in the NMR spectra: ca 1.5:1. ^{1}H-NMR (600 MHz, [D$_4$]MeOH) δ (ppm) 1.31-1.42 (m, 4H), 1.43-1.59

(m, 3H), 1.66-1.77 (m, 2H), 1.84-1.99 (m, 2H), 2.11 (d, *J* 12 Hz, 2H), 2.22-2.28 (m, 2H), 2.49 (d, *J* 13 Hz, 2H), 2.80-2.96 (m, 3H), 2.98-3.07 (m, 3H), 3.09-3.14 (m, 3H), 3.15-3.28 (m, 5H), 3.31-3.38 (m, 3H), 3.40-3.50 (m, 6H), 3.64-3.81 (m, 7H), 3.85 (t, *J* 5.8 Hz, 2H), 3.98 (d, *J* 12 Hz, 2H), 4.24 (s, 2H), 4.40 (d, *J* 18 Hz, 0.4H), 4.43 (d, *J* 18 Hz, 0.6H), 4.58-4.67 (m, 1H), 7.02-7.09 (m, 3H), 7.24-7.29 (m, 1H), 7.32-7.88 (m, 2H), 7.45-7.48 (m, 1H), 7.49-7.52 (m, 1H), 7.60-7.76 (m, 3H), 7.88-7.90 (m, 0.6H), 7.95-7.97 (m, 0.4H), 8.13 (d, *J* 15 Hz, 2H), 8.37 (s, 1H). ^{13}C-NMR (150 MHz, [D$_4$]MeOH) δ (ppm) 24.2, 24.5, 25.1, 27.4, 30.4, 34.3, 36.0, 36.1, 37.2, 43.8, 49.6, 50.5, 50.8, 51.7, 52.3, 54.9, 55.3, 57.4, 57.7, 57.9, 58.0, 61.6, 110.1, 110.7, 115.1 (TFA), 117.0 (TFA), 118.9 (TFA), 120.9 (TFA), 122.4, 122.9, 123.1, 123.6, 126.9, 127.5, 127.8, 127.9, 128.5, 128.8, 129.4, 129.7, 130.0, 130.1, 130.5, 130.9, 131.2, 132.7, 131.9, 132.3, 132.4, 132.9, 133.4, 134.6, 134.9, 135.4, 135.5, 135.7, 136.1, 136.7, 137.0, 140.9, 142.7, 156.1, 162.3 (TFA), 162.6 (TFA), 162.8 (TFA), 163.0 (TFA), 164.9, 165.5, 168.6, 168.8, 168.9, 169.4. RP-HPLC (220 nm): 98% (t_R = 14.6 min, *k* = 4.1). HRMS (ESI): *m/z* [*M*+H]$^+$ calcd. for [$C_{58}H_{77}N_{12}O_5$]$^+$ 1021.6140, found: 1021.6134. $C_{58}H_{76}N_{12}O_5$ · $C_{12}H_6F_{18}O_{12}$ (1021.33 + 684.14).

N^1-(2-(4-(2-Oxo-2,3-dihydro-1*H*-benzo[d]imidazol-1-yl)-[1,4'-bipiperidin]-1'-yl)ethyl)-N^3-(2-(4-(4-(1-(2-oxo-2-(11-oxo-10,11-dihydro-5*H* dibenzo[*b*,*e*][1,4]diazepin-5-yl)ethyl)piperidin-4-yl)butyl)piperazin-1-yl)ethyl)-5-(propionamidomethyl)isophthalamide pentakis(hydrotrifluoroacetate) (115)

Compound **115** was prepared from **114** (20 mg, 11.7 µmol) and **104** (3.2 mg, 18.7 µmol) according to the procedure for the synthesis of **106**. DIPEA: 22 µL, 130 µmol. Purification by preparative HPLC (column: Kinetex XB-C18 5 µm 250 × 21 mm; gradient: 0-25 min: MeCN/0.1% aq TFA 20:80-64:36, t_R = 9 min), yielded compound **115** as white fluffy solid (17 mg, 88%). IR (KBr): 3400, 3070, 2690, 1675, 1545, 1505, 1485, 1460, 1430, 1365, 1200, 1135, 835, 800, 720. Ratio of isomers evident in the NMR spectra: ca 1.5:1. ^{1}H-NMR (600 MHz, [D$_6$]DMSO) δ (ppm) 1.02 (t, *J* 7.6 Hz, 3H), 1.15-1.29 (m, 4H), 1.31-1.47 (m, 3H), 1.53-1.66 (m, 2H), 1.73-1.80 (m, 2H), 1.87-2.05 (m, 4H), 2.16 (q, *J* 7.6 Hz, 2H), 2.34-2.38 (m, 2H), 2.60-2.72 (m, 2H), 2.75-3.97 (m, 4H), 2.97-3.05 (m, 4H), 3.05-3.21 (m, 4H), 3.22-3.31 (m, 4H), 3.31-3.45 (m, 3H), 3.46-3.55 (m, 4H), 3.55-3.62 (m, 4H), 3.65-3.70 (m, 2H), 3.73-3.97 (m, 3H), 4.33 (d, *J* 5.9 Hz, 2H), 4.39 (d, *J* 17 Hz, 0.6H), 4.43 (d, *J* 17 Hz, 0.4H), 4.60 (t, *J* 12 Hz, 1H), 6.93-7.02 (m, 3H), 7.22-7.30 (m, 2H), 7.33-7.35 (m, 1H), 7.42-7.47 (m, 1H), 7.50-7.60 (m, 1H), 7.68-7.77 (m, 2H), 7.80-7.82 (m, 0.6H), 7.86-7.88 (m, 0.4H), 7.88 (s, 2H), 8.21 (s, 1H), 8.41-8.43 (m, 1H), 8.75 (brs, 1H), 8.91 (brs, 1H), 9.61 (brs, 0.6H), 10.66 (Brs, 0.4H), 10.73 (s, 0.4H), 10.78 (s, 0.6H), 10.94 (s, 1H). ^{13}C-NMR (150 MHz, [D$_6$]DMSO) δ (ppm) 9.9, 23.0, 23.5, 23.7, 23.8, 25.4, 25.8, 28.5, 28.6, 32.7, 34.4, 34.8, 35.5, 40.1, 41.8, 46.5, 48.4, 49.0, 50.4, 52.7, 53.2, 54.9, 55.9, 59.5, 108.5, 109.1, 113.6, 115.6, 117.6, 119.5, 120.5, 120.9, 122.3, 124.7, 124.9, 125.5, 127.3,

127.7, 128.3, 128.4, 128.7, 128.9, 129.0, 129.7, 130.0, 130.4, 131.0, 131.6, 133.0, 133.1, 133.8, 134.1, 134.4, 134.7, 135.8, 139.5, 140.4, 141.0, 153.6, 158.2 (TFA), 158.4 (TFA), 158.6 (TFA), 158.8 (TFA), 164.2, 165.7, 166.1, 166.4, 170.3, 173.1. RP-HPLC (220 nm): 99% (t_R = 15.0 min, *k* = 4.2). HRMS (ESI): m/z [*M*+H]$^+$ calcd. for $[C_{61}H_{81}N_{12}O_6]^+$ 1077.6397, found: 1077.6392. $C_{61}H_{80}N_{12}O_6 \cdot C_{10}H_5F_{15}O_{10}$ (1077.39 + 570.12).

1-(2-(3-(Aminomethyl)-5-((2-(4-(4-(1-(2-oxo-2-(11-oxo-10,11-dihydro-5*H*-dibenzo[*b*,*e*][1,4]diazepin-5-yl)ethyl)piperidin-4-yl)butyl)piperazin-1-yl)ethyl)carbamoyl)benzamido)ethyl)piperidin-4-yl 2,2-diphenylacetate pentakis(hydrotrifluoroacetate) (116)

Compound **116** was prepared from **109** (80 mg, 0.27 mmol), **96** (262 mg, 0.27 mmol) and **73** (92 mg, 0.27 mmol) according to the procedure for the synthesis of **110** and **112**. TBTU: 173 mg, 0.54 mmol; HOBt: 73 mg, 0.54 mmol; DIPEA: 95 + 95 µL, 0.54 + 0.54 mmol. Purification by preparative HPLC (column: Kinetex XB-C18 5 µm 250 × 21 mm; gradient: 0-25 min: MeCN/0.1% aq TFA 20:80-95:5, t_R (**112**) = 9 min, t_R (**116**) = 11 min) afforded compounds **112** (30 mg, 6%) and **116** (120 mg, 28%) as white fluffy solids. **116**: ratio of configurational isomers evident in the NMR spectra: ca 1.5:1. ^{1}H-NMR (600 MHz, [D$_4$]MeOH): δ (ppm) 1.26-1.40 (m, 4H), 1.40-1.58 (m, 3H), 1.68-1.73 (m, 2H), 1.81-1.99 (m, 3H), 2.05-2.14 (m, 2H), 2.25-2.26 (m, 1H), 2.78-2.96 (m, 2H), 2.99 (t, *J* 6.7 Hz, 2H), 3.03-3.05 (m, 1H), 3.06-3.10 (m, 2H), 3.11-3.22 (m, 3H), 3.23-3.26 (m, 2H), 3.39-3.46 (m, 6H), 3.55-3.57 (m, 2H), 3.66 (t, *J* 6.2 Hz, 2H), 3.69-3.88 (m, 5H), 4.23 (s, 2H), 4.39 (d, *J* 17 Hz, 0.6H), 4.43 (d, *J* 17 Hz, 0.4H), 5.04-5.09 (m, 1H), 5.18 (d, *J* 18 Hz, 1H), 7.25-7.28 (m, 4H), 7.31-7.38 (m, 8H), 7.45-7.49 (m, 1H), 7,51 (d, *J* 7.8 Hz, 1H), 7.56-7.81 (m, 3H), 7.88-7.90 (m, 0.6H), 7.95-7.96 (M, 0.4H), 8.11-8.13 (m, 2H), 8.36 (s, 1H). ^{13}C-NMR (150 MHz, [D$_4$]MeOH): δ (ppm) 24.5, 25.1, 28.1, 28.9, 30.4, 34.3, 35.8, 36.1, 37.3, 43.8, 49.6, 50.9, 51.9, 54.9, 55.3, 57.4, 57.8, 58.0, 58.1, 66.0, 115.1, 116.9, 117.1 (TFA), 118.9 (TFA), 123.1, 123.7, 126.9, 127.5, 127.8, 127.9, 128.5, 128.9, 129.5, 129.7, 130.1, 130.5, 130.9, 131.2, 131.7, 131.9, 132.2, 132.3, 132.4, 133.0, 133.4, 134.6, 134.9, 135.4, 135.7, 136.1, 136.7, 137.0, 140.0, 141.0, 142.7, 158.8, 159.1, 162.4 (TFA), 162.6 (TFA), 162.8 (TFA), 163.1 (TFA), 164.9, 165.4, 168.6, 168.8, 168.9, 169.4. RP-HPLC (220 nm): 99% (t_R = 17.9 min, *k* = 5.2). HRMS (ESI): *m/z* [*M*+H]$^+$ calcd. for $[C_{60}H_{74}N_9O_6]^+$ 1016.5757, found: 1016.5750. $C_{60}H_{73}N_9O_6 \cdot C_{10}H_5F_{15}O_{10}$ (1016.30 + 570.12).

1-(2-(3-((2-(4-(4-(1-(2-Oxo-2-(11-oxo-10,11-dihydro-5*H*-dibenzo[*b*,*e*][1,4]diazepin-5-yl)ethyl)piperidin-4-yl)butyl)piperazin-1-yl)ethyl)carbamoyl)-5-(propionamidomethyl)benzamido)ethyl)piperidin-4-yl 2,2-diphenylacetate tetrakis(hydrotrifluoroacetate) (117)

Compound **117** was prepared from **116** (15 mg, 9.5 µmol) and **104** (2.9 mg, 16.9 µmol)

according to the procedure for the synthesis of **106**. DIPEA: 16 µL, 92 µmol. Purification by preparative HPLC (column: Kinetex XB-C18 5 µm 250 × 21 mm; gradient: 0-25 min: MeCN/0.1% aq TFA 20:80-95:5, t_R = 11 min), afforded compound **117** as hygroscopic white fluffy solid (12.1 mg, 83%). Anal. calcd. for $C_{63}H_{77}N_9O_7 \cdot C_8H_4F_{12}O_8 \cdot H_{14}O_7$: C 51.54, H 5.79, N 7.62; found: C 51.61, H 5.27, N 7.26. Ratio of isomers evident in the NMR spectra: ca 1.5:1. ^{1}H-NMR (600 MHz, [D$_4$]MeOH): δ (ppm) 1.14 (t, *J* 7.6 Hz, 3H), 1.30-1.41 (m, 4H), 1.43-1.57 (m, 3H), 1.68-1.73 (m, 2H), 1.83-1.96 (m, 3H), 2.03-2.13 (m, 2H), 2.27 (q, *J* 7.6 Hz, 2H), 2.80-2.89 (m, 2H), 2.90-2.94 (m, 3H), 2.98-3.02 (m, 2H), 3.05-3.11 (m, 3H), 3.12-3.19 (m, 2H), 3.23-3.26 (m, 2H), 3.34-3.37 (m, 4H), 3.40-3.48 (m, 2H), 3.55-3.57 (m, 1H), 3.63 (t, *J* 6.2 Hz, 2H), 3.67-3.85 (m, 5H), 4.36-4.42 (m, 1H), 4.44 (s, 2H), 5.04-5.19 (m, 2H), 7.24-7.28 (m, 3H), 7.29-7.39 (m, 10H), 7.46-7.53 (m, 2H), 7.61-7.64 (m, 1H), 7.65-7.76 (m, 1H), 7.89-7.90 (m, 0.6H), 7.92 (d, *J* 9.3 Hz, 2H), 7.96-7.97 (m, 0.4H), 8.21 (s, 1H). ^{13}C-NMR (150 MHz, [D$_4$]MeOH): δ (ppm) 10.4, 24.5, 25.2, 28.2, 29.0, 30.1, 30.4, 34.3, 35.9, 36.1, 37.4, 43.7, 49.6, 50.9, 52.1, 54.9, 55.3, 57.5, 57.8, 58.1, 65.9, 116.9 (TFA), 118.9 (TFA), 123.1, 123.6, 126.4, 126.9, 127.5, 127.9, 128.5, 128.9, 129.4, 129.7, 130.1, 130.5, 130.6, 130.8, 130.9, 131.9, 132.4, 133.0, 133.4, 134.6, 134.9, 135.5, 135.7, 136.2, 137.0, 140.0, 141.0, 141.7, 142.7, 162.0 (TFA), 162.3 (TFA), 162.5 (TFA), 162.8 (TFA), 164.9, 165.4, 168.6, 168.8, 169.5, 170.1, 177.1. RP-HPLC (220 nm): 98% (t_R = 18.9 min, *k* = 5.6). HRMS (ESI): *m/z* [*M*+H]$^+$ calcd. for $[C_{63}H_{78}N_9O_7]^+$ 1072.6024, found: 1072.6013. $C_{63}H_{77}N_9O_7 \cdot C_8H_4F_{12}O_8$ (1072.37 + 456.09).

2-(4-(2-(3-(Aminomethyl)-5-((2-(4-(4-(1-(2-oxo-2-(11-oxo-10,11-dihydro-5*H*-dibenzo[*b*,*e*][1,4]diazepin-5-yl)ethyl)piperidin-4-yl)butyl)piperazin-1-yl)ethyl)carbamoyl)benzamido)ethyl)piperazin-1-yl)ethyl 9*H*-xanthene-9-carboxylate hexakis(hydrotrifluoroacetate) (118)

Compound **118** was prepared from **109** (80 mg, 0.27 mmol), **96** (262 mg, 0.27 mmol) and **80** (102 mg, 0.27 mmol) according to the procedure for the synthesis of **110** and **112**. TBTU: 172 mg, 0.54 mmol; HOBt: 73 mg, 0.54 mmol; DIPEA: 95 + 95 µL, 0.55 + 0.55 mmol. Purification by preparative HPLC (column: Kinetex XB-C18 5 µm 250 × 21 mm; gradient: 0-25 min: MeCN/0.1% aq TFA 20:80-95:5, t_R (**112**) = 9 min, t_R (**118**) = 11 min) afforded compounds **112** (20 mg, 4%) and **118** (70 mg, 15%) as white fluffy solids. **118**: ratio of isomers evident in the NMR spectra: ca 1.5:1. ^{1}H-NMR (600 MHz, [D$_4$]MeOH): δ (ppm) 1.29-1.39 (m, 5H), 1.41-1.60 (m, 3H), 1.67-1.72 (m, 2H), 1.83-2.00 (m, 2H), 2.78 (t, *J* 4.8 Hz, 2H), 2.69-2.72 (m, 4H), 2.97 (t, *J* 6.2 Hz, 2H), 3.03-3.12 (m, 6H), 3.15-3.25 (m, 4H), 3.30-3.51 (m, 8H), 3.66 (t, *J* 6.3 Hz, 2H), 3.68-3.82 (m, 4H), 4.20-4.24 (m, 2H), 4.25 (brs, 2H), 4.39 (d, *J* 17 Hz, 0.6H), 4.43 (d, *J* 17 Hz, 0.4H), 5.10 (s, 1H), 7.07-7.17 (m, 4H), 7.23-7.30 (m, 1H), 7.31-7.39 (m, 6H), , 7.46-7.53 (m, 2H), 7.61-7.65 (m, 1H), 7.66-7.71 (m, 0.6H), 7.73-7.76 (m, 0.4H), 7.89-7.90 (m, 0.6H), 7.94-7.99 (m, 0.4H), 8.10-8.18 (m, 2H), 8.38-8.39 (m, 1H). ^{13}C-NMR (150 MHz, [D$_4$]MeOH): δ

(ppm) 23.1, 23.8, 29.0, 32.9, 34.7, 35.0, 35.9, 42.4, 45.2, 49.5, 50.1, 50.6, 51.3, 53.5, 53.9, 55.1, 55.9, 56.0, 56.4, 56.6, 61.7, 113.5 (TFA), 115.5 (TFA), 116.4, 117.4 (TFA), 118.7, 119.3 (TFA), 121.7, 122.2, 123.3, 125.5, 126.1, 126.4, 126.5, 127.1, 127.5, 128.0, 128.7, 129.0, 129.1, 129.5, 129.8, 130.3, 130.6, 130.8, 130.9, 131.0, 131.6, 132.0, 133.2, 133.5, 134.1, 134.2, 134.3, 135.0, 135.4, 135.6, 139.6, 141.3, 151.5, 160.8 (TFA), 161.0 (TFA), 161.3 (TFA), 163.5, 164.0, 167.2, 167.4, 167.5, 167.8, 171.3. RP-HPLC (220 nm): 96% (t_R = 17.9 min, k = 5.2). HRMS (ESI): *m/z* [*M*+H]$^+$ calcd. for $[C_{61}H_{75}N_{10}O_7]^+$ 1059.5815, found: 1059.5796. $C_{61}H_{74}N_{10}O_7 \cdot C_{12}H_6F_{18}O_{12}$ (1059.33 + 684.14).

2-(4-(2-(3-((2-(4-(4-(1-(2-Oxo-2-(11-oxo-10,11-dihydro-5*H*-dibenzo[*b*,*e*][1,4]diazepin-5-yl)ethyl)piperidin-4-yl)butyl)piperazin-1-yl)ethyl)carbamoyl)-5-(propionamidomethyl)benzamido)ethyl)piperazin-1-yl)ethyl 9*H*-xanthene-9-carboxylate pentakis(hydrotrifluoroacetate) (119)

Compound **119** was prepared from **118** (16 mg, 9.18 µmol) and **104** (2.3 mg, 13.4 µmol) according to the procedure for the synthesis of **106**. DIPEA: 16 µL, 92 µmol. Purification by preparative HPLC (column: Kinetex XB-C18 5 µm 250 × 21 mm; gradient: 0-25 min: MeCN/0.1% aq TFA 20:80-95:5, t_R = 10 min), yielded compound **118** as hygroscopic white fluffy solid (13.3 mg, 86%). Ratio of isomers evident in the NMR spectra: ca 1.5:1. ^{1}H-NMR (600 MHz, [D$_4$]MeOH): δ (ppm) 1.14 (t, *J* 7.6 Hz, 3H), 1.27-1.41 (m, 5H), 1.41-1.57 (m, 3H), 1.67-1.72 (m, 2H), 1.88-1.95 (m, 2H), 2.28 (q, *J* 7.6 Hz, 2H), 2.65-2.71 (m, 4H), 2.78-2.83 (m, 2H), 2.81-2.97 (m, 2H), 2.96-2.98 (m, 3H), 3.01-3.09 (m, 6H), 3.12-3.25 (m, 5H), 3.35-3.45 (m, 4H), 3.65 (t, *J* 6.6 Hz, 2H), 3.69-3.72 (m, 3H), 3.73-3.81 (m, 1H), 4.18-4.25 (m, 2H), 4.39 (d, *J* 17 Hz, 0.6H), 4.43 (d, *J* 17 Hz, 0.4H), 4.46 (s, 2H), 5.10 (s, 1H), 7.10-7.14 (m, 4H), 7.24-7.30 (m, 1H), 7.30-7.34 (m, 3H), 7.34-7.41 (m, 3H), 7.45-7.50 (m, 1H), 7.49-7.53 (m, 1H), 7.59-7.66 (m, 1H), 7.66-7.71 (m, 0.6H), 7.73-7.76 (m, 0.4H), 7.89 (m, 0.6H), 7.93-7.97 (m, 2.4H), 8.23-8.24 (m, 1H). ^{13}C-NMR (150 MHz, [D$_4$]MeOH): δ (ppm) 10.4, 24.5, 25.1, 30.1, 30.4, 34.3, 36.1, 36.4, 37.3, 43.7, 46.6, 50.9, 51.5, 52.0, 52.7, 54.9, 55.3, 56.5, 57.4, 57.5, 57.8, 58.0, 63.1, 116.9 (TFA), 117.9, 118.8 (TFA), 120.1, 123.1, 123.6, 124.6, 126.4, 126.9, 127.5, 127.9, 128.5, 128.9, 129.4, 130.1, 130.4, 130.5, 130.6, 130.7, 130.9, 131.2, 131.7, 132.0, 132.4, 133.0, 133.4, 134.6, 134.9, 135.5, 135.7, 136.1, 137.0, 141.0, 141.7, 142.7, 152.9, 162.1 (TFA), 162.4 (TFA), 162.6 (TFA), 164.9, 165.4, 168.6, 168.8, 169.6, 169.9, 172.7, 177.2. RP-HPLC (220 nm): 96% (t_R = 18.9 min, k = 5.6). HRMS (ESI): *m/z* [*M*+H]$^+$ calcd. for $[C_{64}H_{79}N_{10}O_8]^+$ 1115.6082, found: 1115.6076. $C_{64}H_{78}N_{10}O_8 \cdot C_{10}H_5F_{15}O_{10}$ (1115.39 + 570.12).

5-(Aminomethyl)-*N*^{1}-(2-(4-(4-(1-(2-oxo-2-(11-oxo-10,11-dihydro-5*H*-dibenzo[*b*,*e*][1,4]diazepin-5-yl)ethyl)piperidin-4-yl)butyl)piperazin-1-yl)ethyl)-*N*^{3}-(2-(4-(4-(1-(3-(2-oxo-3,4-dihydroquinolin-1(2*H*)-yl)propyl)piperidin-4-yl)butyl)piperazin-1-

yl)ethyl)isophthalamide heptakis(hydrotrifluoroacetate) (120)

Compound **120** was prepared from **109** (80 mg, 0.27 mmol), **96** (263 mg, 0.27 mmol) and **88** (123 mg, 0.27 mmol) according to the procedure for the synthesis of **110** and **112**. TBTU: 172 mg, 0.54 mmol; HOBt: 73 mg, 0.54 mmol; DIPEA: 94 + 94 µL, 0.54 + 0.54 mmol. Purification by preparative HPLC (Kinetex XB-C18 5 µm 250 × 21 mm; gradient: 0-20 min: MeCN/0.1% aq TFA 10:90-35:65, t_R (**112**) = 18.5 min, t_R (**120**) = 19.1 min) afforded compounds **112** (15 mg, 3%) and **120** (22 mg, 4%) as white fluffy solids. **120**: ratio of isomers evident in the NMR spectra: ca 1.5:1. ^{1}H-NMR (600 MHz, [D$_4$]MeOH): δ (ppm) 1.30-1.41(m, 10H), 1.48-1.62 (m, 4H), 1.69-1.79 (m, 4H), 1.89-1.92 (m, 1H), 1.93-1.98 (m, 2H), 2.06-2.14 (m, 2H), 2.59-2.69 (m, 2H), 2.89-2.95 (m, 5H), 3.00-3.09 (m, 6H), 3.14-3.18 (m, 7H), 3.20-3.27 (m, 5H), 3.37-3.49 (m, 8H), 3.54-3.59 (m, 4H), 3.68-3.80 (m, 7H), 4.06 (t, *J* 6.3 Hz, 2H), 4.24 (s, 2H), 4.39-4.46 (m, 1H), 7.04-7.06 (m, 1H), 7.17-7.23 (m, 2H), 7.24-7.39 (m, 4H), 7.46-7.49 (m, 1H), 7.50-7.53 (m, 1H), 7.61-7.64 (m, 1H), 7.67-7.76 (m, 1H), 7.89 (d, *J* 7.5 Hz, 0.6H), 7.96 (d, *J* 7.6 Hz, 0.4H), 8.12 (s, 2H), 8.38 (s, 1H). ^{13}C-NMR (150 MHz, [D$_4$]MeOH): δ (ppm) 23.7, 24.5, 25.1, 26.1, 30.4, 30.7, 32.6, 34.3, 34.5, 36.0, 36.1, 36.2, 37.1, 37.2, 40.2, 43.8, 49.6, 50.8, 51.7, 51.8, 54.1, 54.9, 55.0, 55.3, 55.7, 57.4, 57.8, 57.9, 58.1, 61.0, 116.1, 116.9 (TFA), 118.1 (TFA), 118.9 (TFA), 123.1, 123.7, 124.8, 126.9, 127.5, 127.9, 128.2, 128.5, 128.8, 128.9, 129.3, 129.5, 130.1, 130.5, 130.9, 131.2, 131.7, 131.9, 132.2, 132.3, 133.0, 133.4, 134.6, 134.9, 135.4, 135.5, 135.7, 136.6, 137.0, 139.6, 141.0, 142.7, 162.0 (TFA), 162.3 (TFA), 162.6 (TFA), 164.9, 165.5, 168.6, 168.8, 168.9, 173.3. RP-HPLC (220 nm): 98% (t_R = 15.4 min, *k* = 4.4). HRMS (ESI): *m/z* [*M*+H]$^+$ calcd. for [$C_{66}H_{93}N_{12}O_5$]$^+$ 1133.7392, found: 1133.7386. $C_{66}H_{92}N_{12}O_5 \cdot C_{14}H_7F_{21}O_{14}$ (1133.54 + 798.16).

3.4.2. Synthesis of the radioligands [^{3}H]106 and [^{3}H]115

The tritiated heterodimeric ligands [^{3}H]**106** and [^{3}H]**115** were prepared by [^{3}H]propionylation of the precursor amines **105a** and **114**, respectively. A solution of succinimidyl [2,3-^{3}H]-proprionate (specific activity: 80 Ci/mmol, purchased from American Radiolabeled Chemicals, St. Louis, MO, via Hartman Analytics, Braunschweig, Germany) (2.5 mCi, 5.5 µg, 31.25 nmol (each)) in hexane/EtOAc (9:1) was transferred from the delivered ampoule to a 1.5-mL reaction vessel with screw cap, and the solvent was removed in a vacuum concentrator (ca 30 min at about 30 °C). A solution of the precursor molecule (**105a**: 0.53 mg, 403 nmol; **114**: 0.52 mg, 305 nmol) in anhydrous DMF/DIPEA (50:1 v/v) (60 µL) was added, and the vessel was vigorously shaken at rt for 1.5 h. 2% aq TFA (40 µL) and MeCN/H_2O (10:90 v/v) (300 µL) were added and the radioligands were purified using an analytical HPLC system (Waters, Eschborn, Germany) consisting of two 510 pumps, a pump control module, a 486 UV/vis detector, and a Flow-one Beta series A-500 radiodetector (Packard, Meriden, CT). A Luna C18

(3 µm, 150 mm × 4.6 mm, Phenomenex, Aschaffenburg, Germany) was used as stationary phase at a flow rate of 0.8 mL/min. Mixtures of 0.05% aq TFA (A) and acetonitrile containing 0.04% TFA (B) were used as mobile phase. The following linear gradient was applied: 0-20 min: A/B 90:10-79:21, 20-25 min: 79:21 (isocratic), 25-27 min: 79:21-5:95, 27-35 min: 5:95. For the purification of each radioligand three HPLC runs were performed (UV detection: 220 nm; no radiometric detection). Each radioligand was collected in a 2-mL reaction vessel with screw cap (t_R ([^{3}H]**106**) = 25.0 min, t_R ([^{3}H]**115**) = 25.2 min). The volume of the combined eluates was reduced in a vacuum concentrator to approx. 400 µL and approx. 300 µL, respectively and ethanol (400 and 300 µL, respectively) was added. The solutions were transferred into 3-mL borosilicate glass vials with conical bottom (Wheaton NextGen 3-mL V-vials). The reaction vessels were rinsed twice with EtOH/water (50:50 v/v) (200 and 300 µL, respectively) and the washings were transferred to the 3-mL glass vials to obtain tentative stocks with volumes of 1200 µL. For the quantification of the radioligands, a four-point calibration was performed with the corresponding 'cold' forms **106** (0.1, 0.2, 0.5, and 0.8 µM) and **115** (0.1, 0.2, 0.5, and 1 µM) using the following HPLC conditions: HPLC system, stationary phase, eluents and flow rate as above; linear gradient for [^{3}H]**106**: 0-20 min: A/B 90:10-69:31, 20-22 min: 69:31-5:95, 22-29 min: 5:95; linear gradient for [^{3}H]**115**: 0-20 min: A/B 90:10-72:28, 20-22 min: 72:28-5:95, 22-29 min: 5:95; injection volume: 100 µL; UV detection: 220 nm. A 2-µL aliquot of each tentative radioligand stock solutions was added to 128 µL of acetonitrile/0.05% aq TFA (10:90 v/v), 100 µL of this solution were analyzed by HPLC, and five times 2 µL were counted in 3 mL of scintillator (Rotiszint eco plus; Carl Roth, Karlsruhe, Germany) with a LS 6500 liquid scintillation counter (Beckmann-Coulter, Munich, Germany). These analyses were performed twice. The molarities of the tentative stock solutions of [^{3}H]**106** and [^{3}H]**115** were calculated from the mean of the peak areas and the linear calibration curves obtained from the peak areas of the standards. To determine the radiochemical purities and to prove the chemical identities, solutions (100 µL) of [^{3}H]**106** (0.18 µM) and [^{3}H]**115** (0.23 µM) spiked with **106** (3 µM) and **115** (3 µM), respectively, were analyzed by RP-HPLC using the system, column, eluents, flow rate, injection volume and UV detection as for the quantification and additionally radiometric detection (flow rate of the liquid scintillator (Rotiscint eco plus/acetonitrile (90:10 v/v)): 4.0 mL/min) The following linear gradient was used: 0-20 min: A/B 90:10-69:31, 20-30 min: 69:31-5:95, 30-38 min: 5:95). The radiochemical purities amounted to 98% and 99%, respectively. The analyses were repeated after storage at -20 °C for 10 months and revealed radiochemical purities of 88% and 98%, respectively. Calculated specific activities: [^{3}H]**106**, 2.420 TBq/mmol (65.40 Ci/mmol), [^{3}H]**115**, 1.815 TBq/mmol (49.06 Ci/mmol). The final activity concentrations were adjusted to 18.50 MBq/mL by the addition of EtOH/water (50:50 v/v), resulting in molarities of 7.64 µM ([^{3}H]**106**) and 10.2 µM ([^{3}H]**115**). Radiochemical yields: [^{3}H]**106**, 33.64 MBq, 36%; [^{3}H]**115**, 32.56 MBq, 35%.

3.4.3. Investigation of the chemical stability

The chemical stability of **106** and **115** was investigated in PBS (pH = 7.4) at 22 ± 1 °C. The incubation was started by addition of a 10 mM solution of the compounds in DMSO (1 µL) to PBS (99 µL) to give a final concentration of 100 µM. After 0, 12, and 48 h, an aliquot (20 µL) was taken and added to acetonitrile/0.04% aq TFA (1:9 v/v) (20 µL). An aliquot (20 µL) of the resulting solution was analyzed by RP-HPLC using a system from Agilent Technologies (composed of a 1290 Infinity binary pump equipped with a degasser, a 1290 Infinity autosampler, a 1290 Infinity thermostated column compartment, a 1260 Infinity diode array detector, and a 1260 Infinity fluorescence detector). A Kinetex-XB C18 2.6 µm, 100 × 3 mm (Phenomenex) served as stationary phase at a flow rate of 0.5 mL/min. The following linear gradient was applied: 0-20 min: 0.04% aq TFA/acetonitrile 10:90-68:32, 20-22 min: 68:32-95:5, 22-28 min: 95:5. The detection wavelength was set to 220 nm.

3.4.4. Cell culture and preparation of cell homogenates

CHO-K9 cell lines stably transfected with the human M_1-M_5 muscarinic receptors were obtained from Missouri S&T cDNA Resource Center (Rolla, MO). Cells were cultured in HAM's F12 medium supplemented with fetal calf serum (Biochrom, Berlin, Germany) (10%) and G418 (Biochrom) (750 µg/mL). CHO-hM_2 cell homogenates were prepared according to a reported procedure with minor modifications[70]: the harvest buffer (50 mM TRIS, 1 mM EDTA) was supplemented with protease inhibitor (SIGMAFAST, Sigma-Aldrich)). Aliquots of 200 µL were transferred to 2-mL cups and stored at -80°C.

3.4.5. MR radioligand binding experiments

All radioligand binding experiments were performed at 22 ± 1 °C. Leibovitz L-15 medium (Gibco, Life Technologies GmbH, Darmstadt, Germany) supplemented with 1% BSA (Serva, Heidelberg, Germany) (in the following referred to as L15 medium) was used as binding buffer throughout. The effects of various MR ligands on the equilibrium binding of [^{3}H]NMS (equilibrium competition binding assay) were determined at intact adherent CHO-hM_xR cells (x = 1-5) in white 96-well plates with clear bottom (Corning Life Sciences, Tewksbury, MA; Corning cat. no. 3610) using the protocol of previously described MR binding studies with [^{3}H]NMS[55] with the following modification: the total volume of L15 medium per well was 200 µL instead of 188 µL, i.e. the cells were covered with L15 medium (160 µL) followed by the

addition of L15 medium (20 µL), neat or containing atropine 10-fold concentrated, and L15 medium (20 µL) containing the radioligand 10-fold concentrated. The concentration of [^{3}H]NMS was 0.2 nM (M_1, M_2, M_3), 0.1 nM (M_4) or 0.3 nM (M_5) and the incubation time was 3 h throughout.

Saturation binding experiments with [^{3}H]**106** and [^{3}H]**115** at live adherent CHO-hM_2 cells were also performed as previously described binding studies with [^{3}H]NMS[55]. The incubation period was 2 h. Nonspecific binding was determined in the presence of atropine (**7**) (500-fold excess to the radioligand).

Saturation binding experiments with [^{3}H]**106** and [^{3}H]**115** at CHO-hM_2 cell homogenates and the investigation of the effects of various MR ligands on equilibrium binding of [^{3}H]**106** and [^{3}H]**115** (equilibrium competition binding assay), investigated at CHO-hM_2 cell homogenates, too, were performed in Primaria 96-well plates (Corning Life Sciences) using a final volume of 100 µL per well. On the day of the experiment, CHO-hM_2 cell homogenates were thawed and re-suspended using a 1-mL syringe (Henke-Sass Wolf GmBh, Tuttlingen, Germany) equipped with a needle (0.90 × 40 mm, B. Braun, Melsungen, Germany) followed by centrifugation at 500 *g* at 4°C for 5 min. The supernatant was discarded and the pellets were re-suspended in L15 medium using a 1-mL syringe equipped with a needle (0.45 × 25 mm, B. Braun). The homogenates were stored on ice until use. The total amount of protein per well was between 19 and 43 µg. Wells were prefilled with 70 µL of L15 medium. For total binding, L15 medium (10 µL), L15 medium (10 µL) containing the radioligand 10-fold concentrated and cell homogenate (10 µL) were added. To determine unspecific binding or the effect of a compound of interest on radioligand equilibrium binding, L15 medium (10 µL) containing atropine 10-fold concentrated (500-fold excess to the radioligand) or the compound of interest (competitor) 10-fold concentrated, L15 medium (10 µL) containing the radioligand 10-fold concentrated and cell homogenate (10 µL) were added. The applied radioigand concentrations for competition binding studies were 2.0 nM ([^{3}H]**106**) and 0.3 nM ([^{3}H]**115**). The plates were shaken during incubation (2 h for saturation and competition binding experiments). After the incubation the homogenates were collected on GF/C filter mats (0.26 mm; Whatman, Maidstone, UK) (pretreated with 0.3% aq polyethylenimine) and washed with cold PBS using a Brandel Harvester (Brandel, Gaithersburg, MD). Filter pieces for each well were punched out and transferred into 1450-401 96-well plates (PerkinElmer). Rotiscint eco plus (Carl Roth) (200 µL) was added, the plates were sealed with a transparent sealing tape (permanent seal for microplates, PerkinElmer, prod. no. 1450–461), vigorously shaken for at least 3 h, and afterwards kept in the dark for at least 1 h prior to the measurement of radioactivity (DPM) with a MicroBeta2 plate counter (PerkinElmer, Rodgau, Germany). In case of saturation binding experiments performed with [^{3}H]**115** in the presence of **15** (applied at increasing fixed concentrations), the total volume per well was 200 µL. Wells were prefilled with 130 µL of L15

medium. For total binding, L15 medium (20 µL), L15 medium (20 µL) containing **15** 10-fold concentrated, L15 medium (20 µL) containing the radioligand 10-fold concentrated and cell homogenate (10 µL) were added. To determine unspecific binding, L15 medium (20 µL) containing atropine 10-fold concentrated (500-fold excess to [^{3}H]**115**), L15 medium (20 µL) containing **15** 10-fold concentrated, L15 medium (20 µL) containing the radioligand 10-fold concentrated and cell homogenate (10 µL) were added.

M_2R association and dissociation experiments with [^{3}H]**106** and [^{3}H]**115** were performed at CHO-hM_2 cell homogenates in Primaria 96-well plates (Corning Life Sciences) using the experimental procedure as for saturation and competition binding experiments at CHO-hM_2 cell homogenates (see above). The concentration of [^{3}H]**106** and [^{3}H]**115** used for association experiments was 2 nM and 0.6 nM, respectively. The incubation was started after different periods of time (between 0 and 120 min) and stopped immediately after the last addition of radioligand by collecting and washing the homogenates on GF/C filter mats using the harvester. Unspecific binding was determined in the presence of **7** (500-fold excess to the radioligand). In case of dissociation experiments a preincubation of the cell homogenates with the radioligand ([^{3}H]**106**: 4 nM, [^{3}H]**115**: 0.6 nM) was performed for 60 min. The preincubation was started after different periods of time ([^{3}H]**106**: between 1 and 180 min, [^{3}H]**115**: between 0 and 150 min) by the addition of the radioligand to the wells prefilled with L15 medium and cell homogenates. The dissociation was started by addition of **7** (1000-fold excess to the radioligand) dissolved in L15 medium (10 µL) (10-fold concentrated). The dissociation was stopped by collecting and washing the homogenates using the harvester. For the determination of unspecific binding **7** (1000-fold excess to the radioligand) was added during the preincubation step.

3.4.6. IP1 accumulation assay

The measurement of M_2R stimulated activation of the G-protein mediated pathway was performed applying the IP-One HTRF® assay (Cisbio, Codolet, France) according to the manufacturer's protocol. In brief, HEK-293 cells were grown to a confluence of approx. 70% and transiently co-transfected with the cDNAs of the human M_2 receptor (Missouri S&T cDNA Rescourse Center) and the hybrid G-protein $G\alpha_{qi5\text{-}HA}$ ($G\alpha_q$ protein with the last five amino acids at the C-terminus replaced by the corresponding sequence of $G\alpha_i$; gift from the J. David Gladstone Institutes, San Francisco, CA)[71-72] applying TransIT-293 Mirus transfection reagent (MoBiTec, Goettingen, Germany). After one day cells were detached from the culture dish with Versene (Life Technologies GmbH, Darmstadt, Germany), seeded into black 384-well plates (10,000 cells/well) (Greiner Bio-One, Frickenhausen, Germany) and maintained for 24 h at 37 °C. After incubation with the test compounds dissolved in stimulation buffer (final concentration

range from 1 pM up to 100 µM) at 37 °C for 1 h the detection reagents were added (IP1-d2 conjugate and Anti-IP1cryptate TB conjugate each dissolved in lysis buffer), and incubation was continued at room temperature for 60 min. Time resolved fluorescence resonance energy transfer (HTRF) was determined using the Clariostar plate reader (BMG, Ortenberg, Germany) measuring fluorescence at 620 (± 10) nm and 670 (± 10) nm (excitation at 330 nm). In the agonist mode each compound (**106**, **115**) was tested in duplicate in three individual experiments in comparison to the reference compound carbachol (**1**, eight experiments). Antagonist properties of **7**, **106** and **115** were determined after preincubation of the cells with **7**, **106** or **115** for 30 min, subsequent addition of the MR agonist **1** (at a final concentration of 300 nM) and continued incubation at 37 °C for 1 h (five independent experiments each).

3.5. Data processing

Retention (capacity) factors were calculated from retention times (t_R) according to $k = (t_R - t_0)/t_0$ (t_0 = dead time). Data of the IP1 accumulation assay (agonist mode) were processed by plotting the ratios (emission 670 nm/emission 620 nm) of the HTRF measurements against log(concentration **1**) and analysis by a four-parameter logistic equation (GraphPad Prism Software 6.0, GraphPad Software, San Diego, CA), followed by normalization (0% = 'top' (maximum of IP1 accumulation), 100% = 'bottom' (basal activity)) of the four-parameter logistic fit and analysis of the normalized data by a four-parameter logistic equation (log(agonist) vs. response - variable slope). Data of the IP1 accumulation assay (antagonist mode) were processed by plotting the fluorescence ratio against log(concentration antagonist) and analysis by a four-parameter logistic equation (GraphPad Prism), followed by normalization (0% = 'top' (IP1 accumulation elicited by **1** (0.3 µM)) of the four-parameter logistic fit, 100% = 'bottom' (basal activity)) and analysis of the normalized data by a four-parameter logistic equation (log(inhibitor) vs. response - variable slope). pIC_{50} values were converted into pK_b values according to the Cheng-Prusoff equation[73] (logarithmic form). Specific binding data (DPM) from saturation binding experiments were plotted against the free radioligand concentration and analyzed by a two-parameter equation describing hyperbolic binding (one site-specific binding, GraphPad Prism) to obtain K_d and B_{max} values. The free radioligand concentration (nM) was calculated by subtracting the amount of specifically bound radioligand (nM) (calculated from the specifically bound radioligand in dpm, the specific activity and the volume per well) from the total radioligand concentration per well. Unspecific binding data from saturation binding experiments were fitted by linear regression. In case of saturation binding experiments with [^{3}H]**115** in the presence of compound **15**, specific binding data (in DPM) were additionally normalized to the B_{max} value and specific binding (%) was plotted against

log(concentration [^{3}H]**115**) followed by analysis using a four-parameter logistic fit (log(agonist) vs. response, applied constraints: bottom = 0%, top = 100%; GraphPad Prism) (*cf*. Figure 10A). Data for the 'Schild' analysis were obtained from the rightward shift ($\Delta p K_d$) of the saturation isotherm and transformation into log(r-1) (where $r = 10^{\Delta p K_d}$). Log(r-1) was plotted against log(concentration **15**) and the data were analyzed by linear regression to obtain the slope and the 'pA_2' value (intercept with the X axis). Specific binding data from association experiments with [^{3}H]**106** and [^{3}H]**115** were analyzed by a two-parameter equation describing an exponential rise to a maximum (one-phase association, GraphPad Prism) to obtain the observed association rate constant k_{obs} and the maximum of specifically bound radioligand (B_{eq}), which was used to calculate specifically bound radioligand (B_t) in %. Data from dissociation experiments (% specifically bound radioligand (B_t) plotted over time) were analyzed by a three-parameter equation (one phase decay, GraphPad Prism) (in case of [^{3}H]**106** 'plateau' was defined as 0) to obtain the dissociation rate constant k_{off}. The association rate constants (k_{on}) were calculated from k_{obs}, k_{off} and the radioligand concentration ([RL]) according to the correlation: $k_{on} = (k_{obs}-k_{off})/[RL]$. Total binding data (DPM) from radioligand competition binding experiments (determination of the effect of various MR ligands on the equilibrium binding of [^{3}H]NMS, [^{3}H]**106** or [^{3}H]**115**) were plotted against log(concentration competitor) and analyzed by a four-parameter logistic equation (log(inhibitor) vs. response-variable slope, GraphPad Prism) followed by normalization (100% = 'top' of the four-parameter logistic fit, 0% = unspecifically bound radioligand (DPM) in case of using [^{3}H]NMS, or 0% = 'bottom' of the four-parameter logistic in case of using [^{3}H]**106** and [^{3}H]**115**) and analysis of the normalized data by a four-parameter logistic equation. IC_{50} were converted to K_i values according to the Cheng-Prusoff equation using K_d values of 1.1 nM ([^{3}H]**106**) and 0.12 nM ([^{3}H]**115**)[73]. Statistical significance was assessed by a one-sample *t*-test. Propagated errors were calculated according to the Gaussian law of errors.

3.6. References

1. Heilker, R.; Wolff, M.; Tautermann, C. S.; Bieler, M., G-protein-coupled receptor-focused drug discovery using a target class platform approach. *Drug Discovery Today* **2009,** *14* (5), 231-240.
2. Salon, J. A.; Lodowski, D. T.; Palczewski, K., The significance of G protein-coupled receptor crystallography for drug discovery. *Pharmacol. Rev.* **2011,** *63* (4), 901-937.
3. Jacoby, E.; Bouhelal, R.; Gerspacher, M.; Seuwen, K., The 7 TM G-protein-coupled receptor target family. *ChemMedChem* **2006,** *1* (8), 760-782.
4. Felder, C. C.; Bymaster, F. P.; Ward, J.; DeLapp, N., Therapeutic opportunities for muscarinic receptors in the central nervous system. *J. Med. Chem.* **2000,** *43* (23), 4333-4353.
5. Hulme, E.; Birdsall, N.; Buckley, N., Muscarinic receptor subtypes. *Annu. Rev. Pharmacol. Toxicol.* **1990,** *30* (1), 633-673.

6. Ellis, J.; Huyler, J.; Brann, M. R., Allosteric regulation of cloned M_1-M_5 muscarinic receptor subtypes. *Biochem. Pharmacol.* **1991,** *42* (10), 1927-1932.
7. Lazareno, S.; Gharagozloo, P.; Kuonen, D.; Popham, A.; Birdsall, N., Subtype-selective positive cooperative interactions between brucine analogues and acetylcholine at muscarinic receptors: radioligand binding studies. *Mol. Pharmacol.* **1998,** *53* (3), 573-589.
8. Gregory, K. J.; Sexton, P. M.; Christopoulos, A., Allosteric modulation of muscarinic acetylcholine receptors. *Curr. Neuropharmacol.* **2007,** *5* (3), 157-167.
9. Conn, P. J.; Christopoulos, A.; Lindsley, C. W., Allosteric modulators of GPCRs: a novel approach for the treatment of CNS disorders. *Nat. Rev. Drug Discovery* **2009,** *8* (1), 41-54.
10. May, L. T.; Leach, K.; Sexton, P. M.; Christopoulos, A., Allosteric modulation of G protein-coupled receptors. *Annu. Rev. Pharmacol. Toxicol.* **2007,** *47*, 1-51.
11. Mohr, K.; Tränkle, C.; Kostenis, E.; Barocelli, E.; De Amici, M.; Holzgrabe, U., Rational design of dualsteric GPCR ligands: quests and promise. *Br. J. Pharmacol.* **2010,** *159* (5), 997-1008.
12. Clark, A.; Mitchelson, F., The inhibitory effect of gallamine on muscarinic receptors. *Br. J. Pharmacol.* **1976,** *58* (3), 323-331.
13. Lüllmann, H.; Ohnesorge, F.; Schauwecker, G.-C.; Wassermann, O., Inhibition of the actions of carbachol and DFP on guinea pig isolated atria by alkane-bis-ammonium compounds. *Eur. J. Pharmacol.* **1969,** *6* (3), 241-247.
14. Croy, C. H.; Schober, D. A.; Xiao, H.; Quets, A.; Christopoulos, A.; Felder, C. C., Characterization of the novel positive allosteric modulator, LY2119620, at the muscarinic M_2 and M_4 receptors. *Mol. Pharmacol.* **2014,** *86* (1), 106-115.
15. Schober, D. A.; Croy, C. H.; Xiao, H.; Christopoulos, A.; Felder, C. C., Development of a Radioligand, [^{3}H] LY2119620, to Probe the Human M_2 and M_4 Muscarinic Receptor Allosteric Binding Sites. *Mol. Pharmacol.* **2014,** *86* (1), 116-123.
16. Birnkammer, T.; Spickenreither, A.; Brunskole, I.; Lopuch, M.; Kagermeier, N.; Bernhardt, G. n.; Dove, S.; Seifert, R.; Elz, S.; Buschauer, A., The bivalent ligand approach leads to highly potent and selective acylguanidine-type histamine H_2 receptor agonists. *J. Med. Chem.* **2012,** *55* (3), 1147-1160.
17. Kagermeier, N.; Werner, K.; Keller, M.; Baumeister, P.; Bernhardt, G.; Seifert, R.; Buschauer, A., Dimeric carbamoylguanidine-type histamine H_2 receptor ligands: A new class of potent and selective agonists. *Bioorg. Med. Chem.* **2015,** *23* (14), 3957-3969.
18. Huber, D.; Hubner, H.; Gmeiner, P., 1, 1′ -Disubstituted ferrocenes as molecular hinges in mono-and bivalent dopamine receptor ligands. *J. Med. Chem.* **2009,** *52* (21), 6860-6870.
19. Kühhorn, J.; Hübner, H.; Gmeiner, P., Bivalent dopamine D_2 receptor ligands: synthesis and binding properties. *J. Med. Chem.* **2011,** *54* (13), 4896-4903.
20. Soriano, A.; Ventura, R.; Molero, A.; Hoen, R.; Casadó, V.; Cortés, A.; Fanelli, F.; Albericio, F.; Lluís, C.; Franco, R., Adenosine A_2A receptor-antagonist/dopamine D_2 receptor-agonist bivalent ligands as pharmacological tools to detect A_2A-D_2 receptor heteromers. *J. Med. Chem* **2009,** *52* (18), 5590-5602.
21. Jacobson, K. A.; Xie, R.; Young, L.; Chang, L.; Liang, B. T., A novel pharmacological approach to treating cardiac ischemia binary conjugates of A_1 and A_3 adenosine receptor agonists. *J. Biol. Chem.* **2000,** *275* (39), 30272-30279.
22. Weiss, S.; Keller, M.; Bernhardt, G.; Buschauer, A.; König, B., Modular synthesis of non-peptidic bivalent NPY Y_1 receptor antagonists. *Bioorg. Med. Chem.* **2008,** *16* (22), 9858-9866.
23. Keller, M.; Teng, S.; Bernhardt, G.; Buschauer, A., Bivalent Argininamide-Type Neuropeptide Y Y_1 Antagonists Do Not Support the Hypothesis of Receptor Dimerisation. *ChemMedChem* **2009,** *4* (10), 1733-1745.
24. Shonberg, J.; Scammells, P. J.; Capuano, B., Design strategies for bivalent ligands targeting GPCRs. *ChemMedChem* **2011,** *6* (6), 963-974.
25. Berque-Bestel, I.; Lezoualc'h, F.; Jockers, R., Bivalent ligands as specific

pharmacological tools for G protein-coupled receptor dimers. *Curr. Drug Discovery Technol.* **2008,** *5* (4), 312-318.
26. Davie, B. J.; Christopoulos, A.; Scammells, P. J., Development of M_1 mAChR allosteric and bitopic ligands: prospective therapeutics for the treatment of cognitive deficits. *ACS Chem. Neurosci.* **2013,** *4* (7), 1026-1048.
27. Valant, C.; Robert Lane, J.; Sexton, P. M.; Christopoulos, A., The best of both worlds? Bitopic orthosteric/allosteric ligands of g protein-coupled receptors. *Annu. Rev. Pharmacol. Toxicol.* **2012,** *52*, 153-178.
28. Valant, C.; Sexton, P. M.; Christopoulos, A., Orthosteric/allosteric bitopic ligands. *Mol. Interventions* **2009,** *9* (3), 125.
29. Disingrini, T.; Muth, M.; Dallanoce, C.; Barocelli, E.; Bertoni, S.; Kellershohn, K.; Mohr, K.; De Amici, M.; Holzgrabe, U., Design, synthesis, and action of oxotremorine-related hybrid-type allosteric modulators of muscarinic acetylcholine receptors. *J. Med. Chem.* **2006,** *49* (1), 366-372.
30. Steinfeld, T.; Mammen, M.; Smith, J. A.; Wilson, R. D.; Jasper, J. R., A novel multivalent ligand that bridges the allosteric and orthosteric binding sites of the M_2 muscarinic receptor. *Mol. Pharmacol.* **2007,** *72* (2), 291-302.
31. Dörje, F.; Wess, J.; Lambrecht, G.; Tacke, R.; Mutschler, E.; Brann, M., Antagonist binding profiles of five cloned human muscarinic receptor subtypes. *J. Pharmacol. Exp. Ther.* **1991,** *256* (2), 727-733.
32. Hammer, R.; Berrie, C.; Birdsall, N.; Burgen, A.; Hulme, E., Pirenzepine distinguishes between different subclasses of muscarinic receptors. **1980**.
33. Gitler, M. S.; Reba, R. C.; Cohen, V. I.; Rzeszotarski, W. J.; Baumgold, J., A novel M_2-selective muscarinic antagonist: binding characteristics and autoradiographic distribution in rat brain. *Brain Res.* **1992,** *582* (2), 253-260.
34. Tränkle, C.; Andresen, I.; Lambrecht, G.; Mohr, K., M_2 receptor binding of the selective antagonist AF-DX 384: possible involvement of the common allosteric site. *Mol. Pharmacol.* **1998,** *53* (2), 304-312.
35. Mohr, M.; Heller, E.; Ataie, A.; Mohr, K.; Holzgrabe, U., Development of a New Type of Allosteric Modulator of Muscarinic Receptors: Hybrids of the Antagonist AF-DX 384 and the Hexamethonio Derivative W84. *J. Med. Chem.* **2004,** *47* (12), 3324-3327.
36. Holzgrabe, U.; De Amici, M.; Mohr, K., Allosteric modulators and selective agonists of muscarinic receptors. *J. Mol. Neurosci.* **2006,** *30* (1), 165-167.
37. Jones, C. K.; Brady, A. E.; Davis, A. A.; Xiang, Z.; Bubser, M.; Tantawy, M. N.; Kane, A. S.; Bridges, T. M.; Kennedy, J. P.; Bradley, S. R., Novel selective allosteric activator of the M_1 muscarinic acetylcholine receptor regulates amyloid processing and produces antipsychotic-like activity in rats. *The Journal of Neuroscience* **2008,** *28* (41), 10422-10433.
38. Bridges, T. M.; Brady, A. E.; Kennedy, J. P.; Daniels, R. N.; Miller, N. R.; Kim, K.; Breininger, M. L.; Gentry, P. R.; Brogan, J. T.; Jones, C. K., Synthesis and SAR of analogues of the M_1 allosteric agonist TBPB. Part I: Exploration of alternative benzyl and privileged structure moieties. *Bioorg. Med. Chem. Lett.* **2008,** *18* (20), 5439-5442.
39. Miller, N. R.; Daniels, R. N.; Bridges, T. M.; Brady, A. E.; Conn, P. J.; Lindsley, C. W., Synthesis and SAR of analogs of the M_1 allosteric agonist TBPB. Part II: Amides, sulfonamides and ureas—The effect of capping the distal basic piperidine nitrogen. *Bioorg. Med. Chem. Lett.* **2008,** *18* (20), 5443-5447.
40. Keov, P.; Valant, C.; Devine, S. M.; Lane, J. R.; Scammells, P. J.; Sexton, P. M.; Christopoulos, A., Reverse engineering of the selective agonist TBPB unveils both orthosteric and allosteric modes of action at the M_1 muscarinic acetylcholine receptor. *Mol. Pharmacol.* **2013,** *84* (3), 425-437.
41. Avlani, V. A.; Langmead, C. J.; Guida, E.; Wood, M. D.; Tehan, B. G.; Herdon, H. J.; Watson, J. M.; Sexton, P. M.; Christopoulos, A., Orthosteric and allosteric modes of interaction of novel selective agonists of the M_1 muscarinic acetylcholine receptor. *Mol. Pharmacol.* **2010,** *78* (1), 94-104.
42. Huang, F.; Buchwald, P.; Browne, C. E.; Farag, H. H.; Wu, W.-M.; Ji, F.; Hochhaus, G.;

Bodor, N., Receptor binding studies of soft anticholinergic agents. *AAPS PharmSci* **2001,** *3* (4), 44-56.
43. Lambert, J. B.; Huseland, D. E.; Wang, G.-t., Synthesis of 1, 3-disubstituted diazolidines. *Synthesis* **1986,** *1986* (08), 657-658.
44. Martinelli, J.; Gugliotta, G.; Tei, L., Synthesis of 6-substituted 6-nitroperhydro-1, 4-diazepines via novel Tandem retro-Henry and Mannich/Michael reactions. *Org. Lett.* **2012,** *14* (3), 716-719.
45. Gugliotta, G.; Botta, M.; Giovenzana, G. B.; Tei, L., Fast and easy access to efficient bifunctional chelators for MRI applications. *Bioorg. Med. Chem. Lett.* **2009,** *19* (13), 3442-3444.
46. Harada, H.; Hirokawa, Y.; Morie, T.; Kato, S., A facile synthesis of 6-amino-1-benzyl-4-methyl-and 6-amino-1, 4-dimethylhexahydro-1*H*-1, 4-diazepines, the amine part of substituted benzamides with a potent serotonin 3 receptor antagonistic activity. *Heterocycles* **1995,** *2* (41), 363-371.
47. Sauerberg, P.; Olesen, P. H.; Nielsen, S.; Treppendahl, S.; Sheardown, M. J.; Honore, T.; Mitch, C. H.; Ward, J. S.; Pike, A. J., Novel functional M_1 selective muscarinic agonists. Synthesis and structure-activity relationships of 3-(1, 2, 5-thiadiazolyl)-1, 2, 5, 6-tetrahydro-1-methylpyridines. *J. Med. Chem.* **1992,** *35* (12), 2274-2283.
48. Rajeswaran, W.; Cao, Y.; Huang, X.-P.; Wroblewski, M. E.; Colclough, T.; Lee, S.; Liu, F.; Nagy, P. I.; Ellis, J.; Levine, B. A., Design, synthesis, and biological characterization of bivalent 1-methyl-1, 2, 5, 6-tetrahydropyridyl-1, 2, 5-thiadiazole derivatives as selective muscarinic agonists. *J. Med. Chem.* **2001,** *44* (26), 4563-4576.
49. Kane, B. E.; Grant, M. K.; El-Fakahany, E. E.; Ferguson, D. M., Synthesis and evaluation of xanomeline analogs—Probing the wash-resistant phenomenon at the M_1 muscarinic acetylcholine receptor. *Bioorg. Med. Chem.* **2008,** *16* (3), 1376-1392.
50. Fang, L.; Jumpertz, S.; Zhang, Y.; Appenroth, D.; Fleck, C.; Mohr, K.; Tränkle, C.; Decker, M., Hybrid molecules from xanomeline and tacrine: Enhanced tacrine actions on cholinesterases and muscarinic M_1 receptors. *J. Med. Chem.* **2010,** *53* (5), 2094-2103.
51. Budzik, B.; Garzya, V.; Shi, D.; Walker, G.; Woolley-Roberts, M.; Pardoe, J.; Lucas, A.; Tehan, B.; Rivero, R. A.; Langmead, C. J., Novel N-substituted benzimidazolones as potent, selective, CNS-penetrant, and orally active M_1 mAChR agonists. *ACS Med. Chem. Lett.* **2010,** *1* (6), 244-248.
52. Thomas, E. A.; Hsu, H. H.; Griffin, M. T.; Hunter, A.; Luong, T.; Ehlert, F. J., Conversion of N-(2-chloroethyl)-4-piperidinyl diphenylacetate (4-DAMP mustard) to an aziridinium ion and its interaction with muscarinic receptors in various tissues. *Mol. Pharmacol.* **1992,** *41* (4), 718-726.
53. Langmead, C.; Austin, N.; Branch, C.; Brown, J.; Buchanan, K.; Davies, C.; Forbes, I.; Fry, V.; Hagan, J.; Herdon, H., Characterization of a CNS penetrant, selective M_1 muscarinic receptor agonist, 77 ‐ LH ‐ 28 ‐ 1. *Br. J. Pharmacol.* **2008,** *154* (5), 1104-1115.
54. Giani, R.; Borsa, M.; Parini, E.; Tonon, G., A new facile synthesis of 11-oxo-10, 11-dihydro-5*H*-dibenzo [*b*, *e*][1, 4] diazepines. *Synthesis* **1985,** *1985* (05), 550-552.
55. Keller, M.; Tränkle, C.; She, X.; Pegoli, A.; Bernhardt, G.; Buschauer, A.; Read, R. W., M_2 Subtype preferring dibenzodiazepinone-type muscarinic receptor ligands: Effect of chemical homo-dimerization on orthosteric (and allosteric?) binding. *Bioorg. Med. Chem.* **2015,** *23* (14), 3970-3990.
56. Buckley, N. J.; Bonner, T. I.; Buckley, C. M.; Brann, M. R., Antagonist binding properties of five cloned muscarinic receptors expressed in CHO-K1 cells. *Mol. Pharmacol.* **1989,** *35* (4), 469-476.
57. Maggio, R.; Barbier, P.; Bolognesi, M. L.; Minarini, A.; Tedeschi, D.; Melchiorre, C., Binding profile of the selective muscarinic receptor antagonist tripitramine. *European Journal of Pharmacology: Molecular Pharmacology* **1994,** *268* (3), 459-462.
58. Copeland, R. A., Conformational adaptation in drug-target interactions and residence time. *Future Med. Chem.* **2011,** *3* (12), 1491-1501.

59. Vauquelin, G., Simplified models for heterobivalent ligand binding: when are they applicable and which are the factors that affect their target residence time. *Naunyn-Schmiedeberg's Arch. Pharmacol.* **2013,** *386* (11), 949-962.
60. Lazareno, S., Quantification of receptor interactions using binding methods. *J. Recept. Signal Transduction* **2001,** *21* (2-3), 139-165.
61. Christopoulos, A.; Kenakin, T., G protein-coupled receptor allosterism and complexing. *Pharmacol. Rev.* **2002,** *54* (2), 323-374.
62. Daval, S. B.; Kellenberger, E.; Bonnet, D.; Utard, V.; Galzi, J.-L.; Ilien, B., Exploration of the orthosteric/allosteric interface in human M_1 muscarinic receptors by bitopic fluorescent ligands. *Mol. Pharmacol.* **2013,** *84* (1), 71-85.
63. Hedlund, P. B.; Carson, M. J.; Sutcliffe, J. G.; Thomas, E. A., Allosteric regulation by oleamide of the binding properties of 5-hydroxytryptamine 7 receptors. *Biochem. Pharmacol.* **1999,** *58* (11), 1807-1813.
64. Kenakin, T., *A pharmacology primer: theory, application and methods*. Academic Press: 2009.
65. Hulme, E. C.; Trevethick, M. A., Ligand binding assays at equilibrium: validation and interpretation. *Br. J. Pharmacol.* **2010,** *161* (6), 1219-1237.
66. Lewandowski, K.; Murer, P.; Svec, F.; Fréchet, J. M., The design of chiral separation media using monodisperse functionalized macroporous beads: effects of polymer matrix, tether, and linkage chemistry. *Anal. Chem.* **1998,** *70* (8), 1629-1638.
67. Burgey, C. S.; Stump, C. A.; Nguyen, D. N.; Deng, J. Z.; Quigley, A. G.; Norton, B. R.; Bell, I. M.; Mosser, S. D.; Salvatore, C. A.; Rutledge, R. Z., Benzodiazepine calcitonin gene-related peptide (CGRP) receptor antagonists: optimization of the 4-substituted piperidine. *Bioorg. Med. Chem. Lett.* **2006,** *16* (19), 5052-5056.
68. Galli, U.; Ercolano, E.; Carraro, L.; Blasi Roman, C. R.; Sorba, G.; Canonico, P. L.; Genazzani, A. A.; Tron, G. C.; Billington, R. A., Synthesis and biological evaluation of isosteric analogues of FK866, an inhibitor of NAD salvage. *ChemMedChem* **2008,** *3* (5), 771-779.
69. Cohen, V. I.; Baumgold, J.; Jin, B.; De la Cruz, R.; Rzeszotarski, W. J.; Reba, R. C., Synthesis and structure-activity relationship of some 5-[[[(dialkylamino) alkyl]-1-piperidinyl] acetyl]-10, 11-dihydro-5*H*-dibenzo [*b*, *e*][1, 4] diazepin-11-ones as M_2-selective antimuscarinics. *J. Med. Chem.* **1993,** *36* (1), 162-165.
70. Hübner, H.; Haubmann, C.; Utz, W.; Gmeiner, P., Conjugated enynes as nonaromatic catechol bioisosteres: synthesis, binding experiments, and computational studies of novel dopamine receptor agonists recognizing preferentially the D_3 subtype. *J. Med. Chem.* **2000,** *43* (4), 756-762.
71. Kruse, A. C.; Ring, A. M.; Manglik, A.; Hu, J.; Hu, K.; Eitel, K.; Hübner, H.; Pardon, E.; Valant, C.; Sexton, P. M., Activation and allosteric modulation of a muscarinic acetylcholine receptor. *Nature* **2013,** *504* (7478), 101-106.
72. Conklin, B. R.; Farfel, Z.; Lustig, K. D.; Julius, D.; Bourne, H. R., Substitution of three amino acids switches receptor specificity of G_q alpha to that of Gi alpha. *Nature* **1993,** *363* (6426), 274-276.
73. Cheng, Y.-C.; Prusoff, W. H., Relation between the inhibition constant (K_i) and the concentration of inhibitor which causes fifty per cent inhibition (I_{50}) of an enzymic reaction. *Biochem. Pharmacol.* **1973,** *22* (23), 3099-108.

Chapter 4

Dibenzodiazepinone-type fluorescently labeled muscarinic receptor ligands

4. Dibenzodiazepinone-type fluorescently labeled muscarinic receptor ligands

4.1. Introduction

Fluorescent GPCR ligands are considered as useful molecular tools complementary to radioligands for studying GPCRs. Compared with radioligands, fluorescent ligands are advantageous, for instance, with respect to safety issues and high costs for disposal. Moreover, appropriate fluorescent ligands can serve to study the localization of receptors in cells by fluorescence microscopy, and to probe the geometry and mechanisms of ligand-receptor interactions and functional responses at a single cell[1-2]. Typically, fluorescent ligands are composed of a pharmacophore (a known agonist or antagonist for the receptor of interest), a linker and the fluorophore[2]. To design fluorescent ligands with receptor binding properties comparable to the parent ligand, several factors need to be taken into consideration (in particular in case of low molecular weight/non-peptide ligands): the attachment site and length of the linker as well as the type of the fluorophore (size, lipophilicity, net charge, etc.)[3] can be crucial. Numerous fluorescent ligands for GPCRs have been reported, for example probes for NPY[4-8], histamine[9-13], opioid[14-16], dopamine[17] and muscarinic receptors[18-26].

Muscarinic acetylcholine receptors (MRs), in humans constituting five subtypes (M_1R-M_5R), are widely distributed in both the peripheral and central nervous systems[27-29], and are involved in the regulation of various physiological functions. The development of MR ligands, which bind with high selectivity to one of the five subtypes, proved to be highly challenging due to the high conservation of the orthosteric binding site among MRs. As allosteric binding sites are less conserved, the design of allosterically or dualsterically binding MR ligands is considered a promising approach to develop ligands with higher subtype selectivity[30-31]. For instance, improved MR subtype binding or functional selectivity was reported for dualsterically/bitopically interacting antagonists such as pirenzepine derivatives[32-34] and the dimeric compound methoctramine[35], as well as for agonists such as McN-A-343[36] and derivatives of AC-42[21, 37].

Various fluorescent MR antagonists such as telenzepine conjugated to Eosin-5 or Cascade Blue dyes[38-39], and pirenzepine labeled with Bodipy FL[40] were used to study the distribution and expression of M_1 receptors in cultured neurons derived from rat visual cortex or presented as alternatives to radiotracers. A series of fluorescent ligands derived from the M_1R-preferring antagonist pirenzepine were synthesized by Ilien and coworkers[23, 41]. The fluorophores were linked with pirenzepine through linkers of varying chain length. Among these compounds, derivative Bo(15)PZ (compound **121**, *cf*. Figure 1) was suggested to bind M_1R in a bitopic

manner, addressing the orthosteric site (via the pirenzepine moiety) and additionally a brucine accessible allosteric site[23]. Compound **122** (para-LRB-AC42, *cf*. Figure 1), representing a derivative of the bitopic agonist AC-42 labeled with lissamine rhodamine B[21], inhibited orthosteric [^{3}H]NMS binding at the M_1R under equilibrium conditions, and was suggested to be competitive with the allosteric modulator **14** (*cf*. Chapter 3). A putative bitopic/dualsteric binding pose for **122** at the human M_1 receptor was supported by molecular modeling studies[21]. In contrast to the M_1R, reports on fluorescent M_2-M_5 receptor ligands are rare.

The observation that dibenzodiazepinone-type heterodimeric ligands, composed of the dibenzodiazepinone scaffold (DIBA, compound **9**), a linker and a second (varying) MR pharmacophore, exhibited throughout high M_2R affinity (K_i < 10 nM) (*cf*. Chapter 3), stimulated us to prepare fluorescently labeled ligands derived from **9**[42], a high affinity M_2R antagonist. As the bulky 'side chain' (comprising the linker and the second pharmacophoric group) in DIBA-derived dimeric ligands was well tolerated with respect to M_2R binding, we anticipated that also bulky fluorophores attached to **9** will not or only marginally affect binding to the M_2R. As the radiolabeled homo- and heterodimeric dibenzodiazepinone-type MR ligands [^{3}H]**11** and [^{3}H]**115**, respectively (*cf*. doctoral thesis of Andrea Pegoli and Chapter 3), were shown to bind dualsterically to the M_2R, the fluorescent ligands presented in this chapter were supposed to exhibit a dualsteric binding mode, too, and were characterized in this respect.

Seven DIBA-derived fluorescent MR ligands were synthesized by linking red-fluorescent fluorophores (*cf*. Figure 2) to the dibenzodiazepinone scaffold using different types of linkers. MR binding data were determined by equilibrium competition binding with [^{3}H]NMS. Two selected fluorescent ligands were characterized by flow cytometry- and high content imaging-based binding studies (saturation and competition binding). Moreover, MR binding was visualized using confocal microscopy.

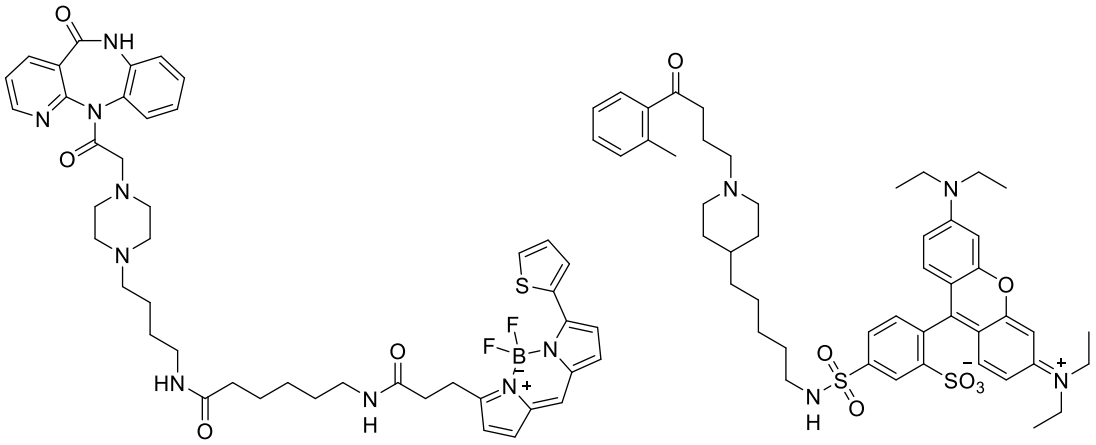

Figure 1. Structures of the fluorescently labeled MR ligands **121** and **122**, which were suggested to exhibit a bitopic/dualsteric binding mode at the M_1 receptor[21, 23].

4.2. Results and discussion

4.2.1. Chemistry

The fluorescent dibenzodiazepinone-type MR ligands were prepared using red fluorescent dyes (emission wavelength > 590 nm) in order to have low background fluorescence when applying the fluorescent ligands at cells. Three different Cy5-related cyanine dyes, i.e. S0223, S0436 and S0387 (emission maximum > 650 nm) (*cf*. Figure 2) as well as the pyrylium dye Py-5 (emission maximum > 600 nm) (*cf*. Figure 2) were used to prepare the fluorescent ligands. The cyanine dyes S0223, S0436 and S0387, exhibiting a low Stokes' shift, can be excited at 635 nm with a red diode laser. Pyrylium dyes such as Py-5, originally developed for the staining of proteins[43], react readily with primary amines at pH > 8 to give the corresponding pyridinium adducts (*cf*. Scheme 1), which are characteristic of a large Stokes' shift and can be excited with an argon laser (488 nm).

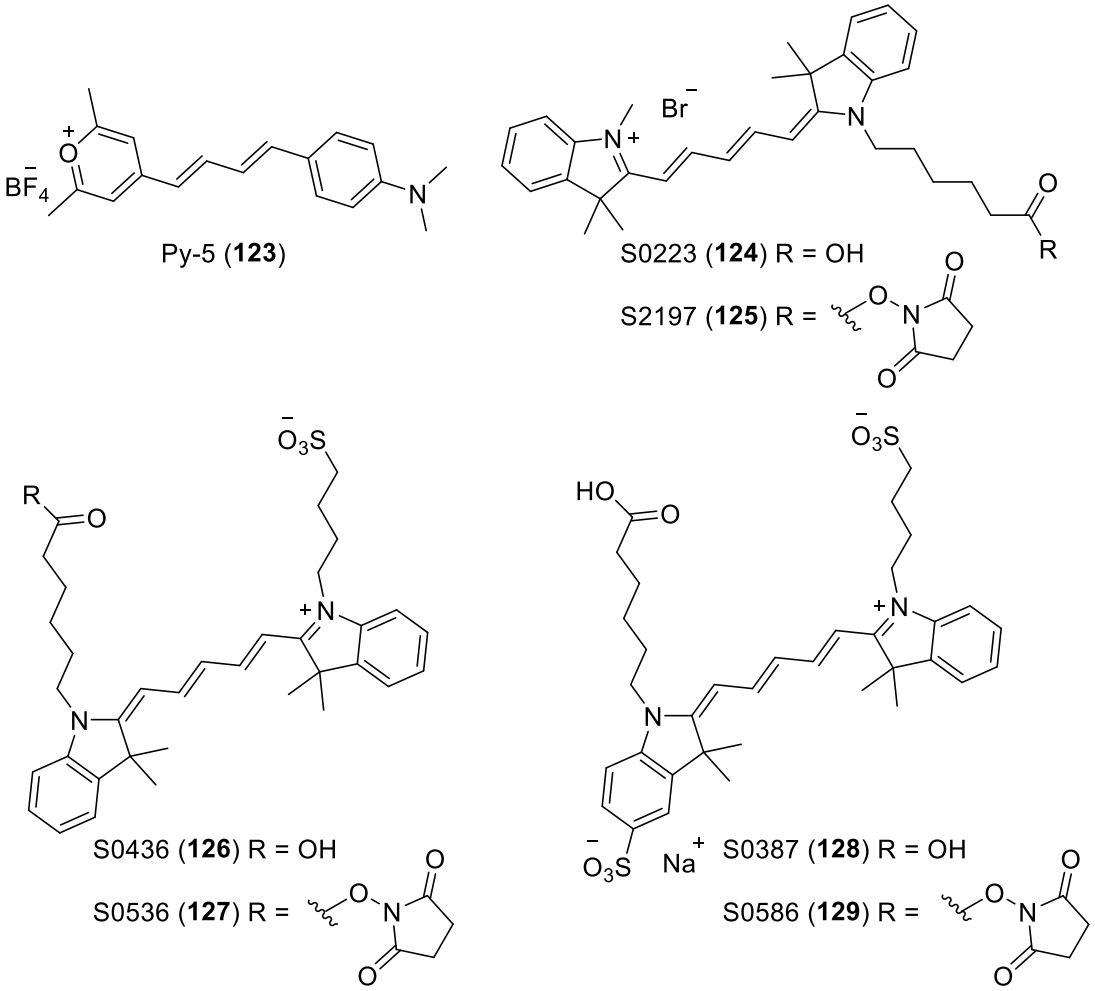

Figure 2. Structures of the fluorescent dyes (**123**, **124**, **126** and **128**) and corresponding succinimidyl esters (**125, 127** and **129**) which were used for the preparation of the fluorescent dibenzodiazepinone-type MR ligands.

Treatment of the DIBA-derived primary amine precursor **10**[44] and **96** (synthesis presented in chapter 3) with the pyrylium dye Py-5 (**123**) (*cf*. Figure 2) gave the fluorescent ligands **130** and **133** (*cf*. Scheme 2). Likewise, treatment of **10** and **96** with the succinimidyl esters **125**, **127** or **129** (*cf*. Figure 2), resulted in the fluorescently labeled DIBA derivatives **131**-**136** (*cf*. Scheme 2).

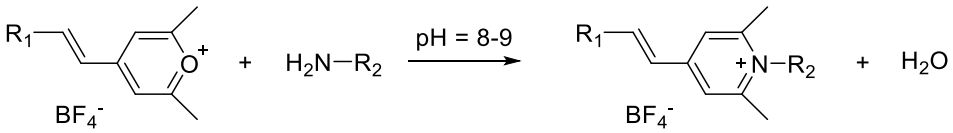

R_1: alkenyl or aryl; R_2: aryl

Scheme 1. Conversion of pyrylium to pyridinium entities through reaction with primary amines.

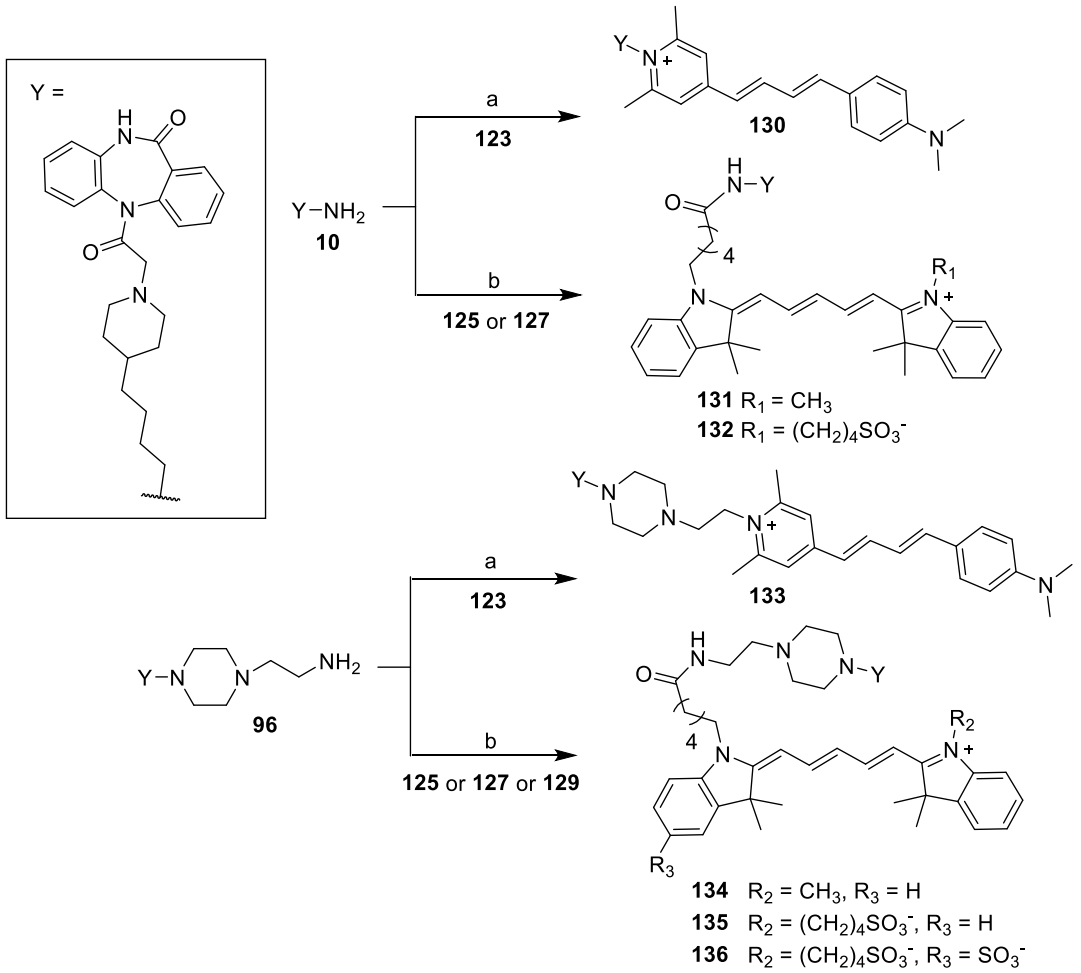

Scheme 2. Synthesis of the fluorescently labeled MR ligands **130-136**. Reagents and conditions: (a) triethylamine, DMF, rt, 2 h, 21% for **130**, 34% for **133**; (b) DIPEA, DMF, rt, 1-2 h, 28-41% for **131**, **132** and **134**-**136**.

4.2.2. Stability of the fluorescent ligand 136

The fluorescent M_2R ligand **136** was investigated with respect to its stability under assay-like

conditions (PBS pH 7.4, 22 °C). No decomposition was observed within the incubation period of 48 h (*cf*. Figure 3).

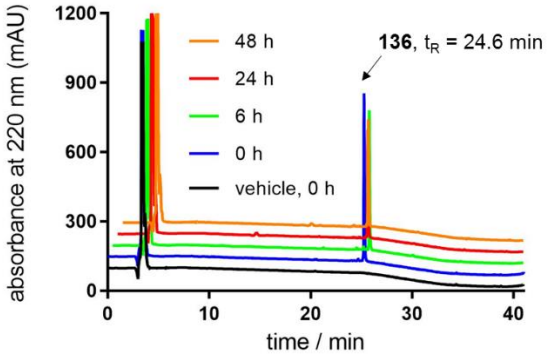

Figure 3. HPLC analysis of **136** after incubation in PBS (pH 7.4) at 23 °C for up to 48 h. **136** showed no decomposition. HPLC conditions see experimental section.

4.2.3. Muscarinic receptor affinity and selectivity

The dibenzodiazepinone-type amine precursors **10** and **96**, and the fluorescent ligands **130-136** were investigated in equilibrium competition binding experiments using the orthosteric antagonist radioligand [^{3}H]N-methylscopolamine ([^{3}H]NMS, [^{3}H]**6**) and live CHO cells stably expressing the human MR subtypes M_1-M_5. The results, expressed as K_i values, are listed in Table 1. Figure 4A shows the sigmoidal curves of fluorescent ligands **130-136** at M_2R. The fluorescent ligands derived from amine precursor **96** (**133-136**), containing the basic piperazine moiety, exhibited higher M_2R affinities compared to the compounds derived from amine precursor **10** (**130-132**) (*cf*. Table 1), which is reflected by the affinities of the precursors **10** and **96** (K_i = 14 and 0.22 nM, respectively). Compound **136**, which bears two sulfonic acid groups at the fluorophore, proved to be the fluorescent ligand with the highest M_2R affinity (K_i = 0.76 nM), suggesting that a negative net charge at the fluorophore is advantageous for M_2R binding. The [^{3}H]NMS displacement curves of ligand **136** at intact CHO-hM_x cells (x = 1-5) are shown in Figure 4B. Obviously, the bulky fluorophore in **136** doesn't prevent receptor binding of the dibenzodiazepinone pharmacophore. Whereas the **96**-derived fluorescent ligands **133-136** showed a preference for the M_2 receptor, the fluorescent ligands derived from **10** exhibited no M_2 over M_4 receptor preference (*cf*. Table 1). For all compounds the M_2R selectivity was most pronounced toward the M_3R and the M_5R. Interestingly, compared to the amine precursor **96**, the M_2R preference of all fluorescent ligands was less pronounced (*cf*. Table 1), indicating that a putative dualsteric binding mode of these ligands didn't result in increased M_2R selectivity.

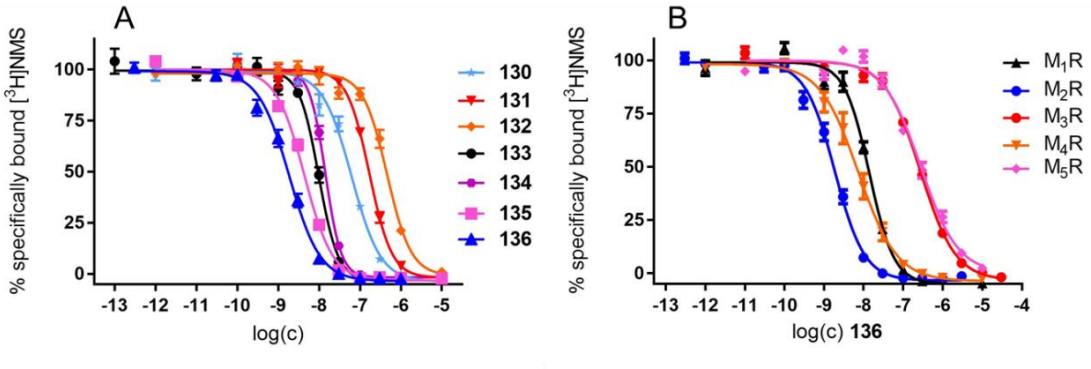

Figure 4. (A) Concentration-dependent effects of compounds **130-136** on [^{3}H]NMS (c = 0.2 nM) equilibrium binding at intact CHO-hM_2 cells. (B) Concentration-dependent effects of compound **136** on equilibrium binding of [^{3}H]NMS at intact CHO-hM_x cells (x = 1-5) (concentration of [^{3}H]NMS: 0.2 nM (M_1R-M_3R), 0.1 nM (M_4R), 0.3 nM (M_5R)). Data were analyzed by four-parameter logistic fits. Data represent mean values ± SEM from at least three independent experiments (performed in triplicate).

Table 1. MR affinities (K_i values) of the amine precursors **10** and **96**, and the fluorescent ligands **130-136** obtained from equilibrium competition binding studies with [^{3}H]NMS at live CHO-hM_x cells (x = 1-5).

Comp.	dye[a]	M_1R		M_2R		M_3R		M_4R		M_5R	
		K_i [nM]	slope[b]	K_i [nM]	slope[b]	K_i [nM]	slope[b]	K_i [nM]	slope[b]	K_i [nM]	slope[b]
10	-	n.d.	n.d.	14 ± 3.2	-0.98 ± 0.07	n.d.	n.d.	n.d.	n.d.	n.d.	n.d.
96	-	7.4 ± 1.6	-0.87 ± 0.12	0.22 ± 0.03	-1.0 ± 0.14	190 ± 0.67	-0.77 ± 0.11	3.6 ± 0.67	-0.83 ± 0.09	230 ± 17	-1.1 ± 0.10
130	**Py-5**	36 ± 6.1	-1.5 ± 0.24	17 ± 3.2	-1.2 ± 0.20	86 ± 12	-1.3 ± 0.06	16 ± 1.1	-1.3 ± 0.04	200 ± 30	-1.6 ± 0.09
131	**S0223**	140 ± 22	-1.3 ± 0.12	54 ± 5.4	-1.6 ± 0.14	640 ± 38	-1.7 ± 0.11	68 ± 3.2	-1.4 ± 0.09	290 ± 63	-1.7 ± 0.16
132	**S0436**	400 ± 37	-1.8 ± 0.29	150 ± 24	-1.5 ± 0.25	960 ± 230	-1.0 ± 0.11	220 ± 9.6	-1.3 ± 0.22	930 ± 240	-1.1 ± 0.24
133	**Py-5**	16 ± 1.6	-1.8 ± 0.19	3.1 ± 0.41	-1.9 ± 0.23	150 ± 9.9	-1.8 ± 0.02	12 ± 4.6	-1.4 ± 0.18	400 ± 71	-1.3 ± 0.20
134	**S0223**	18 ± 1.7	-2.2 ± 0.08	4.5 ± 0.47	-2.3 ± 0.16	88 ± 13	-1.4 ± 0.14	19 ± 3.7	-1.5 ± 0.09	69 ± 7.7	-1.5 ± 0.11
135	**S0436**	12 ± 2.7	-1.9 ± 0.17	1.4 ± 0.18	-1.3 ± 0.14	68 ± 2.4	-1.1 ± 0.03	4.8 ± 2.5	-1.1 ± 0.07	140 ± 1.9	-1.5 ± 0.15
136	**S0387**	5.9 ± 1.1	-1.4 ± 0.17	0.76 ± 0.11	-1.3 ± 0.12	82 ± 5.4	-0.99 ± 0.12	2.5 ± 0.99	-1.0 ± 0.12	150 ± 53	-0.99 ± 0.16

[a]Fluorescent dye used for the preparation of the respective fluorescent ligand. [b]Curve slope of the four-parameter logistic fit. Mean values ± SEM from 3-5 independent experiments (each performed in triplicate). K_d values[44] / applied concentrations of [^{3}H]NMS: M_1R: 0.12 / 0.2 nM; M_2R: 0.090 / 0.2 nM; M_3R: 0.089 / 0.2 nM; M_4R: 0.040 / 0.1 nM; M_5R: 0.24 / 0.3 nM.

4.2.4. Fluorescence properties of compounds 133-136.

The fluorescence quantum yields were determined (reference: cresyl violet perchlorate) for

the fluorescent ligands **133-136** in PBS (pH 7.4) and in PBS with 1% bovine serum albumin (BSA) to study the influence of proteins on the quantum yield (*cf*. Table 2). By selecting compounds **133-136** all types of fluorophores, used in this work, were covered.

Table 2. Fluorescence properties of the fluorescent ligands **133-136** in PBS and PBS containing 1% BSA: excitation/emission maxima and fluorescent quantum yields Φ (reference: cresyl violet perchlorate).

Compound	Dye[a]	PBS		PBS+1% BSA	
		$\lambda_{ex}/\lambda_{em}$	Φ (%)	$\lambda_{ex}/\lambda_{em}$	Φ (%)
133	Py-5	460/713	8.9	484/643	23.8
134	S0223	645/663	19.1	655/675	42.1
135	S0436	648/665	20.9	660/678	30.1
136	S0387	653/669	17.7	656/672	29.0

[a]Fluorescent dye used for the preparation of the respective fluorescent ligand.

All the investigated fluorescent ligands showed a higher quantum yield in PBS with 1 % BSA compared to neat PBS (*cf*. Table 2). The increase in fluorescence quantum yield by adding BSA was most pronounced for **133** and **134** (> 2-fold). This phenomenon can be explained by hydrophobic and electrostatic interactions between the fluorophores and the protein resulting in a reduced molecular motion of the fluorophore and a changed chemical environment.

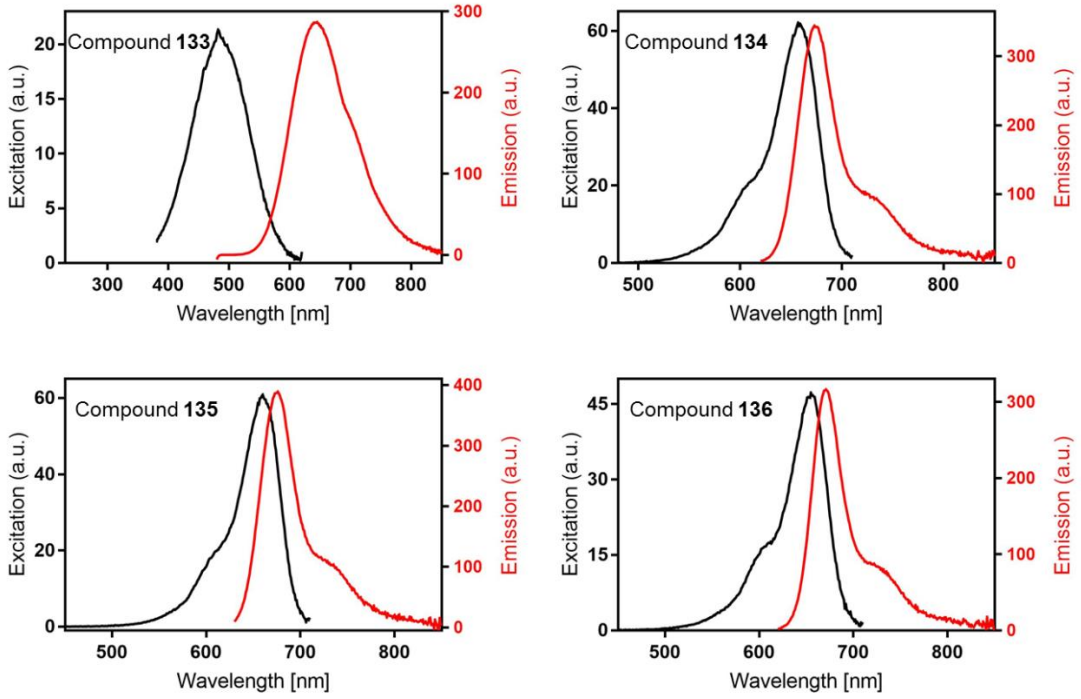

Figure 5. Excitation and corrected emission spectra (recorded at 22 °C) of the fluorescent ligands **133-136** dissolved in PBS supplemented with 1% BSA.

The excitation and corrected emission spectra of **133-136** in PBS containing 1% BSA are depicted in Figure 5, which demonstrates the considerable difference in Stoke's shifts between

the Py-5 labeled ligand (**133**) and the cyanine dye labeled ligands (**134**-**136**), as well as the suitability of **133** to be excited with an argon laser (488 nm) and the compatibility of **134**-**136** with an excitation by the red diode laser (635 nm).

4.2.5. Flow cytometric M_2R binding studies with the fluorescent MR ligands 135 and 136

4.2.5.1. Saturation binding studies

Fluorescent ligands **135** and **136**, which showed excellent M_2R affinity (K_i values < 1.5 nM, *cf*. Table 1) were used for binding studies with flow cytometry. Saturation binding experiments performed with **135** and **136** at intact CHO-hM_2R cells, afforded K_d values of 2.4 nM and 1.0 nM, respectively (*cf*. Figure 6A and 6B, Table 3), which were in good agreement with the K_i values (1.4 and 0.76 nM, respectively, *cf*. Table 1) obtained from competition binding experiments with [^{3}H]NMS at live CHO-hM_2R cells. At concentrations corresponding to the K_d value, unspecific binding amounted to around 10% of total binding for both fluorescent ligands (*cf*. Figure 6A and 6B). The orthosteric antagonist atropine (**7**), used to determine unspecific binding, was capable of completely preventing one-site (monophasic) specific binding of the fluorescent ligands, indicating that **135** and **136** bind to the orthosteric binding pocket of the M_2R.

In addition, saturation binding experiments were performed with **136** at intact CHO-hM_1R cells as well as at intact CHO-hM_4R cells (*cf*. Figure 6C and 6D), resulting in K_d values of 6.5 nM and 8.9 nM, respectively, which were in good agreement with the K_i values (M_1R: 5.9 nM, M_4R: 2.5 nM) obtained from competition binding experiments with [^{3}H]NMS at live CHO-hM_1R and CHO-hM_4R cells (*cf*. Table 1).

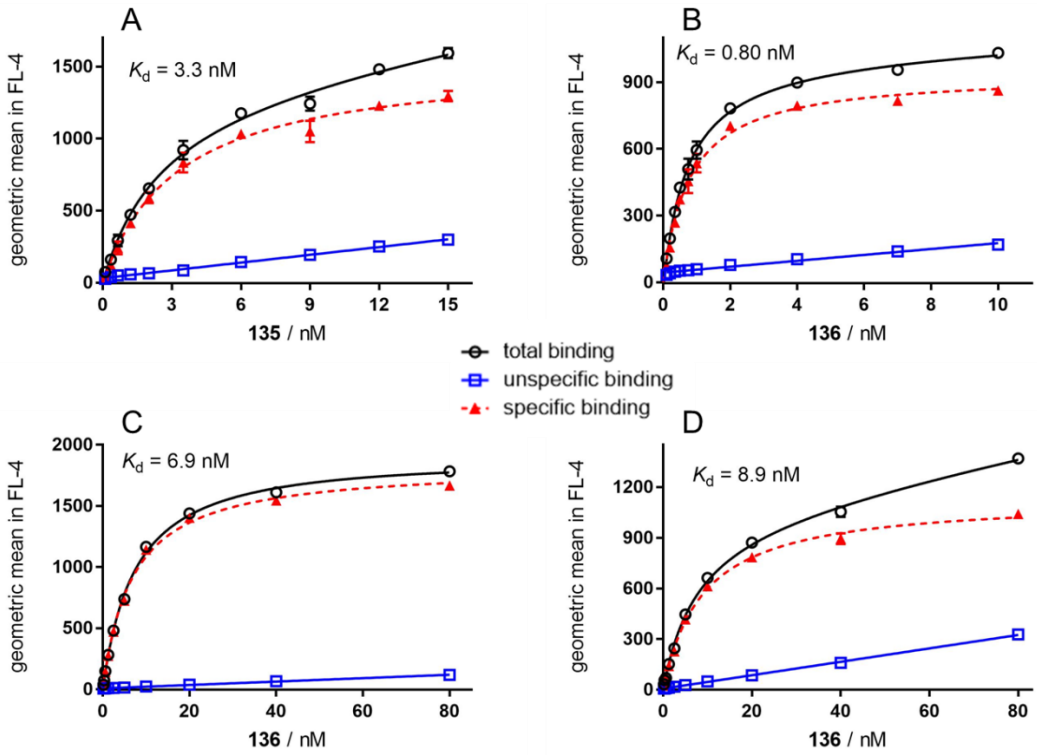

Figure 6. Representative saturation isotherms (specific binding, dashed line) obtained from flow cytometric saturation binding experiments performed with **135** (A) and **136** (B) at intact CHO-hM_2 cells as well as with **136** at intact CHO-hM_1 cells (C) and intact CHO-hM_4 cells (D). Unspecific binding was determined in the presence of atropine (500-fold excess). Cells were incubated with the fluorescent ligands at 22 °C in the dark for 2 h. Experiments were performed in duplicate. Measurements were performed with a FACSCalibur flow cytometer (Becton Dickinson). Specific binding data were analyzed by an equation describing one-site (monophasic) binding. Error bars of specific binding represent propagated errors calculated according to the Gaussian law of errors. Error bars of total and unspecific binding represent the mean ± SEM from at least two independent experiments (each performed in duplicate).

The association and dissociation kinetics of **136** was determined at intact CHO-hM_2R cells at 22 °C using flow cytometry. The association curve reached a plateau after approx. 120 min (*cf*. Figure 7A). The dissociation of **136** from the M_2R was slow ($t_{1/2}$ = 52 min) and incomplete, reaching a plateau at 83% of initial specific binding of **136** (*cf*. Figure 7B). However, the kinetically derived dissociation constant K_d(kin), calculated according to K_d(kin) = k_{off}/k_{on}, amounted to 2.4 nM and was in good agreement with the K_d value (1.0 nM) obtained from saturation binding experiments. An overview of the M_2R binding characteristics of ligand **136**, determined by flow cytometric binding studies, is provided in Table 3.

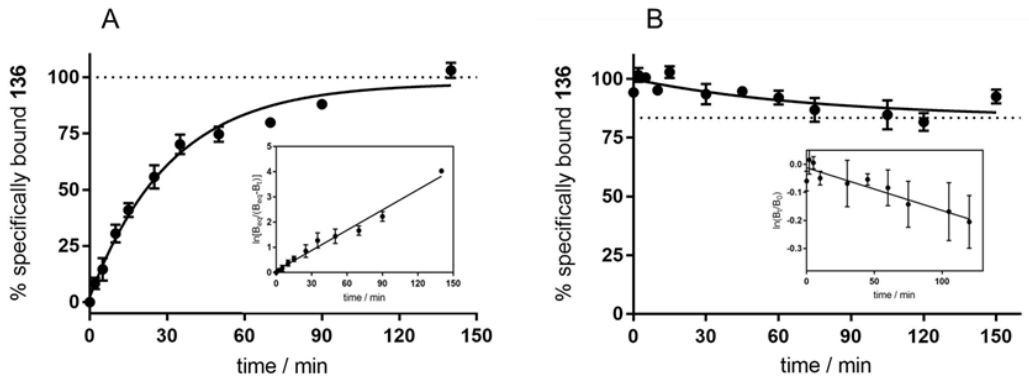

Figure 7. Association and dissociation kinetics of **136** determined at intact CHO-hM_2 cells at 22 °C using a FACSCalibur flow cytometer. A: Association of **136** (c = 3 nM) to the M_2R as a function of time. Inset: ln[B_{eq}/(B_{eq}−B_t)] versus time, k_{obs} = slope = 0.027 min^{-1}. B: Dissociation of **136** (preincubation: 5 nM, 120 min) from the M_2R as a function of time; analyzed by a three-parameter equation describing an (incomplete) monophasic exponential decline ($t_{1/2}$ = 53 min, plateau (dotted line) = 83%). Inset: ln[B_t/B_0] versus time, slope·(−1) = k_{off} = 0.0013 min^{-1}. Data represent the mean ± SEM from two independent experiments (each performed in duplicate).

Table 3. M_2R binding data of the fluorescent ligand **136** determined using flow cytometry.

Saturation binding	Binding kinetics			
K_d(sat) [nM][a]	K_d(kin) [nM][b]	k_{on} [min^{-1}·nM^{-1}][c]	k_{off} [min^{-1}][d]	$t_{1/2}$ [min^{-1}][d]
1.0 ± 0.2	2.4 ± 0.22	0.012 ± 0.0015	0.014 ± 0.0024	52 ± 9.2

[a]Dissociation constant determined by saturation binding at live CHO-hM_2 cells; mean ± SEM from three independent experiments (performed in duplicate). [b]Kinetically derived dissociation constant ± propagated error (K_d(kin) = k_{off}/k_{on}). [c]Association rate constant ± propagated error, calculated from k_{obs}, k_{off} and the applied fluorescent ligand concentration (*cf.* experimental section). [d]Dissociation rate constant and half-life; mean ± SEM from two independent experiments (performed in duplicate).

4.2.5.2. Competition binding.

The suitability of fluorescent ligand **136** as reference compound for the determination of M_2R ligand affinities was explored in competition binding experiments. The fluorescent ligand **136** was used at a concentration corresponding to its K_d value (1 nM). Selected standard MR agonists (**2**), antagonists (**7**, **8**, **11**) and allosteric modulators (**14**, **15**, **16**) were investigated by equilibrium competition binding at live CHO-hM_2R cells using flow cytometry. All types of MR ligands (orthosteric (**2**, **7**), dualsteric (**8**, **11**) and allosteric (**14**, **15** and **16**)) were capable of completely inhibiting specific binding of **136**, resulting in sigmoidal curves that reached 0% specific binding of **136** (*cf*. Figure 8A and 8B). These results were indicative of a competitive mechanism between **136** and the investigated MR ligands. The apparent K_i values (shown in Table 4) were consistent with the K_i or IC_{50} values obtained from equilibrium binding studies with [^{3}H]NMS in the presence of the MR ligands **2**, **7**, **8**, **11** and **14-16**.

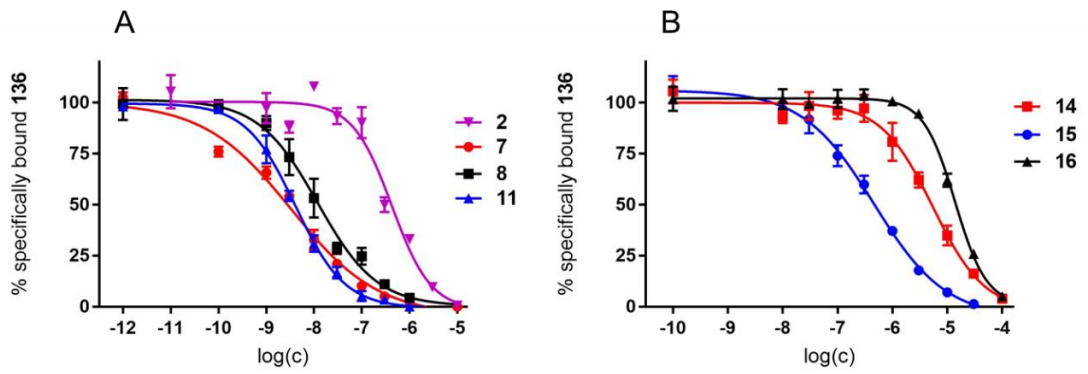

Figure 8. Concentration-dependent effects of various reported orthosteric (**2**, **7**) and dualsteric (**8**, **11**) (A), as well as allosteric (**14**, **15**, **16**) (B) MR ligands on M_2R equilibrium binding of **136** (c = 1 nM) determined at intact CHO-hM_2 cells using a FACSCalibur flow cytometer.

Table 4. M_2R binding data (K_i or IC_{50} values) of various orthosteric (**2**, **7**), allosteric (**14**, **15**, **16**) and dualsteric (**8**, **11**) MR ligands determined with **136** or [^{3}H]NMS.

Compound	**136** K_i [nM][a]	[^{3}H]NMS K_i^* or IC_{50}^{**} [nM]
2	210 ± 5.3	210 ± 59*[b]
7	1.9 ± 0.55	0.94 ± 0.19*[b]
8	6.2 ± 2.4	2.0 ± 0.2*[b]
11	2.1 ± 0.27	0.79 ± 0.10*[b]
14	2700 ± 450	2200 ± 410**[c]
15	250 ± 44	460 ± 130**[c]
16	6900 ± 1200	>10000**[c]

[a]Determined by flow cytometric equilibrium binding studies with **136** (c = 1 nM) in the presence of increasing concentrations of the respective MR ligand at live CHO-hM_2 cells; mean values ± SEM from at least two independent experiments (performed in duplicate). [b]Determined by equilibrium competition binding with [^{3}H]NMS (c = 0.2 nM) at live CHO-hM_2 cells; mean ± SEM from at least three independent experiments (performed in triplicate). [c]IC_{50} values obtained from nonlinear four-parameter logistic curve analyses of data characterizing the inhibition of [^{3}H]NMS (c = 0.2 nM) equilibrium binding at live CHO-hM_2 cells; mean ± SEM from at least 3 independent experiments (performed in triplicate).

4.2.5.3. Saturation binding of the fluorescent ligand 136 in the presence of the allosteric modulator 15.

On one hand, saturation binding experiments with **136** at the M_2R, using the orthosteric antagonist **7** to determine unspecific binding (*cf*. Figure 6B), suggested an interaction of **136** with the orthosteric site of the M_2R. On the other hand, M_2R equilibrium binding of **136** in the presence of the allosteric modulators **14**, **15** and **16** indicated a competitive mechanism between **136** and the allosteric modulators (*cf*. Figure 8B). These findings are consistent with a dulasteric binding mode of ligand **136** at the M_2R. To further elucidate the competitive mechanism between ligand **136** and the allosteric modulator W84 (**15**), saturation binding experiments were performed with the fluorescent ligand **136** in the presence of **15**. This kind

of experiment is equivalent to the Schild analysis based on functional studies with agonists in the presence of antagonists, and was used, e.g. to prove the hypothesis of a competitive interplay between the allosteric modulator brucine and the fluorescent pirenzepine derivative Bo(22)Pz at the M_1R[41]. Figure 9 shows the saturation isotherms of binding of **136** to the M_2R in the absence or presence of different concentrations (0.1, 0.3, 1 and 3 µM) of the allosteric modulator **15**. **15** caused a parallel rightward shift of occupancy curves, going along with an apparent decrease in the affinity of **136**. Based on the shift of the K_d value a 'Schild' plot was constructed (*cf*. Figure 9). The slope factor was not significantly different from unity (slope = 0.85 ± 0.06 (n = 2), P > 0.2), supporting the hypothesis of a competitive mechanism between **15** and **136** and dualsteric binding of **136** at the M_2R.

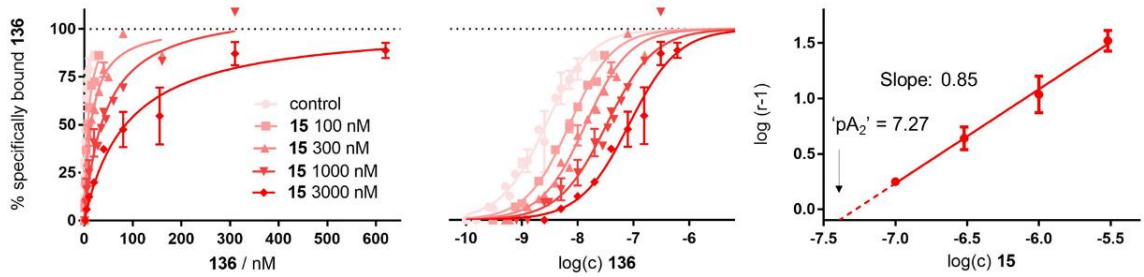

Figure 9. Saturation binding of **136** in the presence of increasing concentrations of **15**. Presented are saturation isotherms of specific binding of **136** to the M_2R in linear scale (left) and semi-logarithmic scale (middle), as well as the "Schild" regression (right) resulting from the rightward shifts (ΔpK_d) of the saturation isotherms (log(r-1) plotted *vs*. log(concentration **15**), where $r = 10^{\Delta pKd}$). The presence of the allosteric modulator **15** led to a parallel rightward shift of the saturation isotherms of **136**. The slope of the linear "Schild" regression was not different from unity (P > 0.2, assessed based on the slope mean value ± SEM (0.85 ± 0.06) from two sets of independent saturation binding experiments (performed in duplicate)) indicating a competitive interaction between **136** and **15**. Data represent mean values ± SEM from at least two independent experiments (performed in duplicate).

4.2.6. Application of the fluorescent ligands 135 and 136 to high content imaging

4.2.6.1. Saturation binding.

The fluorescent ligands **135** and **136** were also applied in plate reader-based, high-content imaging M_2R binding assays, using live CHO-hM_2R cells. The fluorescent ligands **135** and **136** were incubated with CHO-hM_2R cells for 60 min at 22 °C, and directly (without washing of the cells) imaged by the ImageXpress (IX) Ultra plate reader. Figures 10A and 10B show representative saturation binding curves of **135** and **136**. The K_d values amounted to 13 nM and 4.8 nM, respectively. Due to the strong adsorption of the fluorescent ligands **135** and **136** to the 96 well plate (Grenier 655090), high levels of unspecific binding were detected (*cf*. Figure 10A and 10B). The application of a washing step (HBSS+0.1% BSA) after the incubation for 60 min at 22 °C, followed by immediate acquisition of the images, resulted in

considerably lower unspecific binding (at concentrations around the K_d value ca 5% (**135**) and ca 2% (**136**) of total binding) and unaffected K_d values (*cf.* Figure 10C and 10D). The disadvantage of the washing step is the loss of equilibrium conditions, however, as the fluorescent ligands exhibit low off rates (cf. Figure 7B), the fraction of dissociated ligand during the washing step is marginal.

The K_d values obtained by high content imaging were slightly higher than the K_i values (1.4 nM for **135** and 0.76 nM for **136**) derived from radioligand competition binding experiments with [^{3}H]NMS at the M_2R, as well as compared to K_d values (2.4 nM for **135** and 1.0 nM for **136**) obtained from saturation binding using flow cytometry. This deviation might be caused by the strong adsorption of the fluorescent ligands to the plates used for high-content imaging, leading to a decrease in the concentration of 'free' fluorescent ligand. Figure 11 shows representative images acquired with the IX Ultra plate reader after incubation with the fluorescent ligand **136** (c = 10 nM) for 60 min followed by a washing step at M_2R. A clear difference between total and unspecific binding of **136** was observed. K_i and K_d values of **135** and **136** are summarized in Table 5.

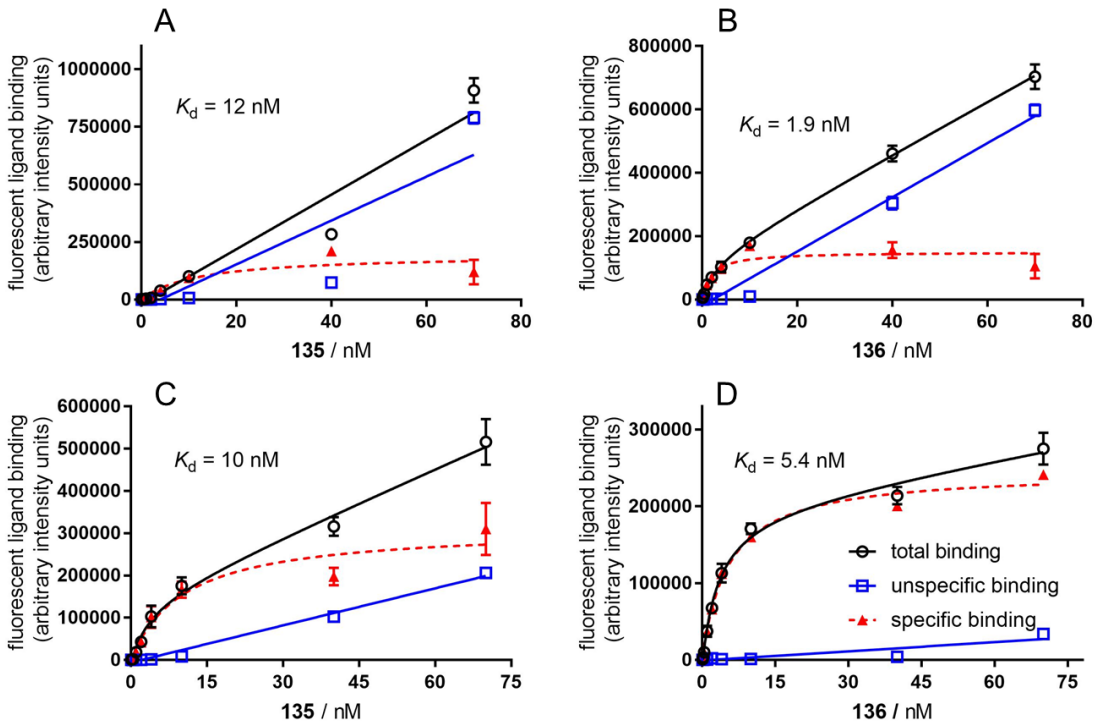

Figure 10. Representative saturation isotherms (specific binding, dashed line) of **135** and **136** obtained from high-content imaging saturation binding experiments at intact CHO-hM_2 cells. (A) (B) Cells were incubated with the fluorescent ligand at 22 °C in the dark for 1 h and directly imaged. Unspecific binding was determined in the presence of atropine (1 µM). (C) (D) Cells were incubated with the fluorescent ligand at 22 °C in the dark for 1 h, plates were washed with HBSS+0.1% BSA before acquisition of the images. Unspecific binding was determined in the presence of atropine (500-fold excess). Experiments were performed in triplicate. Measurements were performed with an IX Ultra Confocal Plate Reader (Molecular Devices). Specific binding data were analyzed by an equation describing one-site (monophasic) binding. Error bars of specific binding represent propagated errors calculated according to the Gaussian law of errors. Error bars of total and unspecific binding represent the SEM (n = 3).

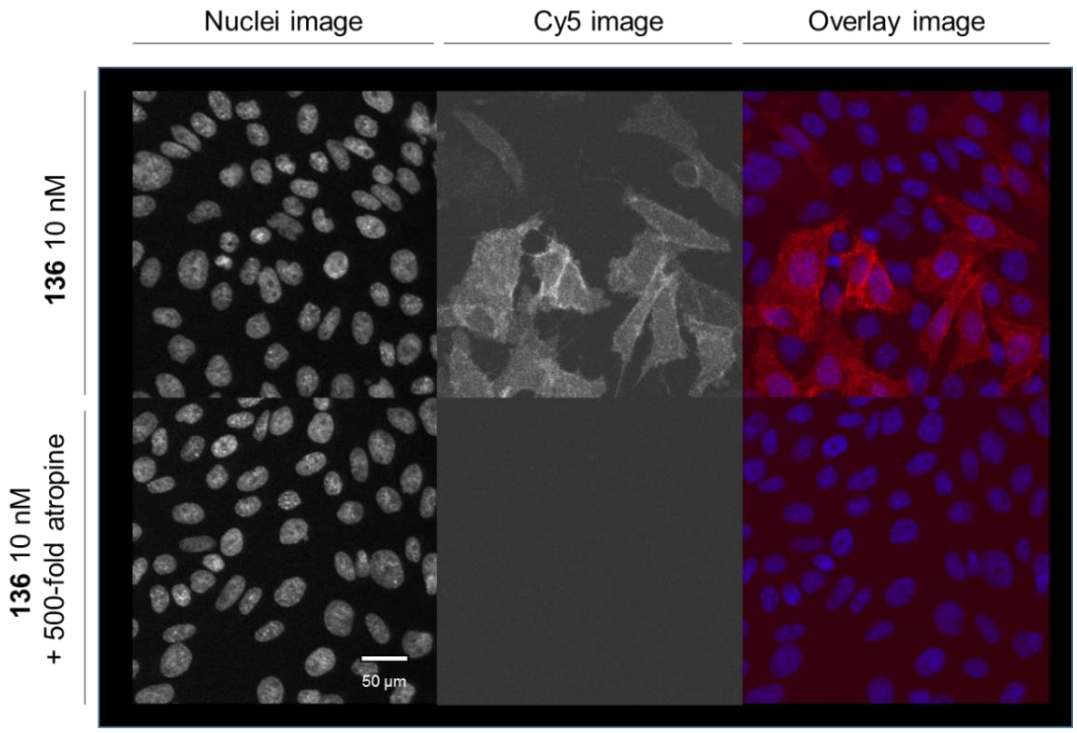

Figure 11. Binding of the fluorescent ligand **136** (c = 10 nM) to live CHO-hM_2 cells investigated by high-content imaging. Images (400 x 400 pixels from original 1000 x 1000 acquisition) were acquired with an IX Ultra platereader after 60 min of incubation in the dark at 22 °C from one of saturation binding experiments performed with **136**. The cells were washed with HBSS+0.1% BSA before imaging. Unspecific binding of **136** was determined in the presence of 500-fold excess of atropine (lower panel). Presented are Hoechst-33342-stained nuclei in greyscale (left), the fluorescence detected in the Cy5 channel in greyscale (centre), and the overlay (right).

Table 5. Comparison of M_2R binding data of **135** and **136**.

Compound	K_i [nM][a]	K_d [nM][b]	K_d [nM][c]	K_d [nM][d]
135	1.4 ± 0.2	2.4 ± 0.6	13 ± 2.5	8.9 ± 1.2
136	0.76 ± 0.11	1.0 ± 0.2	4.8 ± 1.5	3.9 ± 0.78

[a]K_i values taken from Table 1. [b]Dissociation constant from flow cytometric saturation binding studies at live CHO-hM_2 cells; mean ± SEM from three independent experiments (performed in duplicate). [c]Dissociation constant from high-content imaging saturation binding studies at live CHO-hM_2 cells (without performing washing step); mean ± SEM from three independent experiments (performed in triplicate). [d]Dissociation constant from high-content imaging saturation binding studies at live CHO-hM_2 cells (washing step was applied); mean ± SEM from three independent experiments (performed in triplicate).

4.2.6.2. Competition binding.

Ligands **135** and **136** were used as fluorescent probes to study of a range of known muscarinic receptor ligands (including orthosteric antagonist **6** and **7**, orthosteric agonist **2** and **3**, allosteric modulators **14**, **15** and **16**). CHO-hM_2 cells were grown in 96-well plates and incubated with **135** or **136** (fixed concentration, 10 nM) and **2**, **3**, **6**, **7**, **14**, **15** or **16** at increasing concentrations at room temperature for 1 h. Images were directly acquired with the

ImageXpress (IX) Ultra plate reader after incubation without washing. Representative images, obtained from competition binding of **136** with **2**, **6** or **7** are depicted in Figure 12A. Competition binding curves were generated using the mean of arbitrary intensity units from each well (*cf*. Figure 12B and 12C), and K_i values were calculated using the Cheng-Prusoff equation, using the K_d values (8.9 nM for **135** and 3.9 nM for **136**) determined in high-content imaging saturation binding studies (*cf*. Table 5). All the orthosteric ligands **2**, **3**, **6** or **7** investigated were capable of totally inhibiting (displacing) specific M_2R binding of ligands **135** and **136**, which suggested a competitive-like mode between the studied compounds and the fluorescent labeled ligands at the orthosteric receptor site. Moreover, the allosteric modulators **14**, **15** and **16** also fully displaced **136** from the M_2 receptor. In the case of using **136** as the fluorescent probe, the K_i values of **2**, **7**, **14**, **15** and **16** (*cf*. Table 6) correlated well with the K_i values obtained from flow cytometric competition binding studies (*cf*. Table 4). However, when using **135** as fluorescent probe, the K_i values obtained for **2**, **6** and **7** were slightly higher (ca 3-fold) than the K_i values obtained from competition binding experiments with **136**. The binding constants (K_i values) of several MR ligands obtained in these experiments are shown in Table 6.

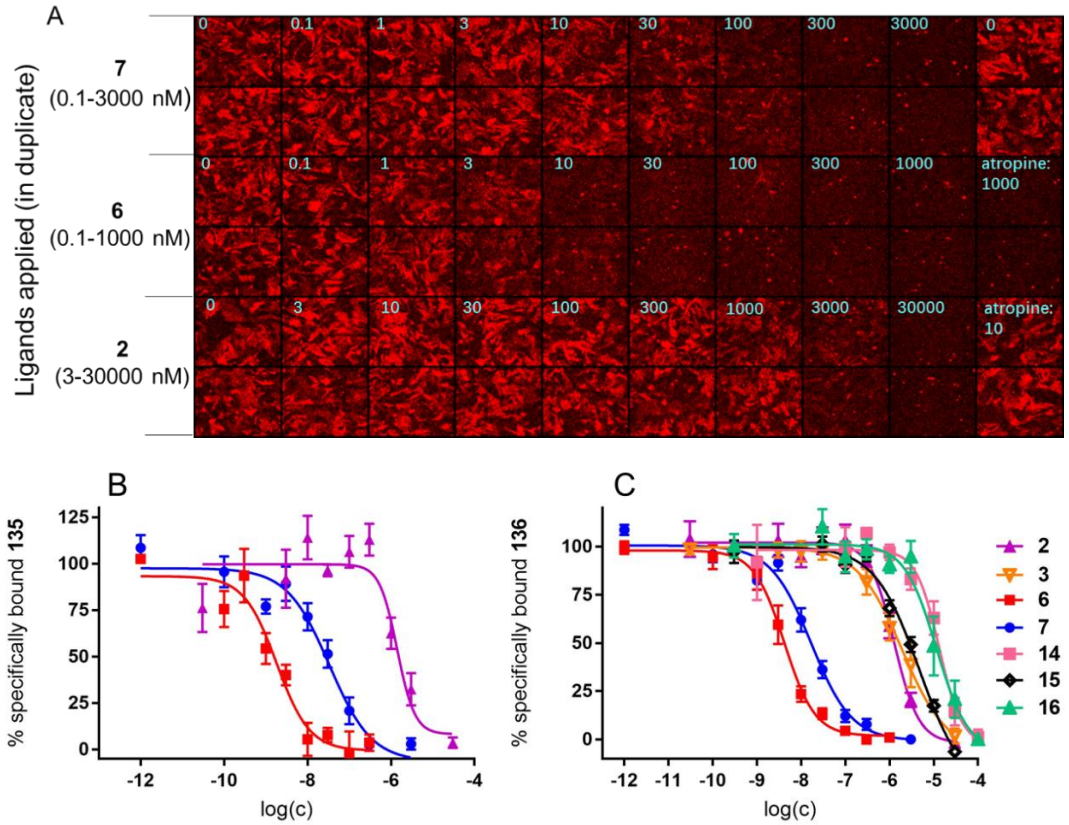

Figure 12. (A) Representative thumbnail fluorescence images acquired with an IX Ultra plate reader of a high-content imaging competition binding assay performed with the fluorescent ligand **136** (c = 10 nM) and **2**, **6** or **7** at live CHO-hM_2 cells in a 96-well plate. Each image from one well represents an area 400 x 400 µm. (B) Concentration-dependent effects of the orthosteric MR ligands **2**, **6** or **7** on M_2R equilibrium binding of **135** determined at intact CHO-hM_2 cells using high-content imaging. (C) Concentration-dependent effects of various reported orthosteric (**2**, **3**, **6** or **7**), allosteric (**14**-**16**) MR

ligands on equilibrium binding of **136** determined at intact CHO-hM_2 cells using high-content imaging.

Table 6. Comparison of M_2R binding data (K_i or IC_{50} values) of various orthosteric (**2**, **3**, **6** and **7**), allosteric (**14**-**16**) MR ligands determined with **135**, **136** or [^{3}H]NMS.

Compound	**135** K_i [nM][a]	**136** K_i [nM][a]	[^{3}H]NMS K_i^* or IC_{50}^{**} [nM]
2	950 ± 220	360 ± 26	210 ± 59*[b]
3	-	800 ± 330	9300*[c]
6	2.6 ± 1.4	0.69 ± 0.14	0.2*[d]
7	15 ± 4.8	4.8 ± 0.92	0.94 ± 0.19*[b]
14	-	3900 ± 760	2200 ± 410**[e]
15	-	1000 ± 130	460 ± 130**[e]
16	-	5000 ± 1000	>10000**[e]

[a]Determined by high-content imaging equilibrium binding studies with **135** (c = 10 nM) or **136** (c = 10 nM) in the presence of increasing concentrations of the respective MR ligand at live CHO-hM_2 cells; mean ± SEM from three independent experiments (performed in duplicate). [b]K_i values taken from Table 4. [c]Jakubík *et al.*[45]. [d]Dei *et al.*[46]. [e]IC_{50} values obtained from nonlinear four-parameter logistic curve analyses of data characterizing the inhibition of [^{3}H]NMS (c = 0.2 nM) equilibrium binding at live CHO-hM_2 cells; mean ± SEM from at least three independent experiments (performed in triplicate).

4.2.6.3. Study of the effect of the allosteric modulator 15 on saturation binding of fluorescent ligand 136.

A series of saturation binding experiments to investigate the effect of the allosteric modulator **15** on the M_2R saturation binding properties of fluorescent ligand **136** was also performed using high content imaging. Figure 13 shows the curves of saturation binding of **136** in the absence or presence of varied concentrations (0.3, 1, 2 and 3 µM) of **15** performed at CHO-hM_2 cells. The results were comparable with the results obtained from the same type of experiment performed using flow cytometry. The presence of **15** led to a parallel rightward shift of the saturation isotherms of ligand **136**. The slope of the linear 'Schild' regression was not different from unity (slope = 0.93 ± 0.11 (n = 3), P > 0.5), suggesting again a competitive interaction between ligand **136** and **15**. The 'pA_2' value of **15** derived from the 'Schild' regression ('pA_2' = 6.80, Figure 13) was in good agreement with the 'pA_2' value obtained from the flow cytometry-based 'Schild' analysis ('pA_2' = 7.27, Figure 9).

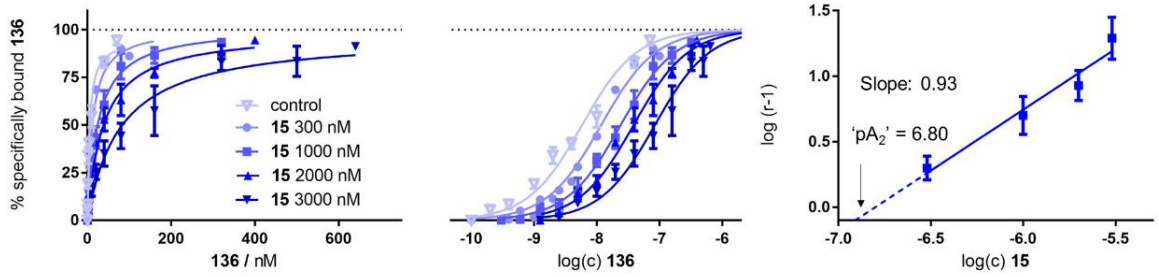

Figure 13. Saturation binding of **136** in the presence of increasing concentrations of **15**. Presented are saturation isotherms of specific binding of **136** to the M_2R in linear scale (left) and semi-logarithmic

scale (middle), as well as the "Schild" regressions (right) resulting from the rightward shifts (ΔpK_d) of the saturation isotherms (log(r-1) plotted *vs*. log(concentration **15**), where $r = 10^{\Delta pKd}$). The presence of the allosteric modulator **15** led to a parallel rightward shift of the saturation isotherms of **136**. The slope of the linear "Schild" regression was not different from unity ($P > 0.5$, assessed based on the slope mean value ± SEM (0.93 ± 0.11) from three sets of independent saturation binding experiments) indicating a competitive interaction between **136** and **15**. Data represent mean values ± SEM from three independent experiments (performed in triplicate).

4.2.7. Application of the fluorescent ligand 136 to confocal microscopy

The fluorescent ligand **136** was also applied in confocal microscopy using live CHO-hM_2R cells. As shown in Figure 14, a clear difference between the total and unspecific binding of **136** (30 nM) to CHO-hM_2R cells was detected by confocal microscopy after different incubation times (5-45 min). Unspecific binding of **136** was determined in the presence of the MR antagonist atropine (10 µM; Figure 14A vs. 14B). The major fraction of fluorescence appeared to be associated to the cell membrane. An increase in intracellular fluorescence was not observed over time.

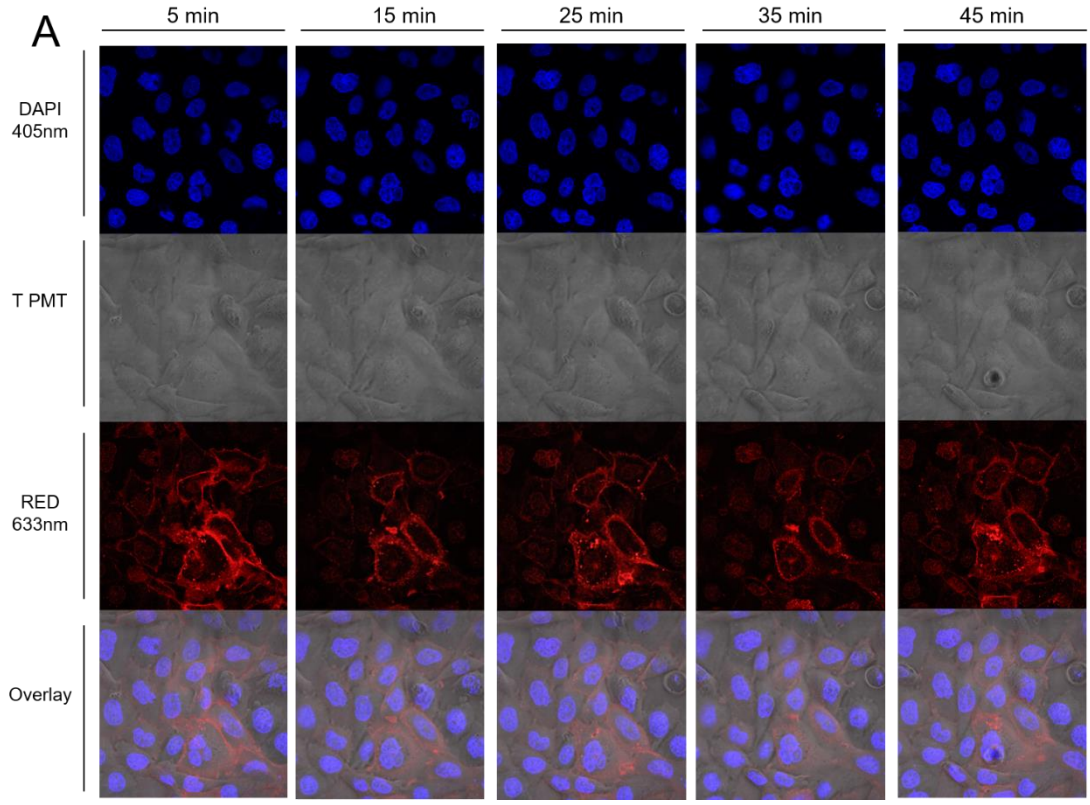

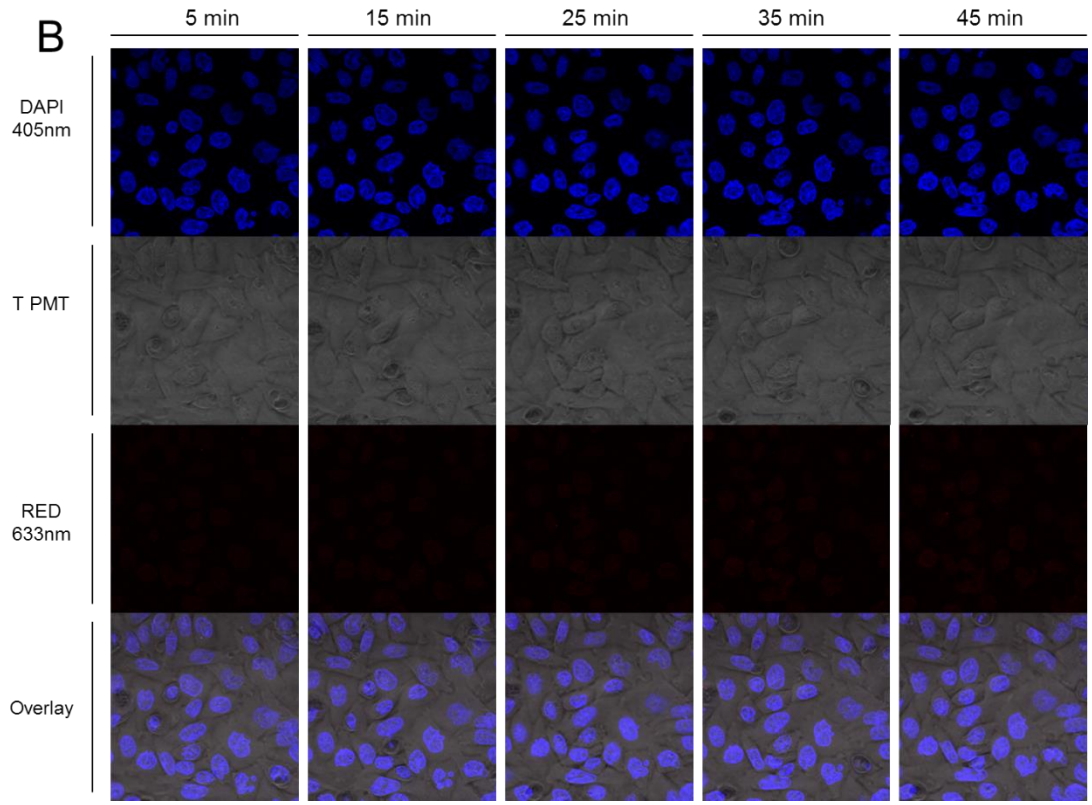

Figure 14. Binding of the fluorescent ligand **136** to CHO-hM_2R cells at 30 °C, visualized by confocal microscopy after 5, 15, 25, 35 and 45 min. (A) Total binding of **136** (30 nM). (B) Unspecific binding of **136** (30 nM) determined in the presence of atropine (10 µM). Images were acquired with a Zeiss LSM710 confocal microscope.

4.3. Conclusion

This work represents the first report on fluorescently labeled dibenzodiazepinone-type M_2 subtype-preferring MR ligands. The dibenzodiazepinone scaffold was linked to fluorophores via two different linkers with respect to lengths and chemical nature (non-basic vs. basic), yielding seven fluorescent ligands. Six of these fluorescent probes exhibited high M_2R affinity (K_i < 55 nM). Variations of the chemical structure of the fluorophores had less impact on M_2R affinity than the type of the linker. The attachment of the cyanine dyes S0436 and S0387 through a linker containing a piperazine moiety yielded the fluorescent ligands with the highest affinity (**135** and **136**: K_i ≈ 1 nM) at M_2R. Application of **135** and **136** to flow cytometry and high content imaging proved that these new fluorescent probes are suited for such techniques. The fluorescent ligand **136** was identified as a valuable, non-radiolabeled pharmacological tool for the determination of MR affinities of MR ligands. M_2R binding studies with **136** in the presence of allosteric modulators strongly suggested that **136** and structurally related ligands bind simultaneously to both the orthosteric (through the dibenzodiazepinone scaffold) and the 'common' allosteric binding site (most likely through the fluorophores) of the M_2R (dualsteric

binding mode). Owing to the low M_2R selectivity, the fluorescent ligand **136** represents a potential fluorescent probe for binding studies at the M_1R and M_4R as well, which was supported by saturation binding studies at the M_1R and M_4R revealing K_d values of 6.5 and 8.9 nM, respectively. Moreover, this work suggests that anchoring an allosteric moiety (here mimicked by the fluorophore) through a linker to the dibenzodiazepinone scaffold might be a promising perspective to develop selective M_2R antagonists according to the dualsteric ligand approach[31, 47-49].

4.4. Experimental section

4.4.1. General experimental conditions

Acetonitrile for HPLC (gradient grade) was obtained from Merck (Darmstadt, Germany). Millipore water was used throughout for the preparation of stock solutions, buffers and HPLC eluents. Bovine serum albumin (BSA) was from Serva (Heidelberg, Germany). DMF, trimethylamine and trifluoroacetic acid were obtained from (Sigma-Aldrich (Deisenhofen, Germany), and N,N-diisopropylethylamine (DIPEA) (99%) was purchased from ABCR (Karlsruhe, Germany). The pyrylium dye Py-5 was synthesized by Mengya Chen in our research group as part of her master thesis. The succinimidyl esters of the fluorescent dyes S0223 (equates to S2197), S0536 (S0436-NHS) and S0586 (S0387-NHS) were obtained from FEW Chemicals (Bitterfeld-Wolfen, Germany). [^{3}H]N-methylscopolamine ([^{3}H]NMS) (specific activity = 80 Ci/mmol) was purchased from American Radiolabeled Chemicals Inc. (St. Louis, MO) via Hartman Analytics GmbH (Braunschweig, Germany). Atropine, N-methylscopolamine (NMS), W84 and gallamine were purchased from Sigma-Aldrich (Deisenhofen, Germany). Oxotremorine sesquifumarate was from MP Biomedicals (Eschwege, Germany). LY2119620 was from Absource Diagnostic (Munich, Germany) and AF-DX 384 was purchased from Abcam (Cambridge, UK). Xanomeline (**2**) was prepared according to described procedures[50] (purity = 97%). Compound **11** was prepared in our lab according to a reported protocol[44]. Polypropylene reaction vessels (1.5 mL) with screw cap (Süd-Laborbedarf, Gauting, Germany) were used for the synthesis of fluorescent ligands, for the investigation of chemical stabilities (**136**) and for the preparation and storage of stock solutions. ^{1}H-NMR spectra were recorded on a Bruker Avance 600 (^{1}H: 600 MHz) (Bruker, Karlsruhe, Germany) with TMS as external standard. High-resolution mass spectrometry (HRMS) analysis was performed on an Agilent 6540 UHD Accurate-Mass Q-TOF LC/MS system (Agilent Technologies, Santa Clara, CA) using an ESI source. Preparative HPLC was performed on a system from Knauer (Berlin, Germany) consisting of two K-1800 pumps and a K-2001 detector. A Kinetex-XB C18, 5 µm, 250 mm × 21 mm (Phenomenex, Aschaffenburg, Germany) served as stationary phase at a

flow-rate of 15 mL/min using mixtures of acetonitrile and 0.1% aq TFA as mobile phase. A detection wavelength of 220 nm was used throughout. Lyophilisation of the collected fractions was performed with an Alpha 2-4 LD apparatus (Martin Christ, Osterode am Harz, Germany) equipped with a RZ 6 rotary vane vacuum pump (Vacuubrand, Wertheim, Germany). Analytical HPLC analysis was performed on a system from Merck-Hitachi (Hitachi, Düsseldorf, Germany) composed of a L-6200-A pump, an AS-2000A autosampler, a L-4000A UV detector, a D-6000 interface. A Kinetex-XB C18, 5 µm, 250 mm × 4.6 mm (Phenomenex, Aschaffenburg, Germany) was used as stationary phase at a flow rate of 0.8 mL/min. Mixtures of acetonitrile (A) and 0.1% aq TFA (B) were used as mobile phase (degassed by Helium purging). The following linear gradient was applied: 0-30 min: A/B 5:95-85:15, 30-32 min: 85:15-95:5, 32-40 min: 95:5. Detection was performed at 220 nm throughout. The oven temperature was 30 °C. The stock solutions (concentrations: 1, 5 or 10 mM) of fluorescent ligands were prepared in DMSO/H_2O (1:1 v/v) and were stored at -80 °C.

The fluorescent ligands were characterized by ^{1}H-NMR spectroscopy, HRMS, and RP-HPLC analysis. The purity (RP-HPLC, detection at 220 nm) of the fluorescent ligands amounted to >96%. Annotation concerning the ^{1}H-NMR spectra of the fluorescent ligands (**130**-**136**): due to a slow rotation about the exocyclic amide group on the NMR time scale, two isomers (ratios provided in the experimental protocols) were evident in the ^{1}H-NMR spectra.

4.4.2. Chemistry: experimental protocols and analytical data

4-((1*E*,3*E*)-4-(4-(Dimethylamino)phenyl)buta-1,3-dien-1-yl)-2,6-dimethyl-1-(4-(1-(2-oxo-2-(11-oxo-10,11-dihydro-5*H*-dibenzo[*b*,*e*][1,4]diazepin-5-yl)ethyl)piperidin-4-yl)butyl)pyridin-1-ium hydrotrifluoroacetate trifluoroacetate (130)

The reaction was carried out in a 1.5-mL eppendorf reaction vessel equipped with a micro stir bar. Compound **10** (2.0 mg, 4.92 µmol) and triethylamine (4.98 mg, 6.8 µL, 49.2 µmol) were dissolved in anhydrous DMF (300 µL) followed by the addition of Py-5 × 1 BF_4^- (**123**) (5.4 mg, 14.8 µmol) in anhydrous DMF (120 µL) and stirring at room temperature in the dark for 2 h. 10% aq TFA (corresponding to 49.2 µmol of TFA) were added. Purification of the product by preparative HPLC (column: Kinetex XB-C18 5 µm 250 × 21 mm; gradient: 0-30 min: MeCN/0.1% aq TFA 5:95-62:38, t_R = 22 min). afforded **130** as a red solid (0.91 mg, 21%). Ratio of configurational isomers evident in the NMR spectra: ca 1.5:1. ^{1}H-NMR (600 MHz, MeOH-d_4): δ (ppm) 1.38-1.44 (m, 2H), 1.46-1.61 (m, 4H), 1.79-1.85 (m, 2H), 1.92-2.06 (m, 2H), 2.78 (s, 6H), 2.88-2.99 (m, 1H), 3.02 (s, 6H), 3.18-3.19 (m, 1H), 3.40-3.42 (m, 1H), 3.42-3.52 (m, 1H), 3.68-3.85 (m, 2H), 4.33-4.37 (m, 2H), 4.40 (d, *J* 18 Hz, 0.6H), 4.43 (d, *J* 18 Hz, 0.4H), 6.57 (d, *J* 18 Hz, 1H), 6.76 (d, *J* 12 Hz, 2H), 6.92-7.01 (m, 2H), 7.25-7.40 (m, 3H), 7.43 (d, *J* 12 Hz,

2H), 7.47-7.54 (m, 2H), 7.61-7.67 (m, 2H), 7.68-7.76 (m, 3H), 7.90-7.91 (m, 0.6H), 7.97-7.98 (m, 0.4H). RP-HPLC (220 nm): 98% (t_R = 19.4 min, k = 5.8). HRMS (ESI): m/z $[M]^+$ calcd. for $[C_{43}H_{50}N_5O_2]^+$: 668.3959, found: 668.3963. $C_{43}H_{50}N_5O_2^+ \cdot C_4HF_6O_4^-$ (668.91 + 227.04).

2-((1*E*,3*E*)-5-((*E*)-3,3-Dimethyl-1-(6-oxo-6-((4-(1-(2-oxo-2-(11-oxo-10,11-dihydro-5*H*-dibenzo[*b*,*e*][1,4]diazepin-5-yl)ethyl)piperidin-4-yl)butyl)amino)hexyl)indolin-2-ylidene)penta-1,3-dien-1-yl)-1,3,3-trimethyl-3*H*-indol-1-ium hydrotrifluoroacetate trifluoroacetate (131)

Compound **131** was prepared from **10** (2.2 mg, 5.42 µmol) and S2197 (2.4 mg, 3.63 µmol) according to the procedure for the synthesis of **130**, but DIPEA (4.69 mg, 6.3 µL, 36.3 µmol) was used instead of triethylamine. Purification by preparative HPLC (column: Kinetex XB-C18 5 µm 250 × 21 mm; gradient: 0-30 min: MeCN/0.1% aq TFA 5:95-90.5:9.5, t_R = 22 min) afforded the product as a blue solid (1.62 mg, 40%). Ratio of configurational isomers evident in the NMR spectra: ca 1.5:1. ^{1}H-NMR (600 MHz, MeOH-d_4): δ (ppm) 1.25-1.35 (m, 5H), 1.42-1.47 (m, 4H),1.47-1.52 (m, 1H), 1.63-1.69 (m, 2H), 1.69 (s, 12H), 1.78-1.84 (m, 2H), 1.85-1.98 (m, 2H), 2.17 (t, *J* 6.0 Hz, 2H), 2.84-2.93 (m, 1H), 2.98-3.04 (m, 1H), 3.11 (t, *J* 6.0 Hz, 2H), 3.18-3.19 (m, 0.5H), 3.31-3.33 (m, 1H), 3.41-3.42 (m, 1H), 3.42-3.44 (m, 0.5H), 3.61 (s, 3H), 3.68-3.74 (m, 1H), 4.08 (t, *J* 12 Hz, 2H), 4.37 (d, *J* 18 Hz, 0.6H), 4.41 (d, *J* 18 Hz, 0.4H), 6.26 (d, *J* 12 Hz, 2H), 6.60 (t, *J* 12 Hz, 1H), 7.24-7.35 (m, 6H), 7.36-7.53 (m, 7H), 7.60-7.64 (m, 1H), 7.67-7.76 (m, 1H), 7.89-7.90 (m, 0.6H), 7.95-7.97 (m, 0.4H), 8.21-8.26 (m, 2H). RP-HPLC (220 nm): 97% (t_R = 25.9 min, k = 8.0). HRMS (ESI): m/z $[M]^+$ calcd. for $[C_{56}H_{67}N_6O_3]^+$: 871.5269, found: 871.5265. $C_{56}H_{67}N_6O_3^+ \cdot C_4HF_6O_4^-$ (872.19 + 227.04).

4-(2-((1*E*,3*E*)-5-((*E*)-3,3-Dimethyl-1-(6-oxo-6-((4-(1-(2-oxo-2-(11-oxo-10,11-dihydro-5*H*-dibenzo[*b*,*e*][1,4]diazepin-5-yl)ethyl)piperidin-4-yl)butyl)amino)hexyl)indolin-2-ylidene)penta-1,3-dien-1-yl)-3,3-dimethyl-3*H*-indol-1-ium-1-yl)butane-1-sulfonatedi(hydrotrifluoroacetate) (132)

Compound **132** was prepared from **10** (1.9 mg, 4.67 µmol) and S0536 (2.2 mg, 3.14 µmol) according to the procedure for the synthesis of **130**, but DIPEA (4.05 mg, 5.5 µL, 31.3 µmol) was used instead of triethylamine. Purification by preparative HPLC (column: Kinetex 5µ-XB-C18 250 × 21 mm; gradient: 0-30 min: MeCN/0.1% aq TFA 5:95-90.5:9.5, t_R = 19 min) afforded the product as a blue solid (1.43 mg, 37%). Ratio of configurational isomers evident in the NMR spectra: ca 1.5:1. ^{1}H-NMR (600 MHz, MeOH-d_4): δ (ppm) 1.26-1.35 (m, 5H), 1.43-1.47 (m, 4H), 1.48-1.54 (m, 2H), 1.64-1.69 (m, 2H), 1.71 (s, 6H), 1.72 (s, 6H), 1.77-1.84 (m, 2H), 1.84-1.89 (m, 1H), 1.92-1.99 (m, 4H), 2.18 (t, *J* 6.0 Hz, 2H), 2.88-2.95 (m, 2H), 3.02-3.06 (m, 1H), 3.13 (t, *J* 6.0 Hz, 2H), 3.18-3.19 (m, 0.5H), 3.31-3.32 (m, 1H), 3.41-3.42 (m, 0.5H), 3.43-3.46 (m, 1H), 3.66-3.80 (m, 2H), 4.08 (t, *J* 6.0 Hz, 2H), 4.10-4.16 (m, 2H), 4.37 (d, *J* 18 Hz,

0.6H), 4.43 (d, *J* 18 Hz, 0.4H), 6.25 (d, *J* 18 Hz, 1H), 6.33-6.36 (m, 1H), 6.60-6.66 (m, 1H), 7.19-7.27 (m, 4H), 7.31-7.35 (m, 2H), 7.36-7.41 (m, 2H), 7.41-7.54 (m, 5H), 7.59-7.65 (m, 1H), 7.66-7.75 (m, 1H), 7.88-7.89 (m, 0.6H), 7.94-7.96 (m, 0.4H), 8.19-8.24 (m, 2H). RP-HPLC (220 nm): 96% (t_R = 24.2 min, k = 7.4). HRMS (ESI): m/z [*M*+H]$^+$ calcd. for [$C_{59}H_{73}N_6O_6S$]$^+$: 993.5307, found: 993.5317. $C_{59}H_{72}N_6O_6S \cdot C_4H_2F_6O_4$ (993.32 + 228.05).

4-((1*E*,3*E*)-4-(4-(Dimethylamino)phenyl)buta-1,3-dien-1-yl)-2,6-dimethyl-1-(2-(4-(4-(1-(2-oxo-2-(11-oxo-10,11-dihydro-5*H*-dibenzo[*b*,*e*][1,4]diazepin-5-yl)ethyl)piperidin-4-yl)butyl)piperazin-1-yl)ethyl)pyridin-1-ium tris(hydrotrifluoroacetate) trifluoroacetate (133)

Compound **133** was prepared from **96** (3.0 mg, 3.08 µmol), Py-5 × 1BF^{4-} (3.65 mg, 9.90 µmol) and triethylamine (5.36 mg, 7.4 µL, 52.9 µmol) according to the procedure for the synthesis of **130**. Purification of the product by preparative HPLC (column: Kinetex XB-C18 5 µm 250 × 21 mm; gradient: 0-30 min: MeCN/0.1% aq TFA 20:80-64:36, t_R = 12 min) afforded the product as a red solid (1.31 mg, 34%). Ratio of configurational isomers evident in the NMR spectra: ca 1.5:1. ^{1}H-NMR (600 MHz, MeOH-d_4): (ppm) δ 1.27-1.31 (m, 4H), 1.35-1.38 (m, 1H), 1.45-1.63 (m, 1H), 1.65-1.77 (m, 2H), 1.86-1.99 (m, 2H), 2.00-2.02 (m, 1H), 2.13-2.22 (m, 1H), 2.59 (t, *J* 12 Hz, 2H), 2.82 (s, 6H), 2.88-2.97 (m, 3H), 3.02 (s, 6H), 3.06-3.16 (m, 4H), 3.17-3.18 (m, 1H), 3.41-3.42 (m, 1H), 3.43-3.47 (m, 1H), 3.53-3.56 (m, 2H), 3.67-3.80 (m, 2H), 4.38 (d, *J* 18 Hz, 0.6H), 4.42 (d, *J* 18 Hz, 0.4H), 4.55 (t, *J* 6.0 Hz, 2H), 6.57 (d, *J* 18 Hz, 1H), 6.75 (d, *J* 6.0 Hz, 2H), 6.92-7.03 (m, 2H), 7.24-7.40 (m, 3H), 7.43 (d, *J* 6.0 Hz, 2H), 7.46-7.54 (m, 2H), 7.51-7.70 (m, 3H), 7.72-7.75 (m, 2H), 7.88-7.93 (m, 0.6H), 7.96-7.98 (m, 0.4H). RP-HPLC (220 nm): 98% (t_R = 16.6 min, k = 4.8); HRMS (ESI): m/z [*M*]$^+$ calcd. for [$C_{49}H_{62}N_7O_2$]$^+$: 780.4960, found: 780.4961. $C_{49}H_{62}N_7O_2^+ \cdot C_8H_3F_{12}O_8^-$ (781.08 + 456.09).

2-((1*E*,3*E*)-5-((*E*)-3,3-Dimethyl-1-(6-oxo-6-((2-(4-(4-(1-(2-oxo-2-(11-oxo-10,11-dihydro-5*H*-dibenzo[*b*,*e*][1,4]diazepin-5-yl)ethyl)piperidin-4-yl)butyl)piperazin-1-yl)ethyl)amino)hexyl)indolin-2-ylidene)penta-1,3-dien-1-yl)-1,3,3-trimethyl-3*H*-indol-1-ium tris(hydrotrifluoroacetate) trifluoroacetate (134)

Compound **134** was prepared from **96** (5.8 mg, 5.95 µmol) and S2197 (3.0 mg, 4.54 µmol) according to the procedure for the synthesis of **130**, but DIPEA (5.87 mg, 7.9 µL, 45.3 µmol) was used instead of trimethylamine and the incubation time period was 1 h instead of 2 h. Purification by preparative HPLC (column: Kinetex XB-C18 5 µm 250 × 21 mm; gradient: 0-30 min: MeCN/0.1% aq TFA 5:95-90.5:9.5, t_R = 19 min) afforded the product as a blue solid (2.06 mg, 31%). Ratio of configurational isomers evident in the NMR spectra: ca 1.5:1. ^{1}H-NMR (600 MHz, MeOH-d_4): δ (ppm) 1.28-1.40 (m, 5H), 1.42-1.57 (m, 5H), 1.57-1.69 (m, 4H), 1.72 (s, 12H), 1,77-1.85 (m, 2H), 1.85-2.02 (m, 2H), 2.21 (t, *J* 6.0 Hz, 2H), 2.63-2.65 (m, 2H),

2.81-2.97 (m, 2H), 2.98-3.05 (m, 3H), 3.18-3.20 (m, 2H), 3.31-3.36 (m, 5H), 3.38-3.50 (m, 2H), 3.62 (s, 3H), 3.66-3.79 (m, 2H), 4.09 (t, *J* 6.0 Hz, 2H), 4.39 (d, *J* 18 Hz, 0.6H), 4.40-4.45 (d, *J* 18 Hz, 0.4H), 6.26 (d, *J* 12 Hz, 2H), 6.59-6.63 (m, 1H), 7.23-7.32 (m, 5H), 7.32-7.43 (m, 3H), 7.46-7,54 (m, 4H), 7.61-7.65 (m, 2H), 7.67-7.76 (m, 1H), 7.89-7.90 (m, 0.6H), 7.96-7.97(m, 0.4H), 8.21-8.26 (m, 2H). RP-HPLC (220 nm): 97% (t_R = 21.9 min, k = 6.6). HRMS (ESI): m/z $[M]^+$ calcd. for $[C_{62}H_{79}N_8O_3]^+$: 983.6270, found: 983.6275. $C_{62}H_{79}N_8O_3^+ \cdot C_8H_3F_{12}O_8^-$ (984.37 + 455.09).

4-(2-((1*E*,3*E*)-5-((*E*)-3,3-Dimethyl-1-(6-oxo-6-((2-(4-(4-(1-(2-oxo-2-(11-oxo-10,11-dihydro-5*H*-dibenzo[*b*,*e*][1,4]diazepin-5-yl)ethyl)piperidin-4-yl)butyl)piperazin-1-yl)ethyl)amino)hexyl)indolin-2-ylidene)penta-1,3-dien-1-yl)-3,3-dimethyl-3*H*-indol-1-ium-1-yl)butane-1-sulfonatetetrakis(hydrotrifluoroacetate) (135)

Compound **135** was prepared from **96** (3.72 mg, 3.81 µmol) and S0536 (2.4 mg, 3.42 µmol) according to the procedure for the synthesis of **130**, but DIPEA (4.42 mg, 5.9 µL, 34.2 µmol) was used instead of trimethylamine and the incubation time period was 1 h instead of 2 h. Purification by preparative HPLC (column: Kinetex XB-C18 5 µm 250 × 21 mm; gradient: 0-30 min: MeCN/0.1% aq TFA 5:95-90.5:9.5, t_R = 18 min) afforded the product as a blue solid (1.59 mg, 30%). Ratio of configurational isomers evident in the NMR spectra: ca 1.5:1.^{1}H-NMR (600 MHz, MeOH-d_4): δ (ppm) 1.28-1.42 (m, 5H), 1.42-1.61 (m, 5H), 1.67-1.71 (m, 4H), 1.71 (s, 6H), 1.72 (s, 6H), 1.73-1.75 (m, 1H), 1.79-1.84 (m, 2H), 1.88-1.92 (m, 2H), 1.93-2.00 (m, 5H), 2.23 (t, *J* 6.0 Hz, 2H), 2.63-2.76 (m, 2H), 2.78-2.98 (m, 3H), 3.02-3.07 (m, 3H), 3.18-3.19 (m, 0.5H), 3.30-3.32 (m, 3H), 3.33-3.37 (m, 3H), 3.41-3.42 (m, 0.5H), 3.43-3.45 (m, 1H), 3.69-3.79 (m, 2H), 4.09 (t, *J* 6.0 Hz, 2H), 4.12-4.17 (m, 2H), 4.38 (d, *J* 18 Hz, 0.6H), 4.42 (d, *J* 18 Hz, 0.4H), 6.27 (d, *J* 18 Hz, 1H), 6.34 (d, *J* 12 Hz, 1H), 6.61-6.67 (m, 1H), 7.25-7.29 (m, 4H), 7.31-7.34 (m, 2H), 7.35-7.43 (m, 3H), 7.44-7.55 (m, 4H), 7.59-7.65 (m, 1H), 7.67-7.76 (m, 1H), 7.88-7.90 (m, 0.6H), 7.96-7.97 (m, 0.4H), 8.19-8.26 (m, 2H). RP-HPLC (220 nm): 96% (t_R = 21.3 min, k = 6.4). HRMS (ESI): m/z $[M+H]^+$ calcd. for $[C_{65}H_{85}N_8O_6S]^+$: 1105.6307, found: 1105.6309. $C_{65}H_{84}N_8O_6S \cdot C_8H_4F_{12}O_8$ (1105.50 + 456.09).

(*E*)-2-((2*E*,4*E*)-5-(3,3-Dimethyl-1-(4-sulfonatobutyl)-3H-indol-1-ium-2-yl)penta-2,4-dien-1-ylidene)-3,3-dimethyl-1-(6-oxo-6-((2-(4-(4-(1-(2-oxo-2-(11-oxo-10,11-dihydro-5*H*-dibenzo[*b*,*e*][1,4]diazepin-5-yl)ethyl)piperidin-4-yl)butyl)piperazin-1-yl)ethyl)amino)hexyl)indoline-5-sulfonate trakis(hydrotrifluoroacetate) (136)

Compound **136** was prepared from **96** (4.46 mg, 4.58 µmol) and S0586 (2.3 mg, 2.94 µmol) according to the procedure for the synthesis of **130**, but DIPEA (4.24 mg, 5.7 µL, 32.8 µmol) was used instead of trimethylamine and the incubation time period was 1 h instead of 2 h. Purification by preparative HPLC (column: Kinetex XB-C18 5 µm 250 × 21 mm; gradient: 0-

30 min: MeCN/0.1% aq TFA 5:95-90.5:9.5, t_R = 15 min) afforded the product as a blue solid (1.45 mg, 30%). Ratio of configurational isomers evident in the NMR spectra: ca 1.5:1. ^{1}H-NMR (600 MHz, MeOH-d_4): δ (ppm) 1.26-1.40 (m, 4H), 1.40-1.56 (m, 4H), 1.59-1.70 (m, 3H), 1.73 (s, 6H), 1.74 (s, 6H), 1.75-1.77 (m, 3H), 1.77-1.87 (m, 2H), 1.89-2.05 (m, 6H), 2.18 (t, *J* 6.0 Hz, 2H), 2.31-2.41 (m, 2H), 2.89 (t, *J* 6.0 Hz, 2H), 2.95-3.01 (m, 2H), 3.01-3.13 (m, 3H), 3.18-3.19 (m, 1H), 3.19-3.22 (m, 1H), 3.19-3.22 (m, 1H), 3.31-3.33 (m, 4H), 3.41-3.42 (m, 1H), 3.45 (d, *J* 10 Hz, 1H), 3.68-3.83 (m, 2H), 4.07 (t, *J* 6.0 Hz, 2H), 4.21-4.23 (m, 2H), 4.38 (d, *J* 18 Hz, 0.6H), 4.43 (d, *J* 18 Hz, 0.4H), 6.21 (d, *J* 12 Hz, 1H), 6.50 (d, *J* 12 Hz, 1H), 6.65-6.71 (m, 1H), 7.22-7.31 (m, 2H), 7.31-7.34 (m, 2H), 7.36-7.46 (m, 3H), 7.44-7.54 (m, 3H), 7.60-7.67 (m, 1H), 7.67-7.75 (m, 1H), 7.81-7.86 (m, 2H), 7.89-7.91 (m, 0.6H), 7.96-7.97 (m, 0.4H), 8.12-8.32 (m, 2H). RP-HPLC (220 nm): 99% (t_R = 17.6 min, k = 5.1). HRMS (ESI): m/z [*M*+H]$^+$ calcd. for $[C_{65}H_{85}N_8O_9S_2]^+$: 1185.5875, found: 1185.5896. $C_{65}H_{83}N_8O_9S_2^- \cdot C_8H_4F_{12}O_8$ (1184.55 + 456.09).

4.4.3. Determination of fluorescence quantum yields

The determination of the fluorescence quantum yields of **133-136** in PBS and PBS containing 1% BSA was performed with a Cary Eclipse spectrofluorimeter and a Cary 100 UV/VIS photometer (Varian Inc., Mulgrave, Victoria, Australia) as described previously with minor modifications[6]. All spectra were recorded using acryl cuvettes (10 × 10 mm, Ref. 67.755, Sarstedt, Nümbrecht, Germany). Fluorescence spectra were recorded at the slit adjustments (excitation/emission) 10/5 nm and 10/10 nm. Table 7 provides an overview of the used concentrations of the fluorescent ligands and the applied excitation wavelengths. The concentration of cresyl violet perchlorate in EtOH was 2 µM. Fluorescence spectra of cresyl violet perchlorate were recorded using an excitation wavelength of 575 nm.

Table 7. Concentrations and excitation wavelengths used for the determination of fluorescence quantum yields.

Compound	concentration [µM]		excitation wavelength [nm]	
	PBS	PBS + 1% BSA	PBS	PBS + 1% BSA
133	15	12	445	470
134	5	5	600	610
135	3	2	610	620
136	2	2	610	610

4.4.4. Investigation of the chemical stability

The stability of the fluorescent ligand **136** was investigated in phosphate buffered saline (pH

7.4). The incubation was started by addition of 10 µL of a 5 mM stock solution of **136** (in DMSO/H_2O 1:1 v/v) to 490 µL of PBS to give a final concentration of 100 µM. After 0 h, 6 h, 24 h, 48 h, an aliquot (120 µL) was taken and added to acetonitrile/H_2O/2% aq TFA (2:4:4 v/v/v) (120 µL). 100 µL of the resulting solution (pH < 4) were analyzed by analytical HPLC on a system from Merck-Hitachi (Hitachi, Düsseldorf, Germany) composed of a L-6200-A pump, an AS-2000A autosampler, a L-4000A UV detector and a D-6000 interface. A Kinetex-XB C18, 5 µm, 250 mm × 4.6 mm (Phenomenex, Aschaffenburg, Germany) served as stationary phase at a flow rate of 0.8 mL/min. The following linear gradient was applied: 0-20 min: acetonitrile/0.1% aq TFA 10:90-36:64, 20-28 min: 36:64-95:5, 28-35 min: 95:5. Detection was performed at 220 nm and the oven temperature was 30 °C.

4.4.5. [^{3}H]NMS competition binding assay

Radioligand binding studies with [^{3}H]NMS were performed at 22 ± 1 °C. Leibovitz L-15 medium (Gibco, Life Technologies GmbH, Darmstadt, Germany) supplemented with 1% BSA (Serva, Heidelberg, Germany) (in the following referred to as L15 medium) was used as binding buffer. The effects of the fluorescent ligands **130**-**136** on the equilibrium binding of [^{3}H]NMS (equilibrium competition binding assay) were determined at intact adherent CHO-hM_xR cells (x = 1-5) in white 96-well plates with clear bottom (Corning Life Sciences, Tewksbury, MA; Corning cat. no. 3610) using the protocol of previously described MR binding studies with [^{3}H]NMS[44] with the following modification: the total volume of L15 medium per well was 200 µL instead of 188 µL, i.e. the cells were covered with L15 medium (160 µL) followed by the addition of L15 medium (20 µL) neat or containing competitors or atropine (10-fold concentrated), and L15 medium (20 µL) containing the radioligand 10-fold concentrated. The concentration of [^{3}H]NMS was 0.2 nM (M_1, M_2, M_3), 0.1 nM (M_4) or 0.3 nM (M_5) and the incubation time was 3 h throughout.

4.4.6. Flow cytometric binding experiments

All flow cytometric binding studies were performed with a FACSCalibur™ flow cytometer (Becton Dickinson, Heidelberg, Germany), equipped with an argon laser (488 nm) and a red diode laser (635 nm), instrument settings were: FSC, E-1; SSC, 280 V; Fl-4, 700−800 V. All samples were prepared and incubated in 1.5 mL reaction vessels (Sarstedt, Nümbrecht, Germany). Samples were prepared in duplicate throughout. Fluorescence signals were recorded in channel FL-4 (excitation: 635 nm, emission: 661 ± 18 nm). Measurements were stopped after counting of 20,000 gated events (highest flow rate).

4.4.6.1. Saturation binding studies at the M_1R, M_2R and M_4R and competition binding with fluorescent ligand 136 at the M_2R

CHO-hM_xR (x = 1, 2 and 4) cells were seeded in a 175-cm^2 culture flask 5-6 days prior to the experiment. Cells were treated with trypsin, suspended in culture medium and centrifuged. The cell pellet was re-suspended in Leibovitz's L15 culture medium (Gibco, Life Technologies, Darmstadt, Germany) supplemented with 1% bovine serum albumin (Serva, Heidelberg, Germany), in the following referred to as L15 medium. The cell density was adjusted $1 \cdot 10^6$ cells/mL. For saturation binding experiments, 490 µL of the cell suspension were added to reaction vessels, 5 µL of a solution of the fluorescent ligand (100-fold concentrated) in DMSO/H_2O (1:1 v/v) and 5 µL of DMSO/H_2O (1:1 v/v), were added to determine total binding. For the determination of unspecific binding (in the presence of atropine at 500-fold access to the fluorescent ligand), 490 µL of the cell suspension were added to reaction vessels, 5 µL of a solution of the fluorescent ligand (100-fold concentrated) in DMSO/H_2O (1:1 v/v) and 5 µL of a solution of atropine (100-fold concentrated) in DMSO/H_2O (1:1 v/v) were added. Compound **135** or **136** was applied at final concentrations of 0.1-15 nM and 0.1-10 nM, respectively, for M_2R binding experiments, and **136** was applied at final concentrations of 0.15-80 nM for M_1R and M_4R binding studies. The incubation period was 2 h.

For competition binding experiments with **136** (c = 1.0 nM) at CHO-hM_2R cells, 5 µL of a solution of the fluorescent ligand (100-fold concentrated) in DMSO/H_2O (1:1 v/v) and 5 µL of a solution of atropine (100-fold concentrated) in DMSO/H_2O (1:1 v/v), to determine unspecific binding (500-fold excess of atropine to **136**), or 5 µL of a solution of the compound of interest (including **2**, **7**, **8**, **11**, **14**, **15** and **16**) (100-fold concentrated) in DMSO/H_2O (1:1 v/v), for competition binding, were premixed in the reaction vessels followed by addition of 490 µL of the cell suspension. The incubation period was 2 h.

M_2R saturation binding experiments with **136** in the presence of various fixed concentrations of **15** were performed as described above with the following modification: vessels were prefilled with 485 µL of M_2R cell suspension. For total binding, L15 medium (5 µL), L15 medium (5 µL) containing **15** 100-fold concentrated, L15 medium (5 µL) containing **136** 100-fold concentrated were added. For unspecific binding, L15 medium (5 µL) containing compound **136** (100-fold concentrated), L15 medium (5 µL) containing **15** (100-fold concentrated) and L15 medium (5 µL) containing atropine 100-fold concentrated (500-fold excess to compound **136**) were added.

4.4.6.2. Association and dissociation kinetics of 136 at CHO-hM$_2$R cells

For association experiments with **136** (c = 3 nM) at CHO-hM$_2$R cells reaction vessels were prefilled with 490 µL of the cell suspension. For total binding DMSO/H$_2$O (1:1 v/v) (5 µL) and DMSO/H$_2$O (1:1 v/v) (5 µL) containing **136** (0.3 µM) were added. To determine unspecific binding DMSO/H$_2$O (1:1 v/v) (5 µL) containing atropine (30 µM) and DMSO/H$_2$O (1:1 v/v) (5 µL) containing **136** (0.3 µM) were added to the cell suspension. The incubation was stopped after different periods of time (0-140 min) by measurement of the samples. In the case of dissociation experiments, cells were preincubated with **136** at a final concentration of 5 nM for 2 h (500 µL total volume per vessel). Unspecific binding was determined in the presence of atropine at a final concentration of 1 µM. After incubation, the cells were centrifuged at room temperature for 3.5 min, the supernatant was removed by suction and the cells were covered with L15 medium (500 µL) containing atropine (2.5 µM) followed by shaking in the dark. After different periods of time (0-150 min), the samples were subjected to measurement by flow cytometry.

4.4.7. High content imaging binding experiments

4.4.7.1. Saturation and competition binding assay

One day prior to the experiment CHO-hM$_2$R cells were seeded at 35,000-40,000 cells per well into the central 60 wells of a black/transparent 96-well plate (Grenier 655090). The medium was removed by suction, the cells were washed with HBSS containing 0.1 % BSA (in the following referred to as HBSS-BSA) (50 µL), and covered with 80 µL of HBSS-BSA containing the permeable nuclear dye H33342 (2 µg/mL, Sigma). To determine total binding HBSS-BSA (10 µL) and HBSS-BSA (10 µL) containing the fluorescent ligand (10-fold concentrated) were added. For the determination of unspecific binding and to study the effect of a compound of interest on M$_2$R binding of the fluorescent ligand (competition binding assay) HBSS-BSA (10 µL) containing atropine or the ‘competitor’ (10-fold concentrated) and HBSS-BSA (10 µL) containing the fluorescent ligand (10-fold concentrated) were added. After incubation at room temperature in the dark for 60 min, images were acquired with the IX Ultra confocal plate reader (Molecular Devices, Sunnyvale CA) to obtain “non-washing” saturation binding curves (*cf*. Figure 10A and 10B), unspecific binding was determined in the presence of atropine (1 µM). After incubation at room temperature in the dark for 60 min, the medium was removed by suction and the cells were washed with HBSS-BSA (50 µL) and covered with HBSS-BSA (50 µL) followed by immediate acquisition of the images using the IX Ultra confocal plate reader to obtain “washing step applying” saturation binding curves (*cf*. Figure 10C and 10D),

unspecific binding was determined in the presence of atropine (500-fold excess to the fluorescent ligand). The washing process was performed within < 2 min. For competition binding experiments, unspecific binding was determined in the presence of atropine (1 µM), plates were directly imaged after incubation for 1 h. Saturation binding experiments were performed in triplicate and competition binding assays were performed in duplicate. In case of competition binding studies the 'competitor' was added to the cells 2 min prior to the addition of fluorescent ligand. One site/well was measured with the plate reader in case of competition binding with **2**, **6** and **7**, and two sites/well were measured in case of saturation binding studies and competition binding experiments with **3**, **14**, **15** and **16**. The excitation laser lines of the Ultra were 405 nm (H33342), 488 nm (FITC), 561 nm (Texas Red) and 635 nm (Cy5), the emission laser lines of the Ultra were 447/60 nm (H33342), 525/50 nm (FITC), 593/40 nm (Texas Red) and 685/40 nm (Cy5).

M_2R saturation binding experiments with **136** in the presence of various fixed concentrations of **15** were performed as described above with the following modification: the cells were covered with 70 µL of HBSS-BSA instead of 80 µL to compensate the extra addition of HBSS-BSA (10 µL) containing **15** (10-fold concentrated). The washing step prior to the measurement was performed.

4.4.8. Confocal Microscopy

One day prior to the experiment CHO-hM_2R cells were trypsinized and seeded in Nunc LabTekTM II chambered coverglasses with 8 chambers (Thermo fisher scientific) (ca. 80000 cells/well). The culture medium was removed, the cells were washed with HBSS-BSA (200 µL) and covered with HBSS-BSA (320 µL). HBSS-BSA (40 µL) and HBSS-BSA (40 µL) with the fluorescent probe (10 fold concentrated) was added for total binding. For unspecific binding HBSS-BSA (40 µL) with the competing agent atropine (final concentration: 10 µM) and HBSS-BSA (40 µL) with the fluorescent probe (10 fold concentrated) were added. Images of total and unspecific binding were acquired after an incubation period of 5-45 min. Confocal microscopy was performed with a zeiss LSM710 confocal microscope. The objective was 63x magnification with oil (1.4NA). The excitation laser lines were 405 nm (2.0%) and 633 nm (10.0%), filter settings were 410-514 nm and 638-759 nm, pinhole settings are 44 µm for both DAPI and Cy5 channels.

4.5. Data processing

Retention (capacity) factors *k* were calculated from retention times (t_R) according to k =

(t_R−t_0)/t_0 (t_0 = dead time). Raw data from flow cytometric experiments were processed with the aid of FloJo software to obtain geometrical mean values of FL-4. Fluorescence images from high content imaging were analyzed using the granularity analysis (2-3-µm-diameter granules; MetaXpress 5.3, Molecular Devices) to obtain values of arbitrary intensity units. Intensity thresholds were adapted to maximize the identification of specifically bound fluorescent ligand (without distinguishing membrane from intracellular localization), by reference to total and unspecific plate controls. Specific binding data from saturation binding experiments (flow cytometry, high content imaging) were plotted against the fluorescent ligand concentration and analyzed by a two-parameter equation describing hyperbolic binding (one site-specific binding, GraphPad Prism) to obtain K_d values. Unspecific binding data from saturation binding experiments were fitted by linear regression. In case of saturation binding experiments with fluorescent labeled ligand **136** in the presence of compound **15**, specific binding data were analyzed by a two-parameter equation describing hyperbolic binding (one site-specific binding, GraphPad Prism) to obtain K_d and B_{max} values. Additionally, specific binding data were normalized to the B_{max} value, specific binding (%) was plotted against log(concentration of **136**) followed by analysis using a four-parameter logistic fit (log(agonist) vs. response, applied constraints: bottom = 0%, top = 100%; GraphPad Prism). Data for the 'Schild' plot were obtained from the rightward shift (ΔpK_d) of the saturation isotherm and transformation into log(r-1) (where $r = 10^{\Delta pK_d}$). Log(r-1) was plotted against log(concentration of **15**) and the data were analyzed by linear regression to obtain the slope and the 'pA_2' value (intercept with the X axis). Specific binding data from association experiments with **136** were analyzed by a two-parameter equation describing an exponential rise to a maximum (one-phase association, GraphPad Prism) to obtain the observed association rate constant k_{obs} and the amount of specifically bound **136** at equilibrium (B_{eq}), which was used to calculate specifically bound **136** (B_t) in %. Data from dissociation experiments (% specifically bound **136** (B_t) plotted over time) were analyzed by a three-parameter equation (one phase decay, GraphPad Prism) to obtain the dissociation rate constant k_{off}. The association rate constant (k_{on}) of **136** was calculated from k_{obs}, k_{off} and the concentration of **136** used for the association experiment according to the correlation: $k_{on} = (k_{obs}-k_{off})/[FL]$. Total binding data from competition binding experiments (determination of the effect of various MR ligands on the equilibrium binding of [^{3}H]NMS, **135** or **136**) were plotted against log(concentration competitor) and analyzed by a four-parameter logistic equation (log(inhibitor) vs. response-variable slope, GraphPad Prism) followed by normalization (100% = 'top' of the four-parameter logistic fit, 0% = unspecifically bound fluorescent ligand determined in the presence of **7**) and analysis of the normalized data by a four-parameter logistic equation. IC_{50} values were converted to K_i values according to the Cheng-Prusoff equation[51]. Statistical significance was assessed by a one-sample t-test.

4.6. References

1. Sridharan, R.; Zuber, J.; Connelly, S. M.; Mathew, E.; Dumont, M. E., Fluorescent approaches for understanding interactions of ligands with G protein coupled receptors. *Biochimica et Biophysica Acta (BBA)-Biomembranes* **2014,** *1838* (1), 15-33.
2. Briddon, S. J.; Kellam, B.; Hill, S. J., Design and use of fluorescent ligands to study ligand–receptor interactions in single living cells. *Receptor Signal Transduction Protocols: Third Edition* **2011**, 211-236.
3. Baker, J. G.; Middleton, R.; Adams, L.; May, L. T.; Briddon, S. J.; Kellam, B.; Hill, S. J., Influence of fluorophore and linker composition on the pharmacology of fluorescent adenosine A_1 receptor ligands. *Br. J. Pharmacol.* **2010,** *159* (4), 772-786.
4. Schneider, E.; Keller, M.; Brennauer, A.; Hoefelschweiger, B. K.; Gross, D.; Wolfbeis, O. S.; Bernhardt, G.; Buschauer, A., Synthesis and characterization of the first fluorescent nonpeptide NPY Y_1 receptor antagonist. *ChemBioChem* **2007,** *8* (16), 1981-1988.
5. Ziemek, R.; Brennauer, A.; Schneider, E.; Cabrele, C.; Beck-Sickinger, A. G.; Bernhardt, G.; Buschauer, A., Fluorescence-and luminescence-based methods for the determination of affinity and activity of neuropeptide Y_2 receptor ligands. *Eur. J. Pharmacol.* **2006,** *551* (1), 10-18.
6. Keller, M.; Erdmann, D.; Pop, N.; Pluym, N.; Teng, S.; Bernhardt, G.; Buschauer, A., Red-fluorescent argininamide-type NPY Y_1 receptor antagonists as pharmacological tools. *Bioorg. Med. Chem.* **2011,** *19* (9), 2859-2878.
7. Dumont, Y.; Gaudreau, P.; Mazzuferi, M.; Langlois, D.; Chabot, J. G.; Fournier, A.; Simonato, M.; Quirion, R., BODIPY® ‐ conjugated neuropeptide Y ligands: new fluorescent tools to tag Y_1, Y_2, Y_4 and Y_5 receptor subtypes. *Br. J. Pharmacol.* **2005,** *146* (8), 1069-1081.
8. Liu, M.; Richardson, R. R.; Mountford, S. J.; Zhang, L.; Tempone, M. H.; Herzog, H.; Holliday, N. D.; Thompson, P. E., Identification of a Cyanine-Dye Labeled Peptidic Ligand for Y_1R and Y_4R, Based upon the Neuropeptide Y C-Terminal Analogue, BVD-15. *Bioconjugate Chem.* **2016,** *27* (9), 2166-2175.
9. Li, L.; Kracht, J.; Peng, S.; Bernhardt, G.; Buschauer, A., Synthesis and pharmacological activity of fluorescent histamine H_1 receptor antagonists related to mepyramine. *Bioorg. Med. Chem. Lett.* **2003,** *13* (7), 1245-1248.
10. Li, L.; Kracht, J.; Peng, S.; Bernhardt, G.; Elz, S.; Buschauer, A., Synthesis and pharmacological activity of fluorescent histamine H_2 receptor antagonists related to potentidine. *Bioorg. Med. Chem. Lett.* **2003,** *13* (10), 1717-1720.
11. Xie, S.-X.; Petrache, G.; Schneider, E.; Ye, Q.-Z.; Bernhardt, G.; Seifert, R.; Buschauer, A., Synthesis and pharmacological characterization of novel fluorescent histamine H_2-receptor ligands derived from aminopotentidine. *Bioorg. Med. Chem. Lett.* **2006,** *16* (15), 3886-3890.
12. Amon, M.; Ligneau, X.; Schwartz, J.-C.; Stark, H., Fluorescent non-imidazole histamine H_3 receptor ligands with nanomolar affinities. *Bioorg. Med. Chem. Lett.* **2006,** *16* (7), 1938-1940.
13. Malan, S. F.; van Marle, A.; Menge, W. M.; Zuliana, V.; Hoffman, M.; Timmerman, H.; Leurs, R., Fluorescent ligands for the histamine H_2 receptor: synthesis and preliminary characterization. *Bioorg. Med. Chem.* **2004,** *12* (24), 6495-6503.
14. Arttamangkul, S.; Alvarez-Maubecin, V.; Thomas, G.; Williams, J. T.; Grandy, D. K., Binding and internalization of fluorescent opioid peptide conjugates in living cells. *Mol. Pharmacol.* **2000,** *58* (6), 1570-1580.
15. Balboni, G.; Salvadori, S.; Dal Piaz, A.; Bortolotti, F.; Argazzi, R.; Negri, L.; Lattanzi, R.; Bryant, S. D.; Jinsmaa, Y.; Lazarus, L. H., Highly selective fluorescent analogue of the potent δ-opioid receptor antagonist Dmt-Tic. *J. Med. Chem.* **2004,** *47* (26), 6541-6546.
16. Houghten, R. A.; Dooley, C. T.; Appel, J. R., De novo identification of highly active

fluorescent kappa opioid ligands from a rhodamine labeled tetrapeptide positional scanning library. *Bioorg. Med. Chem. Lett.* **2004,** *14* (8), 1947-1951.
17. Leopoldo, M.; Lacivita, E.; Passafiume, E.; Contino, M.; Colabufo, N. A.; Berardi, F.; Perrone, R., 4-[ω-[4-Arylpiperazin-1-yl] alkoxy] phenyl) imidazo [1, 2-a] pyridine derivatives: fluorescent high-affinity dopamine D_3 receptor ligands as potential probes for receptor visualization. *J. Med. Chem.* **2007,** *50* (20), 5043-5047.
18. Huwiler, K. G.; De Rosier, T.; Hanson, B.; Vogel, K. W., A fluorescence anisotropy assay for the muscarinic M_1 G-protein-coupled receptor. *Assay Drug Dev. Technol.* **2010,** *8* (3), 351-361.
19. Bonnet, D.; Ilien, B.; Galzi, J.-L.; Riché, S.; Antheaune, C.; Hibert, M., A rapid and versatile method to label receptor ligands using “click” chemistry: Validation with the muscarinic M_1 antagonist pirenzepine. *Bioconjugate Chem.* **2006,** *17* (6), 1618-1623.
20. Tahtaoui, C.; Guillier, F.; Klotz, P.; Galzi, J.-L.; Hibert, M.; Ilien, B., On the use of nonfluorescent dye labeled ligands in FRET-based receptor binding studies. *J. Med. Chem.* **2005,** *48* (24), 7847-7859.
21. Daval, S. B.; Valant, C. I.; Bonnet, D.; Kellenberger, E.; Hibert, M.; Galzi, J.-L.; Ilien, B., Fluorescent derivatives of AC-42 to probe bitopic orthosteric/allosteric binding mechanisms on muscarinic M_1 receptors. *J. Med. Chem.* **2012,** *55* (5), 2125-2143.
22. Hern, J. A.; Baig, A. H.; Mashanov, G. I.; Birdsall, B.; Corrie, J. E.; Lazareno, S.; Molloy, J. E.; Birdsall, N. J., Formation and dissociation of M_1 muscarinic receptor dimers seen by total internal reflection fluorescence imaging of single molecules. *Proc. Natl. Acad. Sci. USA* **2010,** *107* (6), 2693-2698.
23. Tahtaoui, C.; Parrot, I.; Klotz, P.; Guillier, F.; Galzi, J.-L.; Hibert, M.; Ilien, B., Fluorescent pirenzepine derivatives as potential bitopic ligands of the human M_1 muscarinic receptor. *J. Med. Chem.* **2004,** *47* (17), 4300-4315.
24. Lee, P. H.; Miller, S. C.; van Staden, C.; Cromwell, E. F., Development of a homogeneous high-throughput live-cell G-protein-coupled receptor binding assay. *J. Biomol. Screen.* **2008,** *13* (8), 748-754.
25. Ilien, B.; Glasser, N.; Clamme, J.-P.; Didier, P.; Piemont, E.; Chinnappan, R.; Daval, S. B.; Galzi, J.-L.; Mely, Y., Pirenzepine promotes the dimerization of muscarinic M_1 receptors through a three-step binding process. *J. Biol. Chem.* **2009,** *284* (29), 19533-19543.
26. Jones, L. H.; Randall, A.; Napier, C.; Trevethick, M.; Sreckovic, S.; Watson, J., Design and synthesis of a fluorescent muscarinic antagonist. *Bioorg. Med. Chem. Lett.* **2008,** *18* (2), 825-827.
27. Eglen, R. M., Muscarinic receptor subtype pharmacology and physiology. *Prog. Med. Chem.* **2005,** *43*, 105-136.
28. Wess, J.; Eglen, R. M.; Gautam, D., Muscarinic acetylcholine receptors: mutant mice provide new insights for drug development. *Nat. Rev. Drug Discovery* **2007,** *6* (9), 721-733.
29. Eglen, R. M., Overview of muscarinic receptor subtypes. In *Muscarinic Receptors*, Springer: 2012; pp 3-28.
30. De Amici, M.; Dallanoce, C.; Holzgrabe, U.; Traenkle, C.; Mohr, K., Allosteric ligands for G protein-coupled receptors: A novel strategy with attractive therapeutic opportunities. *Med. Res. Rev.* **2010,** *30* (3), 463-549.
31. Lane, J. R.; Sexton, P. M.; Christopoulos, A., Bridging the gap: bitopic ligands of G-protein-coupled receptors. *Trends Pharmacol. Sci.* **2013,** *34* (1), 59-66.
32. Tränkle, C.; Andresen, I.; Lambrecht, G.; Mohr, K., M_2 receptor binding of the selective antagonist AF-DX 384: possible involvement of the common allosteric site. *Mol. Pharmacol.* **1998,** *53* (2), 304-312.
33. Ellis, J.; Seidenberg, M., Competitive and allosteric interactions of 6-chloro-5, 10-dihydro-5-[(1-methyl-4-piperidinyl) acetyl]-11*H*-dibenzo [*b*, *e*][1, 4] diazepine-11-one hydrochloride (UH-AH 37) at muscarinic receptors, via distinct epitopes. *Biochem. Pharmacol.* **1999,** *57* (2), 181-186.
34. Lanzafame, A.; Christopoulos, A.; Mitchelson, F., The allosteric interaction of

otenzepad (AF-DX 116) at muscarinic M_2 receptors in guinea pig atria. *Eur. J. Pharmacol.* **2001,** *416* (3), 235-244.
35. Giraldo, E.; Micheletti, R.; Montagna, E.; Giachetti, A.; Vigano, M.; Ladinsky, H.; Melchiorre, C., Binding and functional characterization of the cardioselective muscarinic antagonist methoctramine. *J. Pharmacol. Exp. Ther.* **1988,** *244* (3), 1016-1020.
36. Valant, C.; Gregory, K. J.; Hall, N. E.; Scammells, P. J.; Lew, M. J.; Sexton, P. M.; Christopoulos, A., A novel mechanism of G protein-coupled receptor functional selectivity muscarinic partial agonist McN-A-343 as a bitopic orthosteric/allosteric ligand. *J. Biol. Chem.* **2008,** *283* (43), 29312-29321.
37. Avlani, V. A.; Langmead, C. J.; Guida, E.; Wood, M. D.; Tehan, B. G.; Herdon, H. J.; Watson, J. M.; Sexton, P. M.; Christopoulos, A., Orthosteric and allosteric modes of interaction of novel selective agonists of the M_1 muscarinic acetylcholine receptor. *Mol. Pharmacol.* **2010,** *78* (1), 94-104.
38. Karton, Y.; Baumgold, J.; Handen, J. S.; Jacobson, K. A., Molecular probes for muscarinic receptors: Derivatives of the M_1-antagonist telenzepine. *Bioconjugate Chem.* **1992,** *3* (3), 234-240.
39. Jacobson, K. A.; Fischer, B.; van Rhee, A. M., Molecular probes for muscarinic receptors: functionalized congeners of selective muscarinic antagonists. *Life Sci.* **1995,** *56* (11), 823-830.
40. Wang, Y.; Gu, Q.; Mao, F.; Haugland, R. P.; Cynader, M. S., Activity-dependent expression and distribution of M_1 muscarinic ACh receptors in visual cortex neuronal cultures. *The Journal of neuroscience* **1994,** *14* (7), 4147-4158.
41. Daval, S. B.; Kellenberger, E.; Bonnet, D.; Utard, V.; Galzi, J.-L.; Ilien, B., Exploration of the orthosteric/allosteric interface in human M_1 muscarinic receptors by bitopic fluorescent ligands. *Mol. Pharmacol.* **2013,** *84* (1), 71-85.
42. Gitler, M. S.; Reba, R. C.; Cohen, V. I.; Rzeszotarski, W. J.; Baumgold, J., A novel M_2-selective muscarinic antagonist: binding characteristics and autoradiographic distribution in rat brain. *Brain Res.* **1992,** *582* (2), 253-260.
43. Wetzl, B. K.; Yarmoluk, S. M.; Craig, D. B.; Wolfbeis, O. S., Chameleon labels for staining and quantifying proteins. *Angew. Chem., Int. Ed.* **2004,** *43* (40), 5400-5402.
44. Keller, M.; Tränkle, C.; She, X.; Pegoli, A.; Bernhardt, G.; Buschauer, A.; Read, R. W., M_2 Subtype preferring dibenzodiazepinone-type muscarinic receptor ligands: Effect of chemical homo-dimerization on orthosteric (and allosteric?) binding. *Bioorg. Med. Chem.* **2015,** *23* (14), 3970-3990.
45. Jakubík, J.; Bačáková, L.; El-Fakahany, E. E.; Tuček, S., Positive cooperativity of acetylcholine and other agonists with allosteric ligands on muscarinic acetylcholine receptors. *Mol. Pharmacol.* **1997,** *52* (1), 172-179.
46. Dei, S.; Bellucci, C.; Buccioni, M.; Ferraroni, M.; Guandalini, L.; Manetti, D.; Martini, E.; Marucci, G.; Matucci, R.; Nesi, M., Synthesis, affinity profile, and functional activity of muscarinic antagonists with a 1-methyl-2-(2, 2-alkylaryl-1, 3-oxathiolan-5-yl) pyrrolidine structure. *J. Med. Chem.* **2007,** *50* (6), 1409-1413.
47. Mohr, K.; Tränkle, C.; Kostenis, E.; Barocelli, E.; De Amici, M.; Holzgrabe, U., Rational design of dualsteric GPCR ligands: quests and promise. *Br. J. Pharmacol.* **2010,** *159* (5), 997-1008.
48. Valant, C.; Robert Lane, J.; Sexton, P. M.; Christopoulos, A., The best of both worlds? Bitopic orthosteric/allosteric ligands of g protein-coupled receptors. *Annu. Rev. Pharmacol. Toxicol.* **2012,** *52*, 153-178.
49. Valant, C.; Sexton, P. M.; Christopoulos, A., Orthosteric/allosteric bitopic ligands. *Mol. Interventions* **2009,** *9* (3), 125.
50. Kane, B. E.; Grant, M. K.; El-Fakahany, E. E.; Ferguson, D. M., Synthesis and evaluation of xanomeline analogs—Probing the wash-resistant phenomenon at the M_1 muscarinic acetylcholine receptor. *Bioorg. Med. Chem.* **2008,** *16* (3), 1376-1392.
51. Yung-Chi, C.; Prusoff, W. H., Relationship between the inhibition constant (K_i) and the concentration of inhibitor which causes 50 per cent inhibition (I_{50}) of an enzymatic

reaction. *Biochem. Pharmacol.* **1973,** *22* (23), 3099-3108.

Chapter 5

Summary

5. Summary

In humans, the family of muscarinic acetylcholine receptors (mAChR, MRs) comprises five subtypes (M_1R-M_5R), which are members of the class A GPCR superfamily and mediate the action of the neurotransmitter acetylcholine in the central and peripheral nervous system. For instance, the M_2R, which binds to $G_{i/o}$ heterotrimeric G-proteins, acts as a presynaptic autoreceptor in the brain and in the periphery. Accordingly, selective M_2R antagonism in the CNS, resulting in enhanced cholinergic transmission, was suggested as an approach to increase cholinergic function in Alzheimer patients. MRs represent important drug targets, however, there is still a need for highly subtype selective MR ligands, as the development of selective agents has been challenging due to the high conservation of the acetylcholine (orthosteric) binding site. Due to the less conserved allosteric binding sites, the dualsteric ligand approach, i.e. the design of compounds, which simultaneously address the orthosteric and allosteric binding sites, is considered a promising strategy to develop MR ligands with improved subtype selectivity.

This work was aiming at the synthesis and pharmacological characterization of dibenzodiazepinone-type heterodimeric MR ligands, which were prepared by linking different monomeric MR ligands (agonists, antagonists, orthosteric and allosteric ligands) through various linkers to a pharmacophoric moiety derived from the dibenzodiazepinone DIBA. The synthesis afforded heterodimeric ligands ('DIBA-xanomeline', 'DIBA-TBPB', 'DIBA-77-LH-28-1', 'DIBA-propantheline' and 'DIBA-4-DAMP') and 'DIBA-DIBA'-type homodimeric ligands. Equilibrium competition binding studies with [^{3}H]NMS at live CHO cells expressing the respective human M_xR subtype (x = 1-5) revealed a M_2R preference of all dimeric ligands with high M_2R affinities (K_i values: 0.08-5.8 nM). These data demonstrated that the type of the linker (short vs. long, basic vs. non-basic, etc.) and the type of the second pharmacophoric group had only little impact on M_2R binding. As non-DIBA-type monomeric and homodimeric reference compounds exhibited considerably lower M_2R affinities than the synthesized DIBA-derived ligands, the high M_2R affinity of the heterodimeric dibenzodiazepinone-type ligands is most likely conferred by the 'dibenzodiazepinone' pharmacophore.

Two tritium-labeled DIBA-derived heterodimeric ligands ('DIBA-xanomeline'- and DIBA-TBPB'-type) were prepared and characterized by saturation and kinetic binding studies at the hM_2R. Saturation binding experiments showed that these ligands address the orthosteric site of the M_2R. The 'DIBA-TBPB'-type dimeric radioligand ([^{3}H]**115**) exhibited a very high M_2R affinity (K_d value 0.13 nM). The investigation of the effect of allosteric MR ligands (gallamine, W84, LY2119620) on the equilibrium binding of [^{3}H]**115**, and saturation binding studies with [^{3}H]**115** in the presence of the allosteric MR ligand W84 (Schild-like analysis) strongly

suggested a competitive mechanism between [^{3}H]**115** and the investigated allosteric ligand. Consequently, these data revealed that DIBA-derived heterodimeric ligands such as **115** exhibit a dualsteric binding mode at the M_2R.

Moreover, a series of fluorescently labeled, monomeric DIBA-derived ligands was prepared by conjugation of cyanine dyes or a pyrylium dye via different linkers to the dizenzodiazepinone scaffold. Except for one compound, the fluorescent probes exhibited high M_2R affinity (K_i < 55 nM). Interestingly, the structure of the fluorophores had less impact on the M_2R affinity than the nature of the linker. The fluorescent ligands **135** and **136**, bearing red-emitting cyanine dyes attached via linkers with a basic piperazine moiety, exhibited the highest M_2R affinity (K_i ca. 1 nM). The M_2R preference of the fluorescent ligands was less pronounced compared to the amine-functionalized precursor molecules, i.e. attachment of the lipophilic fluorophores resulted in a decrease in M_2R selectivity. Application of **135** and **136** to flow cytometry and high content analysis proved that these new fluorescent probes are suited for such techniques. The fluorescent ligand **136** was identified as a valuable molecular tool for the determination of MR affinities of MR ligands. M_2R binding studies with **136** in the presence of allosteric modulators strongly suggested that **136** and structurally related ligands bind simultaneously to both the orthosteric (via the dibenzodiazepinone scaffold) and the ‘common’ allosteric binding site (most likely via the fluorophores) of the M_2R, thus exhibiting a dualsteric binding mode, too.

In conclusion, this work afforded new radiolabeled and fluorescently labeled molecular tools for the M_2R and suggests dibenzodiazepinone-type MR ligands as an interesting compound class to develop highly selective M_2R ligands according to the dualsteric ligand approach.

Chapter 6

Appendix

6. Appendix

6.1. ^{1}H-NMR and ^{13}C-NMR spectra of compounds 41, 46, 53-55, 67, 95-102, 105a, 106-108, 110-120 and 130-136

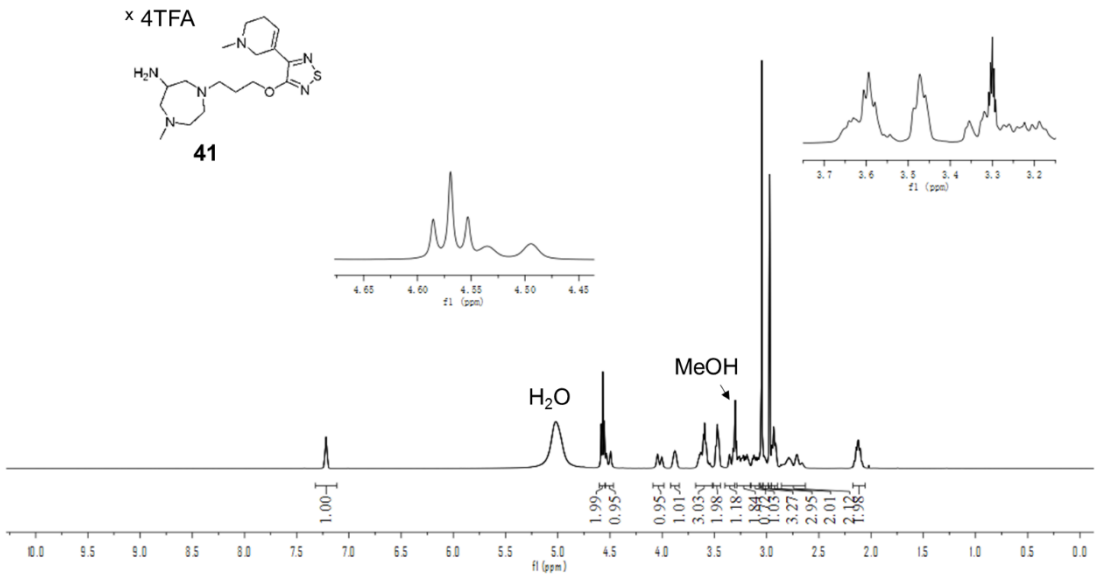

^{1}H-NMR spectrum (400 MHz, [D$_4$]MeOH) of compound **41**.

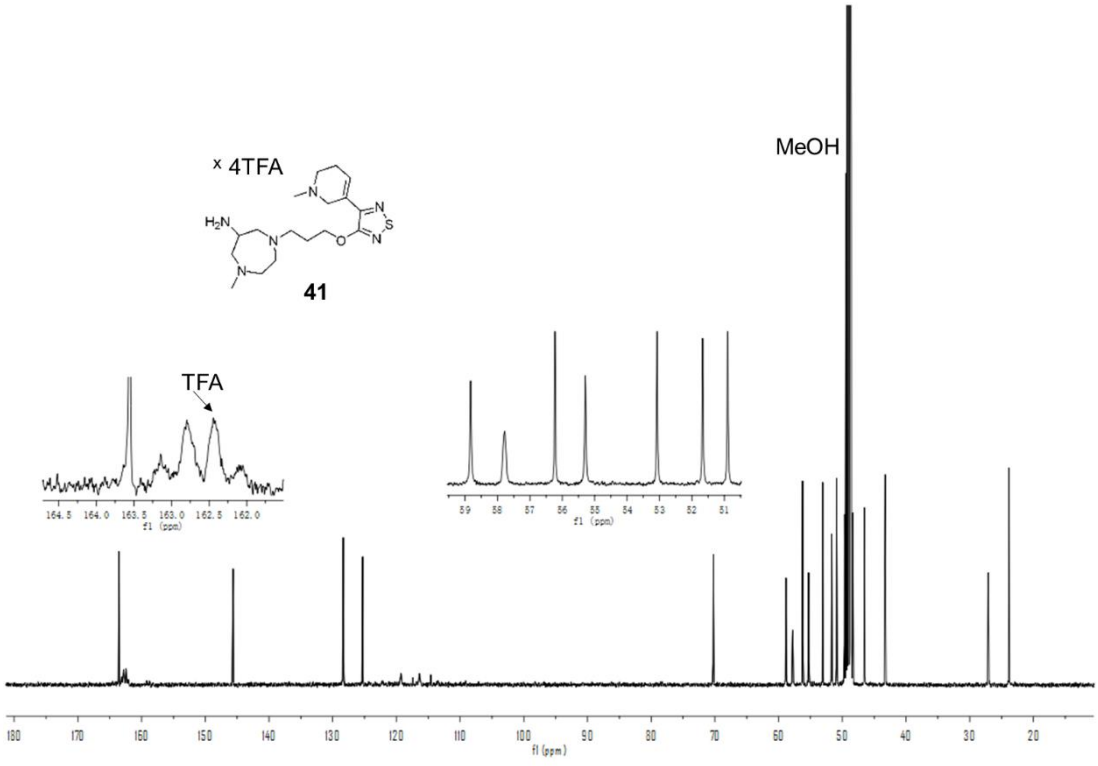

^{13}C-NMR spectrum (100 MHz, [D$_4$]MeOH) of compound **41**.

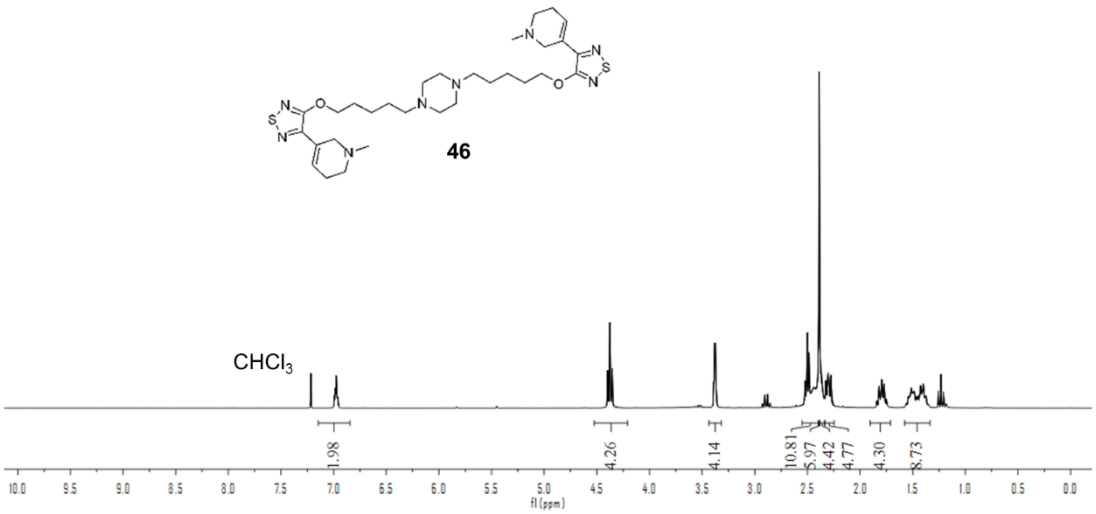

^{1}H-NMR spectrum (300 MHz, $CDCl_3$) of compound **46**.

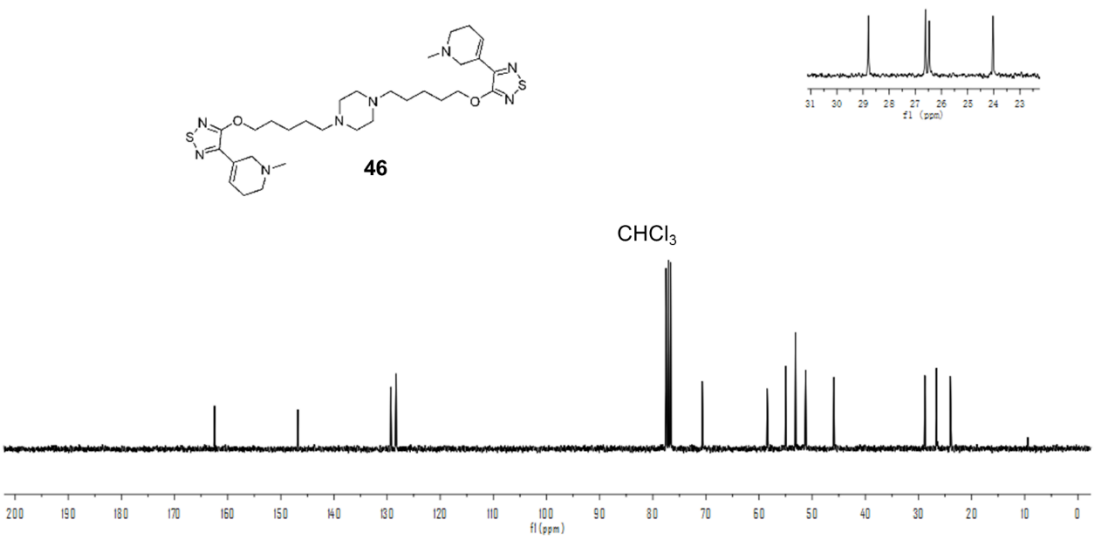

^{13}C-NMR spectrum (75 MHz, $CDCl_3$) of compound **46**.

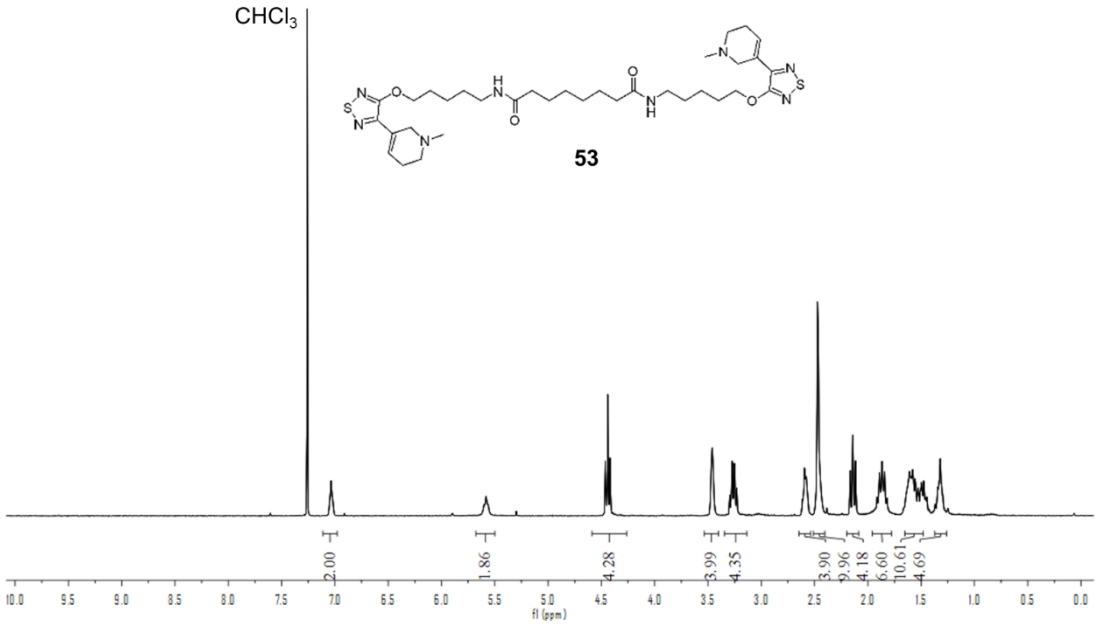

^{1}H-NMR spectrum (300 MHz, $CDCl_3$) of compound **53**.

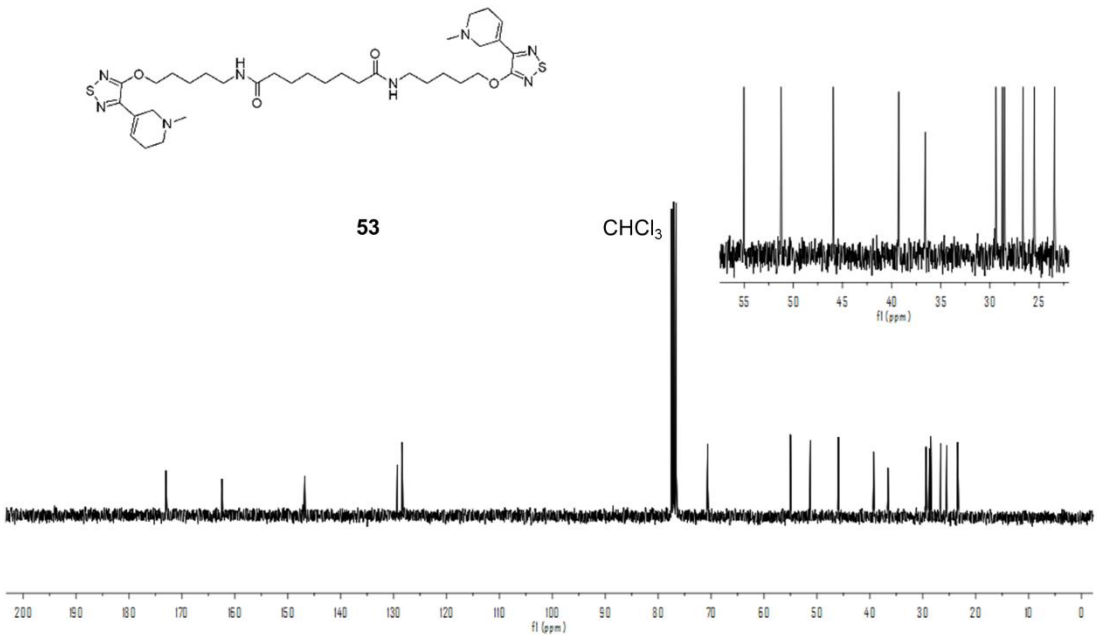

^{13}C-NMR spectrum (75 MHz, $CDCl_3$) of compound **53**.

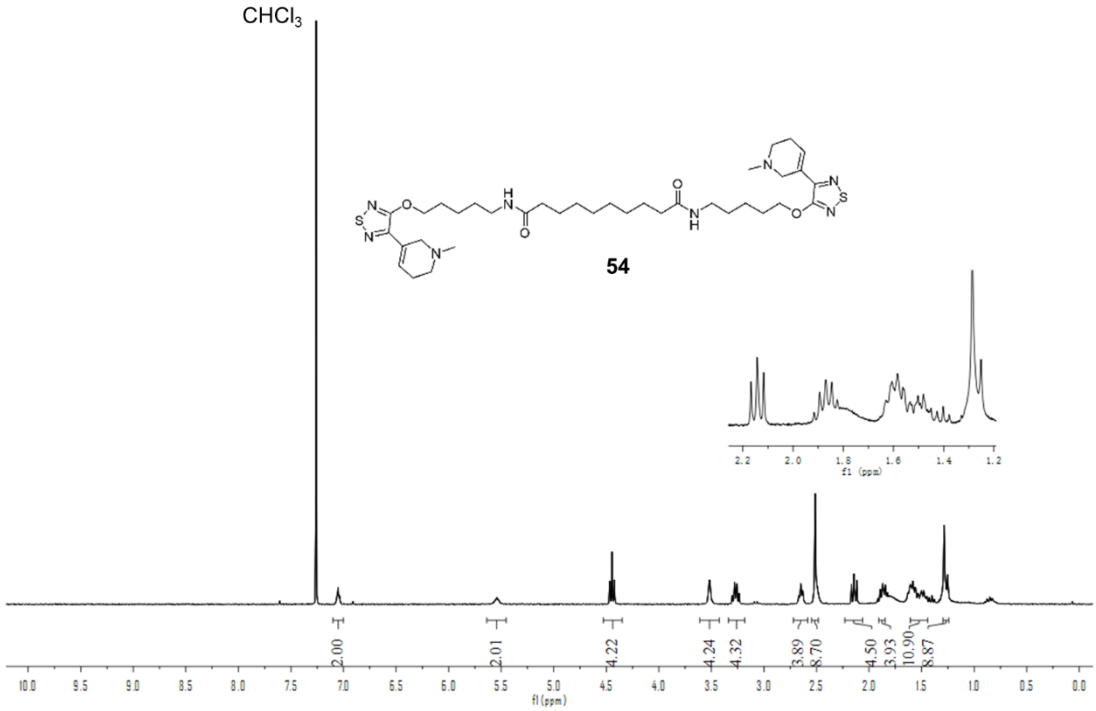

^{1}H-NMR spectrum (300 MHz, $CDCl_3$) of compound **54**.

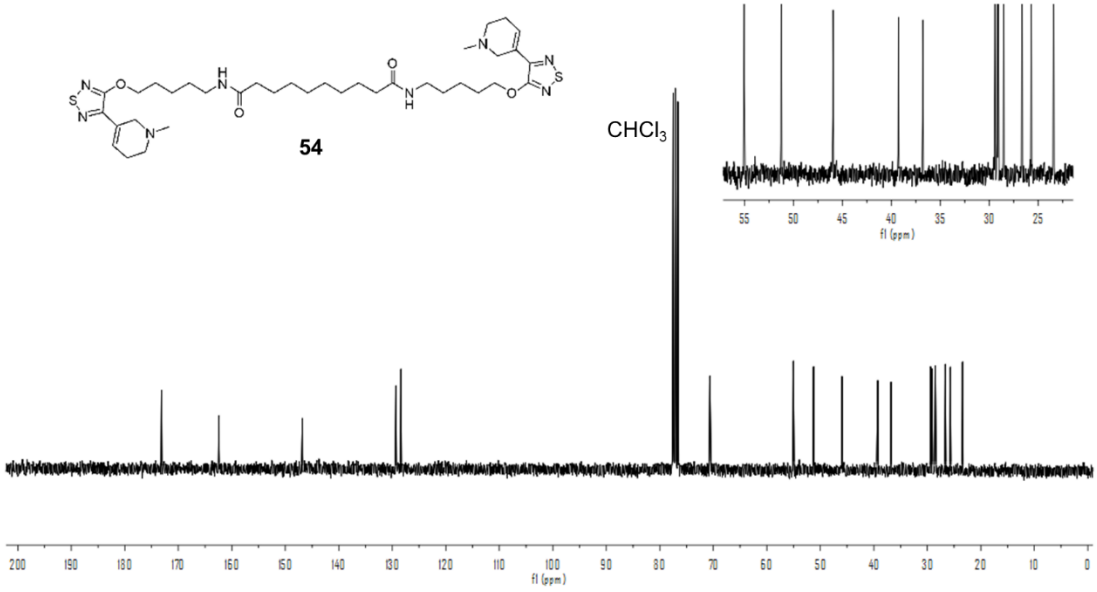

^{13}C-NMR spectrum (75 MHz, $CDCl_3$) of compound **54**.

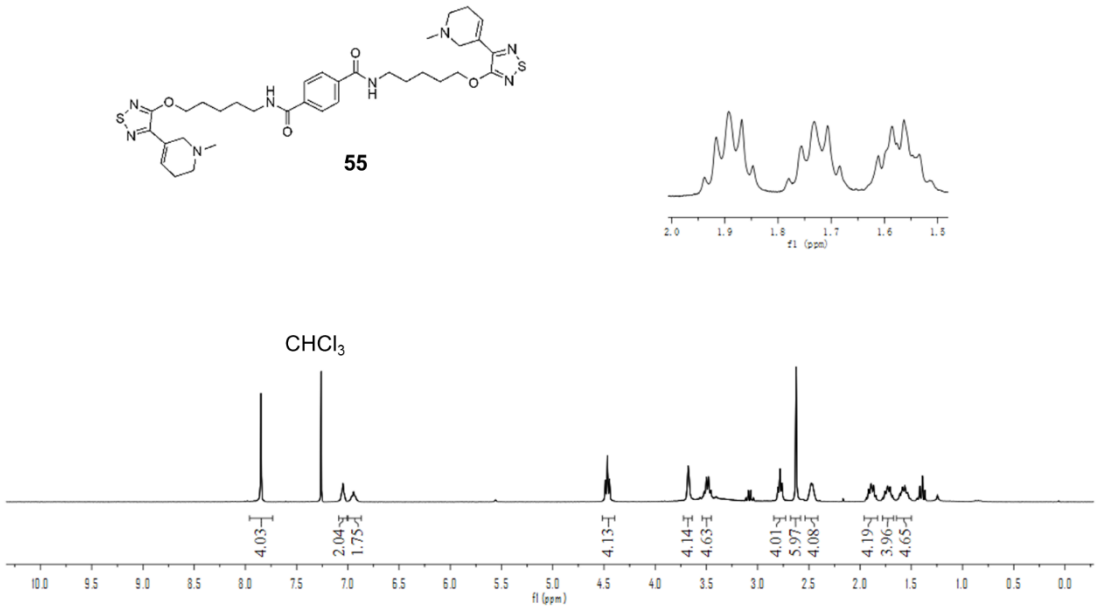

^{1}H-NMR spectrum (300 MHz, $CDCl_3$) of compound **55**.

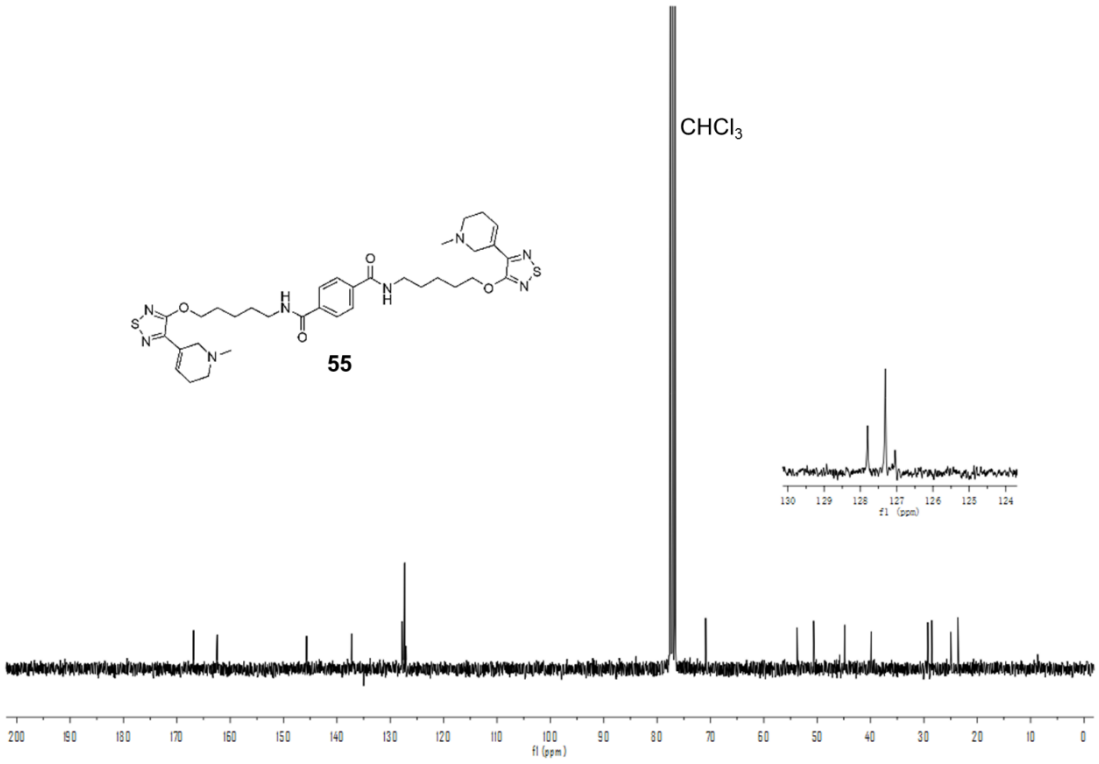

^{13}C-NMR spectrum (75 MHz, $CDCl_3$) of compound **55**.

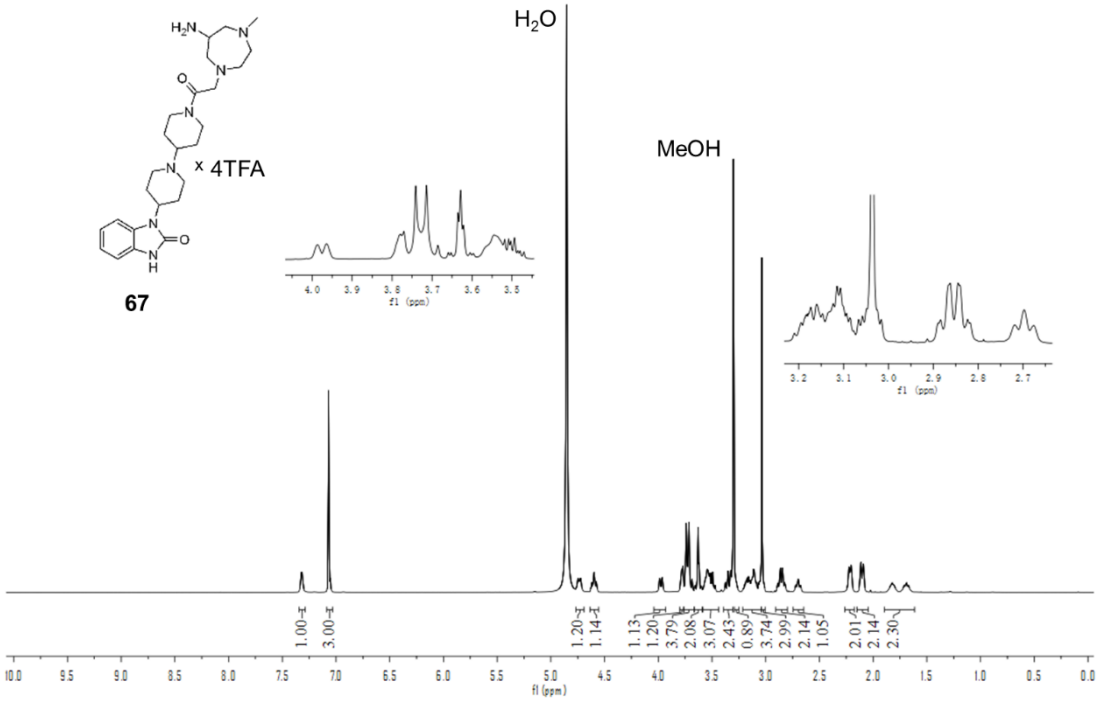

^{1}H-NMR spectrum (600 MHz, [D$_4$]MeOH) of compound **67**.

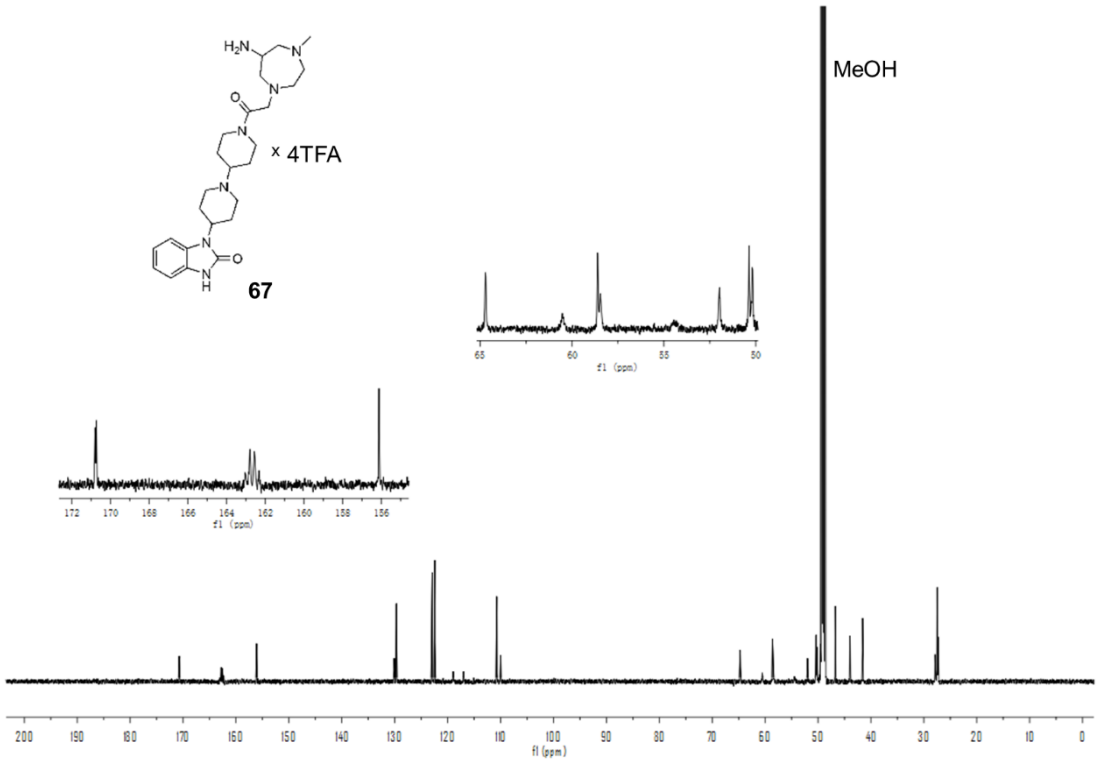

^{13}C-NMR spectrum (150 MHz, [D$_4$]MeOH) of compound **67**.

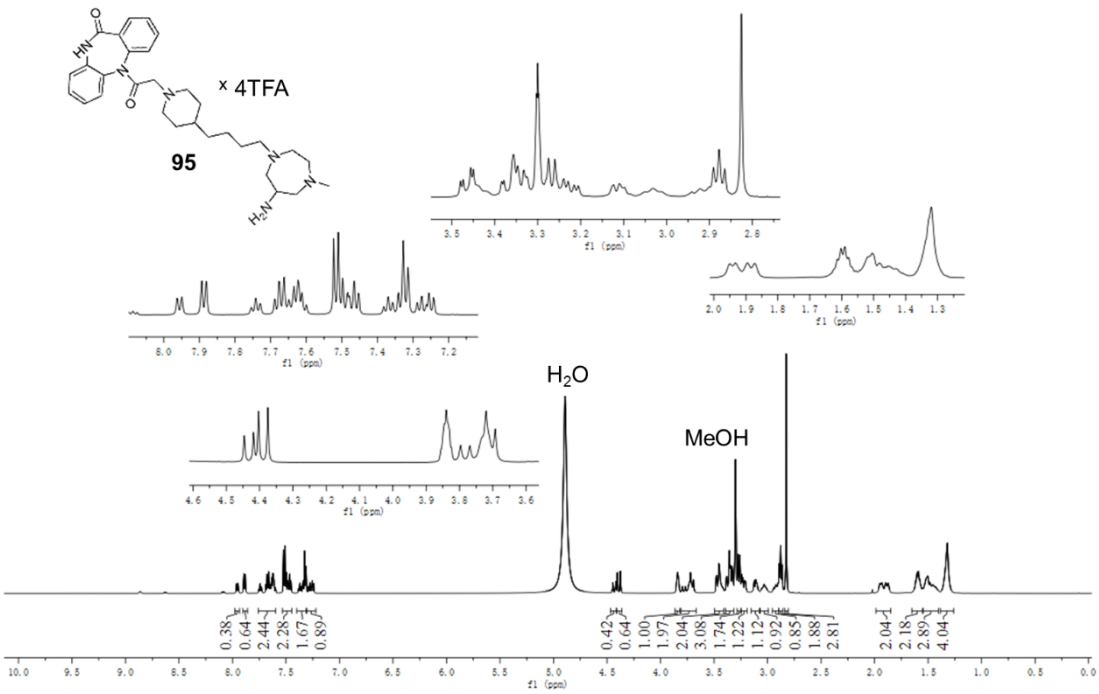

^{1}H-NMR spectrum (600 MHz, [D$_4$]MeOH) of compound **95**.

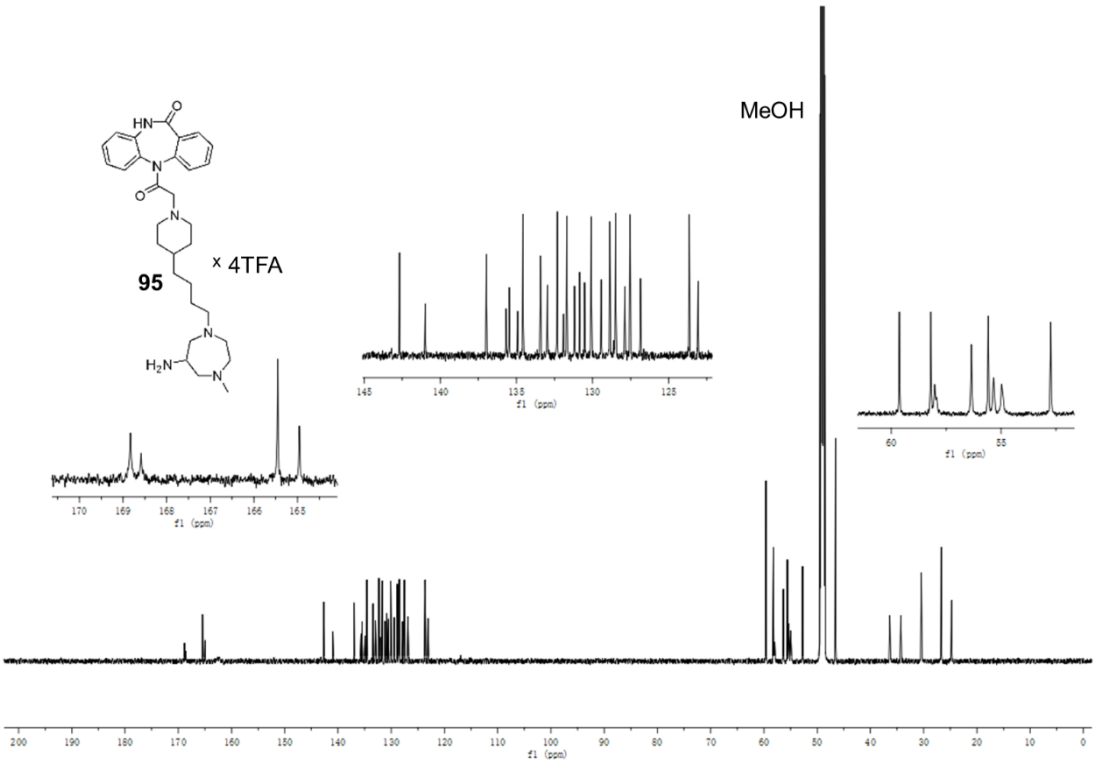

^{13}C-NMR spectrum (150 MHz, [D$_4$]MeOH) of compound **95**.

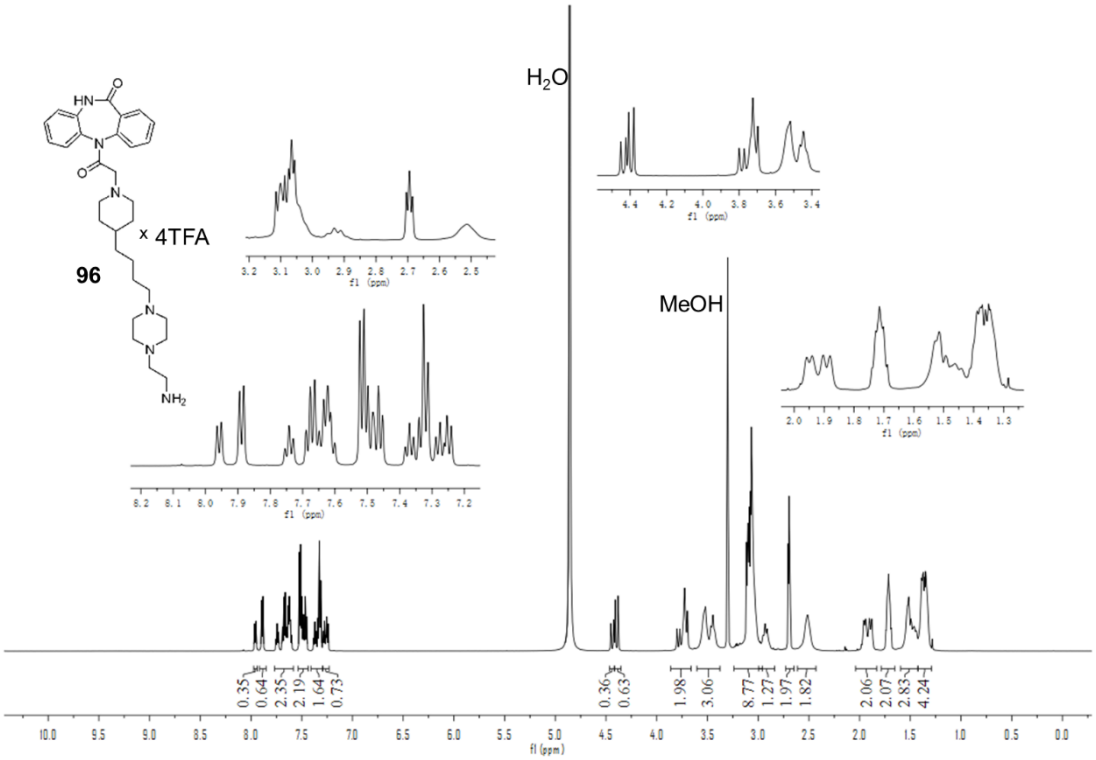

^{1}H-NMR spectrum (600 MHz, [D$_4$]MeOH) of compound **96**.

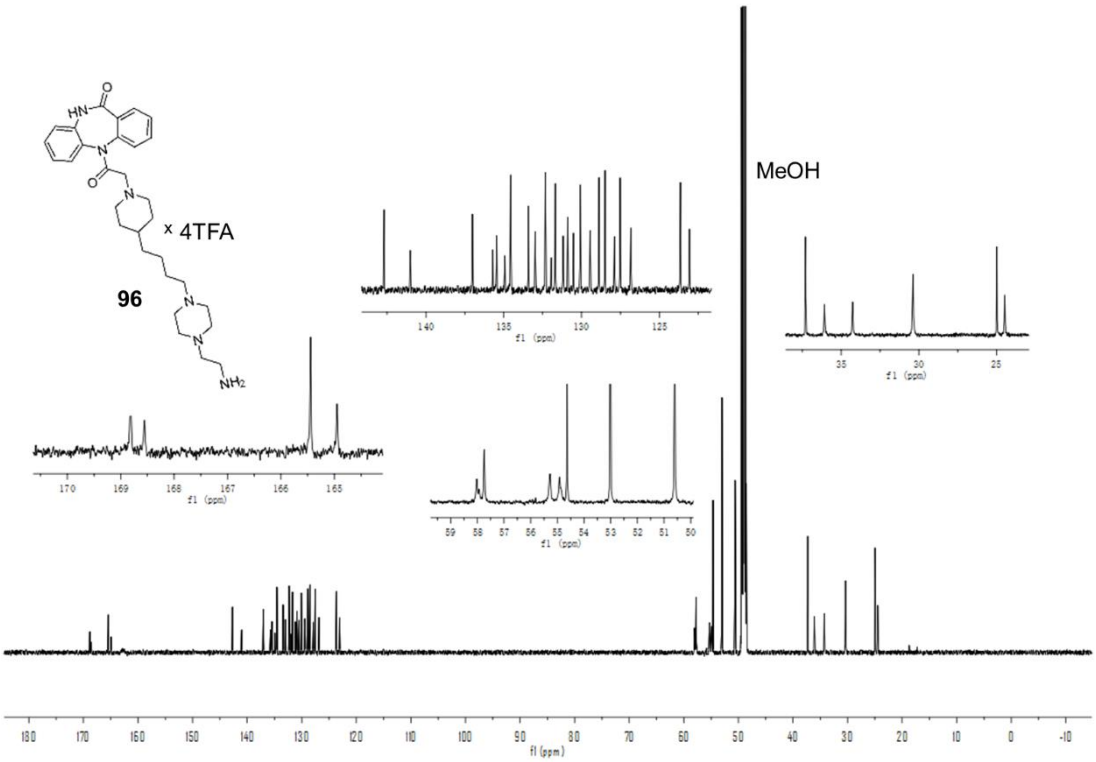

^{13}C-NMR spectrum (150 MHz, [D$_4$]MeOH) of compound **96**.

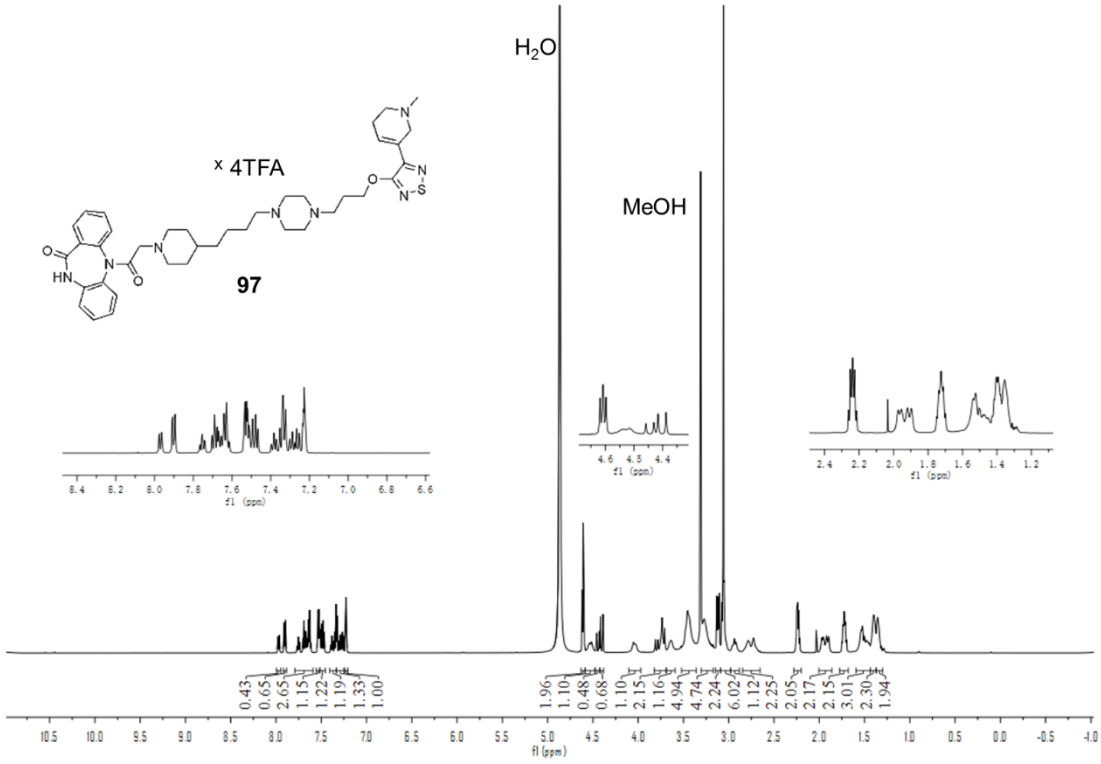

^{1}H-NMR spectrum (600 MHz, [D$_4$]MeOH) of compound **97**.

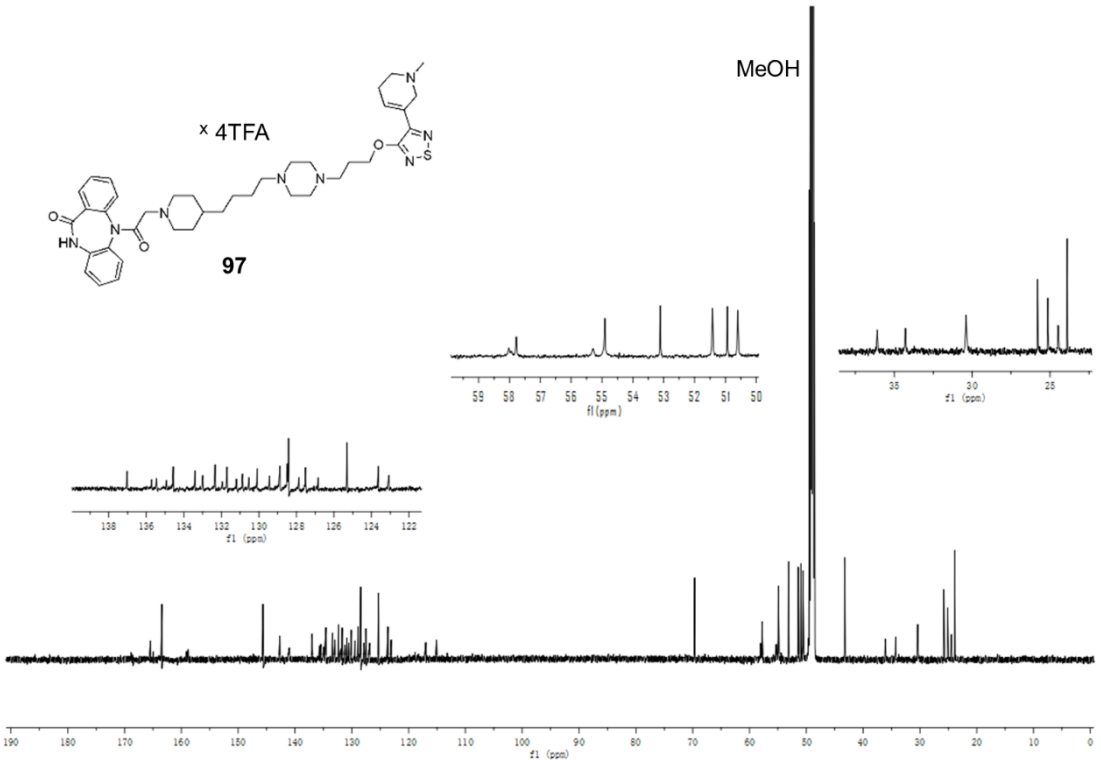

^{13}C-NMR spectrum (150 MHz, [D$_4$]MeOH) of compound **97**.

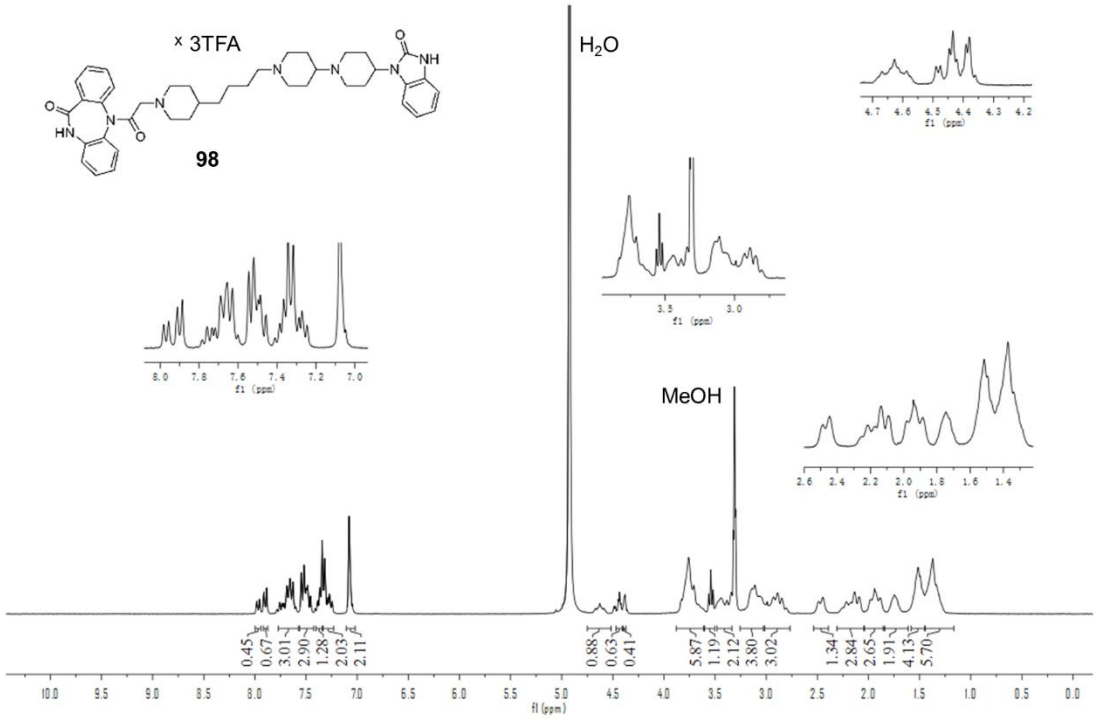

^{1}H-NMR spectrum (300 MHz, [D$_4$]MeOH) of compound **98**.

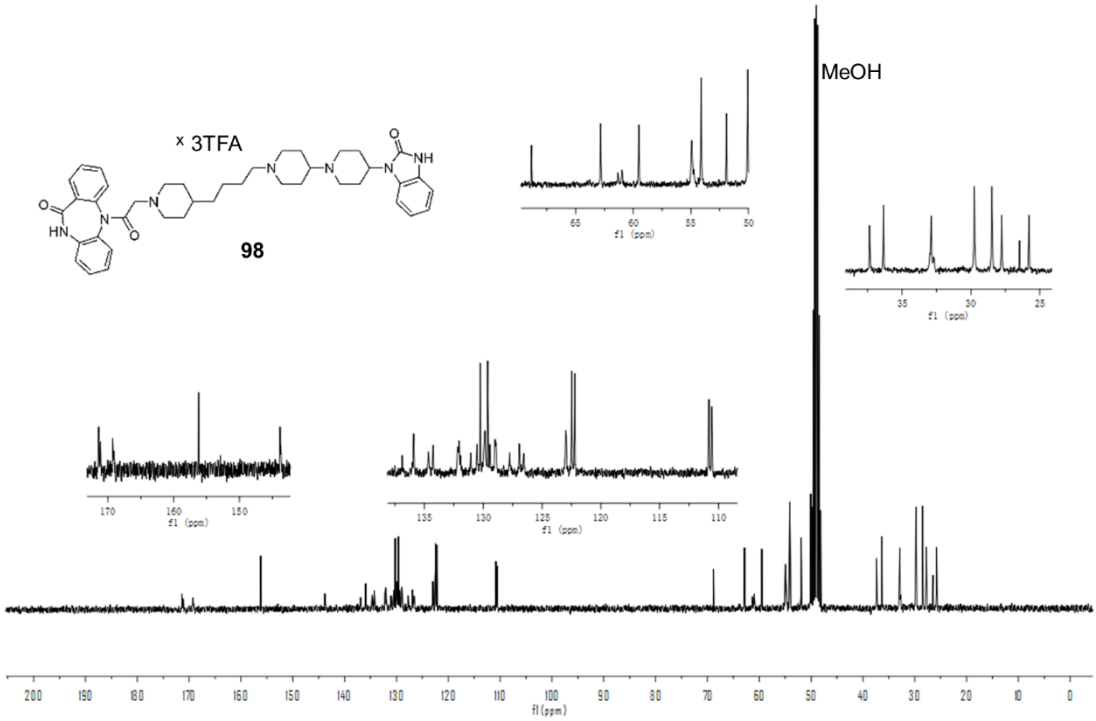

^{13}C-NMR spectrum (75 MHz, [D$_4$]MeOH) of compound **98**.

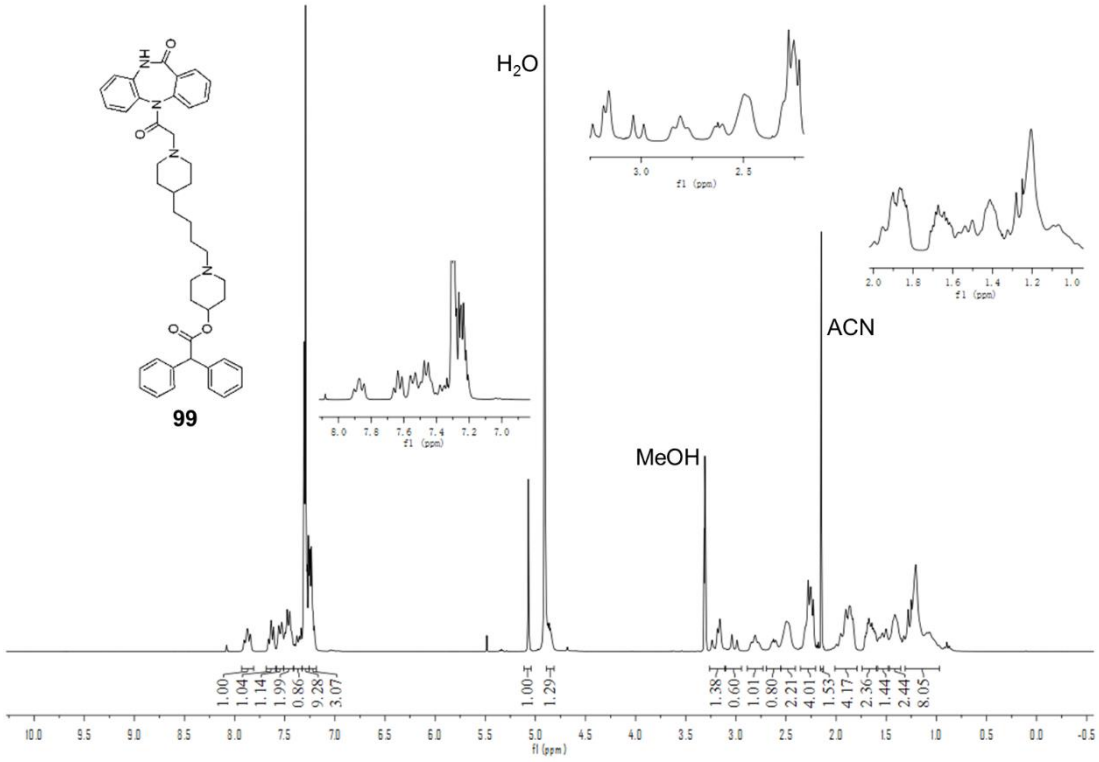

^{1}H-NMR spectrum (300 MHz, [D$_4$]MeOH) of compound **99**.

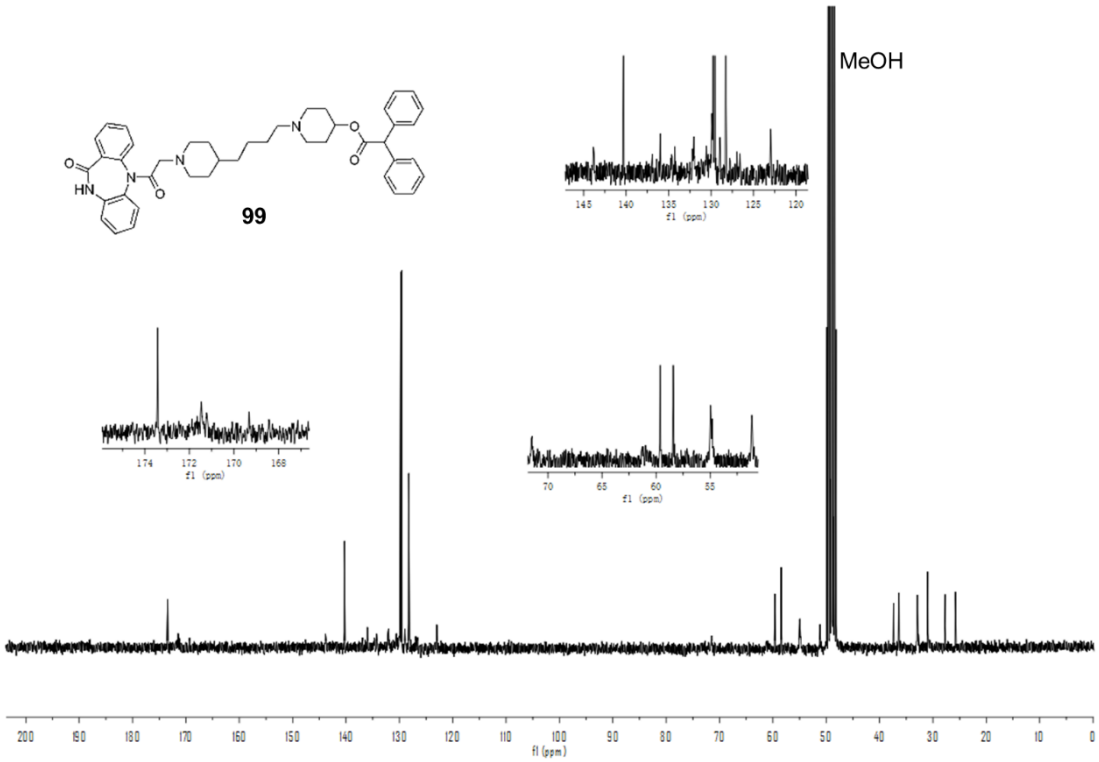

^{13}C-NMR spectrum (75 MHz, [D$_4$]MeOH) of compound **99**.

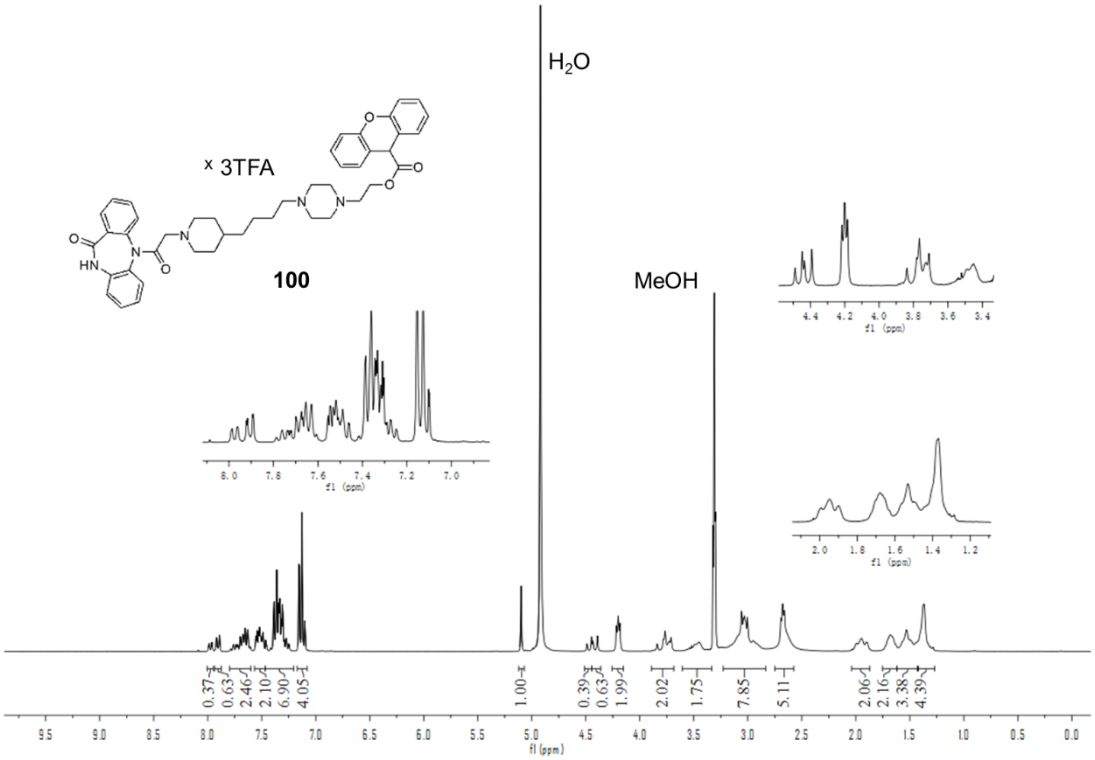

^{1}H-NMR spectrum (300 MHz, [D$_4$]MeOH) of compound **100**.

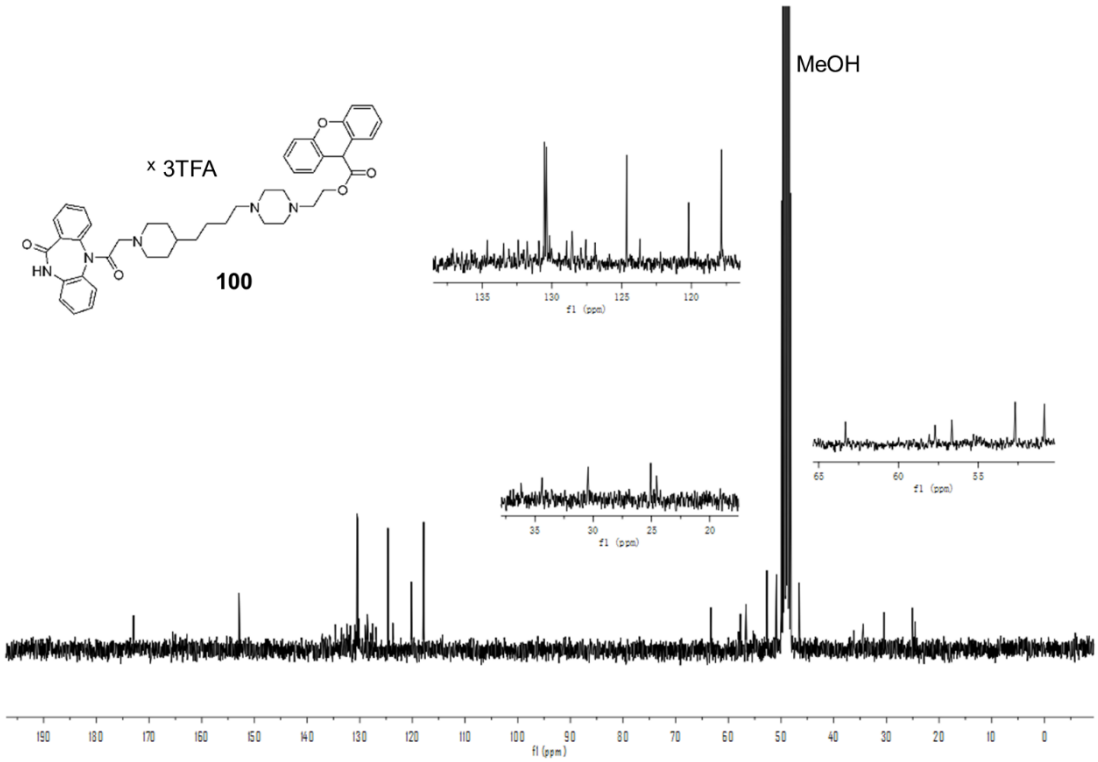

^{13}C-NMR spectrum (75 MHz, [D$_4$]MeOH) of compound **100**.

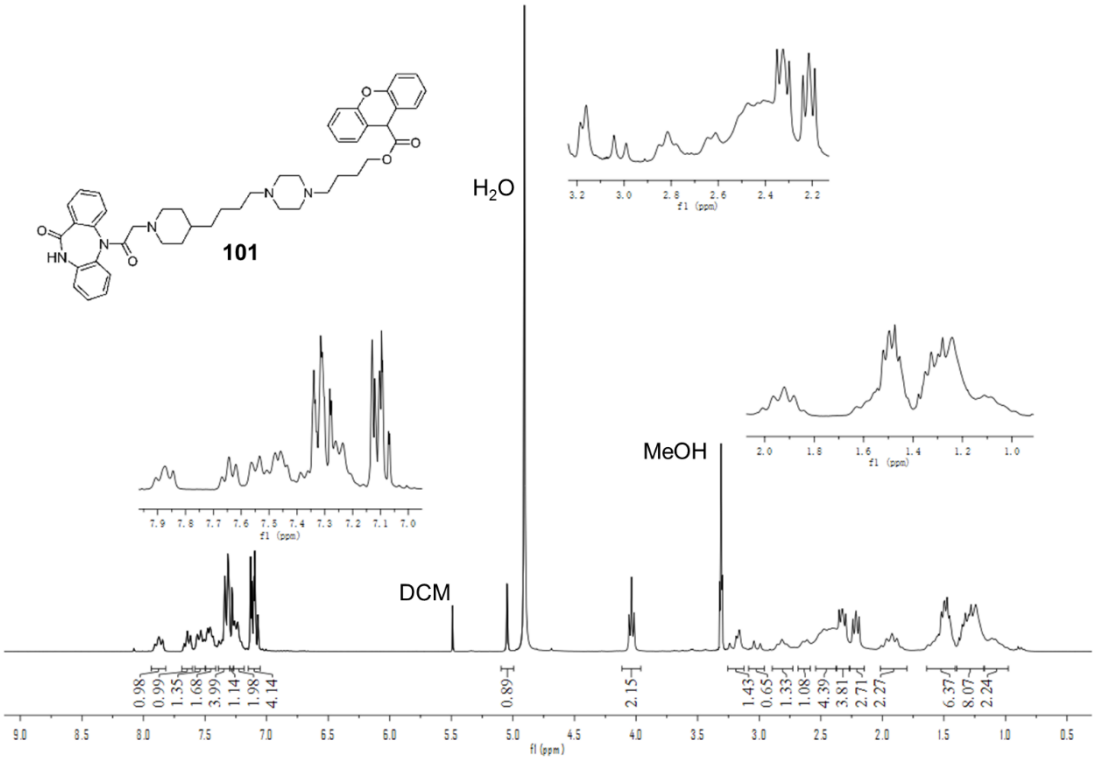

^{1}H-NMR spectrum (300 MHz, [D$_4$]MeOH) of compound **101**.

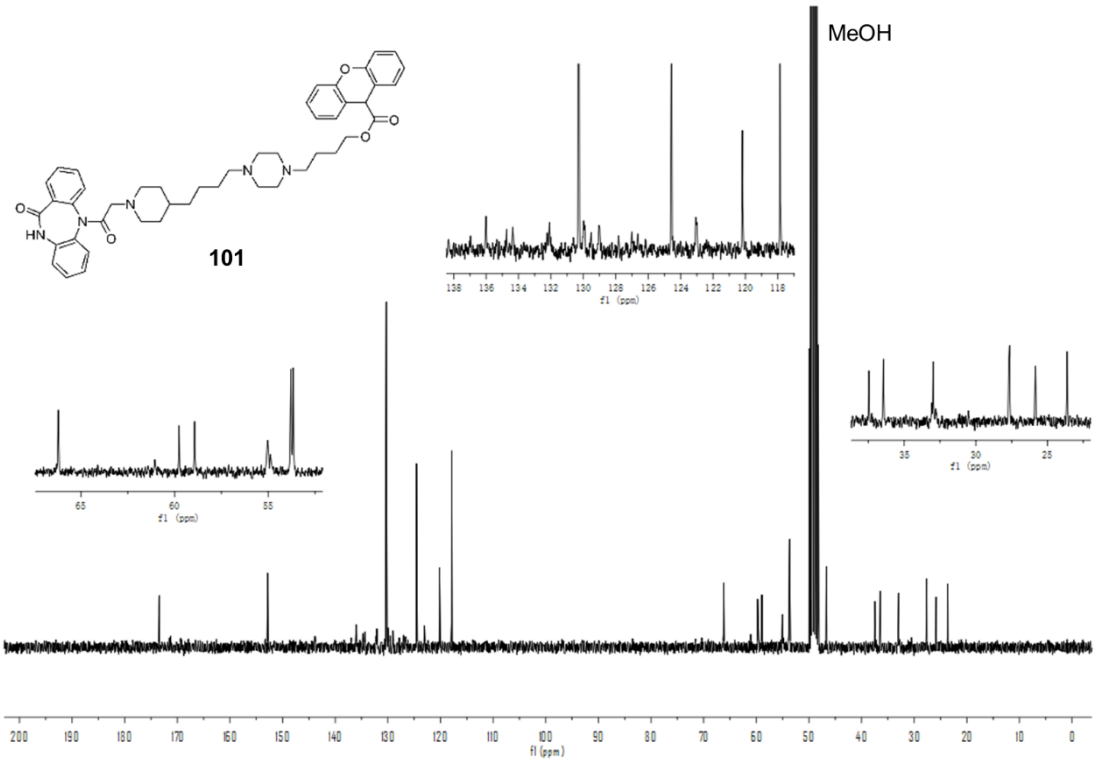

^{13}C-NMR spectrum (75 MHz, [D$_4$]MeOH) of compound **101**.

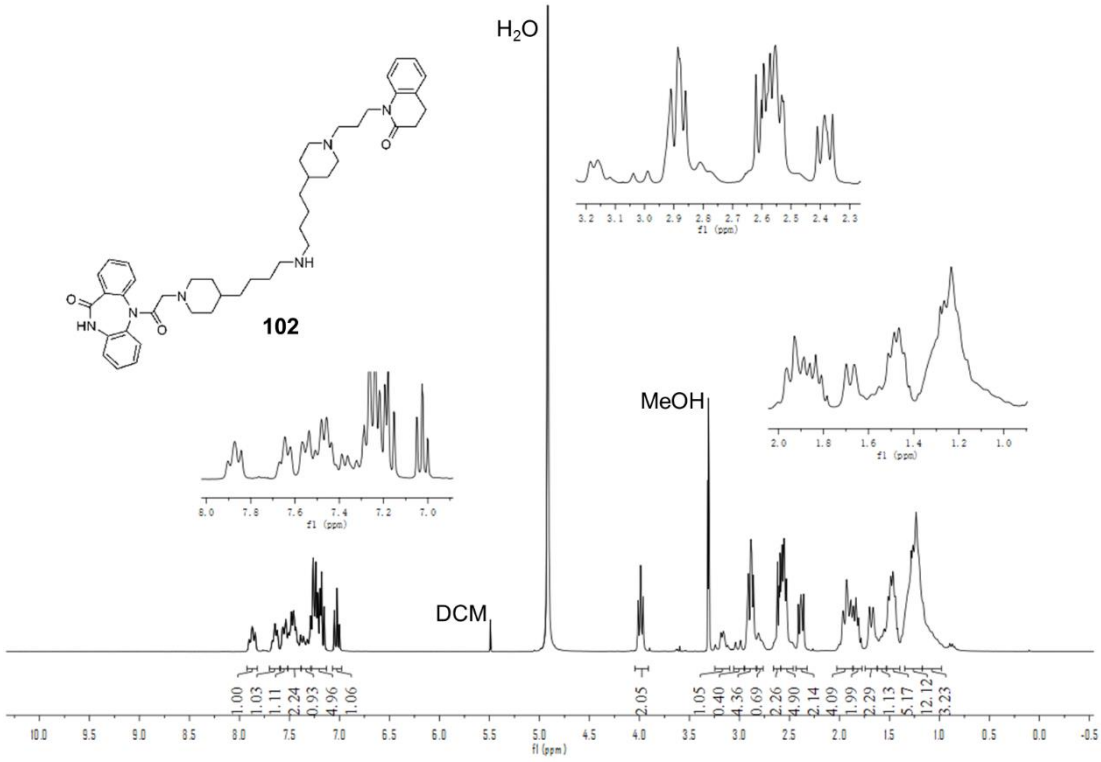

^{1}H-NMR spectrum (300 MHz, [D$_4$]MeOH) of compound **102**.

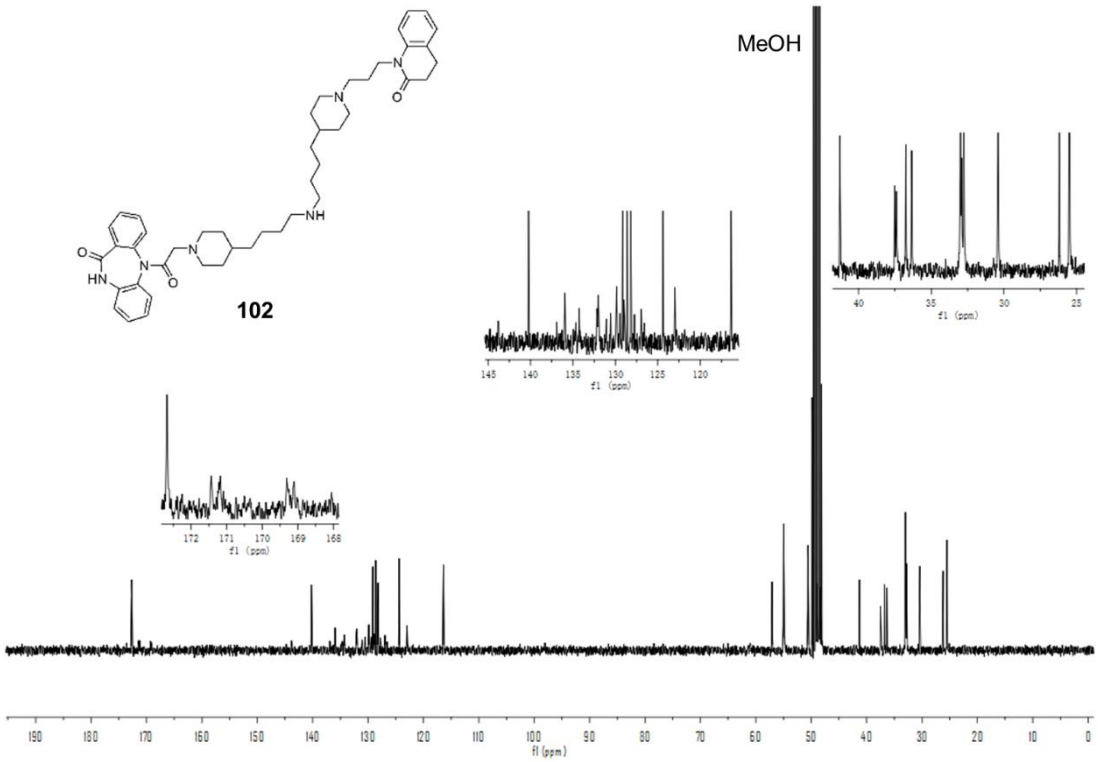

^{13}C-NMR spectrum (75 MHz, [D$_4$]MeOH) of compound **102**.

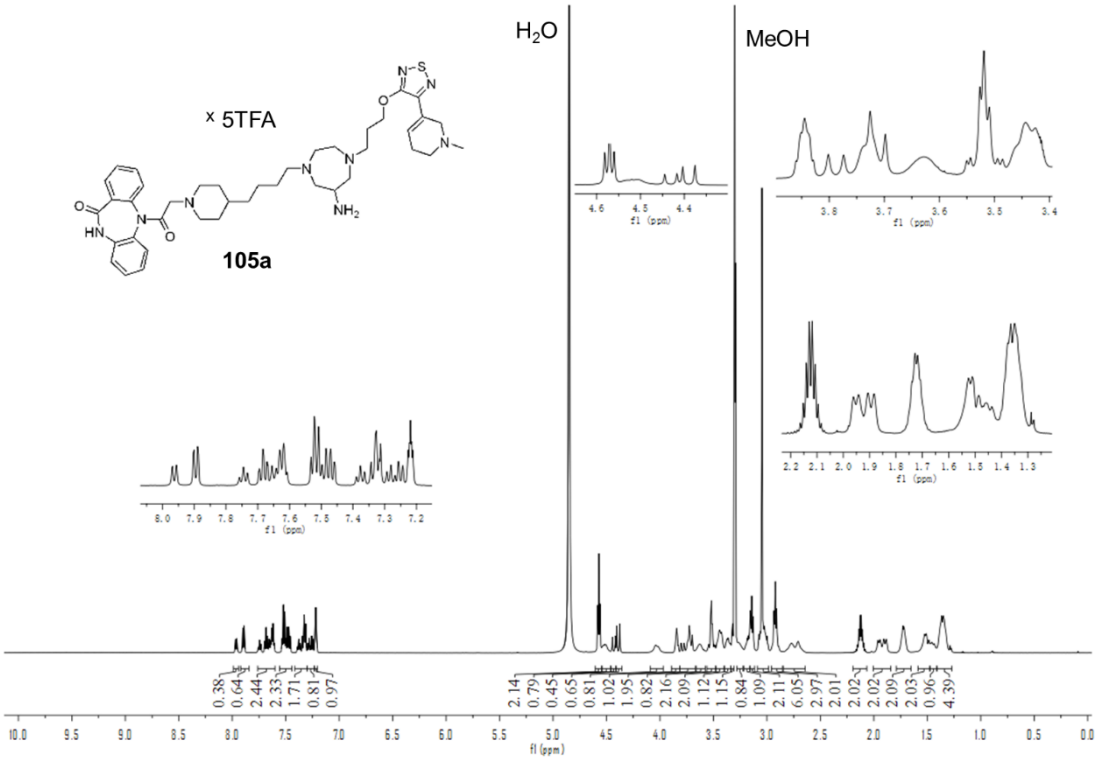

^{1}H-NMR spectrum (600 MHz, [D$_4$]MeOH) of compound **105a**.

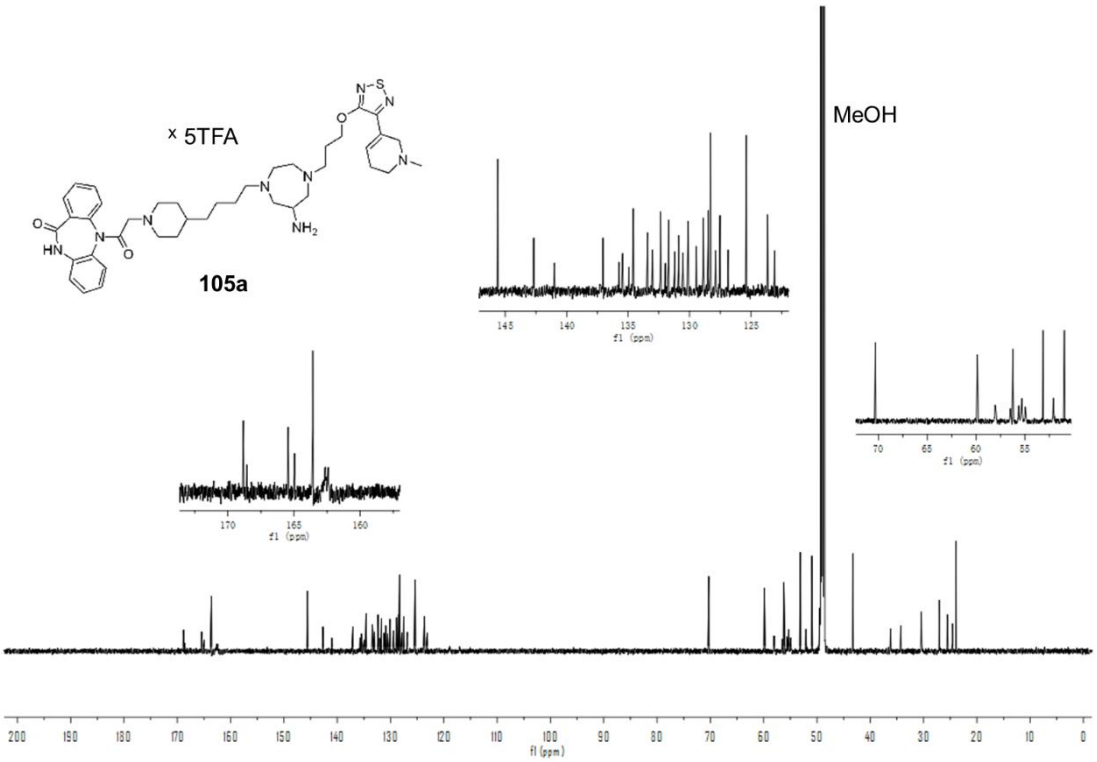

^{13}C-NMR spectrum (75 MHz, [D$_4$]MeOH) of compound **105a**.

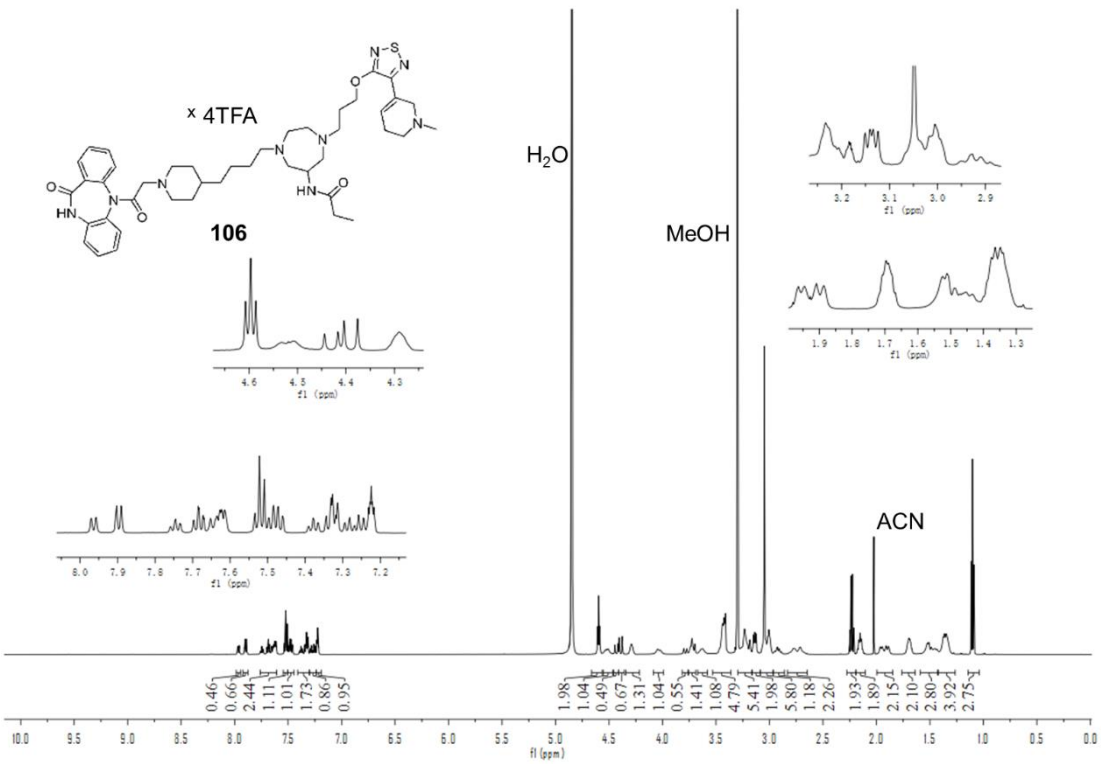

^{1}H-NMR spectrum (600 MHz, [D$_4$]MeOH) of compound **106**.

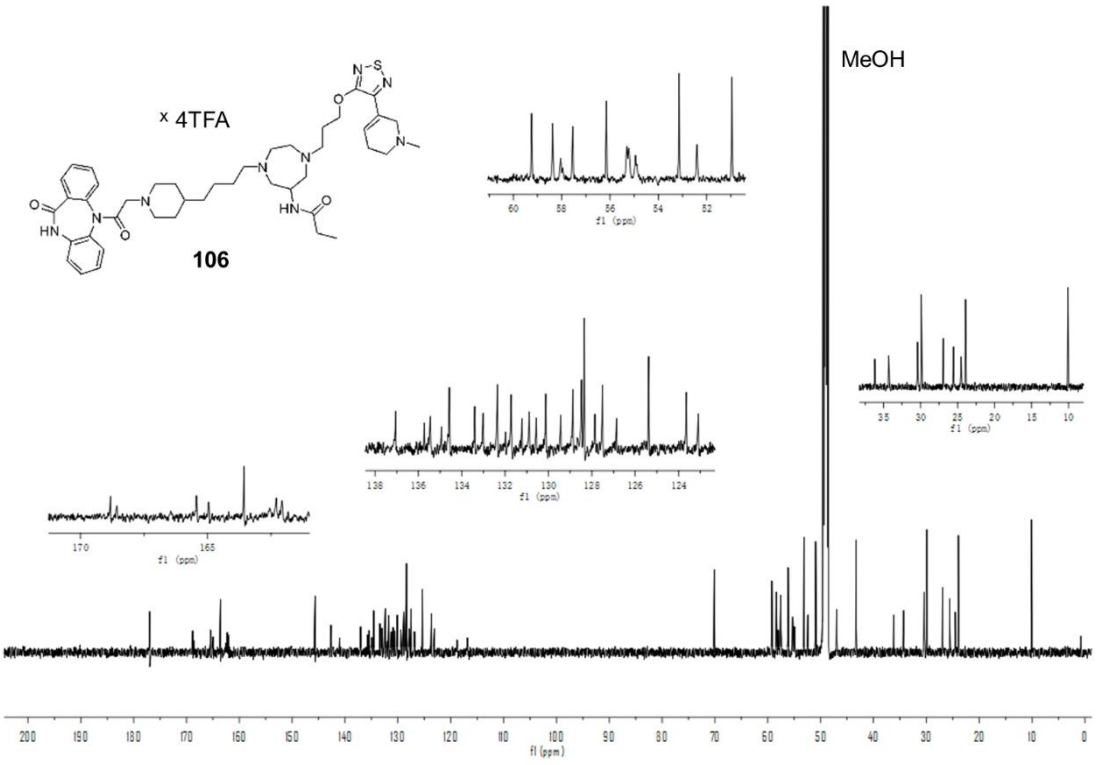

^{13}C-NMR spectrum (150 MHz, [D$_4$]MeOH) of compound **106**.

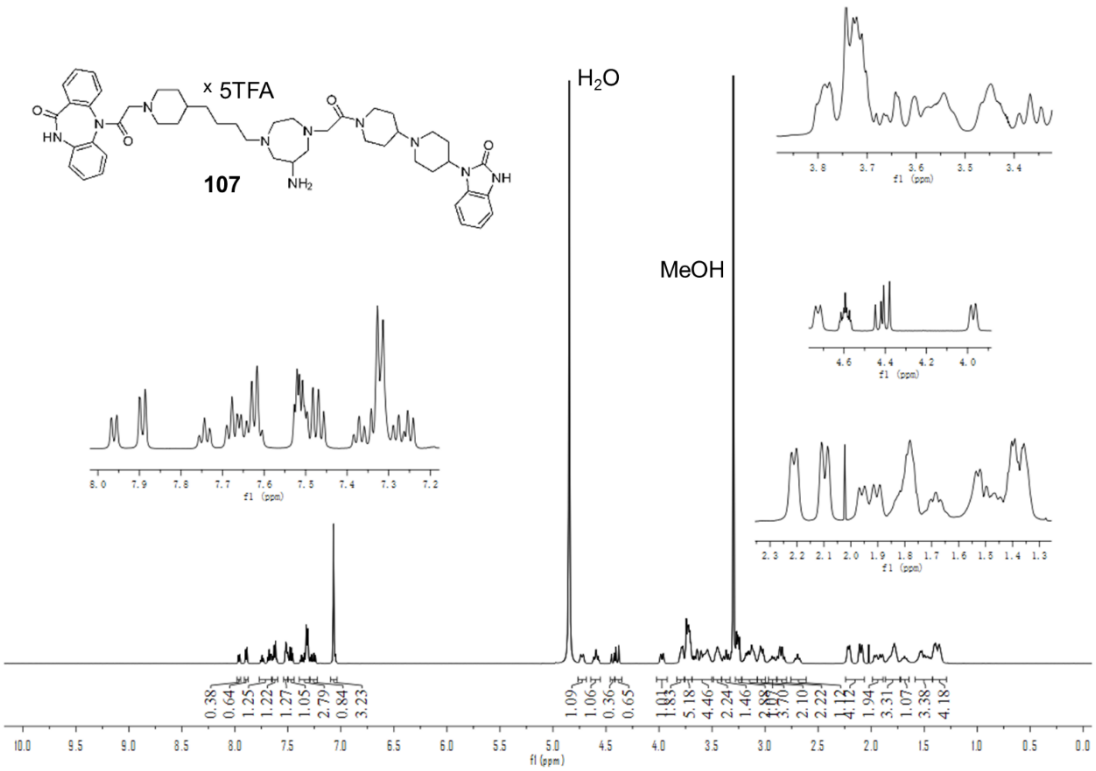

^{1}H-NMR spectrum (600 MHz, [D_4]MeOH) of compound **107**.

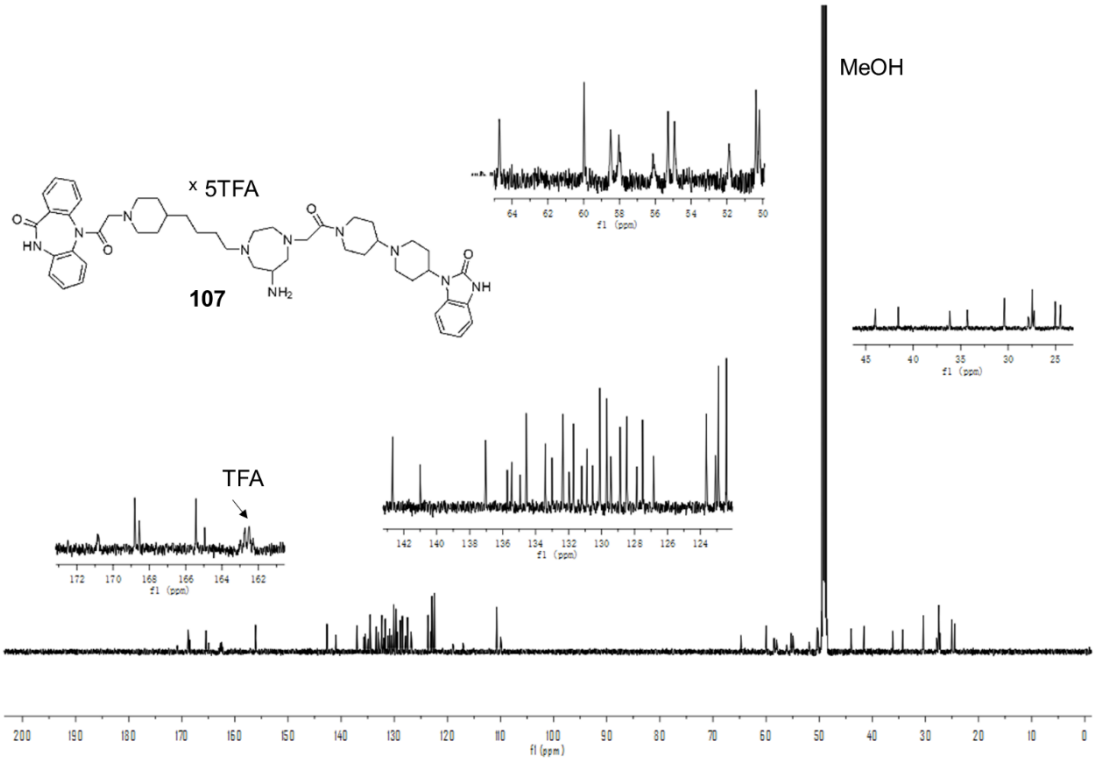

^{13}C-NMR spectrum (150 MHz, [D_4]MeOH) of compound **107**.

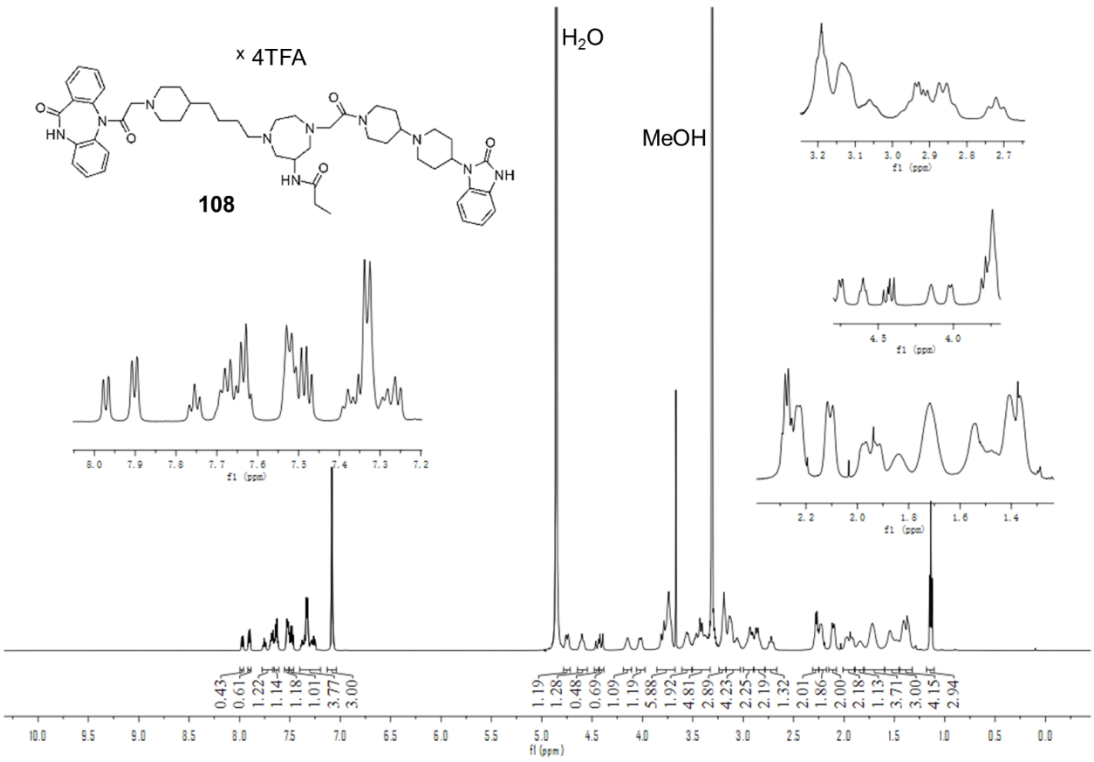

^{1}H-NMR spectrum (600 MHz, [D_4]MeOH) of compound **108**.

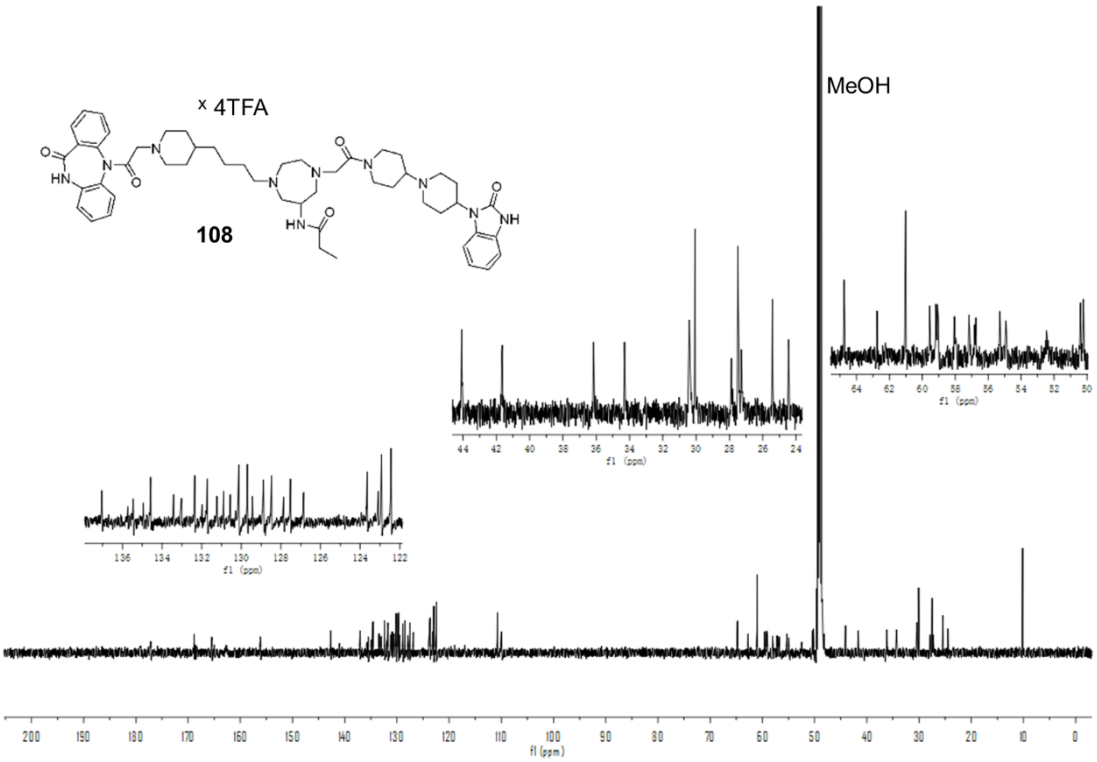

^{13}C-NMR spectrum (150 MHz, [D_4]MeOH) of compound **108**.

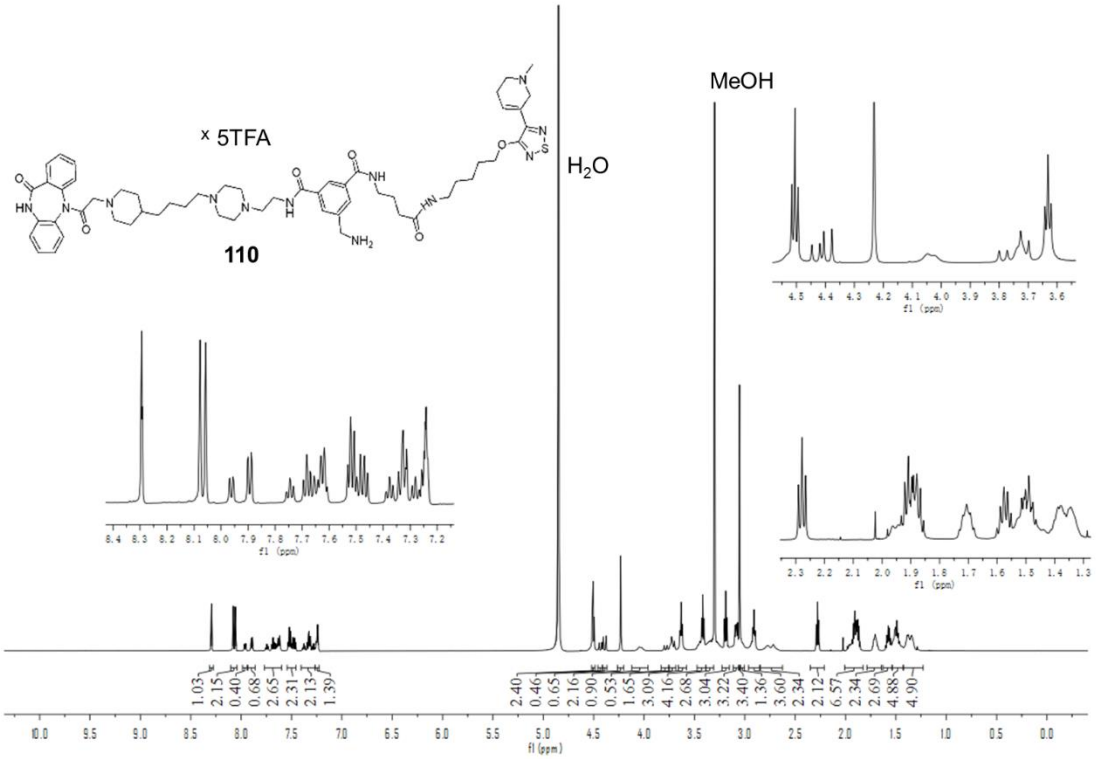

^{1}H-NMR spectrum (600 MHz, [D$_4$]MeOH) of compound **110**.

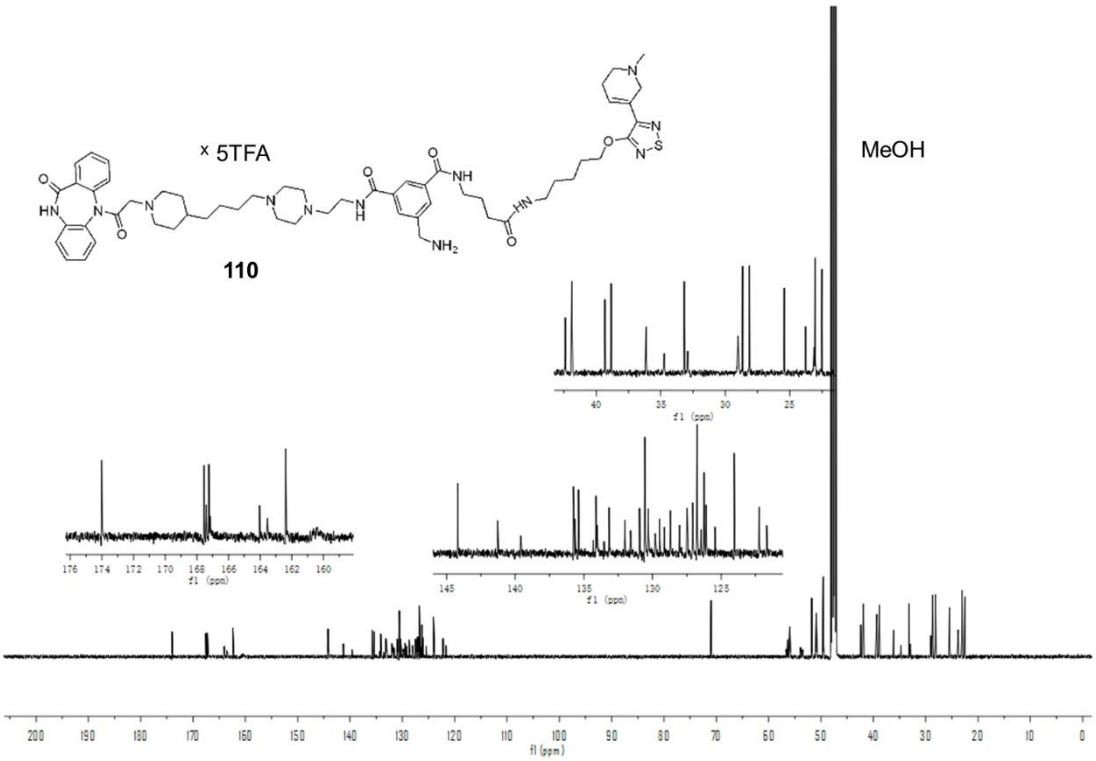

^{13}C-NMR spectrum (150 MHz, [D$_4$]MeOH) of compound **110**.

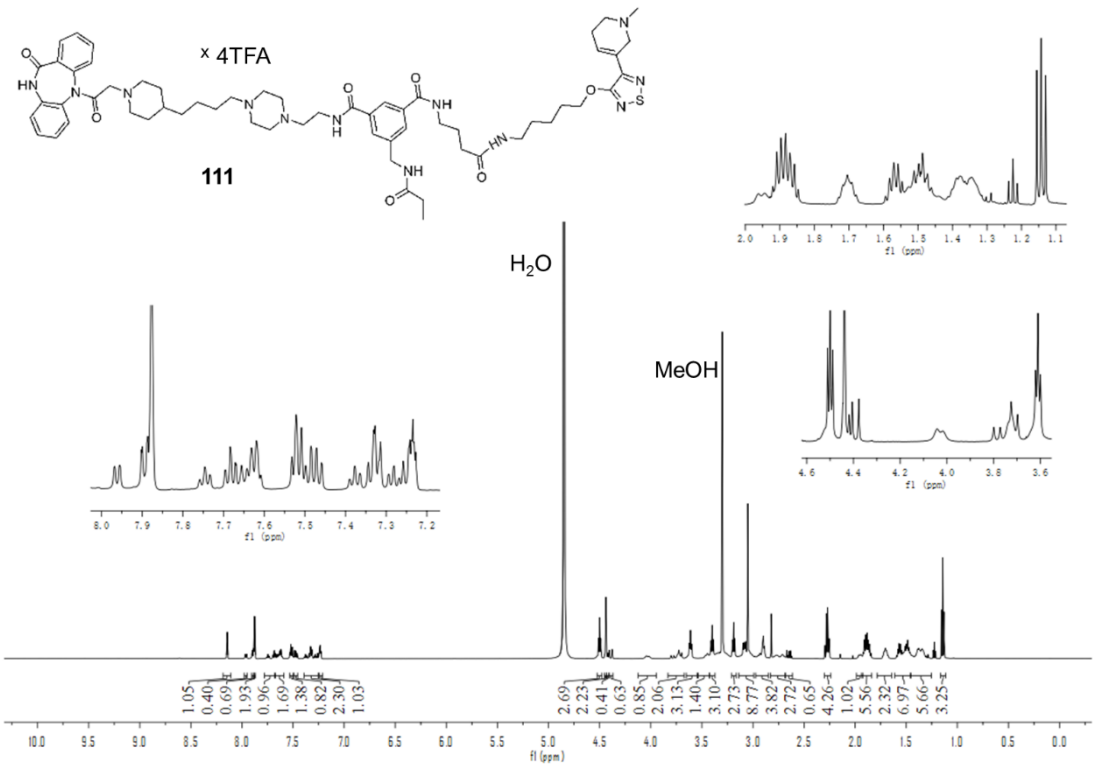

^{1}H-NMR spectrum (600 MHz, [D$_4$]MeOH) of compound **111**.

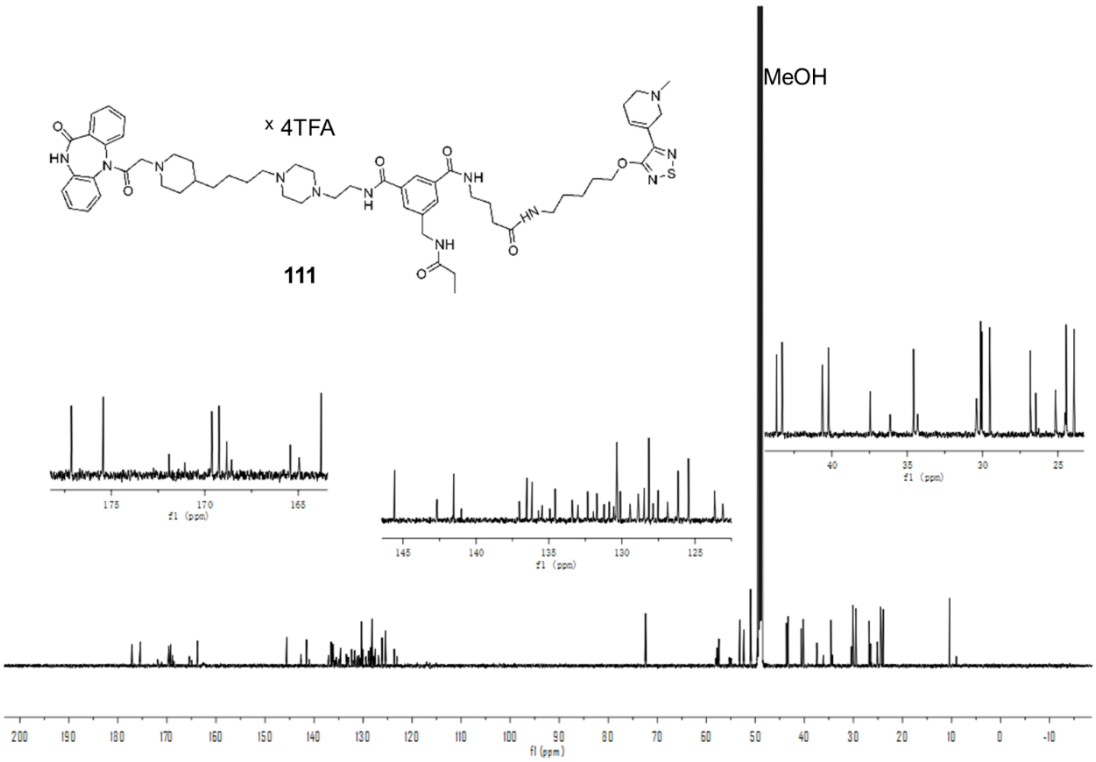

^{13}C-NMR spectrum (150 MHz, [D$_4$]MeOH) of compound **111**.

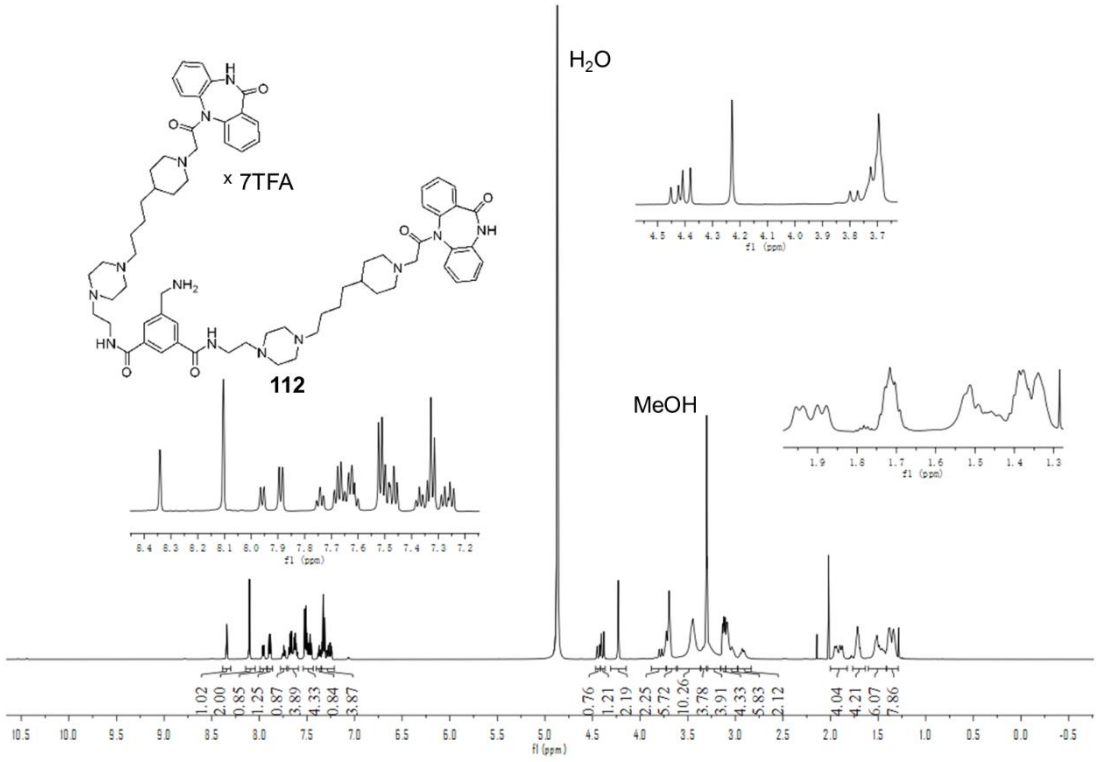

^{1}H-NMR spectrum (600 MHz, [D$_4$]MeOH) of compound **112**.

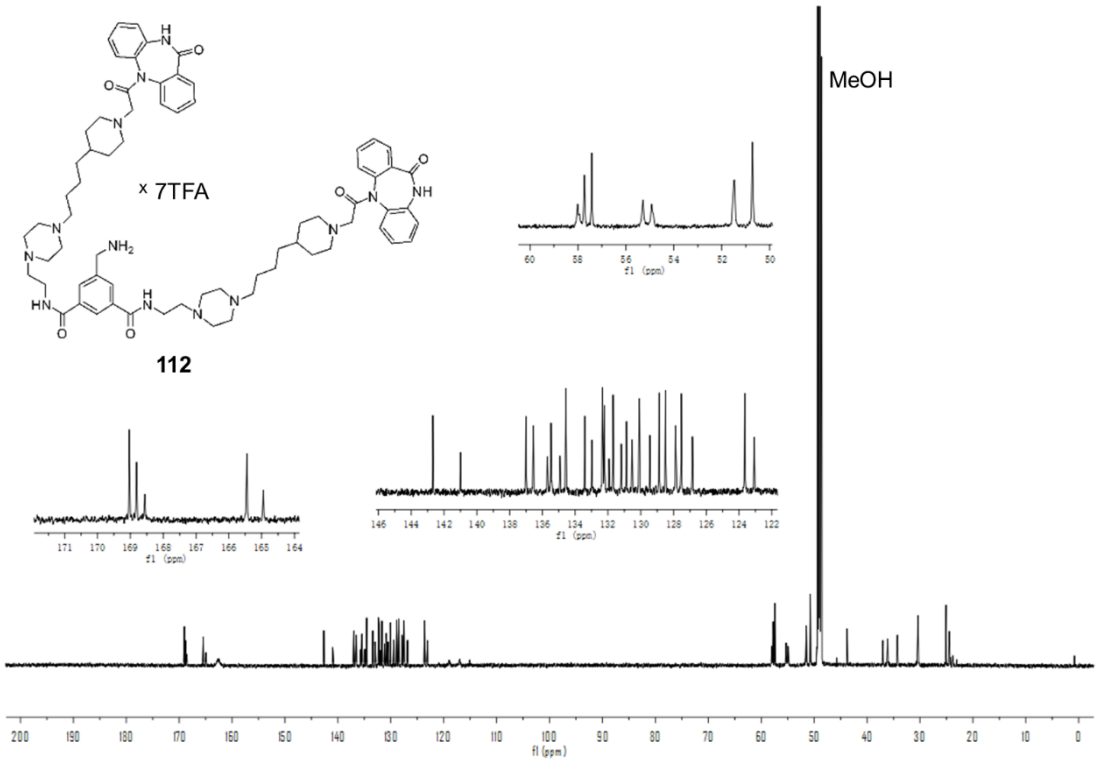

^{13}C-NMR spectrum (150 MHz, [D$_4$]MeOH) of compound **112**.

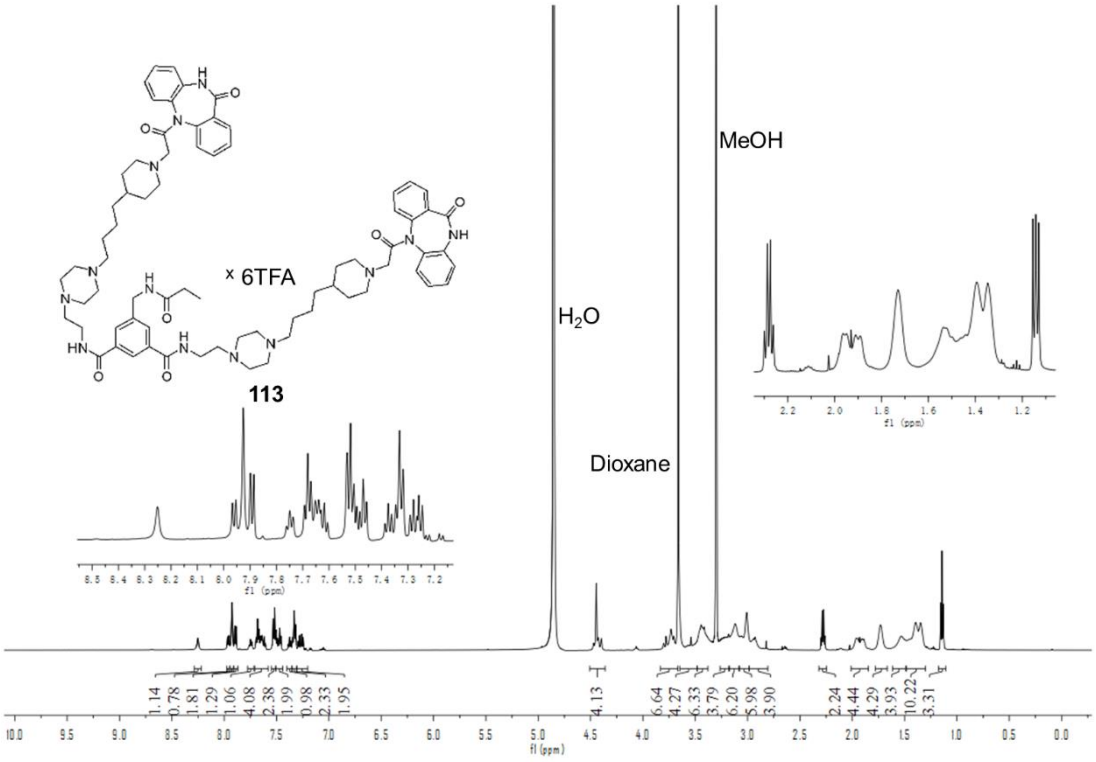

^{1}H-NMR spectrum (600 MHz, [D$_4$]MeOH) of compound **113**.

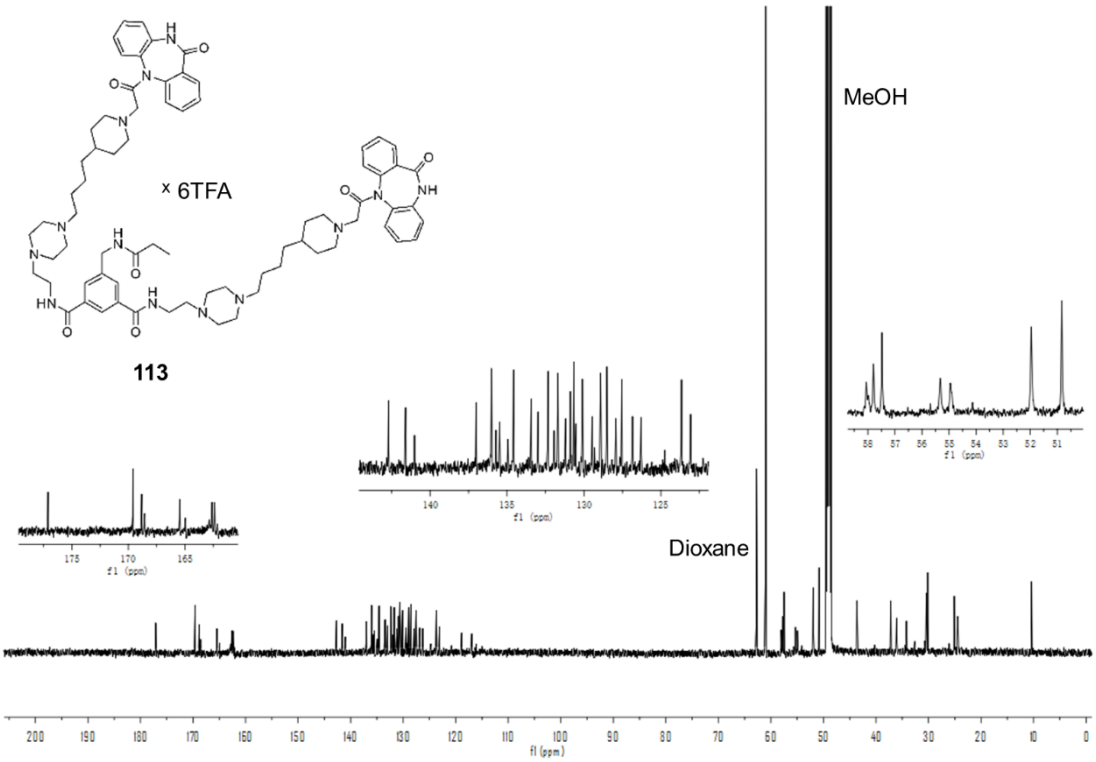

^{13}C-NMR spectrum (150 MHz, [D$_4$]MeOH) of compound **113**.

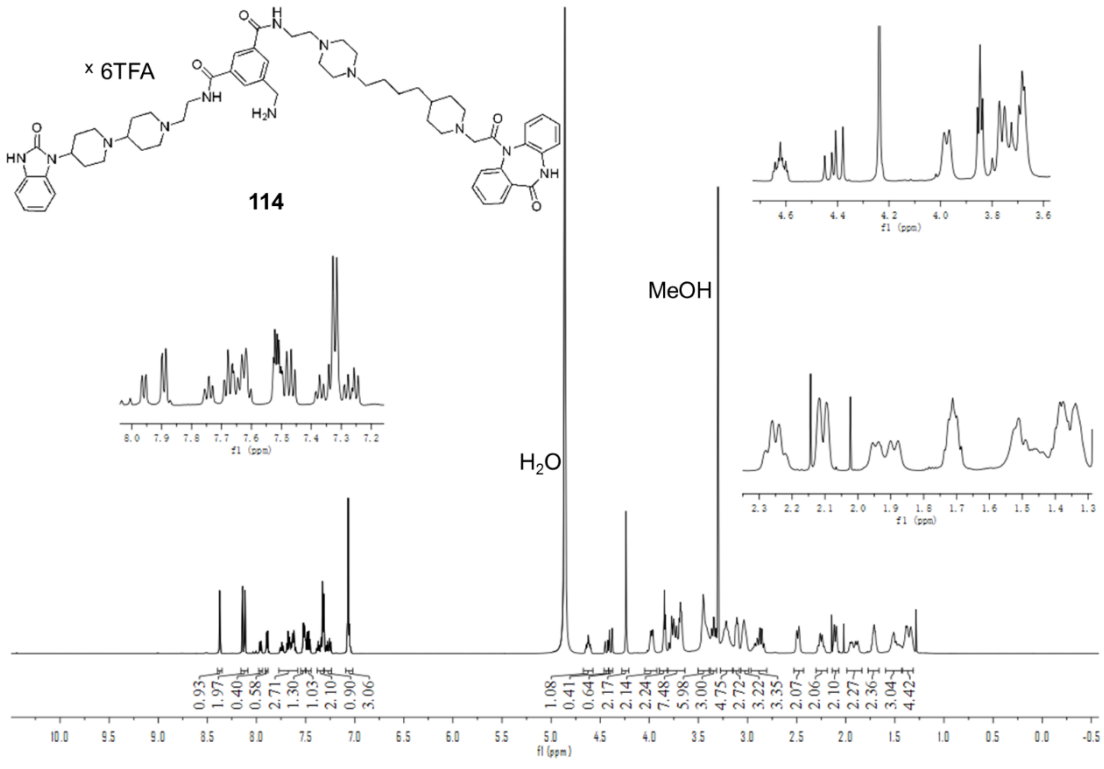

^{1}H-NMR spectrum (600 MHz, [D$_4$]MeOH) of compound **114**.

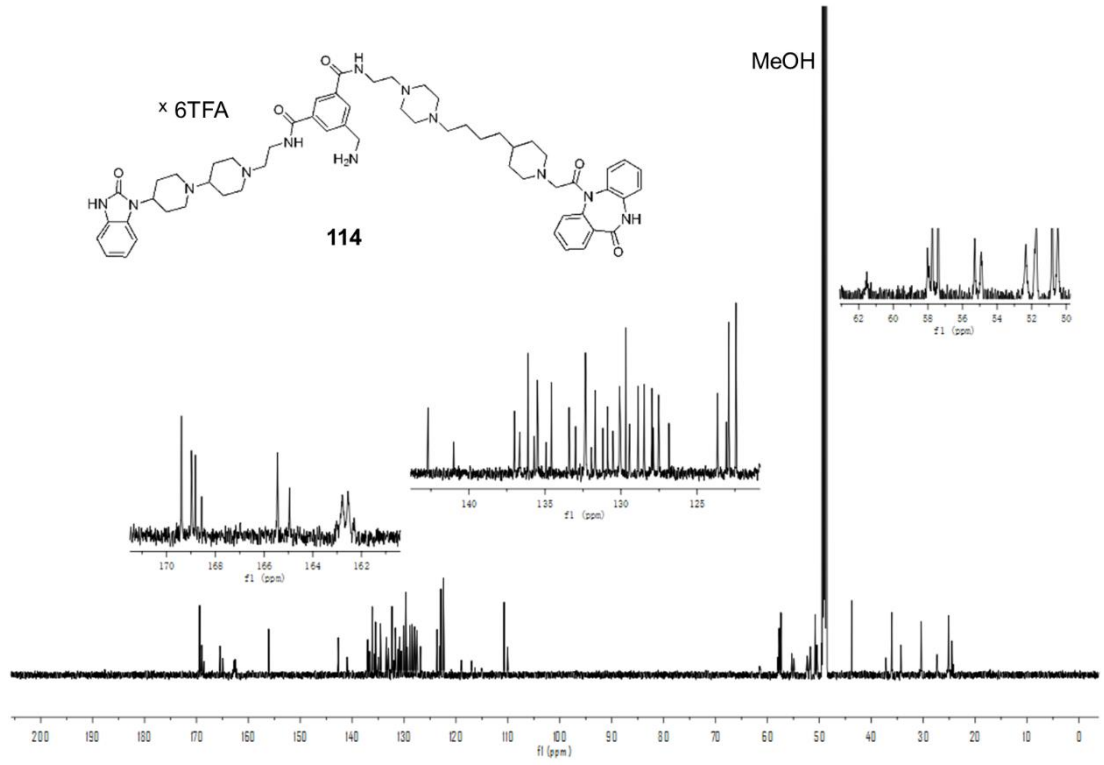

^{13}C-NMR spectrum (150 MHz, [D$_4$]MeOH) of compound **114**.

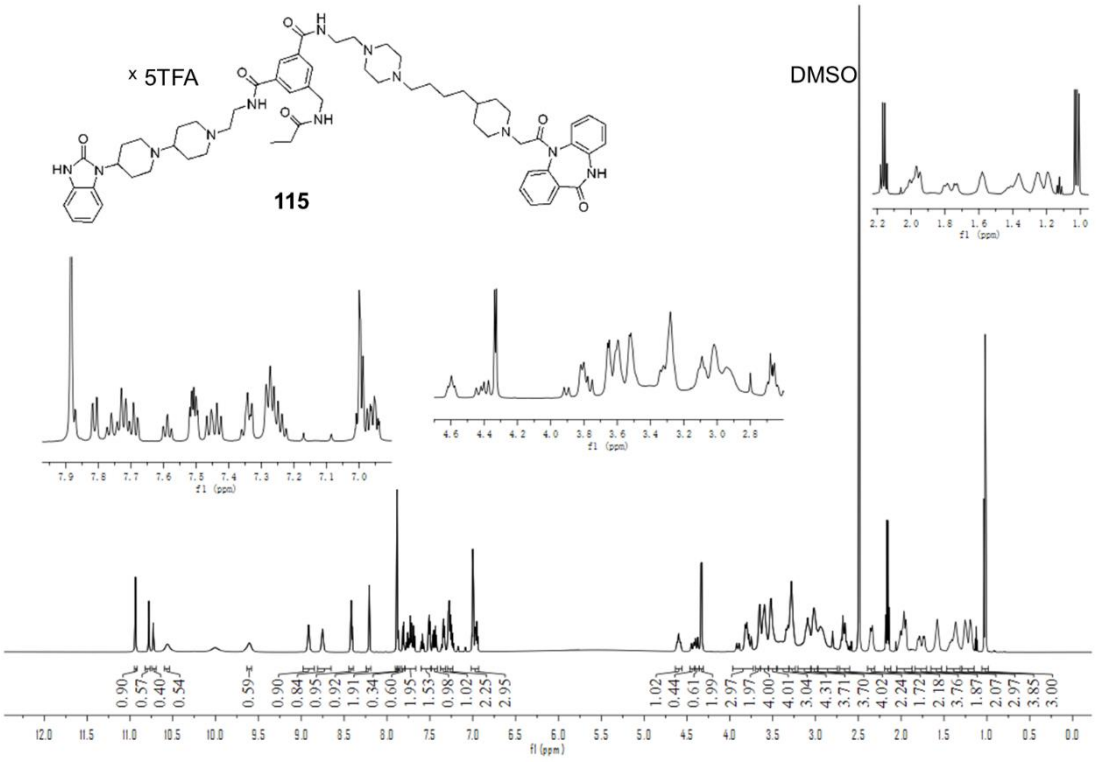

^{1}H-NMR spectrum (600 MHz, [D_6]DMSO) of compound **115**.

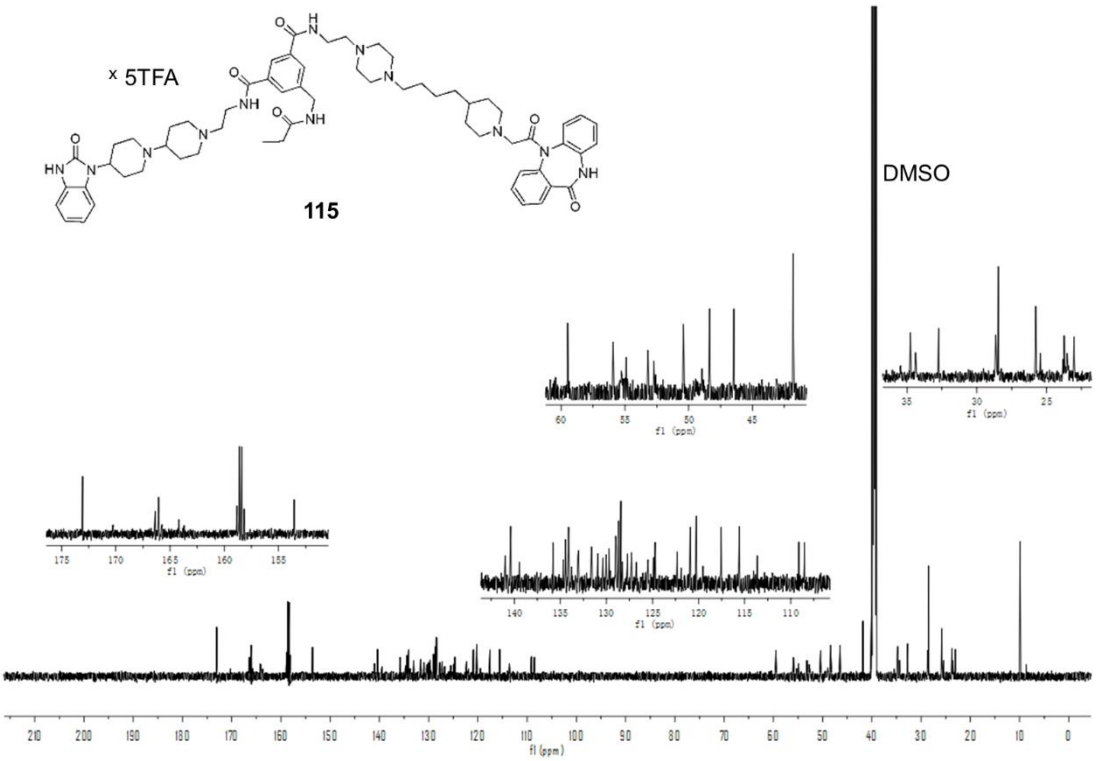

^{13}C-NMR spectrum (150 MHz, [D_6]DMSO) of compound **115**.

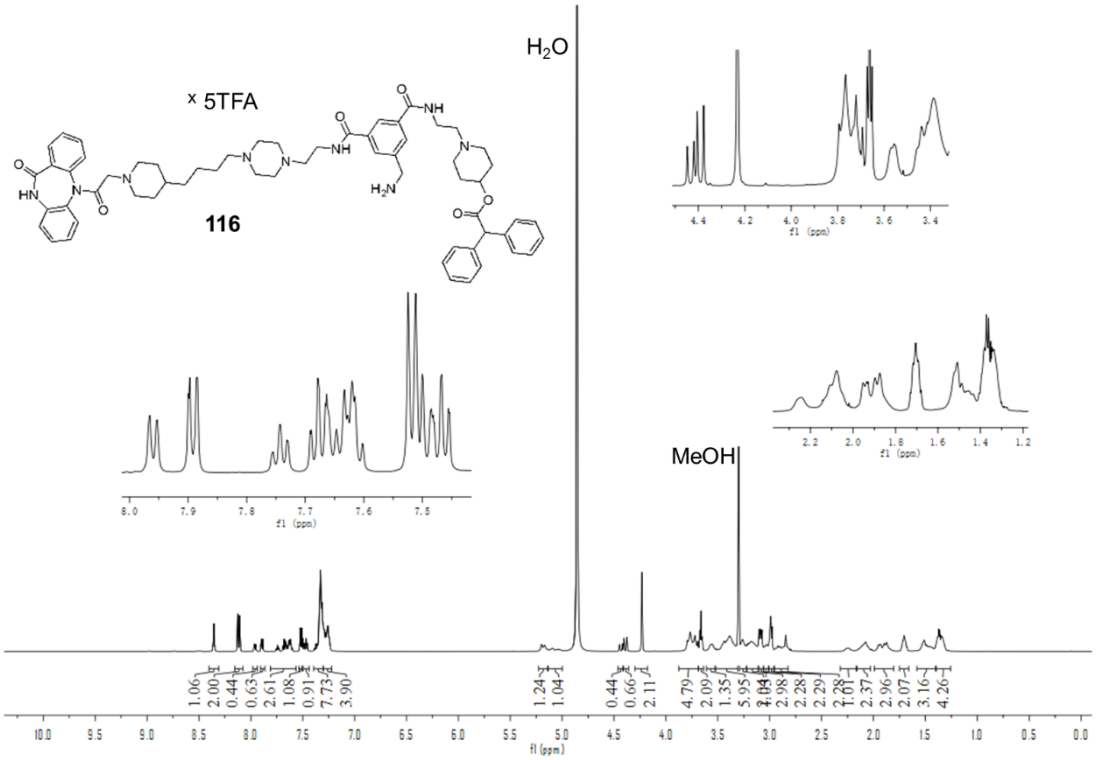

^{1}H-NMR spectrum (600 MHz, [D$_4$]MeOH) of compound **116**.

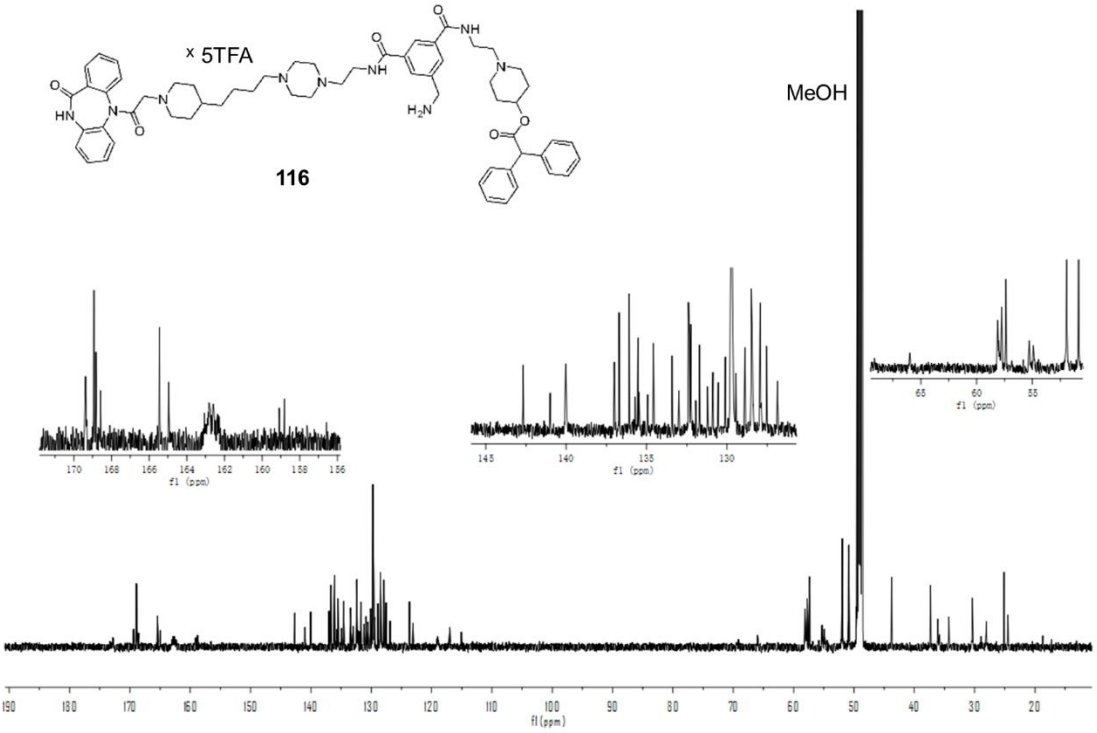

^{13}C-NMR spectrum (150 MHz, [D$_4$]MeOH) of compound **116**.

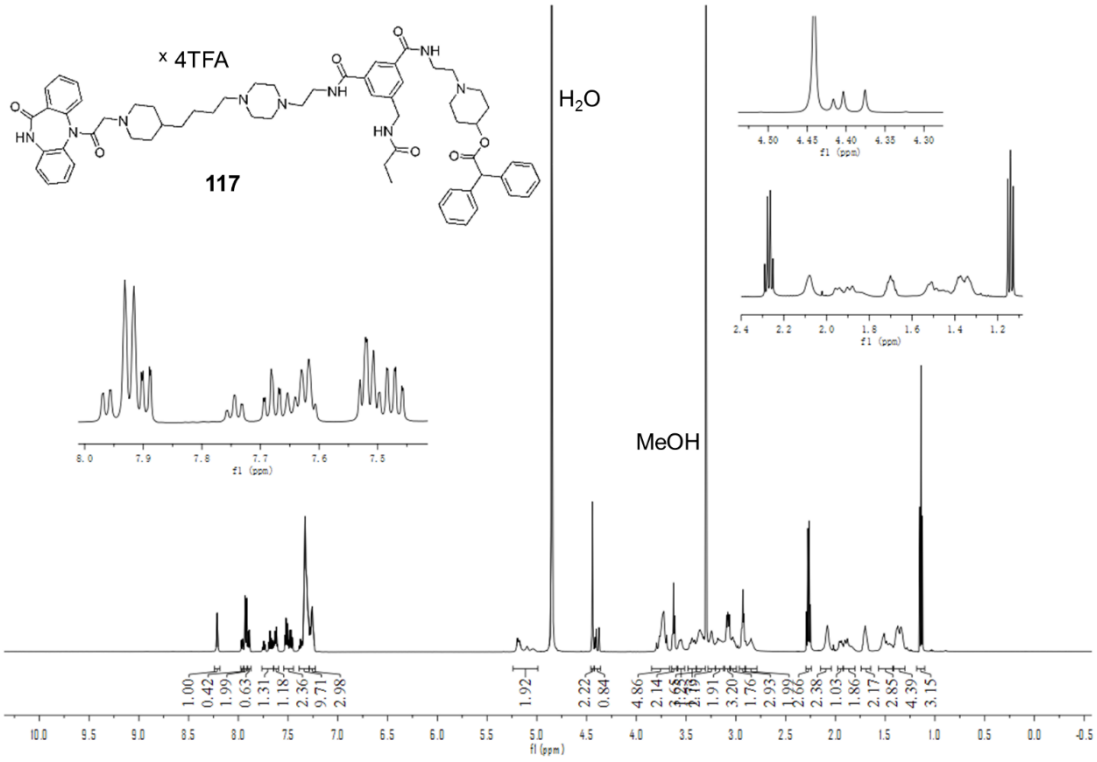

^{1}H-NMR spectrum (600 MHz, [D$_4$]MeOH) of compound **117**.

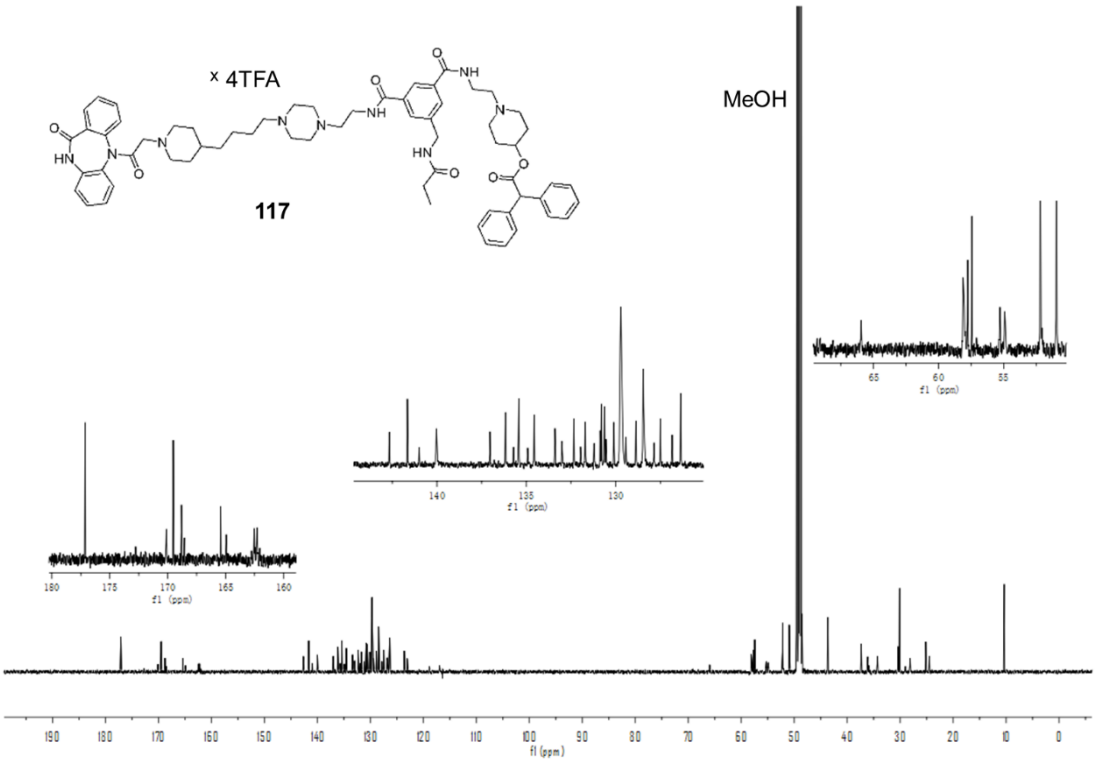

^{13}C-NMR spectrum (150 MHz, [D$_4$]MeOH) of compound **117**.

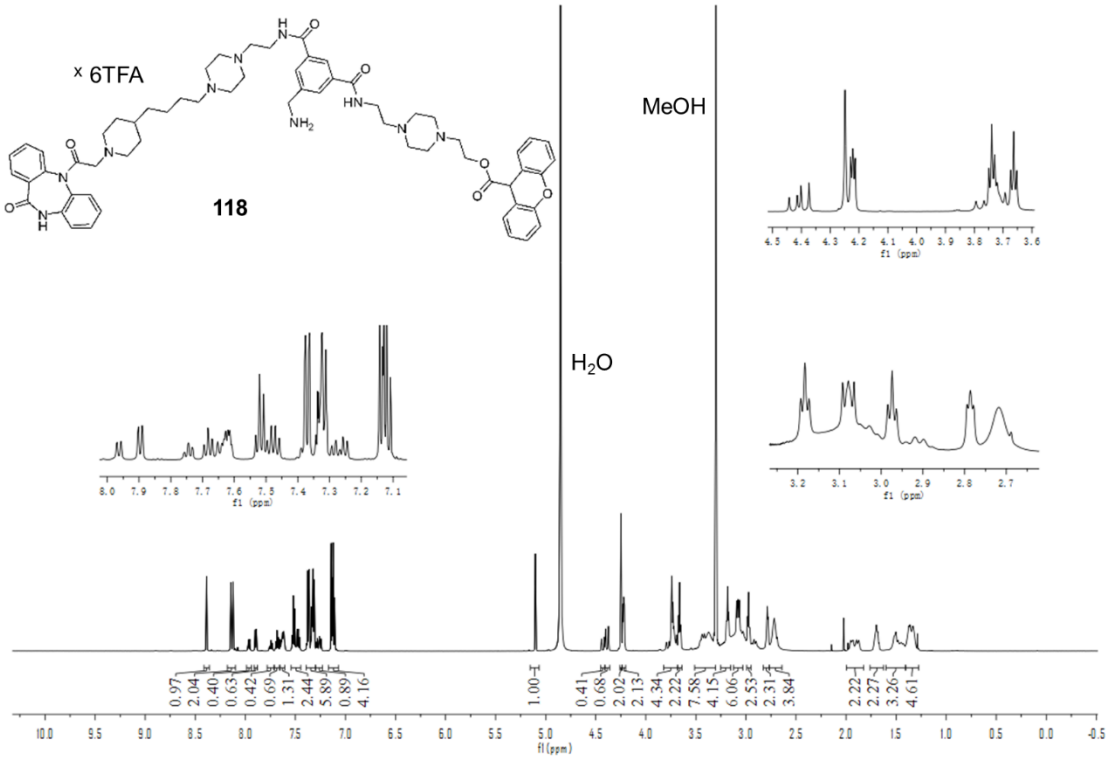

^{1}H-NMR spectrum (600 MHz, [D$_4$]MeOH) of compound **118**.

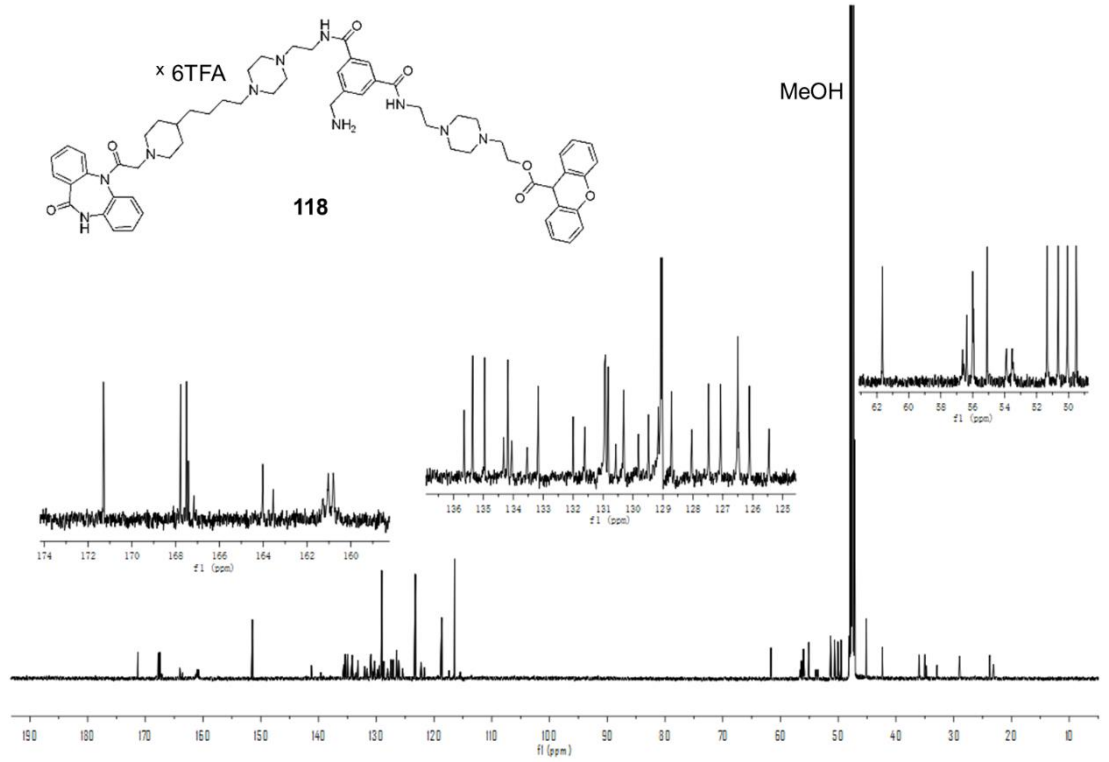

^{13}C-NMR spectrum (150 MHz, [D$_4$]MeOH) of compound **118**.

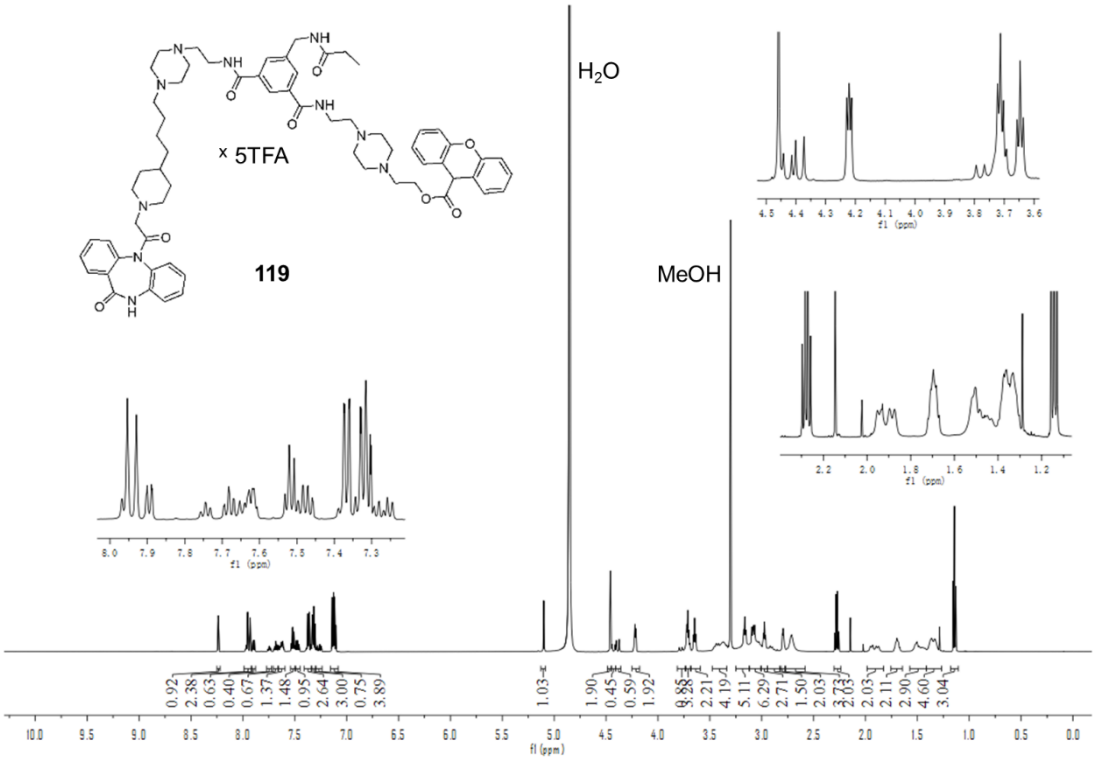

^{1}H-NMR spectrum (600 MHz, [D$_4$]MeOH) of compound **119**.

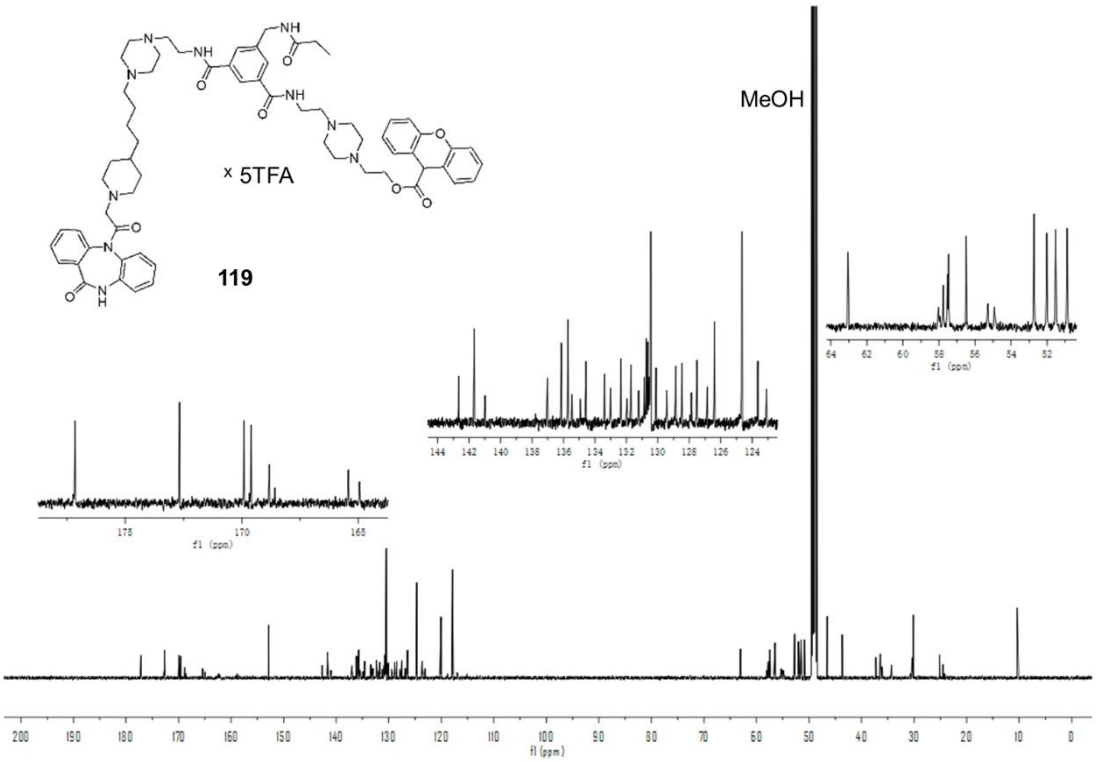

^{13}C-NMR spectrum (150 MHz, [D$_4$]MeOH) of compound **119**.

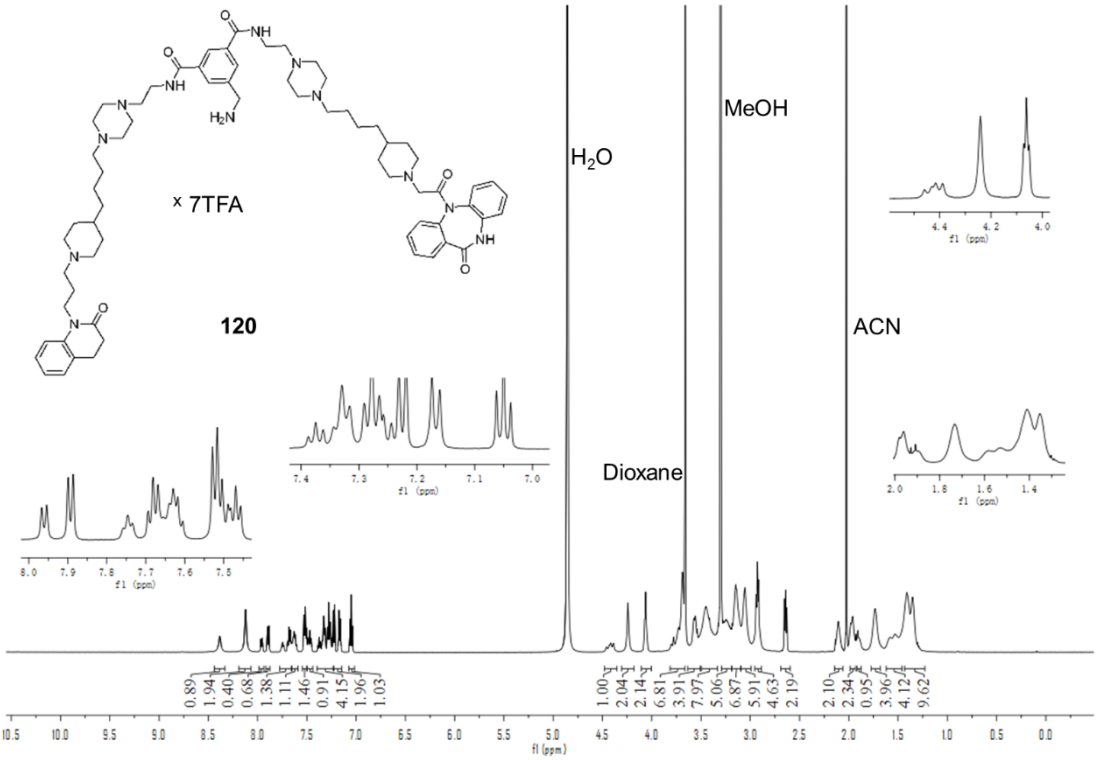

^{1}H-NMR spectrum (600 MHz, [D$_4$]MeOH) of compound **120**.

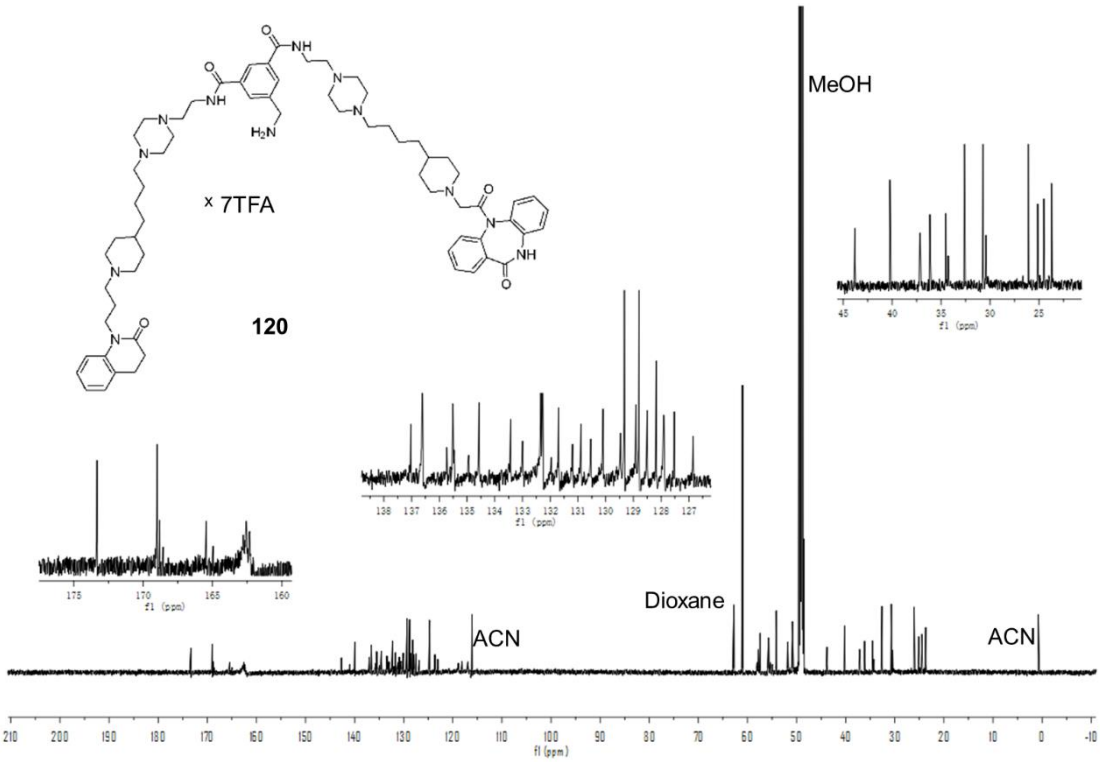

^{13}C-NMR spectrum (150 MHz, [D$_4$]MeOH) of compound **120**.

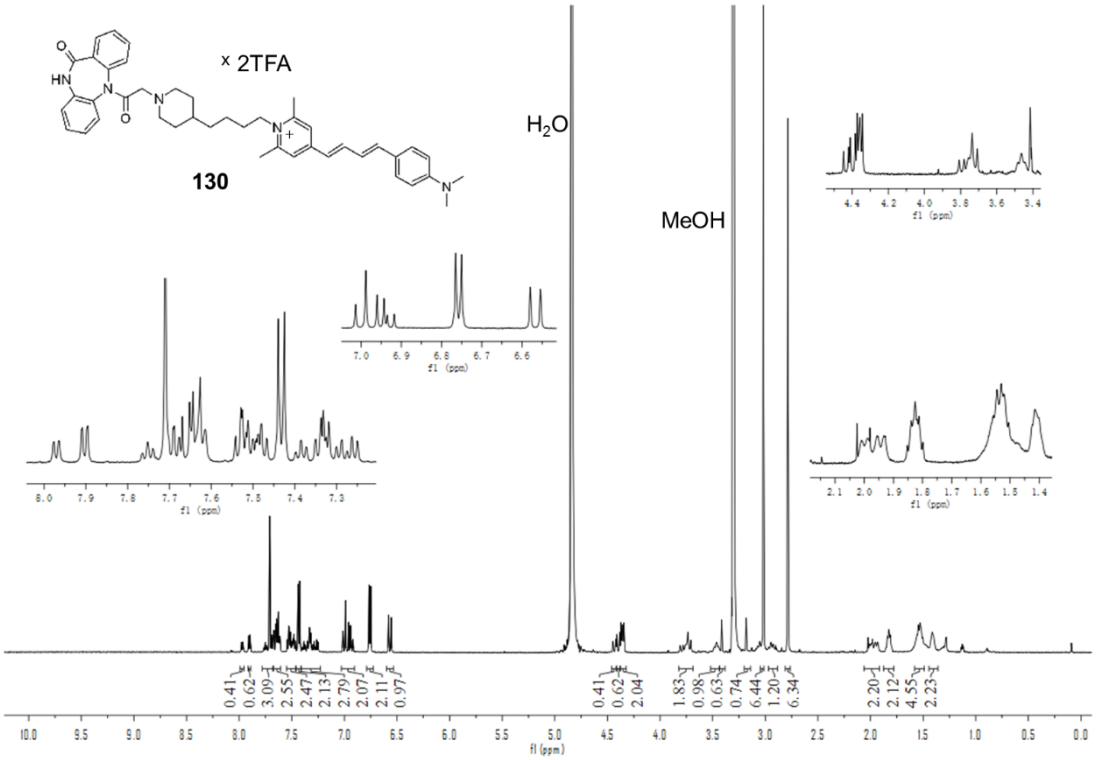

^{1}H-NMR spectrum (600 MHz, MeOH-d_4) of compound **130**.

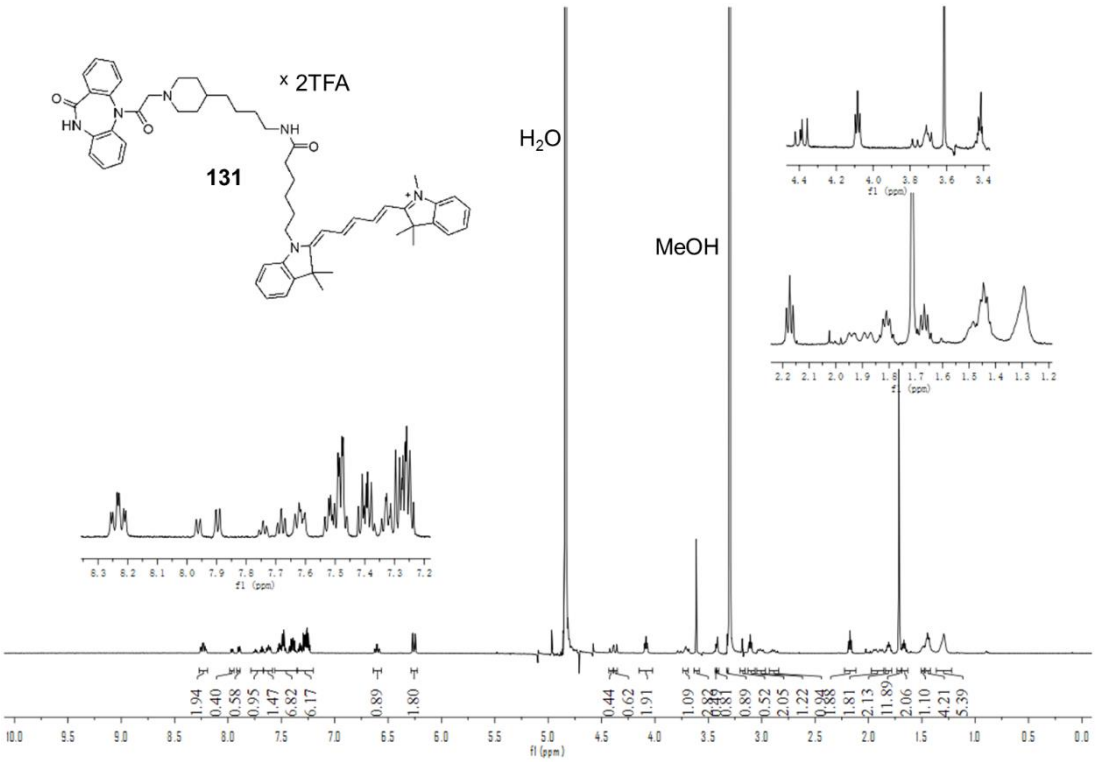

^{1}H-NMR spectrum (600 MHz, MeOH-d_4) of compound **131**.

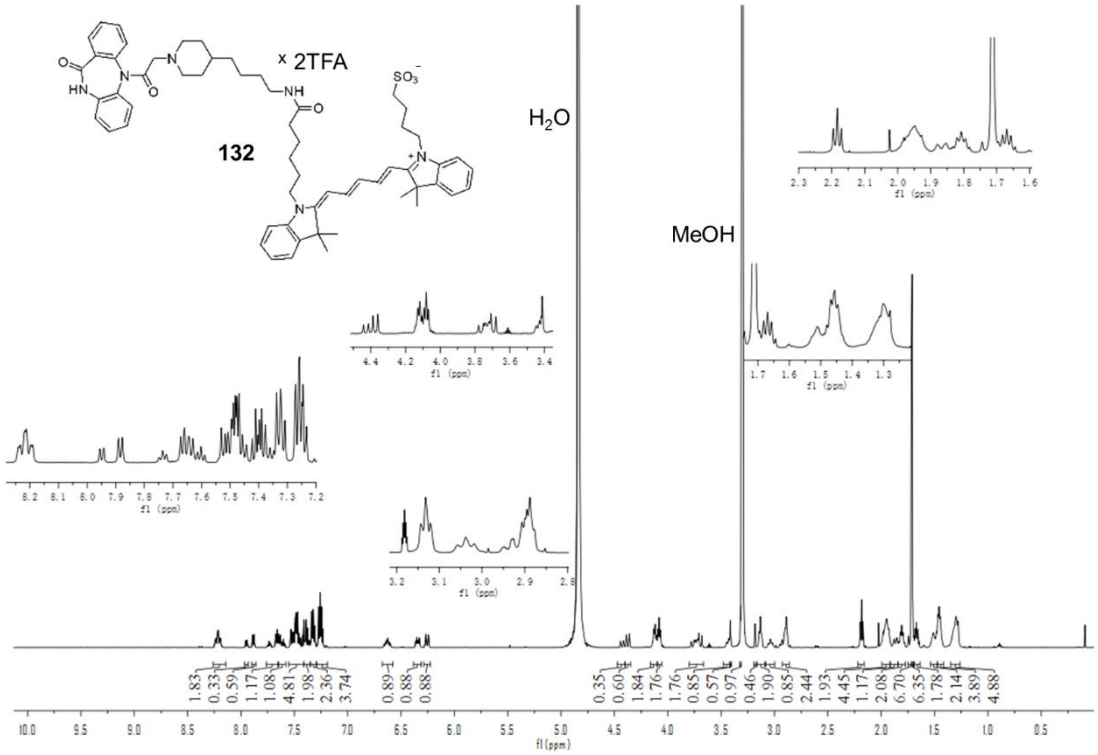

^{1}H-NMR spectrum (600 MHz, MeOH-d_4) of compound **132**.

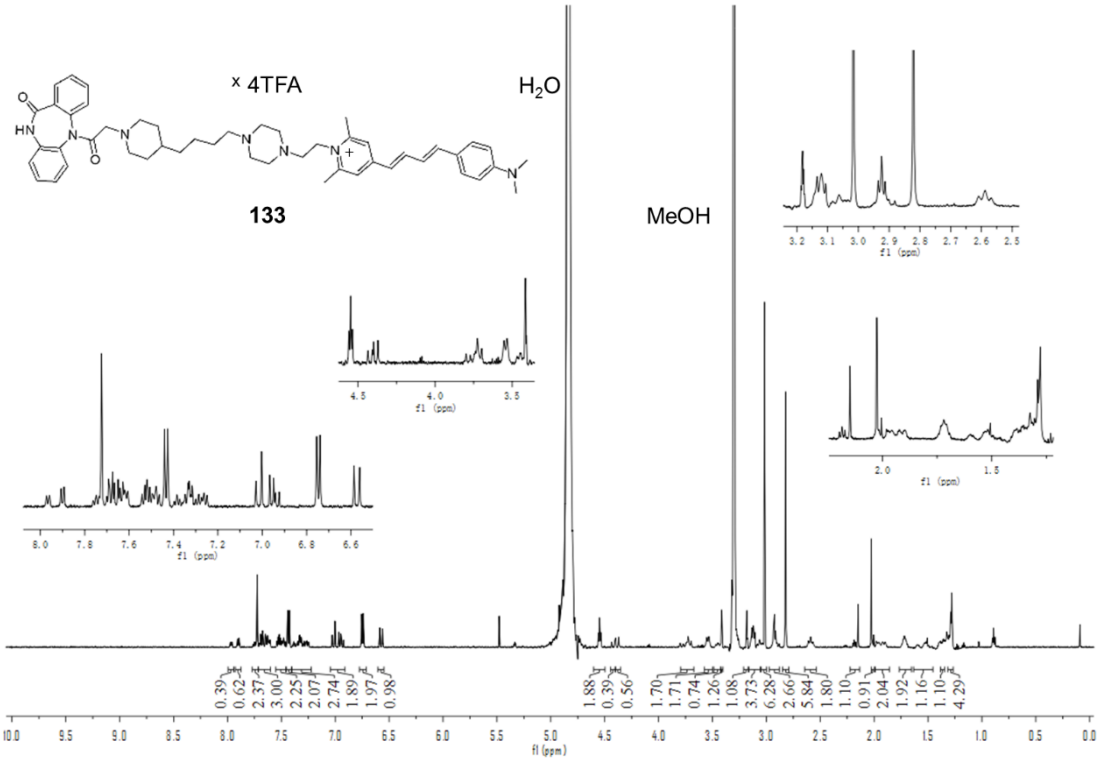

^{1}H-NMR spectrum (600 MHz, MeOH-d_4) of compound **133**.

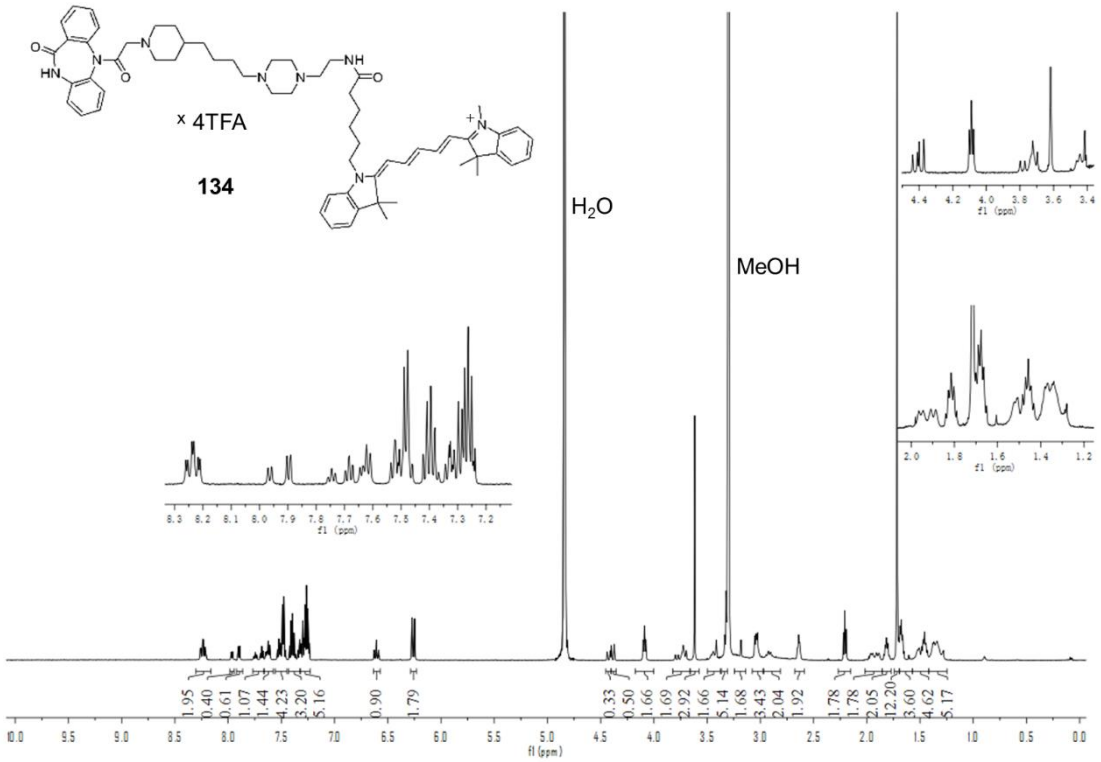

1H-NMR spectrum (600 MHz, MeOH-d4) of compound **134**.

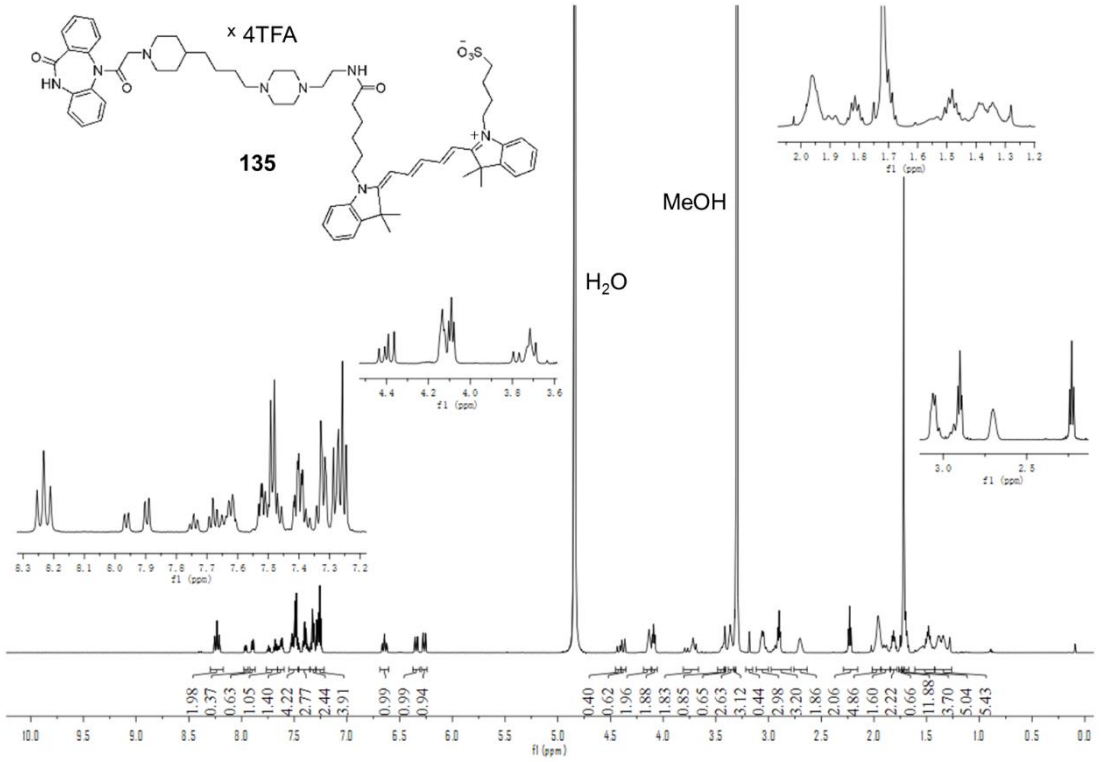

^{1}H-NMR spectrum (600 MHz, MeOH-d_4) of compound **135**.

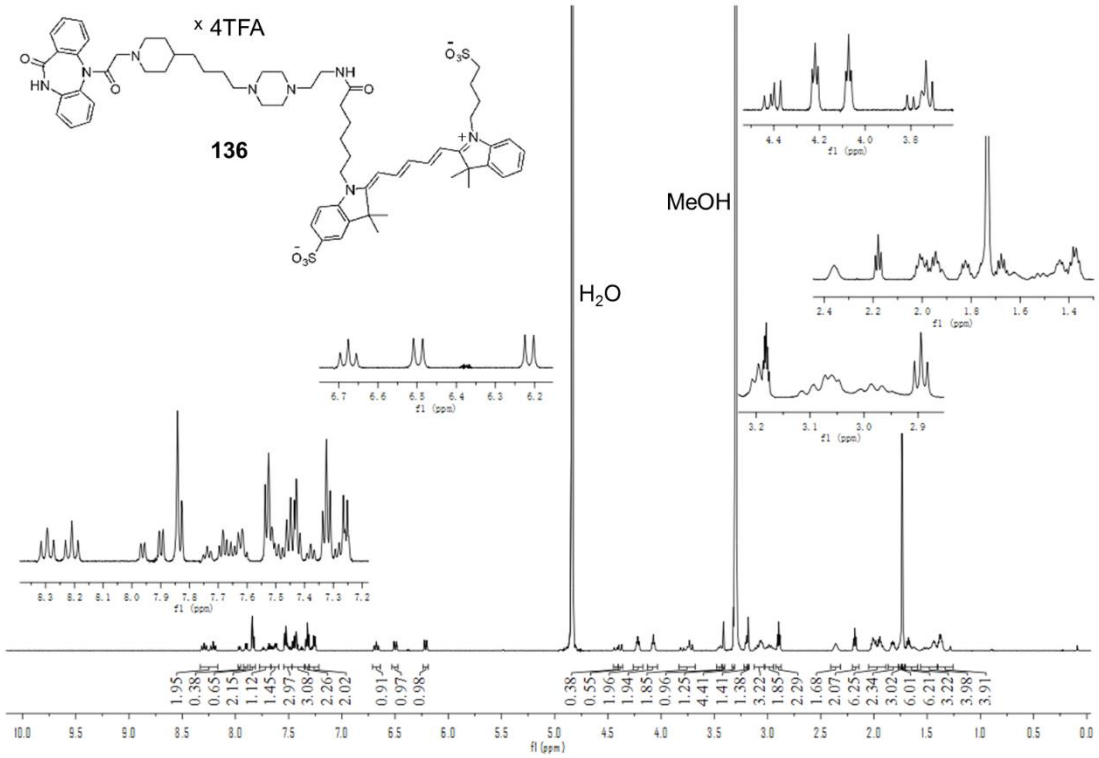

^{1}H-NMR spectrum (600 MHz, MeOH-d_4) of compound **136**.

6.2. RP-HPLC chromatograms of compounds 41, 46, 53-55, 67, 95-102, 105a, 106-108, 110-120 and 130-136

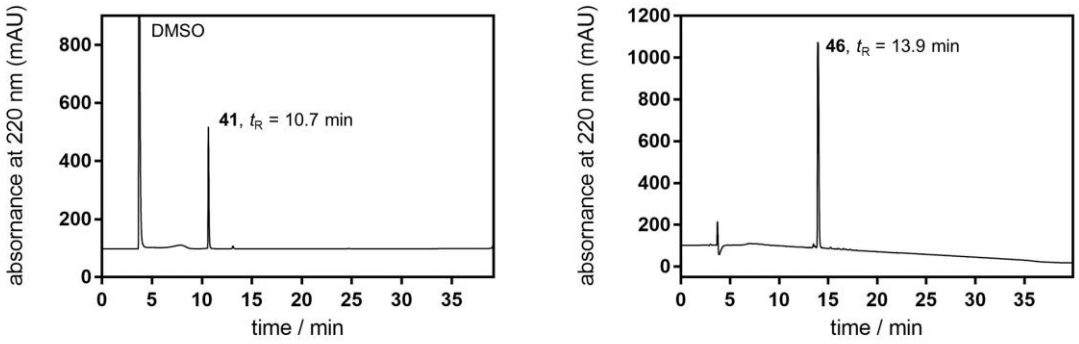

RP-HPLC analysis (purity control) of **41** and **46**.

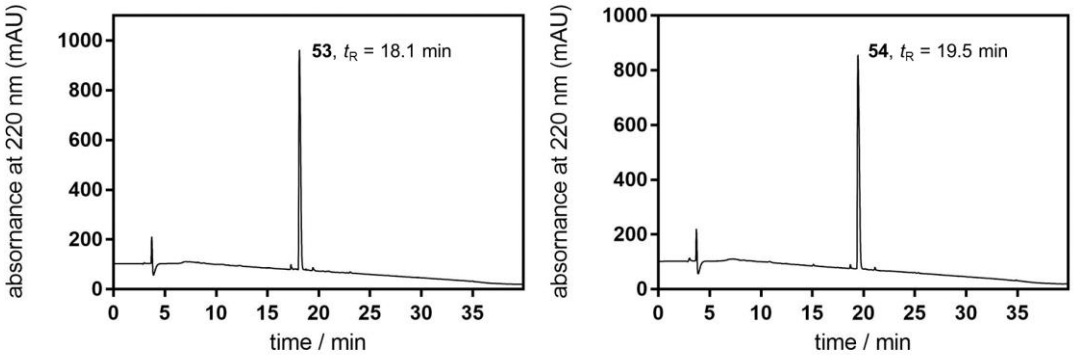

RP-HPLC analysis (purity control) of **53** and **54**.

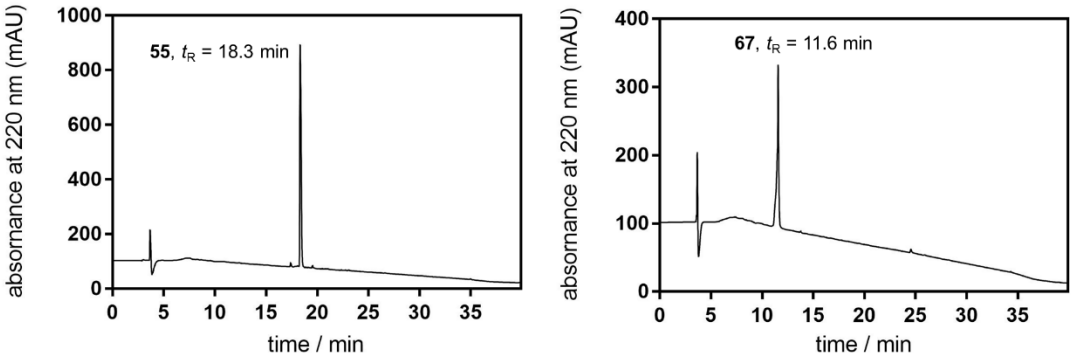

RP-HPLC analysis (purity control) of **55** and **67**.

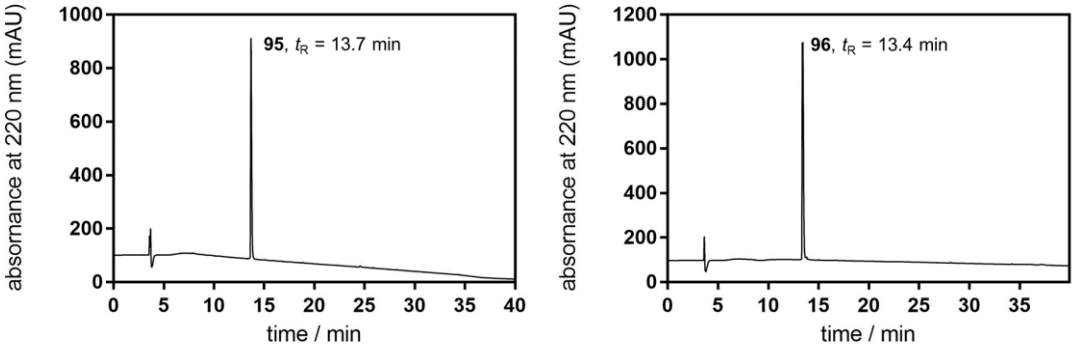

RP-HPLC analysis (purity control) of **95** and **96**.

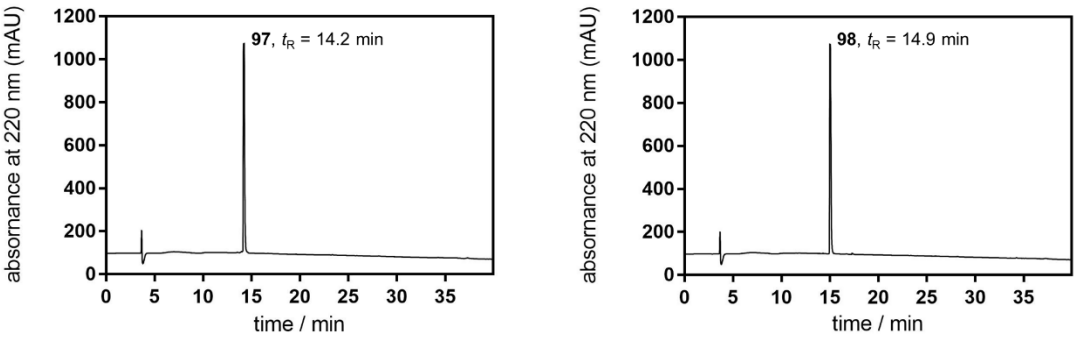

RP-HPLC analysis (purity control) of **97** and **98**.

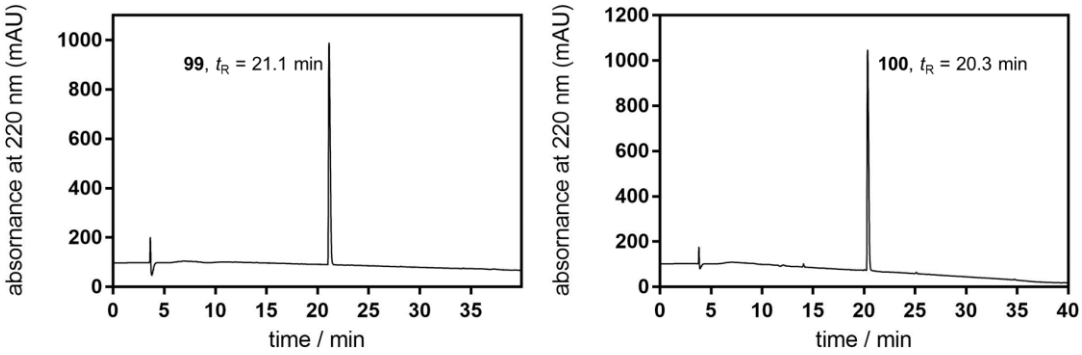

RP-HPLC analysis (purity control) of **99** and **100**.

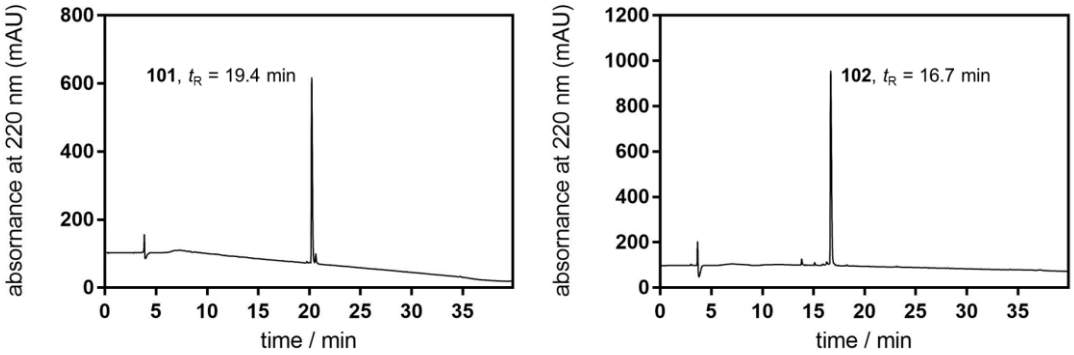

RP-HPLC analysis (purity control) of **101** and **102**.

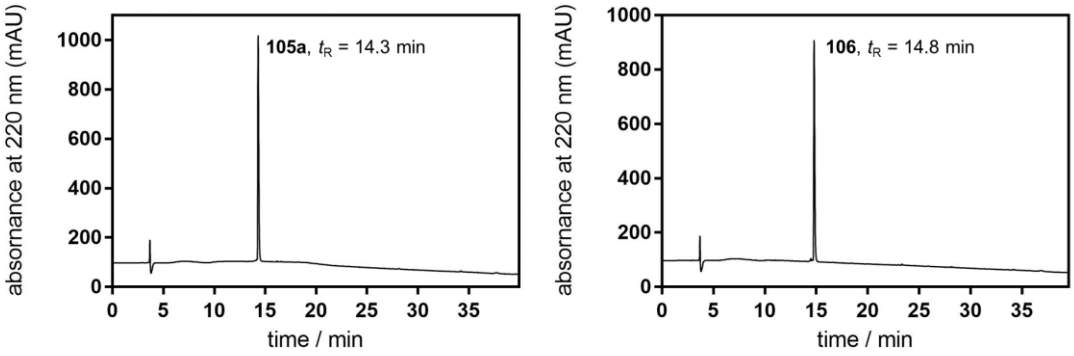

RP-HPLC analysis (purity control) of **105a** and **106**.

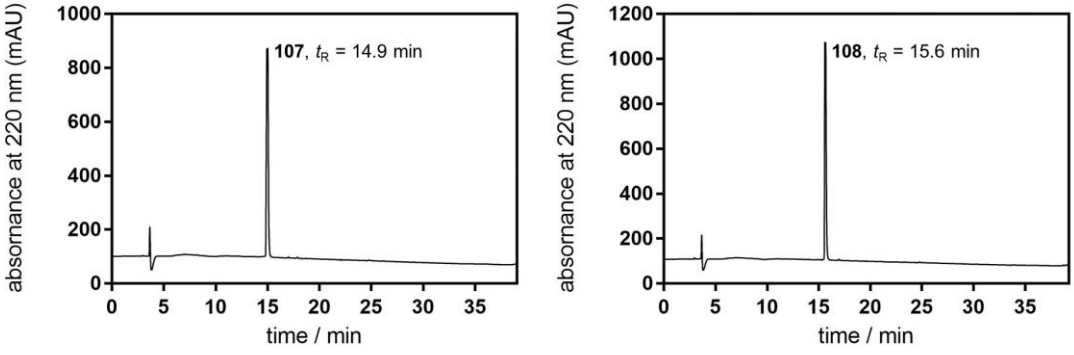

RP-HPLC analysis (purity control) of **107** and **108**.

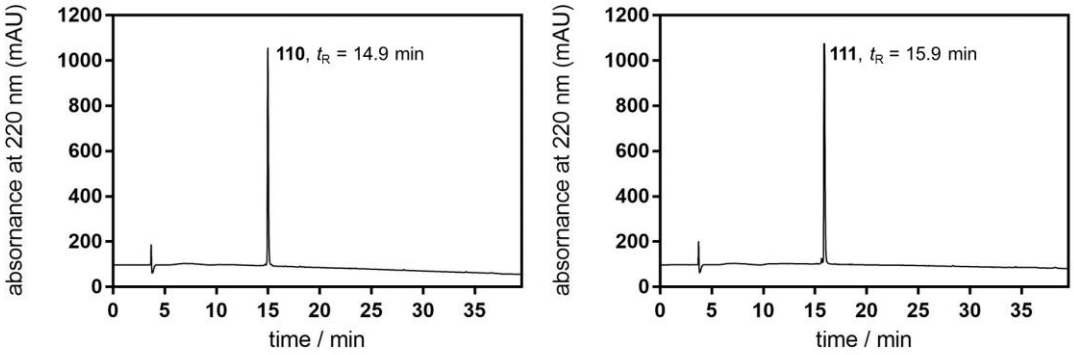

RP-HPLC analysis (purity control) of **110** and **111**.

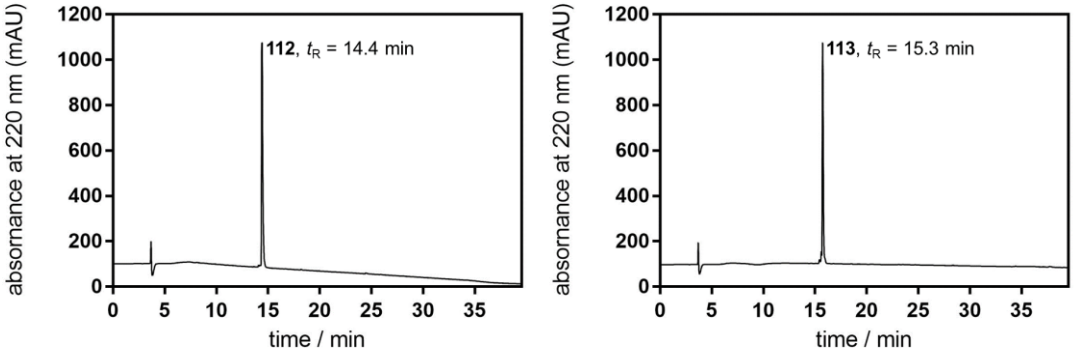

RP-HPLC analysis (purity control) of **112** and **113**.

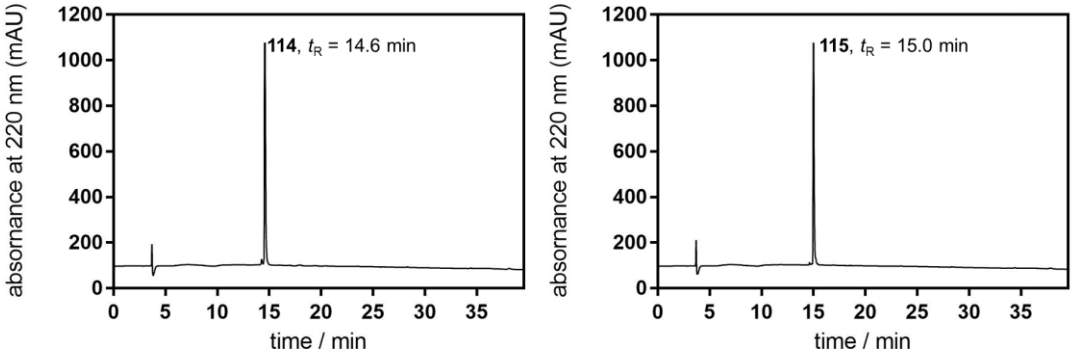

RP-HPLC analysis (purity control) of **114** and **115**.

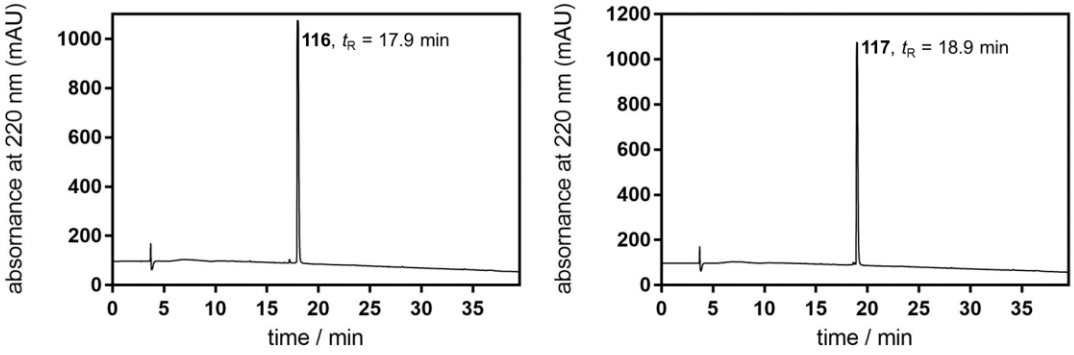

RP-HPLC analysis (purity control) of **116** and **117**.

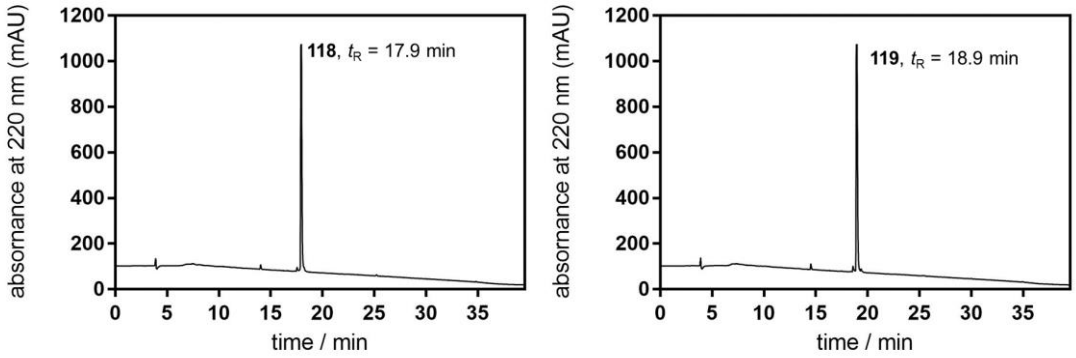

RP-HPLC analysis (purity control) of **118** and **119**.

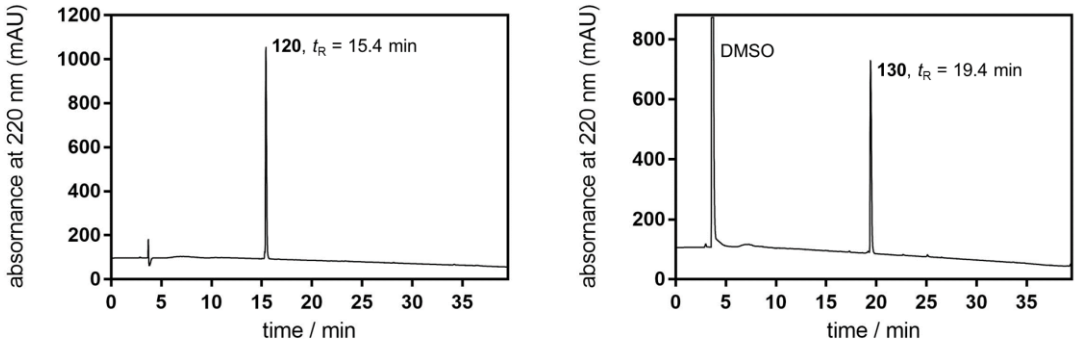

RP-HPLC analysis (purity control) of **120** and **130**.

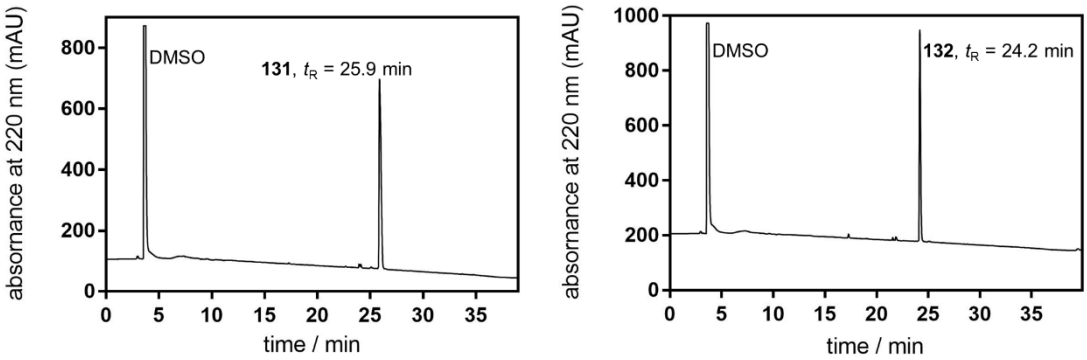

RP-HPLC analysis (purity control) of **131** and **132**.

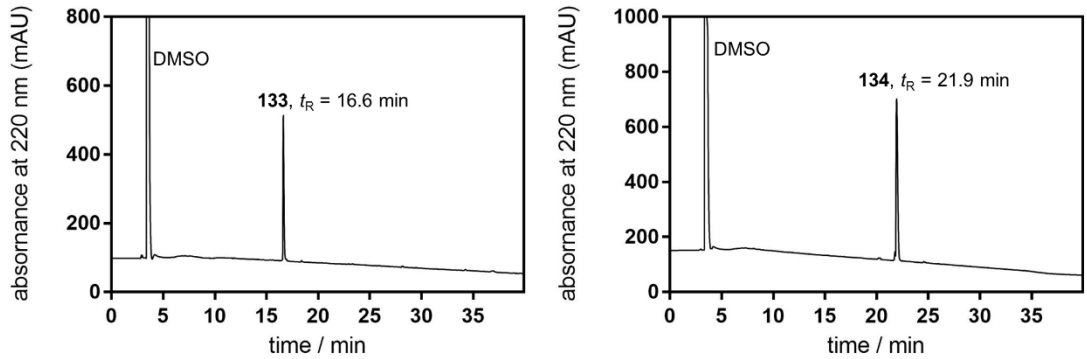

RP-HPLC analysis (purity control) of **133** and **134**.

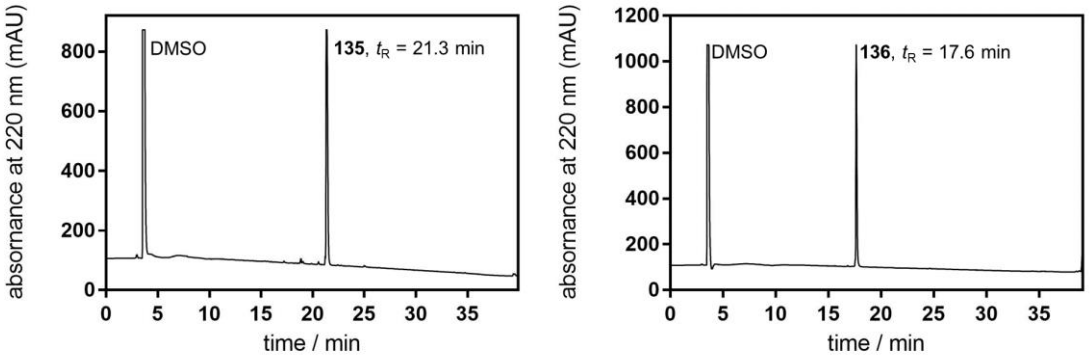

RP-HPLC analysis (purity control) of **135** and **136**.

6.3. Abbreviations

α	intrinsic activity or selectivity factor
A	agonist
abs	absolute
AC	adenylyl cyclase
aq	aqueous
atm	atmosphere
Boc	*tert*-butoxycarbonyl
Boc_2O	di-*tert*-butyl dicarbonate
Bq	becquerel
B_{max}	the maximal specific binding of a ligand
BRET	bioluminescence resonance energy transfer
brs	broad singlet
BSA	bovine serum albumin
$[Ca_{2+}]_i$	intracellular calcium ion concentration
calcd.	calculated
cAMP	cyclic 3', 5'-adenosine monophosphate
CH_2Cl_2	dichloromethane
$CHCl_3$	chloroform
CH_3CN	acetonitrile
CHO-cells	Chinese hamster ovary cells
Ci	curie
CNS	central nervous system
COSY	correlated spectroscopy
cpm	counts per minute
d	day(s) or doublet
DAG	diacylglycerol
δ	chemical shift
DCC	N,N'-dicyclohexylcarbodiimide
DCM	dichloromethane
dd	doublet of doublets
DIPEA	diisopropylethylamine
DMAP	4-dimethylaminopyridine
DMF	dimethylformamide
DMSO	dimethylsulfoxide

DMSO-d_6	per-deuterated dimethylsulfoxide
EC_{50}	agonist concentration which induces 50 % of the maximum response
EDC	*N*-(3-dimethylaminopropyl)-*N*′-ethylcarbodiimide hydrochloride
eq	equivalents
EtOAc	ethylacetate
Et_2O	diethylether
EtOH	ethanol
FACS	fluorescence activated cell sorter
FCS	fetal bovine serum
Fl-1, Fl-2, Fl-3, Fl-4	fluorescence channels (Flow cytometer)
FRET	fluorescence resonance energy transfer
G	G-Protein
GDP	guanosine diphosphate
GTP	guanosine triphosphate
GPCR	G-protein coupled receptor
h	hour(s) or human
HCl	hydrochloric acid
HMBC	heteronuclear multiple bond correlation
HSQC	heteronuclear single quantum correlation
HOBt	1-Hydroxybenzotriazole hydrate
HPLC	high-performance liquid chromatography
HRMS	high resolution mass spectrometry
Hz	hertz
IC_{50}	radioligand binding assay: ligand concentration inhibiting the binding of a radioligand by 50 %
IP_3	inositol-1,4,5-trisphosphate
IR	infrared
J	coupling constant
k	capacity factor
K_b	dissociation constant (functional assay)
KBr	potassium bromide
K_2CO_3	potassium carbonate
K_d	dissociation constant (saturation binding)
$KHSO_4$	potassium bisulfate
K_i	dissociation constant (competition binding)
k_{obs}	observed rate constant
k_{off}	dissociation rate constant
k_{on}	association rate constant
L	liter
$LiAlH_4$	Lithiumaluminiumhydrid
L15	Leibovitz medium without phenol red
m	multiplet
M	molar (mol/L)
mAU	milli absorbance units
MeCN	acetonitrile
MeOH	methanol
MeOH-d_4	per-deuterated methanol
MeI	methyl iodide
mol	mole (s)
min	minute(s)
µ	micro

mp	melting point
MR	Muscarinic receptor
M_xR	Muscarinic M_x receptor (x = 1, 2, 3, 4, 5)
MS	mass spectrometry
n	nano or amount of substance
$NaHCO_3$	sodium bicarbonate
NaI	sodium iodide
Na_2SO_4	sodium sulfate
NEt_3	triethylamine
NHS	N-hydroxysuccinimide
NMR	nuclear magnetic resonance
NPY	neuropeptide Y
OBD	orthosteric binding domain
PBS	phoshpate buffered saline
PE	petroleum ether
pEC_{50}	negative decadic logarithm of the molar concentration of the agonist causing 50 % of the maximal response
Ph	phenyl
Ph_3P	triphenylphosphine
PIP_2	Phosphatidylinositol-4,5-bisphosphate
PKC	protein kinase C
PLCβ	phospholipase Cβ
pK_b	negative decadic logarithm of the dissociation constant (functional assay)
pK_i	negative decadic logarithm of the dissociation constant (competition binding assay)
ppm	parts per million
Py	pyridyl or pyrylium
q	quartet
ref	reference
R_f	retardation factor
RGS	regulator of G-protein signaling
RP	reversed phase
rpm	revolutions per minute
rt	room temperature
s	singulet
sat.	saturated
SEM	standard error of the mean
t	triplet
t_0	dead time
TBDPS	*tert*-butyldiphenysily
TBTU	2-(1*H*-Benzotriazole-1-yl)-1,1,3,3-tetramethylaminium tetrafluoroborate
TFA	trifluoroacetic acid
THF	tetrahydrofuran
TLC	thin layer chromatography
	TM transmembrane
TM	transmembrane
TMS	trimethylsilyl
t_R	retention time
UV	ultraviolett